Univerza
v Ljubljani
Fakulteta
za gradbeništvo
in geodezijo

Jamova 2
1000 Ljubljana, Slovenija
telefon (01) 47 68 500
faks (01) 42 50 681
fgg@fgg.uni-lj.si

Podiplomski program Gradbeništvo
Konstrukcijska smer

Kandidat:
Jure Klopčič

Analiza in napoved pomikov za predore, grajene v permo-karbonskih skrilavcih

Doktorska disertacija št. 196

Mentor:
izr. prof. dr. Janko Logar

Somentor:
izr. prof. dr. Tomaž Ambrožič

Ljubljana, 15. 9. 2009

BIBILIOGRAFSKO-DOKUMENTACIJSKA STRAN IN IZVLEČEK

UDK: **528.48:624.19(043.3)**

Avtor: **Jure Klopčič**

Mentor: **izr. prof. dr. Janko Logar**

Somentor: **izr. prof. dr. Tomaž Ambrožič**

Naslov: **Analiza in napoved pomikov za predore, grajene v permo-karbonskih skrilavcih**

Obseg in oprema: **235 str., 11 pregl., 137 sl., 11 en.**

Ključne besede: **gradnja predorov, 3D meritve pomikov, avtomatiziran sistem obdelave podatkov, merski podatki, raziskovalni rov, 3D meritve pomikov pred čelom, avtomatsko prepoznavanje tarč, povratne 3D numerične analize, ekstrapolacijska metoda napovedi pomikov, anizotropija hribinske mase**

Izvleček:

V zadnjih petnajstih letih je bilo v okviru avtocestnega programa na slovenskem avtocestnem omrežju zaradi razgibanega reliefa zgrajenih precej predorov. Od leta 1997 in gradnje predora Golovec dalje se v Sloveniji pri gradnji vseh avtocestnih predorov kot integralni del geološko-geotehnične spremljave izvaja meritve 3D pomikov notranje obloge. Analiza in interpretacija teh meritev omogoča oceno ustreznosti vhodnih projektnih parametrov ter optimizacijo podporja in delovnih procesov glede na izmerjeni in pričakovani odziv predora. V okviru naloge so bili merski podatki iz trinajstih predorov, zgrajenih od leta 1998 dalje, skupaj z geološkimi popisi izkopnih čel urejeni v obsežno bazo podatkov. Za prikaz in analizo teh podatkov je bil nadalje izdelan lastni računalniški programski paket, imenovan Predor. Posebnost paketa je avtomatski sistem za obdelavo merskih in geoloških podatkov iz predorov v gradnji, shranjevanje v že omenjeno bazo ter izdelavo nazornih grafičnih in tekstovnih poročil v realnem času. Osrednji del naloge je posvečen analizi merjenih pomikov iz predorov, zgrajenih v mehkih skrilavih hribinah permo-karbonske starosti (Trojane, Golovec, Šentvid). Analiza teh pomikov izkazuje bolj ali manj izrazito anizotropno obnašanje hribine tako v prečnem prerezu kot tudi vzdolž predorske osi. Numerične povratne analize so kot eno izmed možnosti za modeliranje merjenega odziva izkazale zelo nizko vrednost strižnega modula vzdolž diskontinuitet. Na primeru vzdolžnega pomika v izkopani prostor smo ugotovili, da je velikost pomikov izkopanega prostora in s tem delež pomikov pred čelom predora močno odvisen od usmerjenosti diskontinuitet glede na os predora. Podrobno so opisani in analizirani predvsem vzdolžni pomiki v smeri napredovanja izkopa pod padajočim nadkritjem kot posledica anizotropije hribine. Izvedli smo ogromno število 3D numeričnih analiz, da bi ugotovili delež predpomikov in velikost vplivnega območja pred čelom predora za različne relativne naklone diskontinuitet glede na os predora in različne kombinacije materialnih parametrov anizotropne hribinske mase. Med projektiranjem predora Šentvid je bil za določitev geološko najprimernejšega položaja priključnih kavern izdelan raziskovalni rov, v katerem so se nato med gradnjo glavnega predora pred čelom kalote le-tega na daljšem odseku rova izvajale meritve 3D pomikov. Podrobno je prikazana zasnova in sama izvedba eksperimenta, ki je bil po dostopnih podatkih izveden prvič. Izmerjeni pomiki so bili ustrezno obdelani, prikazani so dobljeni rezultati in opravljena analiza opaženih deformacijskih vzorcev glede na zabeleženo geološko zgradbo. Izdelane so bila tudi 3D numerične študije opaženih fenomenov ter vpliva raziskovalnega rova in njegovega položaja na pomike pred čelom.

BIBILIOGRAPHIC-DOCUMENTALISTIC INFORMATION AND ABSTRACT

UDC: **528.48:624.19(043.3)**

Author: **Jure Klopčič**

Supervisor: **Assoc. Prof. Janko Logar, Ph.D.**

Co-adviser: **Assoc. Prof. Tomaž Ambrožič, Ph.D.**

Title: **Analyses and prediction of displacements for tunnels in foliated rock mass of Perm-Carboniferous age**

Notes: **235 pp., 11 tab., 137 fig., 11 eq.**

Keywords: **tunnelling, 3D displacement measurements, automatic system for data processing, monitoring data, exploratory tunnel, 3D displacement measurements ahead of the face, automatic target recognition (ATR), 3D numerical back calculations, extrapolation prediction method, rock mass anisotropy**

Abstract:

Due to diversified topography a number of tunnels have been constructed on Slovenian motorway network in the last 15 years after the implementation of the National motorway construction programme. 3D displacement measurements of the primary lining has been applied as an integral part of the observational method on all tunnel construction sites since the Golovec tunnel construction in 1997. Analysis and interpretation of the measured displacements allow the verification of the design parameters, support optimization and optimization of construction processes. Monitoring data from the 13 tunnels, constructed after 1998, were collected and arranged in the database in the framework of this thesis together with face logs. Further on, a computer code Predor (means Tunnel in Slovene) was developed for graphical presentation and analysis of these data. Code comprises also a system for automatic handling of the incoming data from construction sites and for the preparation of graphical reports in real time. The main emphasis of the work was given to the analysis of measured displacements in tunnels, situated in soft foliated rock mass of Carboniferous age (the Trojane, Golovec and Šentvid tunnels). Monitored displacements display more or less pronounced anisotropic response in the cross section as well as in the longitudinal section. To model the observed response, back analyses with numerical calculations suggested very low value of shear modulus along the discontinuities. Special attention was paid to the analysis of well documented longitudinal displacements in the excavation direction under decreasing overburden due to anisotropy of the rock mass. It was found out that the magnitude of final measured displacements and thus portion of pre-displacements strongly depends on the relative discontinuity orientation to the tunnel axis. A large number of numerical simulations was performed to define the portion of pre-displacements and the extent of pre-face domain for different discontinuity orientations and different sets of material properties of the anisotropic rock mass. To locate the merging caverns of the Šentvid tunnel in most favourable rock mass conditions the exploratory tunnel was constructed in the design stage and enabled 3D displacement measurements ahead of the top heading face of the main motorway tunnel during its construction. Extensive information about the scheme and execution of this experiment is given (no reports have been found so far of any similar experiments). Monitored displacements were analyzed according to mapped geological structure. Further on, the observed phenomena and the influence of the exploratory tunnel and its position on the displacements were studied with 3D numerical calculations.

ZAHVALA

Doktorska disertacija je rezultat raziskovalnega dela na Katedri za mehaniko tal z laboratorijem in Katedri za geodezijo Fakultete za gradbeništvo in geodezijo Univerze v Ljubljani. Raziskovalno delo je financiralo Ministrstvo za visoko šolstvo, znanost in tehnologijo Republike Slovenije preko Javne agencije za raziskovalno dejavnost Republike Slovenije v okviru programa usposabljanja mladih raziskovalcev.

Izvedbo meritev prostorskih pomikov v raziskovalnem rovu predora Šentvid je financirala Družba za avtoceste Republike Slovenije (DARS). Lastnik geotehničnih in geoloških podatkov iz slovenskih avtocestnih predorov je prav tako DARS. Z vsemi potrebnimi podatki sta me oskrbovala Andrej Štimulak iz podjetja DDC svetovanje inženiring iz Ljubljane in Janez Maurer iz podjetja Elea iC iz Ljubljane. Geološke pojme mi je pojasnjeval Igor Ajdič iz podjetja Gracen iz Ljubljane.

Pri izvajanju zahtevnih in dolgotrajnih meritev v raziskovalnem rovu predora Šentvid so mi pomagali Tomaž Ambrožič, Sonja Gamše, Aleš Marjetič in Janko Logar, ki jim ni bilo težko v petek in svetek tudi ob najbolj nemogočih nočnih urah iti s čelado na glavi, svetilko v roki in škornji na nogah v včasih ne najbolj varen in prijeten raziskovalni rov. Zahvala gre na tem mestu tudi Milanu Črepinšku iz podjetja ZIL inženiring in Bogdanu Balohu iz podjetja SCT za pomoč pri logističnih problemih ter Andreju Štimulaku iz podjetja DDC svetovanje inženiring – sod, težka vrtalka, »puher« in nakovalo mi bodo za vedno ostali v spominu. In nenazadnje: zahvala velja tudi vsem neimenovanim predorskim delavcem in inženirjem iz podjetja SCT, ki so nam po svojih najboljših močeh pomagali pri celotni izvedbi tega edinstvenega eksperimenta, hvala jim predvsem za skrb za našo varnost.

Somentorju izr.prof.dr. Tomažu Ambrožiču se zahvaljujem, da me je vzel pod svoje okrilje kot mladega raziskovalca.

Mentorju izr.prof.dr. Janku Logarju lahko rečem le: HVALA! Da ste mi dali prostor v svoji pisarni in me prenašali ves ta čas, za vse kritične pripombe, za vse vzpodbude, za odgovor na vsak moj zakaj, za vse... Brez Vas te naloge ne bi bilo. HVALA!

Ne nazadnje dolgujem zahvalo še mojim staršem, ki sta me vseskozi spodbujala in mi pomagala na moji poti. Hvala tudi Katarini, ki mi je stala ob strani (skoraj) do konca...

CONTENT

LIST OF FIGURES

KAZALO SLIK

LIST OF TABLES

SEZNAM PREGLEDNIC

1.0 Introduction

Researches of traffic streams predict enlargement of personal and goods transport by 40% by year 2020 compared to the present situation. Because of daily migrations from suburban towns and countryside to city centres on work-days and in opposite direction during weekends, and due to massive migrations of tourists towards tourist destinations in summer, different traffic routes like highways, railways and regional connecting roads are becoming more and more important. Present routes can hardly cope with all the traffic, which is why new traffic connections will have to be built or the existing will have to be extended. The expansion of areas intended for traffic routes reduces the agricultural area as well as areas intended for relaxation and natural resorts. Despite rapid development of environmentally friendly vehicles the traffic is still one of the major pollutants with exhausts of heavy metals and gases. Therefore especially in sensible environments like Alpine world the construction of new traffic routes has to meet high environmental standards to be accepted by the society that has become more sensitive about ecological issues.

The space for the construction of traffic network in highly populated areas is limited and the prices of land are increasing, thus making new traffic routes very expensive. On the other hand, the pollution and noise due to the traffic in urban areas reduce the quality of life for the inhabitants.

Lack of space on the surface, increasing environmental awareness and care for the quality of the residential areas lead to the design and construction of underground structures. Improved knowledge about the construction and behaviour of these structures and rapid development of new technologies enables placing a wide range of activities beneath the surface (power plants, tunnels on traffic routes, parking houses, production plants, repositories of nuclear waste materials and energy recourses in forthcoming future). A large expansion of underground facilities forces also construction of such structures in unfavourable conditions, which have been avoided in the past or even considered impossible.

Since the ancient times the construction of tunnels and underground spaces has been a big challenge for engineers. This challenge is even greater if the underground spaces are constructed in faulted and heterogeneous rock mass of low strength and of high deformability. Although a lot of time and money have been spent recently in the design stage to establish a reliable and accurate geological model of the rock mass on the site of a future project, inconvenient geological surprises still occur. To minimize the risk of such situations during the construction of tunnels and other underground structures according to conventional tunnelling method (often also referred to as shotcrete method or NATM), the observational approach was introduced already by Rabcewicz (1965) and Peck (1969) and has been later on widely accepted as its integral part (Vavrovsky et al, 1987; Schubert et al, 2003).

Evaluation and interpretation of the monitoring data enable the verification of the design parameters, quality control, optimization of the construction and observation of the rock mass response to the tunnel excavation (Schubert et al, 2003). In case of construction of underground structures the observational approach consists of geological and geotechnical monitoring.

Geological monitoring typically includes geological drafts of the excavation faces produced by site geologist, often in a very limited time and unpleasant working conditions. These face logs supplement the geological model with interpolation and extrapolation of acquired data to the surrounding rock mass. However, in last decade tremendous advance has been achieved in various techniques and technologies for collecting information about rock mass using remote sensing photogrammetric and/or laser methods, such as high-resolution cameras (Gaich et al, 2006) or laser scanners, for producing digital 3D surfaces and for rock mass characterization like identification of joint spacing, dip directions, strike, etc. (Tonon, 2006).

In the last two decades really fast development has also occurred in the area of geotechnical monitoring. Several methods are available nowadays to observe the underground structure response due to the stress redistribution around an opening, caused by its excavation (Kavvadas, 2003). The response of the underground structure can be monitored using geodetic and/or geotechnical methods. Geodetic methods like terrestrial laser scanning and 3D total station measurements are used for monitoring the convergence of the circumference of the underground structure and the surface above tunnels in absolute coordinates, while the geotechnical methods enable recording of relative displacements in the surrounding rock (Kontogianni, 2005) and strains and/or stresses in the rock and in structural elements.

Different geotechnical methods allow measurements of the axial forces in rock bolts (Kavvadas, 2003), measurements of the displacements of the surrounding rock mass with single- and multi-point extensometers (Kavvadas, 2003), measurements of the radial and tangential stress state within the tunnel lining and/or on the interface between ground and tunnel lining with pressure cells (*DGSI*), measurements of the horizontal rock mass movements with vertical inclinometers when a shallow tunnel is constructed, to mention only the most common methods. For mainly research purposes some other geotechnical methods have been applied: horizontal inclinometer, installed in a pipe roof for measuring the displacements ahead of the tunnel face (Volkmann et al, 2005), vertical multi-point extensometer installed from the surface to the tunnel crown to investigate the distribution of the displacements to the surface, sliding micrometers, chain deflectometers (Kavvadas, 2003), etc. Geotechnical methods usually allow monitoring of the underground structure - rock mass response out of the excavated cross section.

For a long time the only geodetic method used in underground works was the steel convergence tape for measuring the convergences of the tunnel circumference. The accuracy of such measurements can be very high (±0.3 to 0.5 mm) in optimum measuring conditions, but in most cases it turned out to be much lower (Steindorfer, 1998). Comparison of several consecutive measurements offered limited information about the tunnel response, since only relative distances from one observation point to another in a certain cross section were obtained. Deviatoric behaviour could only be detected.

An important advance has been achieved with absolute displacement monitoring. Improvements in the surveying instruments and techniques as well as the computer software allow the determination of absolute position of each measuring point in real time, enabling to track its movements in space.

A lot of effort has been devoted in the last few years to terrestrial laser scanning that allows monitoring of the entire contour of an opening, but lacks accuracy. Due to uneven surface of the lining (usually shotcrete) the accuracy is in the range of a few centimetres and usually does not satisfy the accuracy requirements. However, the advantage of recording the absolute position of a very large number of points sometimes outweighs relatively low accuracy of individual points. With further development of equipment and software tools it is believed that the accuracy of laser scanning will be significantly improved.

In comparison to laser scanning the 3D geodetic measurements of the optical reflector targets using electronic tachymeters with integrated distance measurement give information on the underground structure response in selected points only. General accuracy of this method is rather higher if compared to laser scanning and is in the range of a few millimetres (Kavvadas, 2003), depending on the accuracy of the applied geodetic instrument, the type and the distance to the reflectors (Kontogianni, 2007) and the conditions on the site (presence of dust in the area, the size of an opening, the length of tunnel). The number of the targets that are mounted on the primary lining in each of the measuring sections and the distances between consecutive measuring sections depend on the geological conditions and the size of an opening; typical distance between measuring sections is 1-2 tunnel diameters (Rabensteiner, 1996). Due to high accuracy the systematic monitoring of the absolute displacements with total station geodetic instruments have become an everyday practice at construction sites around the world.

To gain as much information from the displacement monitoring data as possible, several plots are used for graphical representation, enabling the evaluation of the tunnel – rock mass response and estimation of the rock mass structure in the vicinity of excavated section (Schubert et al, 2003). The radial (e.g. vertical and horizontal) displacements are most commonly used for the assessment of the

tunnel behaviour due to the well established relationships between convergence and face advance (Guenot et al, 1985). An increased deformation rate of the tunnel circumference is expected within the first few days after the excavation of the observed cross section. With further face advance the displacements increments converge to zero and increase again in the influence area ahead of the face of the next excavation stage (bench, invert). The stress changes induced by tunnel excavation and subsequent deformations occur in the surrounding rock mass, rapidly attenuating at a distance of 2-3D (D = tunnel diameter), sometimes to 4D along the tunnel axis (Kontogianni, 2005). Using analytical functions ((Guenot et al, 1985; Barlow, 1986; modifications by Sellner (2000)) the radial displacements can be reliably anticipated and modelled. The magnitude and the shape of the deformation curve can even be predicted in advance for the sections to be excavated using special computer codes (Sellner, 2000). Unlike radial displacements, longitudinal displacements were disregarded for a long time in the interpretation of monitoring data, but have been gaining more and more attention since findings of Schubert, as they allow prediction of the rock mass conditions well ahead of the face (Schubert et al, 2002; Schubert et al, 2005).

In last two decades a more extensive use of underground space has started also in Slovenia. The largest portion of the underground structures represent tunnels on the motorway network. Apart from motorway tunnels only some hydro tunnels and a single railway tunnel were constructed. Repository for permanent nuclear waste disposal, repository for natural gas and a number of railway tunnels are at the moment in the design stage.

Since 1990 and especially since 1994 when the National Motorway Construction Programme was implemented, a large number of tunnels have been constructed on Slovenia's motorway network (more than 15 km of double-tube tunnels and one single-tube tunnel with the length of approximately 250 m). The majority of these tunnels are situated in fair to good rock (in limestone and flysch or flysch-like formations). Construction in these rock formations is less demanding due to minor rock mass pressures onto the primary lining. In general, only minor convergences occurred; larger displacements were limited to some fault zones or zones of weathered material. On the other hand some of the tunnels (Trojane, Golovec, V Zideh and Debeli hrib tunnels, partly Karavanke and Jasovnik tunnels) were constructed or are currently under construction (the Šentvid tunnel) in clastic soft rock mass of Permian and Carboniferous age, where considerable rock mass pressures, large convergences, overbreaks and instability of the slopes above the tunnel as well the instability of face caused difficulties during tunnelling. In these projects it was almost impossible to establish a reliable geological model of the area of future tunnel prior to construction, since such rock mass is densely

foliated and due to intensive tectonics of the area folded to a large extent. The presented circumstances significantly affected the excavation progress and final costs of the tunnel.

Monitoring data that were collected during construction of these projects provides invaluable experience for future projects in similar ground conditions and should be therefore properly stored and analyzed.

1.1 Scope of work

The monitoring of absolute 3D displacements of tunnel linings in Slovenia started in 1997 with the construction of the Golovec tunnel. Monitoring data from the tunnels, where the 3D displacements of the targets were continuously recorded, were collected and arranged in the database in the framework of this thesis together with face logs. A short description of tunnel projects important for this work is given in Chapter 2.

A computer code Predor (means Tunnel in Slovene) was developed for managing these data and enables different graphical outputs and analyses. Later on the code was upgraded with an automatic system for handling of the incoming data from construction sites and for the preparation of graphical reports. The system has already been successfully applied in three recently constructed tunnels on the motorway network. A short overview of software capabilities and experiences with automatic system is presented in Chapter 3.

Monitoring data of tunnels in soft foliated rock mass were systematically studied using Predor code and compared to geological structure to identify characteristic deformation patterns. Back calculations were performed to find the most suitable numerical description of material behaviour together with material parameters for future projects in similar rock mass conditions. Investigation was performed for the radial and longitudinal displacements of the primary lining as well as displacements of the surface. According to reviewed literature, unexpected longitudinal displacement pattern that was observed under declined overburden and in particular geological conditions is described in Chapter 4 together with other analyses of the tunnel response in anisotropic rock mass conditions.

The Šentvid tunnel comprises the junction of a twin tube motorway tunnel and two ramp tunnels in soft foliated rock mass. In the design stage an exploratory tunnel was constructed to locate the junctions. During the construction of the main motorway tunnel, 3D displacements of the primary lining of the exploratory tunnel were recorded in 8-month period just ahead of the main tunnel. No reports of any similar experiments have been found so far. Extensive information about the

experiment, discussion about the results and numerical analyses of the observed phenomena are given in Chapter 5.

During the analysis of the longitudinal displacements the dependence of the magnitude of final measured displacements and the portion of pre-displacements on the relative discontinuity orientation to the tunnel axis was observed. A large number of 3D numerical analyses was performed to investigate this dependence. Results and practical application of fitting the particular analytical function to the measured displacements in the anisotropic rock using calculated parameters are presented in Chapter 6.

The most important findings and observations of performed studies are exposed again and summarized in concluding Chapter 7.

2.0 Tunnel projects in Slovenia

To provide an adequate and efficient road system, improve road safety, ensure the integration with the broader European area and to achieve more balanced economic development of all Slovenian regions, in 1994 an accelerated construction of motorways started with the implementation of the National Motorway Construction Programme. Since then 472 kilometres of new two-lane and four-lane motorways and highways have been constructed and given over to the traffic (*DARS, Built motorways and expressways*). Due to diversified topography of Slovenia (Fig. 2-1) several tunnels are situated or planned on the motorway and highway network. 15 two-lane tunnels with the total length of 30 kilometres have already been constructed, while 4 tunnels with the total length of 3.1 km are currently under construction and will be given over to traffic presumably in 2009. Some others are in the design or tender stage.

The construction of all motorway tunnels in Slovenia followed the principles of the New Austrian Tunnelling Method (NATM). The 3D displacement measurements of the primary lining started with the Golovec tunnel project on the eastern bypass of Ljubljana in 1997 and since then a continuous 3D displacement monitoring have become an everyday practice on tunnel construction sites in Slovenia.

Figure 2-1. Relief map of Slovenia with motorway and highway network.

Slika 2-1. Reliefna karta Slovenije z vrisanim avtocestnim omrežjem.

In order to facilitate the analyses of valuable monitoring data from completed projects to serve as an important experience for future projects, the 3D displacements data from all tunnel projects with considerable displacements, e.g. in soft rock mass, that were constructed on the Slovenian motorway

network after the commencement of the 3D displacement monitoring were collected and arranged in a database. For the moment the database comprises monitoring data from 13 tunnel projects, situated in different geological formations. Some of the tunnels are situated in stable rock mass conditions with only minor measured displacements of the primary lining. On the other hand, some projects were executed in unfavourable tunnelling conditions where large convergences were measured, roof collapses occurred occasionally, considerable influence to the surface was monitored and in one of the projects adjacent infrastructure in the influence area above the tunnel was damaged.

2.1 Tunnel projects in database

Tunnels, constructed in fair geological conditions that are included in the database, are (arranged in an alphabetical order):

Table 2-1. Data about tunnel projects in fair geological conditions.

Preglednica 2-1. Podatki o predorih, grajenih v dobrih geološko-geotehničnih pogojih.

tunnel	type	length [m]	construction time	No. of MS	avg. dist. between MS	targets/MS TH+bench
Barnica	2 lanes 2 tubes	254 + 283	2007 - 2009	34	15.8	7 5 + 2
Cenkova	2 lanes 2 tubes gallery	353 + 353 + 353	2007 - 2009	53 (tun.) + 27(gal.)	13.3 (tun.) 13.1 (gal.)	5 (tun.) 3 + 2 3 (gal.)
Dekani	2 lanes 2 tubes	2148 + 2112	2002 - 2004	168	25.4	5 3 + 2
Leščevje	2 lanes 2 tubes	352 + 351	2008 - 2009	36	19.5	5 3 + 2
Ljubno	3 lanes 1 tube	235	2006 - 2007	23	10.2	5 3 + 2
Tabor	2 lanes 2 tubes	497 + 648	2007 - 2009	64	17.9	7 5 + 2
Vodole	2 lanes 2 tubes gallery	219 + 221 + 220	2007 - 2009	55 (tun.) + 24 (gal.)	8.0 (tun.) 9.2 (gal.)	5 (tun.) 3 + 2 3 (gal.)

- *The Barnica tunnel and the Tabor tunnel*

These are double tube two-lane tunnels situated on the Razdrto – Vipava expressway and run with shallow overburden (maximum of 53 m above the Barnica tunnel and 64 m above the Tabor tunnel) through Flysch and slope debris formations. Both tunnels are situated very close together. The length of the mined tunnels is 254 m of the left tube and 283 of the right tube of the Barnica tunnel, and 497

m and 648 m of the left and the right tube, respectively, of the Tabor tunnel. The construction of the tunnels started in 2007 and they will be given over to the traffic in 2009. Since they are constructed in fair conditions, no major convergences were measured on 34 measuring cross sections in the Barnica tunnel and 64 measuring sections in the Tabor tunnel. Each measuring section comprises 7 targets.

- *The Cenkova tunnel*

It is located on the A5 motorway in north-eastern Slovenia from Maribor to Pince (border to Hungary). The geological situation was characterized by Miocene clastic sediments, consisting mainly of clays, sands, gravels and poorly litified sandy marls of grey and brown colour. Due to traffic reasons both tubes of the twin tube two-lane tunnel are situated next to each other. To reduce the influence of the second tube construction on the primarily excavated tube, a 353 m long central gallery was constructed first in order to form a concrete central pillar between both tubes. The excavation of the main tunnel tubes started in April 2007 and took one year. 53 measuring sections including 5 targets were installed in 353 m long main motorway tunnel and further 27 sections with 3 targets in the central gallery.

- *The Dekani tunnel*

It is a double tube two-lane tunnel on the A1 motorway from Ljubljana to Koper and is situated near Koper. The geological situation of the tunnel is characterised by Eocene clastic formations with characteristic alternation of marl, sandstone and calcarenite (Flysch) (Beguš et al, 2003). The length of the excavated section of the left and the right tube is 2148 m and 2112 m, respectively (Beguš et al, 2004). The construction started in 2002 and was completed in 2004. The excavation of both tubes proceeded from both portals simultaneously. 168 measuring cross sections were installed with 5 targets.

- *The Leščevje tunnel*

The double tube two-lane tunnel runs through fissured micritic limestone of grey colour with intercalations of clayey sand in minor faults. It is situated on the A2 Ljubljana – Novo mesto motorway near Trebnje. The length of the left tube is 352 m and of the right tube 351 m. The construction started in 2008 and the tunnel will be put into operation presumably in 2010. 5 targets were installed in each of the 36 measuring cross sections.

- *The Ljubno tunnel*

Former A2 Karavanke – Ljubljana expressway with bi-directional traffic was expanded to motorway. Therefore an additional 235 m long tube with three lanes was constructed under low overburden (maximum of 30 m) in stiff overconsolidated Oligocene silt called “sivica”. The tunnel driving started in July 2006 and was finished in December 2006. 23 measuring sections were located inside the tunnel

with 5 measuring points. The existing tube will be widened from a two to a three-lane tunnel by the end of 2010.

- The Vodole tunnel

It is situated on the A1 Ljubljana-Maribor motorway and forms part of the Maribor highway. The alignment runs with shallow overburden through a variety of tertiary sediments (clayey to silty marlstone with intercalations of fine to medium grained sandstone). Like in the case of the Cenkova tunnel, the two tunnel tubes of the Vodole tunnel have a common central pillar that was constructed in the 220 m long central gallery. The excavation of the central gallery started in November 2007 and took 3 months to complete. The excavation of both tubes (length of the left tube is 219 m and 221 m of the right tube) started in March after concreting the central pillar and finished in August 2008. 24 measuring sections with 5 targets were installed in the central gallery and altogether 55 measuring sections with 7 points in the tunnel.

The displacements of the described tunnel projects were inspected and compared to the geological model. Since these tunnels are not constructed in soft and foliated rock mass, the analysis and the interpretation of the monitoring data is not included in this work. Nevertheless, all displacement measurements from these projects are included in the database and available for analysis.

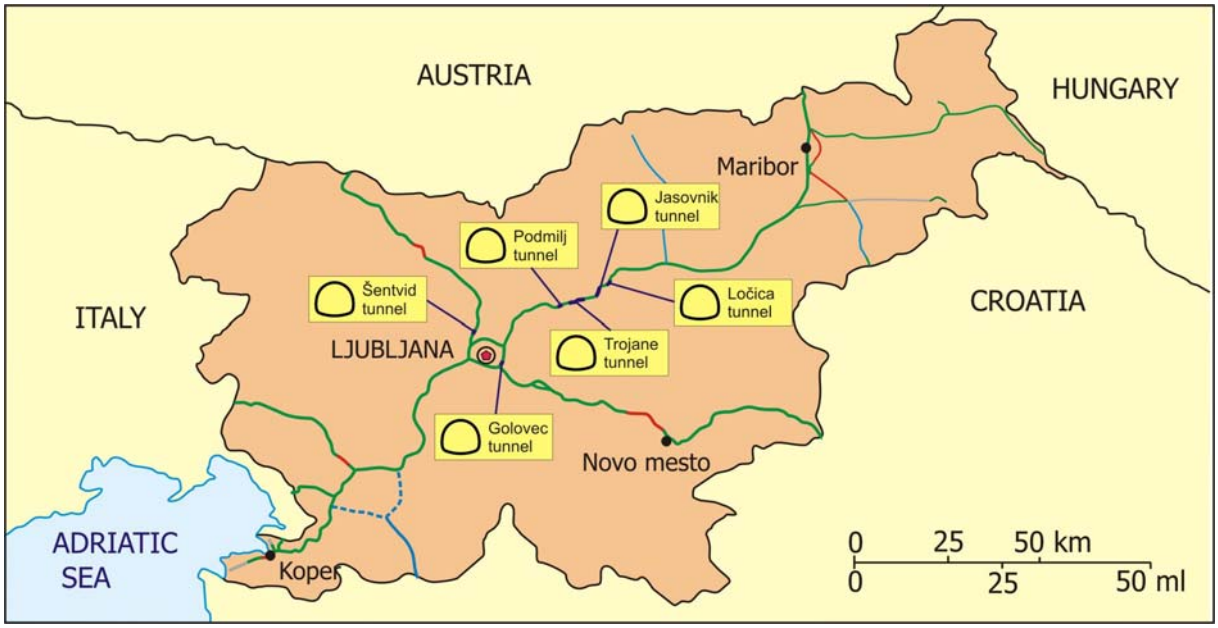

Figure 2-2. Position of the Trojane, Šentvid, Golovec, Jasovnik, Ločica and Podmilj tunnels on the motorway network in Slovenia.

Slika 2-2. Položaj predorov Trojane, Šentvid, Golovec, Jasovnik, Ločica in Podmilj na slovenskem avtocestnem omrežju.

A detailed analysis of the monitoring data and further numerical modelling was performed for the following six tunnels: the Trojane tunnel, the Šentvid tunnel, the Golovec tunnel, the Jasovnik tunnel, the Ločica tunnel and the Podmilj tunnel. The locations of these tunnels on the Slovenian motorway network are shown in Fig. 2-2.

According to the macro tectonic division of Slovenia, the area of the six abovementioned tunnels belongs to Internal Dinarides and Southern Alps (Placer, 1999a). From the structural point of view the area belongs to Sava folds, situated in the triangle named Sava compressive wedge between the Periadriatic tectonic zone, the Idrija tectonic zone and the Mid-Hungarian tectonic zone (Placer, 1999b). Older rock mass of Permian and Carboniferous age is usually found in anticlines, while the rock mass of tertiary age is found in synclines. In between is the rock mass of different ages (predominantly Triassic formation, including some Jurassic and Cretaceous formations). In geological history these Mesozoic rocks were thrusted over older Perm-Carboniferous rock mass. In later phase the area was cut with faults in E-W and NW-SE (Dinaric) directions (Premru, 1974).

2.2 The Trojane tunnel

2.2.1 General information

The Trojane tunnel is nearly 3 km long (length of the northern tube is 2.840 m (2.812 m of excavated tunnel) and 2.931 m of the southern tube (2.850 m of excavated tunnel)) and is the longest two-lane double tube motorway tunnel in Slovenia. It is situated on the Slovenian A1 Maribor – Koper motorway that connects the capital city Ljubljana with Maribor, 2nd largest city in Slovenia (Fig. 2-2). Theoretical excavated cross section of the tunnel tube is 89 m^2 with equivalent tunnel diameter of 10 m. The distance between both tube axes is 40 m and reaches up to 75 meters under the Trojane village (Fig. 2-3). The overburden above the tunnel varies from 2 m in the Učak valley up to 140 m. The construction commenced on September 15, 2000 and was completed on March 25, 2004 (Schubert P. et al, 2005). The excavation proceeded from both portals in both tubes simultaneously. Lengths of excavated sections on each individual site are shown in Fig. 2-3.

The most demanding part of the project was the tunnel construction under the Trojane village with low overburden from 10 to 25 m (Fig. 2-4). The eastern part of the tunnel (section of approximately 500 m) was excavated under populated area, under main, regional and local roads and a regional gas pipeline. Several numerical analyses were performed to assess the influence of the tunnel construction on the surface (maximum calculated settlements up to 36 millimetres (Likar, 1999)) and to select appropriate support class (different types of SCC support classes according to ÖNORM B 2203 were used). Following the initial design, the construction of the northern tube caused only minor influence

on the above structures, while the excavation of the southern tube (in this section situated below a slope, deeping to south, in unfavourable geological conditions and less overburden) caused large settlements (up to 25 cm) and damages to adjacent structures (Logar et al, 2004; Likar et al, 2004a). The tunnelling was stopped and additional investigations and analyses were carried out to determine possible measures for limiting the influence of the tunnel construction. An extensive monitoring programme (Likar et al, 2004b) was established to enable proper and timely measures (vertical inclinometers (Štimulak et al, 2002), horizontal inclinometer above the tunnel crown (Volkmann et al, 2005), 3D measurements of the geodetic points in cross sections and along the tunnel axis, vertical and horizontal multiple point extensometers).

2.2.2 Rock mass description

The tunnel alignment is situated in the rock mass of Carboniferous age (about 280 million years old). The rock mass consists mainly of densely foliated soft claystone of dark grey to black colour and includes lenses of stiffer grey siltstone. Some more competent sandstone lenses were included locally (Fig. 2-4). Due to intensive tectonics the rock is folded. Several sub vertical to vertical fault zones up to several meters thick were mapped, filled with low-bearing and highly deformable gouge clay. The rock is locally weathered up to the depth of 15 m (Beguš et al, 2005). The general direction of the foliation is to the North, but can be locally chaotic due to tectonics. The foliation of the rock mass together with unfavourable dip angle of the layers affected the stability of the tunnel and the tunnelling conditions.

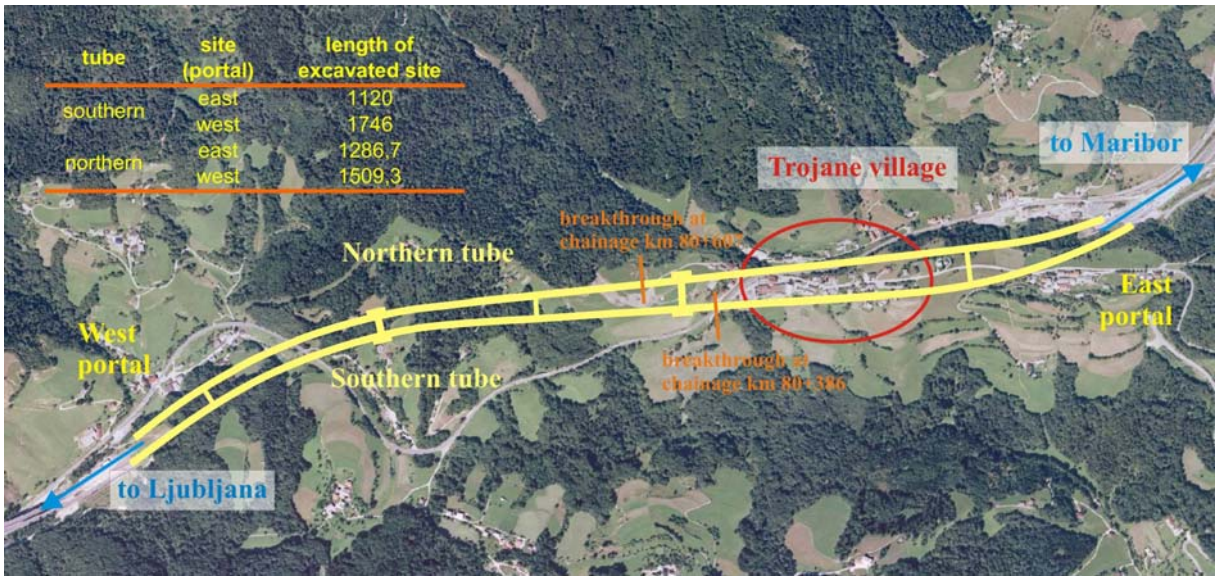

Figure 2-3. Layout of the Trojane tunnel.

Slika 2-3. Situacija predora Trojane.

The slopes above the tunnels are generally close to the limit equilibrium. These circumstances significantly influenced the tunnelling conditions under low overburden (eastern part). Consequently, the excavation affected the surface and existing nearby structures.

The majority of tunnelling conditions were classified in categories C3 (42%) and SCC of different types (under the populated area in eastern part - 36%), followed by C2 (12%) and PC (8%).

The GSI values were being assessed continuously during tunnelling (Štimulak et al, 2004). The majority of rock mass was assigned a GSI value between 20 and 25 with minimum and maximum value of 10 and 55, respectively.

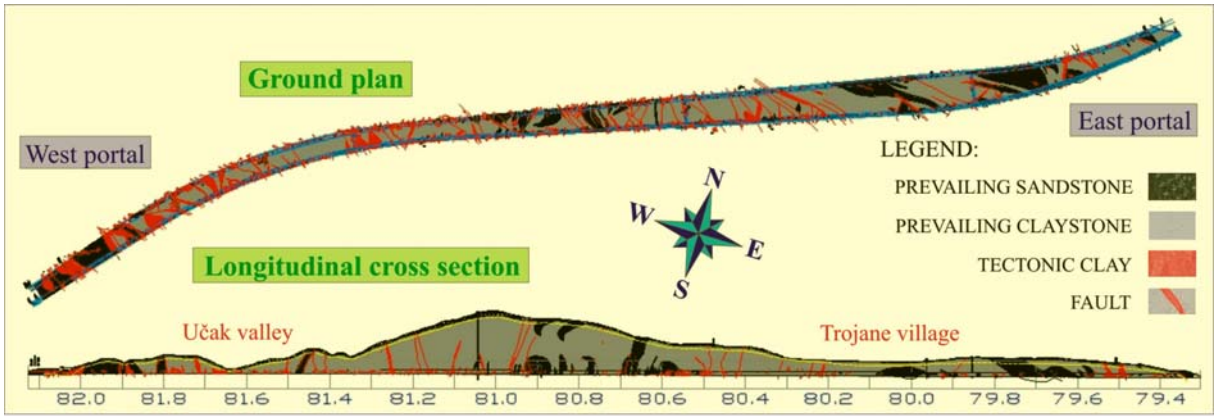

Figure 2-4. Geological ground plan and longitudinal cross section of the Trojane tunnel.

Slika 2-4. Vzdolžni geološki prerez in geološka situacija predora Trojane.

2.2.3 Monitoring programme

The 3D displacements of the primary lining were measured geodetically in sections that were placed on average each 14.6 m over the entire length of the tunnel (altogether 389 measuring cross sections – details are given in Table 2.2). Higher density of measuring sections in the east lot of the southern tube is due to previously described problems with tunnelling beneath the Trojane village. Five points were observed in each measuring section, three in the top heading and two on the bench sidewalls. Only in some sections in the parking niches 7 targets were installed.

Due to difficult geomorphologic conditions and tunnelling under regional and local roads, a regional gas pipeline and populated area, an extensive surface monitoring system was established in the mentioned parts. The 3D surface displacements were monitored along a considerable length of both tunnel axes, especially in the eastern part (88 points above the left tube in the total length of 1200 m and 66 points above the right tube in the total length of 1240 m – a detailed disposition is given in

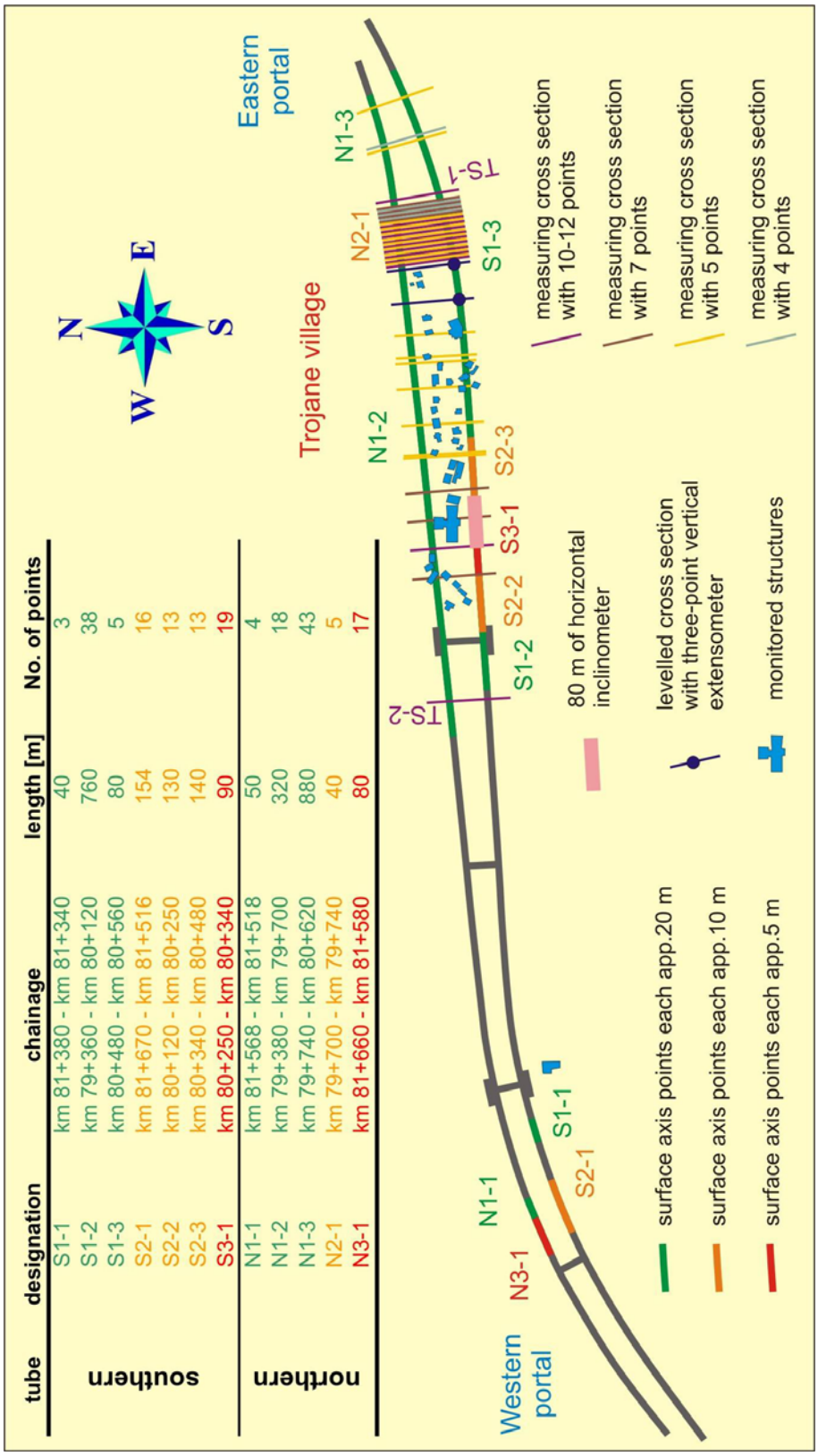

Figure 2-5. Scheme of surface monitoring at the Trojane tunnel.

Slika 2-5. Shematski prikaz površinskega opazovanja nad predorom Trojane.

Fig. 2-5). A large number of surface cross sections were installed to observe the behaviour perpendicular to the tunnel axis (in total 43 cross sections with 4, 5, 7 or 10-12 points in each – location and number of points are shown in Fig. 2-5). Before driving the tunnel beneath the Trojane village, a large area above the tunnel tubes was monitored to define the influence area due to the tunnelling (25 cross sections at the mutual distance of 5 m, covering the total length of 120 m). Since no housing facilities are located in the western part of the tunnel alignment, only surface points in the axis of the tunnel in the Učak valley were monitored due to low overburden, covering a length of approximately 130 m.

Table 2-2. Number of measuring cross sections and lengths of the individual construction sites in the Trojane tunnel.

Preglednica 2-2. Število merskih profilov in dolžina izkopa na vsakem od napadnih mest v predoru Trojane.

tube	site (portal)	length of excavated section	No. of MS	average distance between MS
southern	east	1120	94	11.,9
	west	1746	111	15.7
northern	east	1286.7	81	15.9
	west	1509.3	103	14.7

All structures in the expected influence area of the tunnel (40 in the eastern part, e.g. in the Trojane village and 1 in western part just above the Učak valley – the monitored structures are shown in Fig. 2-5) were equipped with at least three points that were levelled when the tunnel was driven beneath (Štimulak et al, 2004).

To understand better the influence area of the tunnel, especially the disposition of the displacements from the tunnel to the surface, a three-point vertical extensometer supplemented with a cross section of five levelled targets was installed close to Garni hotel in the eastern part, as shown in Fig. 2-5 (Štimulak et al, 2002).

In the southern tube of the Trojane tunnel, beneath the famous tourist restaurant, an 80 m section was equipped with a horizontal inclinometer system to evaluate the utilization of the pipe roof system (Likar et al, 2004c). An in-place horizontal chain inclinometer was installed at the beginning of each pipe roof field and the measurements were taken in 1 minute intervals. The onset of the chain inclinometer was measured to track absolute position and obtain absolute instead of relative displacements (Likar et al, 2004c).

2.3 The Šentvid tunnel

2.3.1 General information

The Šentvid tunnel system links the Slovenian A2 Karavanke-Ljubljana motorway to the Ljubljana ring motorway. Regarding the construction method, the tunnel project is divided in two parts. The northern part was constructed with cut&cover method in 1984 during the construction of the Ljubljana-Kranj motorway. The total length of the cut&cover section at that time was 247 m (*DARS, Predori*) and it consisted of 4 two-lane tunnels (2 ramp tunnels for the connection of the Celovška street to the motorway and 2 for the future tunnel under the Šentvid hill). During the preparatory works for the Šentvid tunnel, in spring 2004 the two tunnels of the cut&cover section were extended under the Celovška street to the foothill, where the northern construction site was situated. The total length of the cut&cover section is at present 423 m, as seen in Fig. 2-6.

Figure 2-6. Layout of the Šentvid tunnel.

Slika 2-6. Situacija predora Šentvid.

The initial design in the early 90's foresaw only a partial connection of the Celovška street to the motorway using the existing ramp tunnels in the cover section to the direction Kranj (Žigon et al, 2006a). The reason was the uncertainty of the experts that the construction of a full connection in the

Šentvid hill (with the knowledge and the technology of that time) was feasible. This would be the only junction without a full connection of the city to the motorway. Since the traffic situation in this part of the city is among the most critical ones in Slovenia and it will aggravate with the new residential areas, the full connection is crucial.

In 2003 several variants were studied to provide full junction (four 2-lane tunnels with junction at the southern portal where enough space is available; two 2-lane tunnels and a 2-lane city tunnel with bidirectional traffic – junction at the southern portal; two 2-lane motorway tunnels and two connecting tunnels from the northern portal to the merging cavern and a 3-lane motorway further to the south (Pulko, 2004)). They were compared according to economical aspects, traffic safety and construction aspects. The variant with merging caverns was selected as the most appropriate and feasible solution.

The design foresaw two large merging caverns with a cross section of more than 300 m^2 (span of 24 m and height of 16 m). Financial risks and possible schedule delay risks connected to the construction of the underground structure of this size on the basis of the geological model of that time would be unacceptable for the Client. To obtain more reliable geological model and material parameters of the rock mass and consequently to determine the most favourable positions of the future merging caverns in terms of geological and geotechnical criteria, an exploratory tunnel with extensive geological and geotechnical testing program was suggested by a group of experts (Žigon et al, 2004).

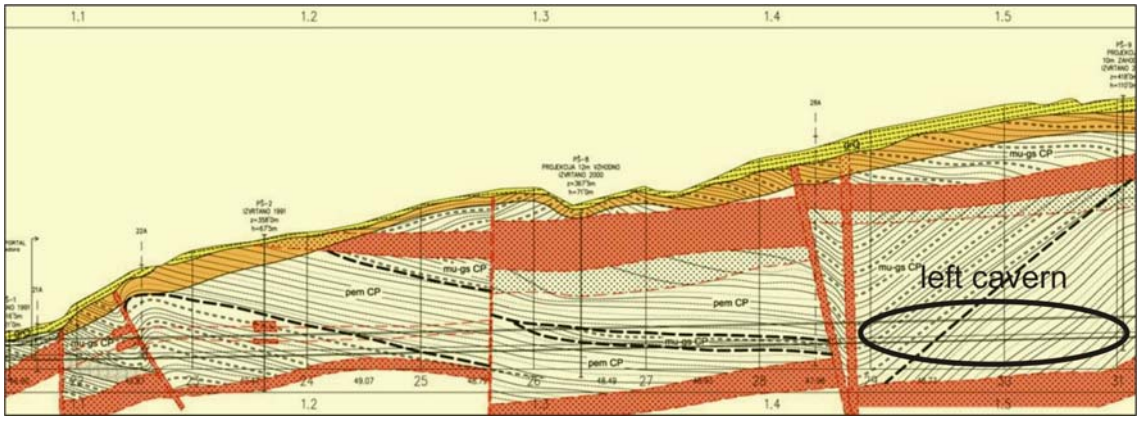

Figure 2-7. Initial geological interpretation in longitudinal section of the Šentvid hill before the exploratory tunnel was constructed (left tube, north part).

Slika 2-7. Vzdolžni geološki prerez Šentviškega hriba pred gradnjo raziskovalnega rova (leva cev, severni del).

The initial design of the tunnel alignment with the merging caverns was positioned according to the geological model at that time (Fig. 2-7 - position of the left cavern is marked) and was based on core

drilling and geological mapping. Predicted positions of the right and left cavern were 480 m and 369 m (reserve position 453 m (Črepinšek, 2006)), respectively, from northern portal as shown in Fig. 2-8. The construction of the exploratory tunnel according to the principles of the NATM (application of the shotcrete, steel arches, wire mesh and rock bolting) started in May 2004 with an access gallery from the northern portal towards the axis of the future right tunnel tube. After approximately 90 m the exploration gallery entered the future right tube and continued along the axis towards south. To accelerate the construction the installation of the wire meshes and rock bolts was omitted (except in fault zones and at the enlargements) and only micro reinforced shotcrete was used.

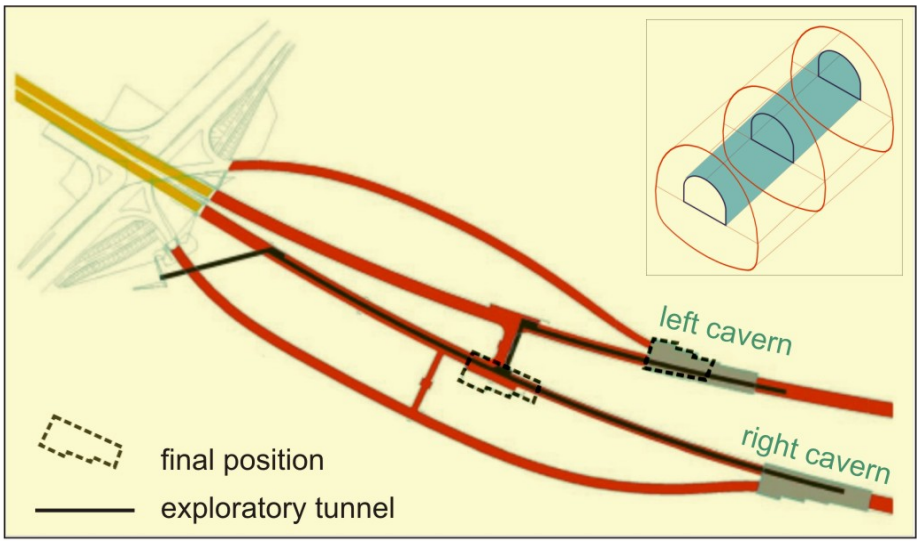

Figure 2-8. Initial tunnel alignment with the position of both caverns and exploratory tunnel alignment (Jemec, 2006).

Slika 2-8. Prvoten potek trase s prikazom položaja obeh kavern in trase raziskovalnega rova (Jemec, 2006).

At a distance of 239 m from the northern portal a block of firm sandstone was encountered (Črepinšek, 2006). Further analysis confirmed the location of the right cavern at this chainage. Afterwards excavation continued through a 40 m long cross passage to the left tube and followed the left tube axis for approximately 150 m to reach the reserve position for the left merging cavern. Based on the measured displacements, mapped lithological units, the degree of fracturing and the degree of tectonisation the decision for the position of the left merging cavern at a distance of 369 m from the northern portal was taken. The total length of the constructed exploration gallery was 655 m (Table in Fig. 2-9) and was completed in December 2004. Geotechnical testing finished in February 2005. The initially foreseen length of the exploration gallery was 800 m. Its alignment was not precisely defined

with the design and it depended on the actual geological and geotechnical conditions of the rock mass (Žigon et al, 2006b).

Regular cross section of the exploratory tunnel (13 m^2 as seen in Fig. 2-9) depended on the size of the tunnelling equipment (Žigon et al, 2004) for excavation, bolt drilling, dense shotcrete application and transport of the excavated material. Three larger openings (in both future caverns and at the cross passage in the right tube, as plotted in Fig. 2-9) were executed to enable the extensive geotechnical testing of the rock mass and core drilling. Position of the bottom of the exploratory tunnel in the cross section is on the level of the top heading excavation (Fig. 2-8). The tunnel alignment raises from the northern portal towards the southern. Maximum overburden reaches 115 m.

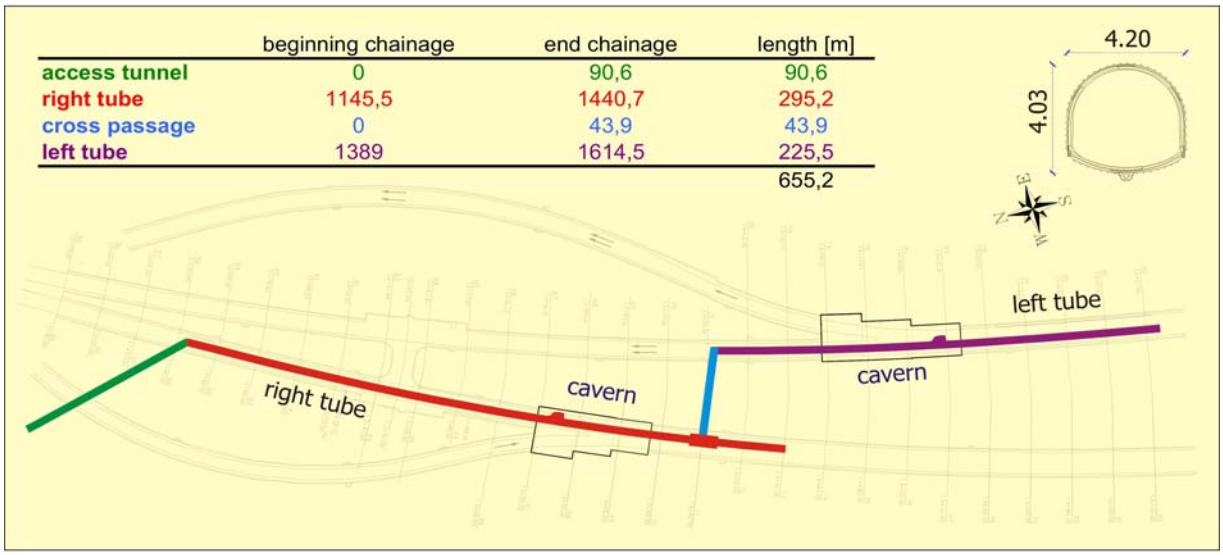

Figure 2-9. Executed alignment and cross section of the exploratory tunnel.

Slika 2-9. Izvedena trasa raziskovalnega rova ter njegov prečni prerez.

The exploratory tunnel allowed the establishment of a more reliable geological model (Fig. 2-10) and enabled the in-situ geotechnical testing (core drilling, geophysical surveys, extensometers). The geodetic measurements of the 3D displacements during the exploratory tunnel construction improved the knowledge about the rock mass behaviour and its response to the tunnel excavation.

Since the excavation of the exploration gallery exceeded the determined time schedule (to accelerate the construction from August 2004 onwards the micro-fibre reinforced shotcrete was applied instead of wire mesh and rock bolting), the design and tender of the motorway tunnel system started before the completion of the exploratory tunnel. The position of the right cavern was already known and the feasibility report completed, therefore the tender foresaw a 2-lane tunnel for the left

tube and a connection in the tunnel for the right tube. A special amendment was inserted in the tender that the tunnel alignment can change during the construction if the left cavern was feasible (Popit et al, 2006). The construction of the motorway tunnel started in December 2004 from the northern portal.

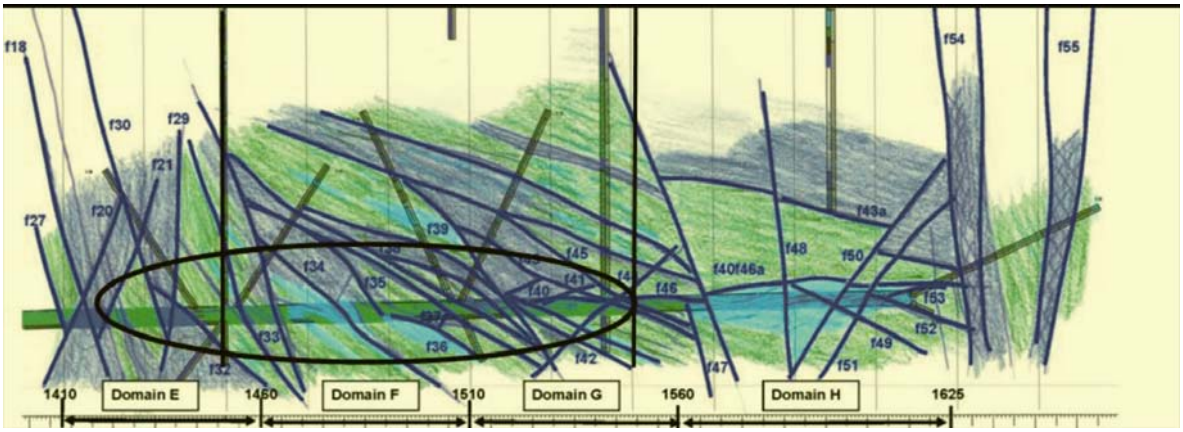

Figure 2-10. Geological interpretation in longitudinal section of the Šentvid hill in the area of the left cavern after the excavation of the exploratory tunnel.

Slika 2-10. Vzdolžni geološki prerez Šentviškega hriba na območju leve kaverne glede na podatke, pridobljene z gradnjo raziskovalnega rova.

On the basis of the findings from the exploratory tunnel as input parameters for 3D numerical calculations a feasibility study (Žigon et al, 2005) in March 2005 confirmed that the construction of both caverns in the determined sections was feasible and the expected convergences could be controlled with economically reasonable primary support. The layout of the final alignment was eventually determined and is shown in Fig. 2-11. The length of the left tube is 1036 m and of the right tube 1061.5 m. Lengths and cross section sizes of the connecting ramps, 2-lane and 3-lane tunnels and caverns (Črepinšek, 2006) are given in the table in Fig. 2-11.

Due to the possibility of reactivation of a fossil landslide in poor ground conditions above the southern portal (Žigon et al, 2004), the preparatory works for the portal structures avoided the deep cuts. Large diameter piles were constructed on both sides of each 3 lane tunnel tube in the length of approximately 100 m along the axis and a thin soil cover above the tunnel was increased in thickness using cement stabilisation. The excavation from the southern portal started in June 2005.

The breakthrough of the right tube, where more favourable geological conditions were encountered, was in December 2006. In June 2007 the excavation works were completed also in the left tube. Due to the time delay in preparation of the documentation for the connecting tunnels, only the motorway tunnel was given over to traffic in July 2008. Before concreting the inner lining of the

cavern, 80 m of the ramp tunnels were excavated from the cavern to the northern portal in order to prevent any larger influence on the motorway tunnel during the construction of ramp tunnels. Ramp tunnels with a junction on the Celovška street are currently under construction and will be operational presumably in the beginning of 2010.

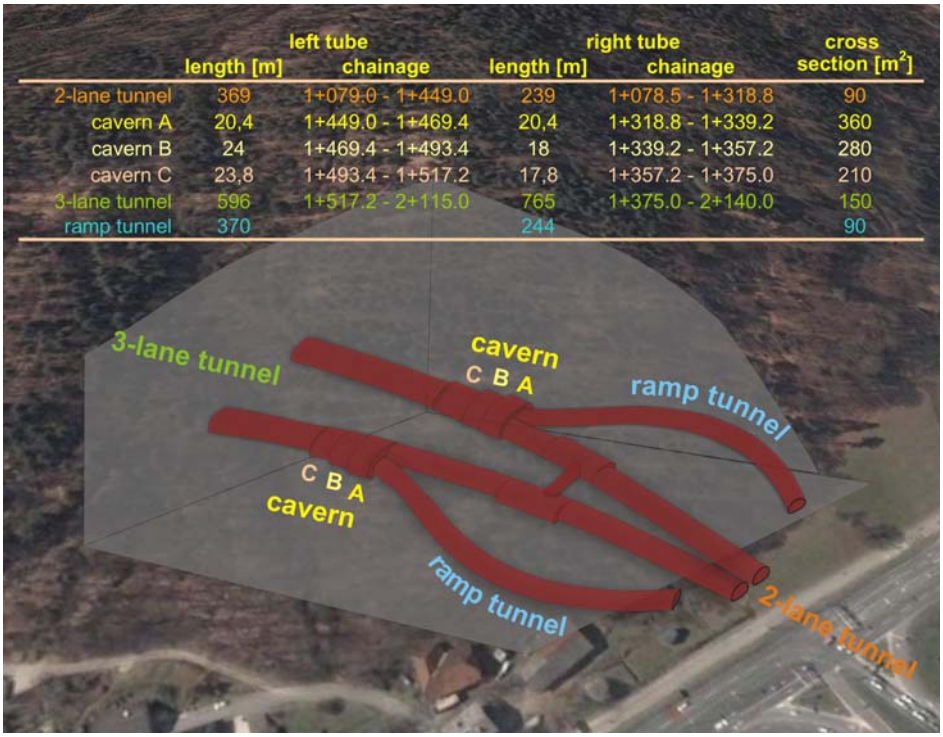

Figure 2-11. Final scheme of the underground junction of the Šentvid tunnel.

Slika 2-11. Izvedbena shema podzemnega vozlišča v predoru Šentvid.

Some new, heavy duty types of support were used at the Šentvid tunnel for the first time in Slovenia. Special yielding elements were used to avoid possible excessive deformations and consequently cracking of the shotcrete in the caverns, where the remedial measures would be almost impossible or at least very costly and time consuming due to the large dimensions. Lining stress controllers (LSC) make the lining more flexible, allow controlled development of loads in the lining and at the same time provide support resistance against deformation which was not possible in case of just leaving gaps between the segments (Schubert, 1996; Schubert et al, 1998). A special type of self-drilling anchors (IBI) was used that allow re-grouting of the anchor (*ALWAG, Self drilling anchors*) if the contact between the anchor and the rock mass is damaged due to excessive deformation. Another advantage compared to IBO anchor is full bonding with the rock mass along the total length of the anchor, which was proven at the test field in the Šentvid tunnel (Črepinšek, 2006).

Beside useful information that contributed to the successful execution of the main motorway tunnel, the exploration gallery enabled the observations of the rock mass – support system behaviour ahead of the face of the main tunnel during its execution. Details of this experiment and results are given in Chapter 5.

2.3.2 Rock mass description

The Šentvid tunnel alignment passes through densely foliated clastic sedimentary rocks of carboniferous age, mainly sandstones, siltstones and clayey slates. The region has undergone intense tectonic deformations, presumably during several deformation phases. Due to intensive tectonics the rock is folded, fault zones are up to several meters thick and consist mainly of gouge clay. The rock mass itself is very heterogeneous and anisotropic (Fig. 2-12).

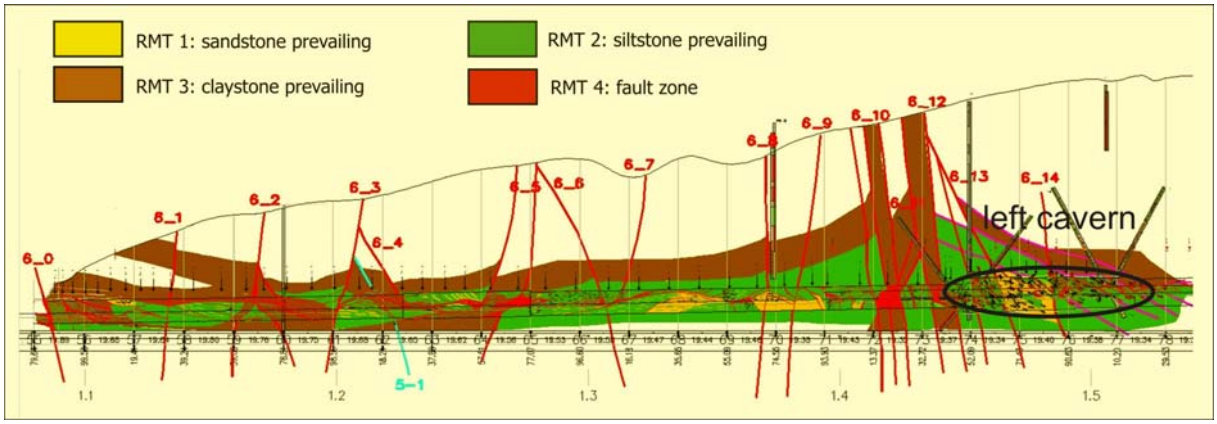

Figure 2-12. Geological interpretation in longitudinal section of the Šentvid hill after the excavation of the motorway tunnel – left tube, northern part.

Slika 2-12. Končni vzdolžni geološki prerez Šentviškega hriba po izgradnji avtocestnega predora - leva cev, severni del.

The quantity of water that percolates from the surface into the tunnel tube is small. Water appears mainly in fault zones. Together with deformations that occur due to tunnelling this water causes the increase of the water content along the foliation and consequently the decrease of rock suction, which affects mechanical properties of the rock mass and impairs the tunnelling conditions in the vicinity of the fault zones. Several smaller overbreaks occurred in such conditions.

Encountered tunnelling conditions for the Šentvid tunnel system were in the range from fair to very poor (Čadež et al, 2004a).

2.3.3 Monitoring programme

Very complex geology and geometry of the Šentvid tunnel demanded a comprehensive monitoring scheme to monitor properly the tunnel response. The density of the measuring sections and the number of monitored targets depended primarily on the rock mass conditions as well as on the geometry of cross section. Thus, the highest density was in both caverns, where an average distance between measuring sections amounted to 5-6 m and each of the measuring sections comprised 10 targets (Table 2.3). In two and three lane tunnel 7 and 9 targets were monitored, respectively. The density of measuring sections was also higher compared to the Trojane tunnel.

Table 2-3. Number of measuring cross sections and lengths of the individual construction sites in the Šentvid tunnel.

Preglednica 2-3. Number of measuring cross sections and lengths of the individual construction sites in the Trojane tunnel.

		No. of MS	No. of points	Section length	Average distance between MS
left tube	2-lane	35	7	321	9,2
	parking niche	6	9	48	8,0
	cavern A	4		20,4	5,1
	cavern B	4	10	24	6,0
	cavern C	4		23,8	6,0
	3-lane	59	9	596	10,1
right tube	2-lane	20	7	191	9,6
	parking niche	5	9	48	9,6
	cavern A	4		20,4	5,1
	cavern B	3	10	18	6,0
	cavern C	3		17,8	5,9
	3-lane	71	9	765	10,8

2.4 The Golovec tunnel

2.4.1 General information

The Golovec tunnel was the first three lane double tube motorway tunnel constructed in Slovenia. It forms a part of Ljubljana motorway ring and provides a connection from northern Slovenia to southwest (Koper) and southeast (Novo mesto) – Fig. 2-13. Theoretical tunnel cross section is 148 m^2 with the height of 10.5 m and the span of 14.1 m. The length of the excavated section in western and eastern tunnel tube is 578 and 545 m, respectively. The distance between the axes of both tubes is about 50 m and is nearly constant. The overburden above the tunnel reaches up to 80 m.

The preparatory works for the portal cuttings, which caused a large landslide at the southern portal, started in October 1995. A 10 to 15 m thick layer of weathered rock and soil started to move in the area of 20.000 m^2 (Popovič et al, 1998) and affected the portal area of the designed tunnel. On the basis of extensive ground investigation of the southern as well as northern slope, remedial measures for the landslide stabilization were undertaken to allow further works in the tunnel. After almost two years and significant modification of the original design by construction of heavy retaining structures and galleries at both portals the tunnel excavation itself started in the western tube in June 1997 from the southern portal only.

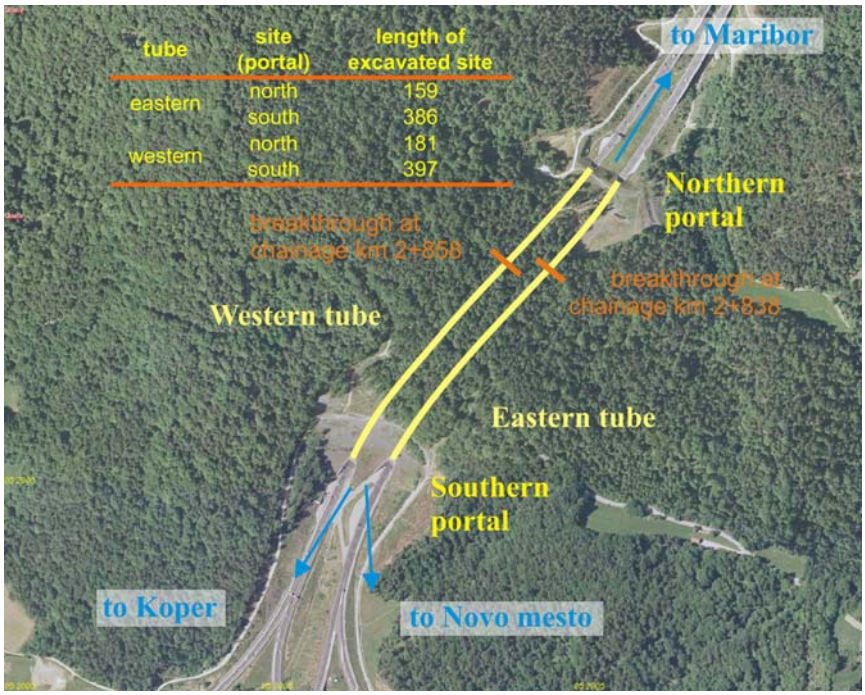

Figure 2-13. Layout of the Golovec tunnel.

Slika 2-13. Situacija predora Golovec.

Section close to southern portal was excavated in extremely weak and tectonically damaged claystone and significant deformation in the tunnel and on the surface was observed (Popovič et al, 1998). Since deformations exceeded tolerable values, some changes were introduced to the original design (use of pipe roof, temporary invert, maintaining face stability with bolts or supporting core, thicker primary lining, closing the support ring at closest distance from top heading face (Fifer et al, 2004)). These countermeasures allowed successful further excavation with reasonable advance rates. Following modified design, the excavation of the eastern tube started in March 1998. Due to the exceeded contractual deadline the excavation at the northern portals commenced in April 1998. The breakthrough of the western tube was in August 1998 and of the eastern tube in March 1999.

The Golovec tunnel was the first tunnel project in Slovenia where 3D geodetic displacement measurements of the primary lining were performed continuously.

2.4.2 Rock mass description

Like the Trojane and Šentvid tunnels the Golovec tunnel alignment is also situated in foliated Perm-Carboniferous clastic soft rock. The ground consists of sandstone, siltstone and tectonic clay in fault zones (Fig. 2-14) and is therefore extremely heterogeneous and anisotropic. Layers of siltstone usually alternate with layers of sandstone in the thickness of a few centimetres or decimetres (Fifer et al, 2004). The contacts between these two prevailing lithological units are smooth, sometimes filled with clay, and caused stability problems if the dip direction of layers was into the excavated area (Beguš et al, 200). Sandstone was usually fissured with several systems of joints, thus enabling percolation of water in the excavated sections. Within the fault zones the tectonic clay with the lenses of tectonically deformed sandstone and siltstone was observed. The fault zones together with the weathered claystone layers acted as hydro-geological barriers (Popovič et al, 1998). The dip direction of layers was generally to S or SE (Fig. 2-14 – longitudinal section), but could locally vary due to intensive tectonics in past.

The majority of rock mass was assigned a GSI value between 15 and 35 (Popovič et al, 1998).

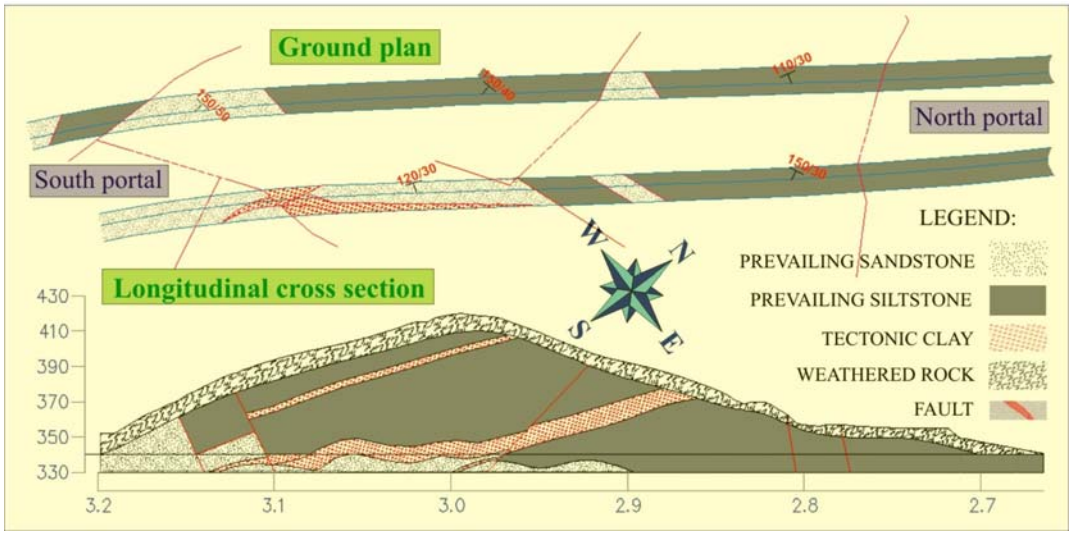

Figure 2-14. Geological ground plan and longitudinal section of the Golovec tunnel.

Slika 2-14. Vzdolžni geološki prerez in geološka situacija predora Golovec.

2.4.3 Monitoring programme

Due to the mentioned landslide at the southern portal a surface displacement monitoring programme was established above the entire tunnel. To track the sliding movement, 22 vertical

inclinometers were installed (Popovič et al, 1999) and equipped with targets for geodetic surveying (shown with green dots in Fig. 2-15). The targets (15 at the southern portal and 14 at the northern portal) were installed on the pile walls and on the entrance galleries of both portals to observe the effectiveness of the support structures. 20 individual targets (dots of violet colour in Fig. 2-15) were also installed in the expected or observed influence area of the tunnel. 3D positions of the targets were recorded once a week to once a fortnight, depending on the face advance and its position (Fifer et al, 2004). Additionally the settlements of the points in three cross sections were monitored.

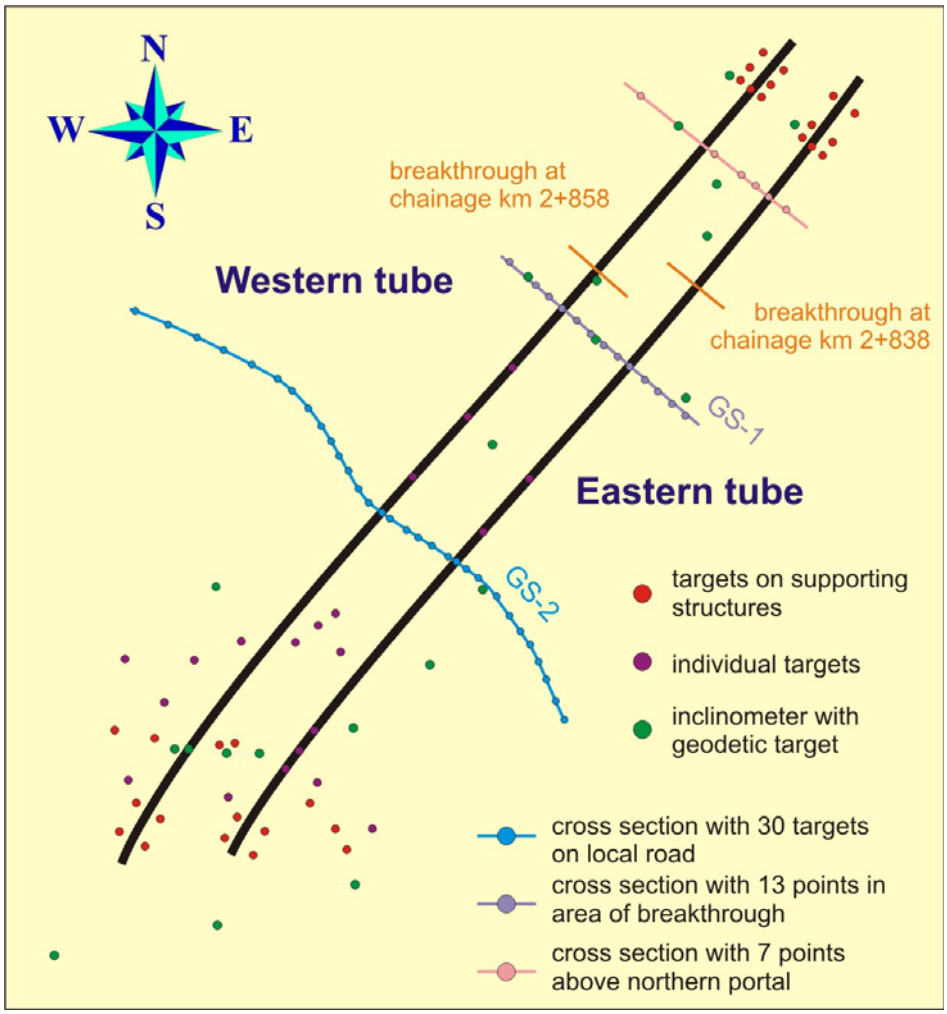

Figure 2-15. Scheme of surface monitoring at the Golovec tunnel.

Slika 2-15. Shematski prikaz površinskega opazovanja nad predorom Golovec.

Inside the tunnel 97 monitoring sections with 5 measuring points were installed. Relatively high density of the measuring sections (one measuring section per 11 m of the tunnel on average) is the consequence of the stability problems and extremely heterogeneous rock mass.

2.5 The Jasovnik tunnel

2.5.1 General information

The Jasovnik tunnel is situated in the vicinity of the Trojane tunnel. It is a two-lane double tube tunnel. The length of the southern and the northern tube is 1612 and 1633 m, respectively. Theoretical cross section of the tunnel tube is the same as in the Trojane tunnel (89 m^2). The distance between both tube axes is 40 m and remains constant along the tunnel as shown in Fig. 2-16. The overburden reaches 250 m. The area above the tunnel is not populated. The construction of the Jasovnik tunnel started with portal excavations in spring 1999. Excavation proceeded in both tubes simultaneously from eastern portals (heading Ljubljana) only and commenced in August 1999. The excavations were completed in October 2000 (Čadež et al, 2001).

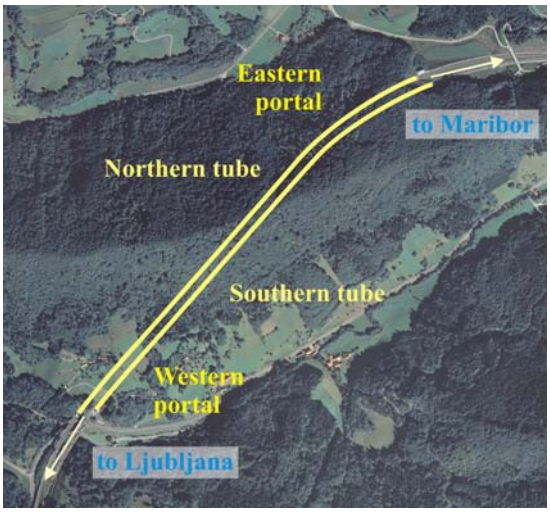

Figure 2-16. Layout of the Jasovnik tunnel.

Slika 2-16. Situacija predora Jasovnik.

2.5.2 Rock mass description

The Jasovnik tunnel alignment runs through diversified lithologic structure. The geological situation is characterized with different types of upper Triassic massive carbonatic rocks in the first approximately 1000 m (Čadež et al, 2001). Dolomite and dolomitic breccia changed in the first and last part of this section to limestone and in the central part to dolomitic limestone (Fig. 2-17). The geological-geotechnical conditions were favourable due to high rock mass strength and low tectonic damages of the area. The rock mass was categorized according to ÖNORM B 2203 classification mainly as A2 and B1.

In the last 600 m to the west portal the tunnel alignment entered the middle Triassic Pseudozilian shale and siltstone beds with intercalations of sandstone and tuff rocks (Čadež et al, 2001). The tunnelling conditions in this part were more demanding and the measured displacements much larger than in the first 1000 m, especially in the shales and siltstones, while in section with dominating tuff formations the measured displacements decreased. The difficulty of the tunnel construction depended on the amount of clay in the composition of the rock mass. The tunnelling conditions were classified in categories C2 and C3 in shales and siltstones and in B2 in tuff section (Čadež et al, 2001).

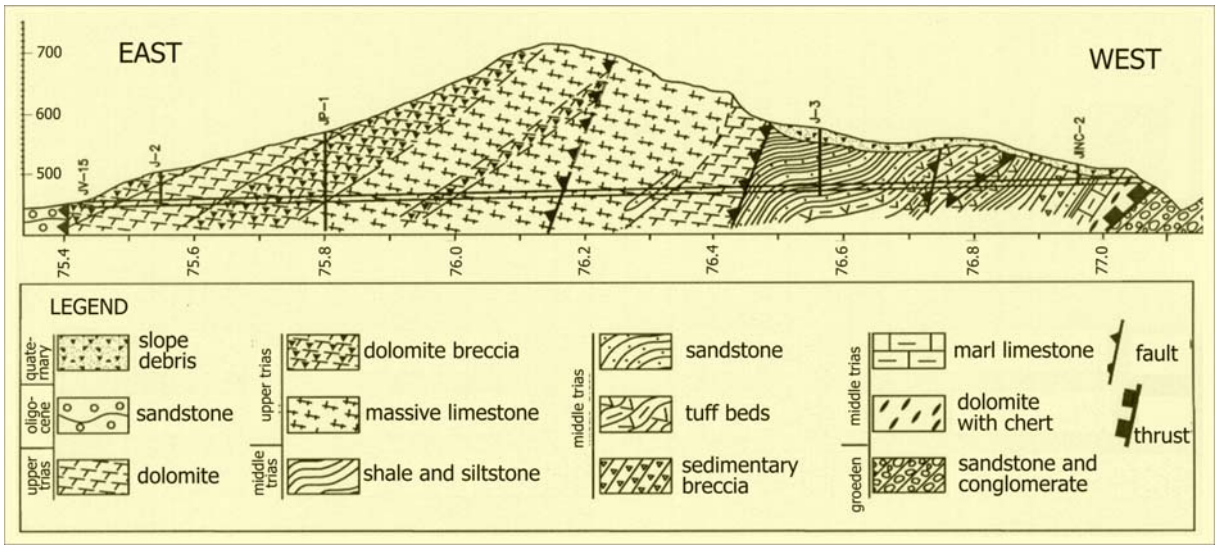

Figure 2-17. Geological longitudinal section of the southern tube of the Jasovnik tunnel (Čadež et al, 2001).

Slika 2-17. Vzdolžni geološki prerez južne cevi predora Jasovnik (Čadež et al, 2001).

Generally the beds dip with 40°-70° to the N. Especially soft clayey to silty rocks are gradually folded and transformed into tectonic gouge in the fault zones or near contacts with stiffer rocks. Two bigger fault zones were observed (Čadež et al, 2001).

The excavation was performed using drill and blast technique in stiff rocks (dolomite, limestone, tuffs) and by mechanical excavators in soft rock mass (shales, siltstones).

2.5.3 Monitoring programme

The monitoring programme consisted of 106 measuring cross sections with 5 points in the tunnel (3 in top heading area, 2 in bench area), 2 inclinometers above the axes of both tunnel tubes at the western portal and some measuring points and inclinometers on the retaining structure at the western portal of the southern tube. The inclinometers were monitored only during the construction of the portal structures.

The distance between the measuring sections in the tunnel depended on the predicted and observed tunnelling conditions. In the first 1000 m the measuring sections were situated on average each 50 m (21 measuring sections in the right tube, 20 in left tube) and in the last 600 m at a distance of 10-20 m (32 measuring sections in the left tube and 33 in the right tube).

2.6 The Ločica tunnel

2.6.1 General information

The Ločica tunnel is a two-lane double tube tunnel and has the same cross section of the tunnel tube as the Trojane and Jasovnik tunnels. The length of the southern tunnel tube is 797 m and of the northern tube 756 m. The distance between the tubes is 40 m and is constant (Fig. 2-18). The maximum overburden above the tunnel reaches 105 m. The crest of the hill above the Ločica tunnel is almost flat and extends over 300 m along the tunnel axis (Fig. 2-19). No important infrastructure or housing facilities are situated on the surface in the expected influence area of the tunnel. The portal excavations started in July 1999. Both tubes were excavated simultaneously from eastern portals (heading towards Ljubljana) only. The excavations started in October 1999 and were completed in April 2000 (Čadež et al, 2000).

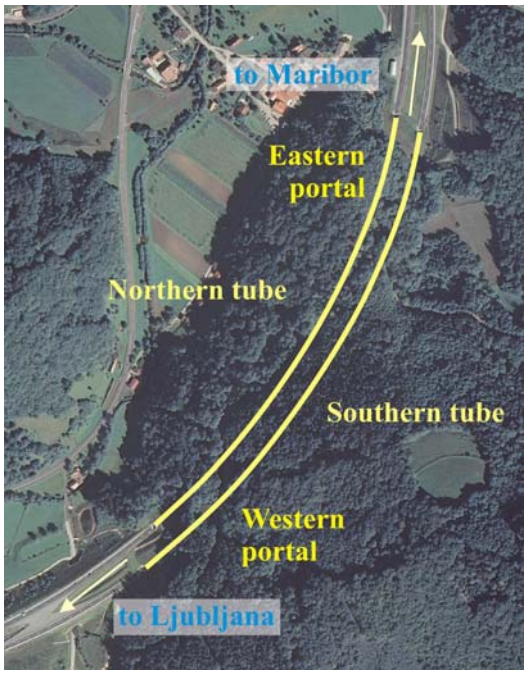

Figure 2-18. Layout of the Ločica tunnel.

Slika 2-18. Situacija predora Ločica.

2.6.2 Rock mass description

The tunnel alignment runs through Upper Triassic siltstones and mudstones with intercalations of marly limestones. The main lithologic unit is siltstone. Rock mass is folded and cut by few minor faults. Only one bigger fault was mapped at the western portal (Čadež et al, 2000). Unlike the other three presented projects, the geological-geotechnical conditions in the Ločica tunnel were better than predicted. The main reason could be the presence of the carbonate and volcanic material during the sedimentation of silty and muddy matrix. Recristallisation of these particles within matrix resulted in harder and less deformable rock mass than expected.

The tunnelling conditions were classified in categories B2 (about 83%) and C2 (Čadež et al, 2000).

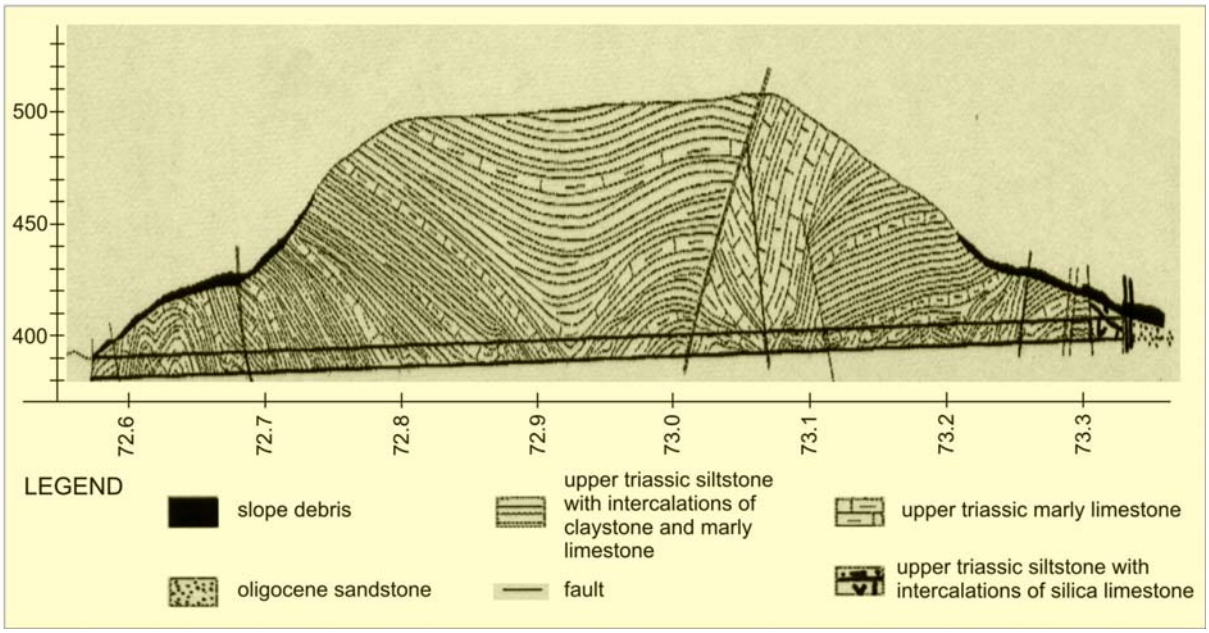

Figure 2-19. Geological longitudinal cross section of the southern tube of the Ločica tunnel (Čadež et al, 2000).

Slika 2-19. Vzdolžni geološki prerez južne cevi predora Ločica (Čadež et al, 2000).

2.6.3 Monitoring programme

Since the ground conditions were fair, only 48 measuring cross sections were installed in both tunnel tubes (one measuring section per 35 m on average, 22 measuring sections in the right tube, 26 in the left tube). All measuring sections included 5 targets (3 in top heading, 2 in bench excavation). The area above the tunnel is not populated and no surface monitoring was needed.

2.7 The Podmilj tunnel

2.7.1 General information

The Podmilj tunnel is the last of four tunnels constructed to pass the Trojane ridge on the A1 motorway Ljubljana – Maribor. It is constructed as a two-lane double tube tunnel with the length of the southern tunnel tube of 500 m and of the northern tube 552 m. The peak of the Dobnarše hill reaches 162 m above the tunnel crown and no infrastructure or housing facilities are located there. The construction started with portal excavations in spring 2002 and the tunnel driving started at the end of 2002. Both tubes were mainly excavated simultaneously from eastern portals (heading towards Ljubljana), only shorter sections were excavated from western portals (approximately 100 m in the northern and 37 m in the southern tube (Čadež et al, 2004b), as shown in Fig. 2-20). The excavations were completed in July 2003.

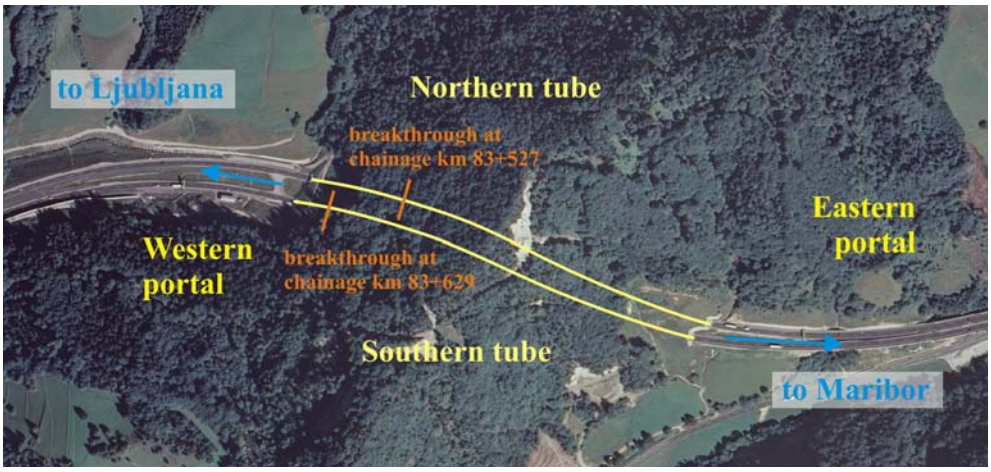

Figure 2-20. Layout of the Podmilj tunnel.

Slika 2-20. Situacija predora Podmilj.

2.7.2 Rock mass description

Like the Jasovnik tunnel, the Podmilj tunnel alignment also runs through a variety of lithologic structures. The first 220 m in the southern tube and 250 in the northern tube from the eastern portal are characterized by massive Middle Triassic dolomite of light grey colour (Fig. 2-20). Further excavation was performed in diversified Lower Triassic Scythian layers (dolomite of yellow and grey colour prevails) in the length of approximately 40 m. The excavation in this part was performed with drill and blast technique in top heading – bench sequence.

At chainage km 83+415 in the southern and km 83+343 in the northern tube the tunnel alignment entered lower Gröden sandstone, siltstone and claystone layers of Permian age and of violet colour.

Intercalations of white, completely crushed rock mass were usually found at the contact of sandstone and claystone in thickness of meters (Čadež et al, 2004b), especially in the northern tube. Petrographic analysis revealed presence of epsomite ($MgSO_4$ x $7H_2O$). Its re-crystallisation with swelling potential increases the pressures of the rock mass to the tunnel lining. In the southern tube Upper Scythian layers were entered again in the top heading excavation for about 65 m between chainages km 83+552 and km 83+615. Both tubes are close to the western portal, situated in soft foliated rock of Permian and Carboniferous age in the length of approximately 20-30 m. The excavation in the second part was performed with mechanical excavators and partially with drill and blast technique in top heading-bench-invert excavation sequence.

The rock mass is folded and crushed in the vicinity of the thrust contacts between different rock layers. Only one larger fault was mapped in Middle Triassic dolomite, a few tens of meters before the thrust contact with Scythian layers. The rock mass in between is crushed and cracked to high extent (Čadež et al, 2004b). The tunnelling conditions were classified mainly in categories B2 (about 41%) and C2 34% (Čadež et al, 2004b). Some B2 with the invert (13%) and C3 (8%) categories were also applied.

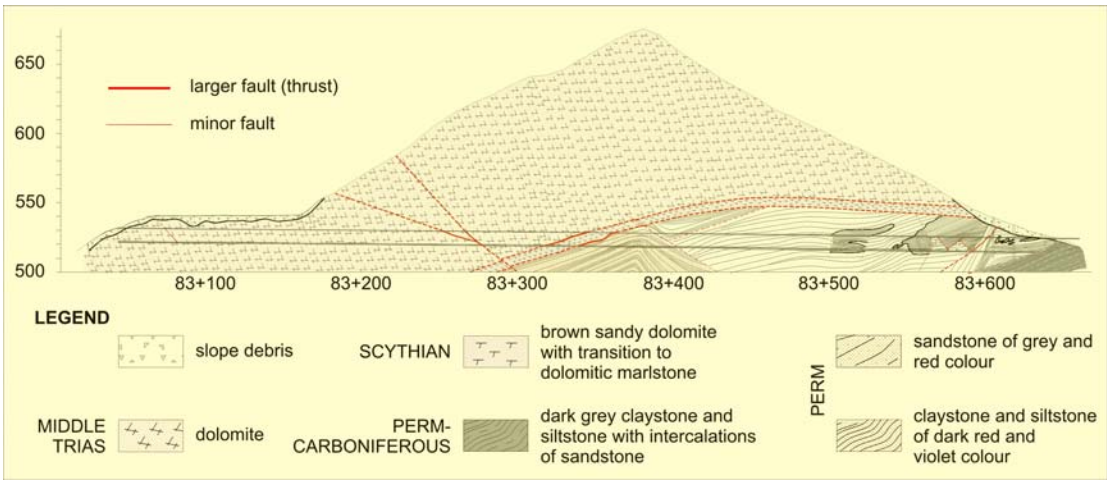

Figure 2-21. Geological longitudinal section of the northern tube of the Podmilj tunnel.

Slika 2-21. Vzdolžni geološki prerez severne cevi predora Podmilj.

2.7.3 Monitoring programme

The ground conditions were fair along the Podmilj tunnel and 48 measuring cross sections were installed in both tunnel tubes (one measuring section per 22 m on average, 23 measuring sections in the northern tube and 25 in the southern tube). Although the measured displacements were much larger in the second (Gröden) part of the tunnel, the density of the measuring sections remained the same. Each measuring section consists of 5 targets, 3 in top heading, 2 in bench excavation. No surface monitoring was needed, since the area above the tunnel is covered by forest.

3.0 Predor code

In modern tunnelling a large quantity of data is acquired every day, if we assume that due to the safety requirements usually double tube tunnels with unidirectional traffic are constructed on motorway networks and that the tunnelling progresses at least from both portals simultaneously to reduce the project construction time. Sometimes, construction sites are formed even at an intermediate location, e.g. by access tunnels or shafts, to shorten the construction time (Henke et al, 2004). With a fast development of the geodetic equipment the number of targets in measuring sections constantly increases and the distance among measuring sections decreases to provide more detailed data on the tunnel – rock mass response. In more demanding tunnelling conditions several sets of measurements can be performed each day.

According to the principles of the observational method stated in Eurocode 7-1 "the response time of the instruments and the procedures for analyzing the results shall be sufficiently rapid in relation to the possible evolution of the system", therefore the acquired monitoring data (geodetic measurements, geotechnical measurements, face logs) shall be properly inserted in the database and readily presented in a graphic way as soon as possible to enable the analysis and interpretation by the designers, contractors and supervising engineers.

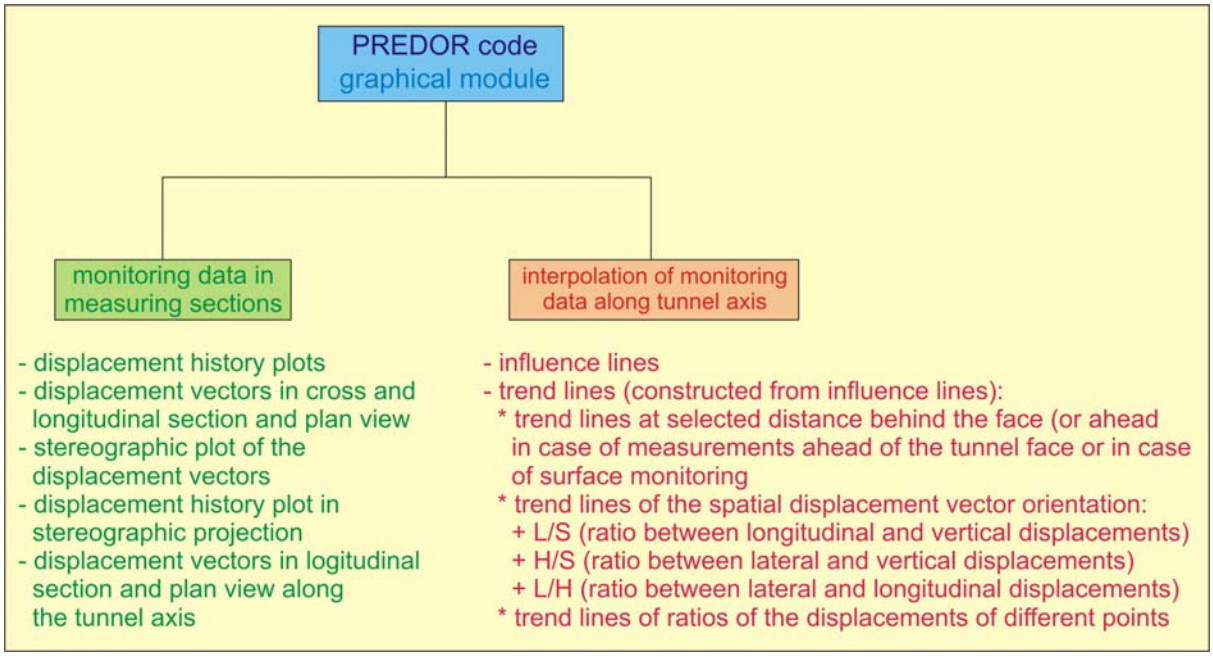

Figure 3-1. Range of different graphical presentations incorporated in the Predor code.

Slika 3-1. Nabor grafičnih izrisov, ki so vključeni v program Predor.

Several commercial software codes are available nowadays for building a database of the tunnel projects and providing graphical presentation of complex monitoring data in different ways (*GeoFit*; *Tunnel:monitor*; Schmuck, 2009).

In order to enable our own development and research in the field of interpretation of monitoring data obtained during tunnelling, a new software was developed. The Predor code is a task oriented database with extensive tools for data control and correction and especially for graphical presentation of original and interpreted data collected by 3D geodetic measurements during tunnelling. The development of the Predor code started as part of the graduation thesis (Klopčič, 2004) and set the basis of database structure and allowed basic graphical presentations. Further development made the code more universal. In present stage any cross section, any number of measuring points in a cross section and any scheme of the excavation works can be implemented within the tunnel project. Different types of monitoring data files for the input of displacements or construction phases advance data can be manipulated.

The Predor code enables different graphical presentations of the monitoring data from the tunnel as well as from the surface monitoring (Fig. 3-1).

If the face logs of the excavation faces were inserted in a database, the Predor code enables placement of the face log under the plotted displacement vectors in the cross section to allow direct comparison of the geology and measurements. The Predor code also comprises geological module for direct comparison of selected geological parameters to the measured displacements.

Geological accompaniment, geodetic and geotechnical monitoring on the sites are usually not performed by the same company. To collect and distribute monitoring data to the client, responsible for the analysis and interpretation of these data, and finally to make the requested graphical presentation takes valuable time.

To reduce time needed for the collection of daily monitoring data, for the verification of the data for possible errors, for their analysis and storing in previously prepared database, for the preparation of a comprehensive report with required graphical presentations and its sending to predefined clients inside the Predor code, an automatic system for processing monitoring data in tunnels was developed. This system was already applied in three recently constructed tunnel projects in Slovenia (the Barnica tunnel, the Leščevje tunnel and the Tabor tunnel). Details on the data flow of the automatic system and experience from the three tunnel projects are given below.

3.1 Automatic procedure for data input

Different types of data can be processed at this stage by the automatic monitoring system:

- 3D displacement or levelling data of the targets, mounted on the primary lining,
- 3D displacement or levelling data of the targets on the surface in the expected influence area above the tunnel,
- data about construction phase advance,
- face logs of different excavation faces.

For each project and/or project site a database shall be predefined with all the required parameters: axis of the tunnel and overburden, given as a polygon in discrete points, geometrical data of all different tunnel contours, scheme of the inclination of the tunnel cross section and expected tunnelling categories along the tunnel axis, as well as the template of a face log. Within the expected tunnelling categories the displacement thresholds for each component of the displacement vector must be defined on the basis of calculations or comparable experiences from other sites in similar conditions. These thresholds can be later on manually updated by the operator of the automatic system.

Before starting an automatic monitoring system, the following properties shall be defined for each individual project site:

- filename extensions that are characteristic for each individual project site,
- thresholds for checking gross errors of face advance and 3D displacement data, which are automatically calculated from the axis data and geometry data of cross sections and must be checked and confirmed by the operator,
- list of senders of the incoming data,
- list of receivers of error warnings (surveyors, supervising engineer, contractor),
- the template of the Microsoft Word document and the types of graphical output, if the reports are required by the client,
- list of receivers of the reports,
- timeline when the daily reports are produced if the measurements are executed several times a day; if only one set of measurements is planned and executed per day, a daily report is produced just after the monitoring data has been received and inserted in the database,
- timeline when weekly or monthly reports shall be executed.

The incoming monitoring data are received from the site surveyors and geologists by email or are uploaded to an agreed FTP server. It is of high importance that the incoming data are in a predefined

form and properly marked with the filename extensions defined for each individual project. The 3D displacement or levelling data can be given in an absolute Gauss-Krueger coordinate system directly from the total station instrument or in a local coordinate system of the tunnel. A requested format of 3D geodetic monitoring data and the construction phase advance data is an ASCII TXT file, while face logs can be processed as JPEG, BMP or PDF formats (due to easier handling the JPEG format is preferred).

If data are received by email, a Microsoft Outlook application is used for handling the email and its attachments. A special Outlook watcher handling Outlook Object Model was developed that recognizes the expected sender and downloads the belonging attachments to a user-specified folder on a local disc. This folder or FTP server is checked in regular user specified time intervals. If attachments with expected filename extensions containing 3D displacement data or construction phase advance data from active project site are found, the automatic system starts. Incoming face logs can not trigger the automatic system.

At the beginning of the automatic process the list of tasks according to the incoming data and previously defined requirements is prepared. All further actions are then executed according to this list. The automatic procedure is locked during the execution of the prescribed actions and any incoming data during this time will be processed in next session.

ASCII files with 3D displacement monitoring data are checked at the beginning for possible typing errors or gross errors in the process of acquiring 3D positions. Target positions are checked with regard to the axis data, the geometry of the cross section and the last measured position of the target. Similarly, the data on the advance of the construction phases are checked with regard to the last known position of the excavation faces and the average and maximum face advance. If any mistakes are detected, an error message is send to predefined clients to notify them about the mistake. The automatic process for such site is stopped and is waiting for reply from the input data provider.

The checked displacement data are then calculated from global to local coordinate system, if provided in the Gauss-Kruegger (or any other) coordinate system and inserted into the database of automatic monitoring system. All data in the database are saved in local coordinate system with the origin at the axis of a tunnel. To enable the use of monitoring data also with other codes, the Predor code allows exporting of the data in different formats.

During the development of the automatic procedure special attention was paid to the recognition of any anomalies of the displacement curves. Based on experience obtained by inserting monitoring data of already completed projects in the database, three different cases of irregular displacement curves

were identified in general. The first case is characterised by only one measurement that differs from the remainder of the displacement curve, usually due to minor error during the acquisition of the target position. The second case is when the target has been destroyed and has actually moved from the original position. The last case deals with the shifted position of the tunnel reference points with regard to the outer reference points due to the long lasting deformation of the tunnel lining. Recognition of the described three cases was incorporated to the following procedure and is based on several consecutive steps.

When the displacement data are transformed in the local coordinate system, an automatic procedure thoroughly examines the calculated data. If an individual calculated value of the displacement vector differs significantly from the last value in the database or from the value of other points in the same measuring section and exceeds previously defined tolerable thresholds when no excavation activities are ongoing in the vicinity, the target is marked and the monitoring data are not inserted in the database. A temporary file with a complete displacement history is written for such target, since causes for the unexpected measurement are not clear from this single measurement. If only a minor error occurred during the acquisition of the removed target position, subsequent measurement will be within thresholds from the last value in the database and the removed value will be deleted (case 1 in Fig. 3-2).

Especially in longer tunnels, constructed in unfavourable geological conditions with squeezing and creeping rock mass, surveyors usually encounter problems when determining the reference points for daily convergence measurements (long-term response of the rock mass aggravates the selection of the stabilised sections and/or targets). In these cases the polygon of the tunnel network has to be checked regularly with a tie to the outer (stable) reference points and positions of the tunnel reference points corrected if the new positions differ from previous. The positions of all monitored targets are therefore altered, but for all targets simultaneously, taking into account the translation and rotation of the coordinate system.

A special case occurs when the subsequent measurement is not found within thresholds, either from the last value in the database or from the removed value. A warning message is produced, the data of the problematic monitoring section are blocked and the intervention of the operator is demanded. The automatic procedure does not stop in this case and the remainder of the monitoring data are checked. Further incoming data for the problematic measuring section are inserted only in the file with original data of the monitoring section and not in the database.

Several causes influenced the decision for the intervention by the operator. As already mentioned, thresholds are set on the basis of the calculation results or on the basis of comparable experience in the project preparation phase before the automatic system is initiated. If worse geological conditions are encountered than predicted, the displacements rates can significantly increase and therefore thresholds must be modified. If the target was physically moved twice during three subsequent measurements, the operator of the automatic system must manually shift the displacement curve to the expected value. A blockade of the monitoring section is removed and the monitoring data in the database can be further managed by the automatic system.

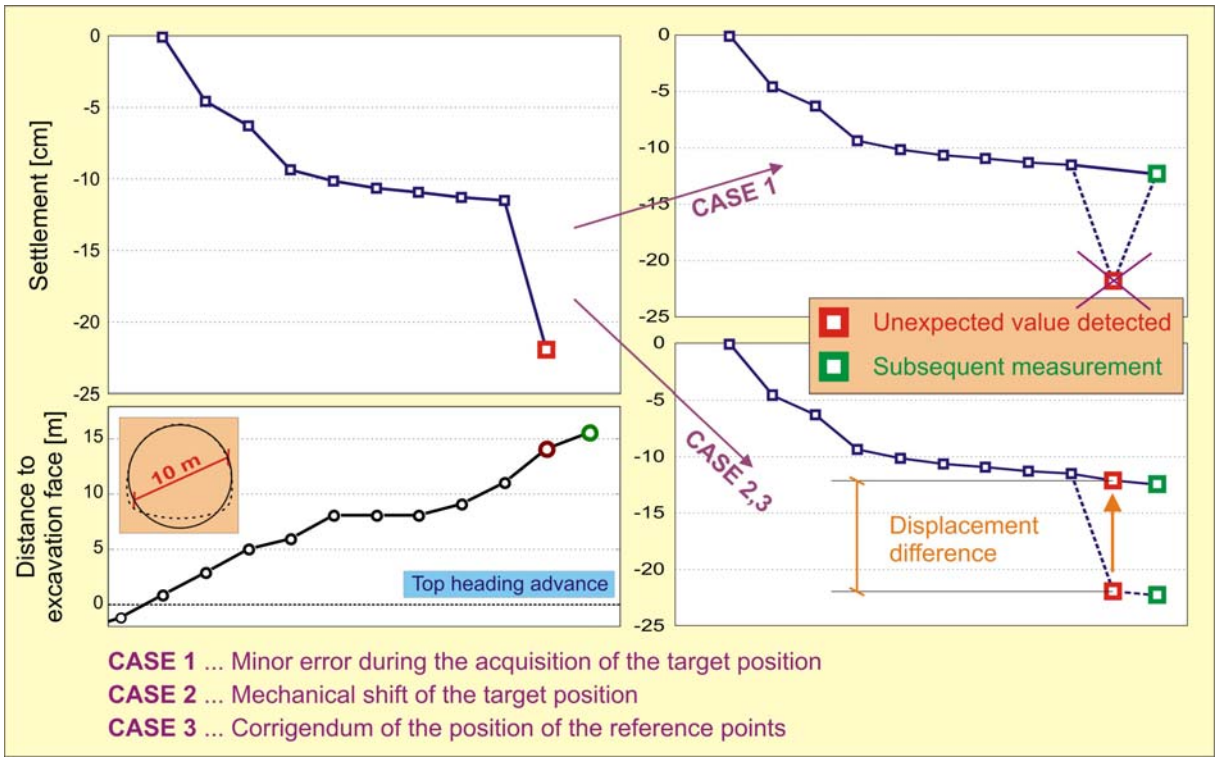

Figure 3-2. Handling with the displacement history curves when unexpected values of the displacements are detected.

Slika 3-2. Popravljanje krivulj časovnega poteka pomikov, ko je bila prepoznana nepričakovana velikost pomika.

If the target has been mechanically destroyed and then rebuilt or just stroked by any means (excavator, blasting), the removed position presents the first measurement of the new target position. In this case all three curves of the displacement vector components have to be moved to presumed value which is assessed by the slope of the displacement curve between the last two values of each component in the database and by the influence of nearby excavation activities (case 2 in Fig. 3-2).

The displacement difference between the last "old" and the first "new" position of the target is stored and later on added to all calculated values of this target. The automatic system also stores the original (not corrected) displacement curve of such target.

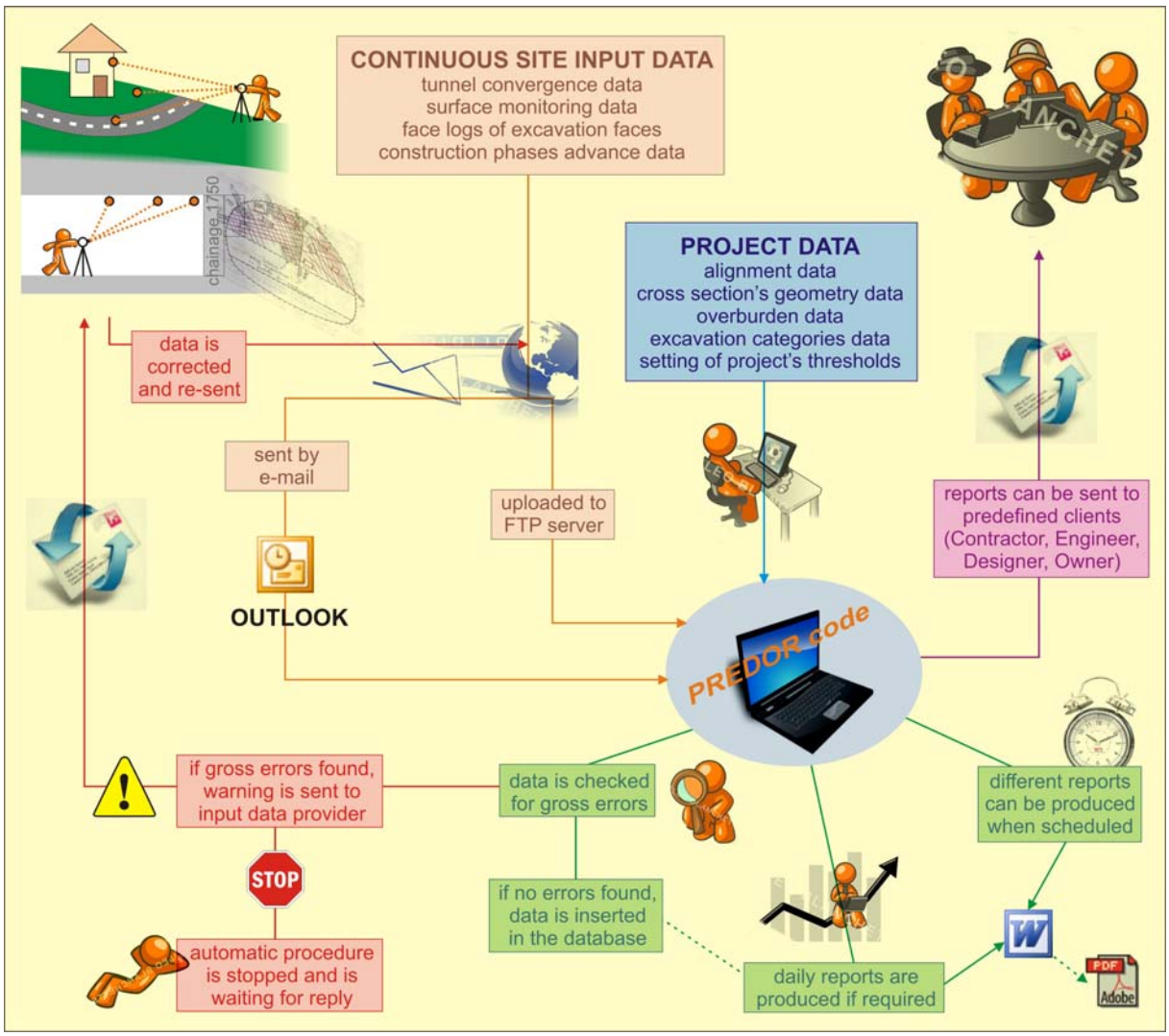

Figure 3-3. Schematic flowchart of the automatic system for processing monitoring data in tunnels.

Slika 3-3. Shematski prikaz delovanja avtomatskega sistema za obdelavo podatkov geodetskega in geološkega opazovanja v predorogradnji.

As soon as the displacement monitoring data have been checked and corrected, if needed, the automatic system adds them to the database. Further on the excavation phase advance data that have already been checked during the search for gross errors is inserted in the database. In the last step the face logs are copied. If a new measuring section has been installed and a face log of the excavation

face in the vicinity is provided, the sketch of the geological structure is recognized, cut from the form and placed to a special folder. It can then be plotted together with the displacement vectors in cross section. The data input for the present project is completed. If no other activities for the project are scheduled, the same procedure re-runs for all other projects on the list. If the execution of the reports is planned, the report is produced and sent to predefined clients.

Automatic system significantly facilitates the data input, but plain data are not applicable for a day-to-day use. Therefore, the automatic system was upgraded and in this stage allows preparation of comprehensive graphical output with all required graphical presentations and information for the decision making on site.

3.2 Automatic procedure for graphical report preparation

A complete range of the listed graphical formats of the monitoring data as shown in Fig. 3-1 can be inserted in a report. In order to offer as much information as possible in condensed form, special graphical presentations were developed in cooperation with the decision making staff on site. These graphical forms can be divided in three groups – report pages RP1, RP2 and RP3, as follows:

- report page RP1.1 of the individual tunnel cross section (a sample is shown in Fig. 3-4); the form comprises displacement history plots in three directions with belonging construction phase advance data and plots of displacement vectors in longitudinal and cross section with lined face log if inserted; the data on the overburden and tunnelling category are provided together with the remarks that are generated by the automatic system in case of shifting any of the displacement curves during the check of the input monitoring data (remarks can also be added manually by the operator of the automatic system and are stored for later reports).

- report page RP1.2 of the individual surface cross section (a sample is shown in Fig. 3-5); the form is quite similar to the RP1.1 and also comprises displacement history plots in three directions with belonging construction phase advance data; displacement vectors are plotted in cross section with marked surface and the positions of the tunnel tubes; settlements of all targets are also plotted with the influence lines.

- report page RP2 of the displacements along the tunnel axis (a sample is shown in Fig. 3-6); the form comprises three plot objects where all in Fig. 1 listed graphical presentations can be plotted (influence lines, trend lines, displacement vectors along axis); remarks can be added manually by the operator of the automatic system.

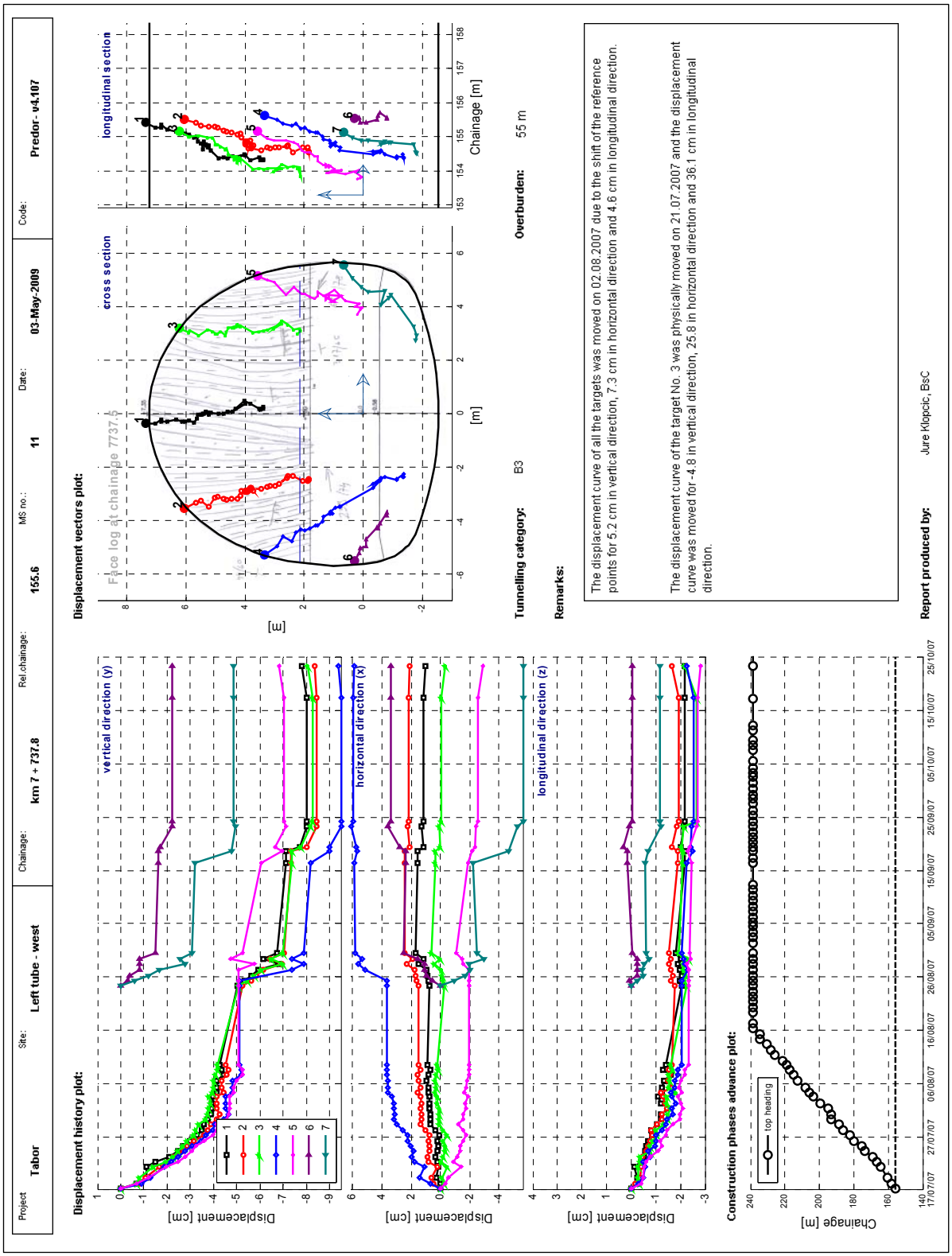

Figure 3-4. Sample of the report page RP1.1 of the individual tunnel cross section.

Slika 3-4. Primer poročila RP1.1 za posamezni merski profil v predoru.

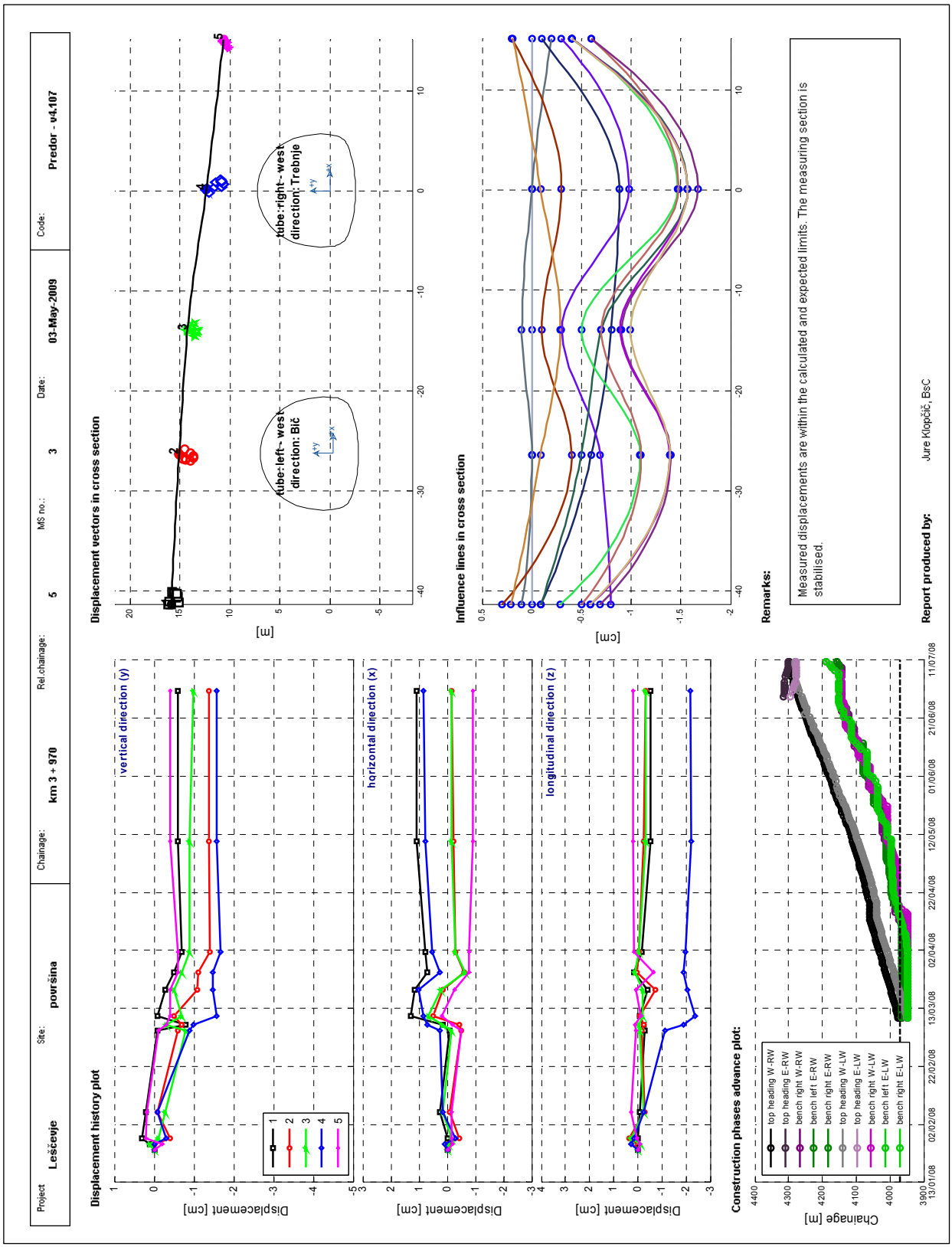

Figure 3-5. Sample of the report page RP1.2 of the individual surface cross section.

Slika 3-5. Primer poročila RP1.2 za posamezni merski profil na površini.

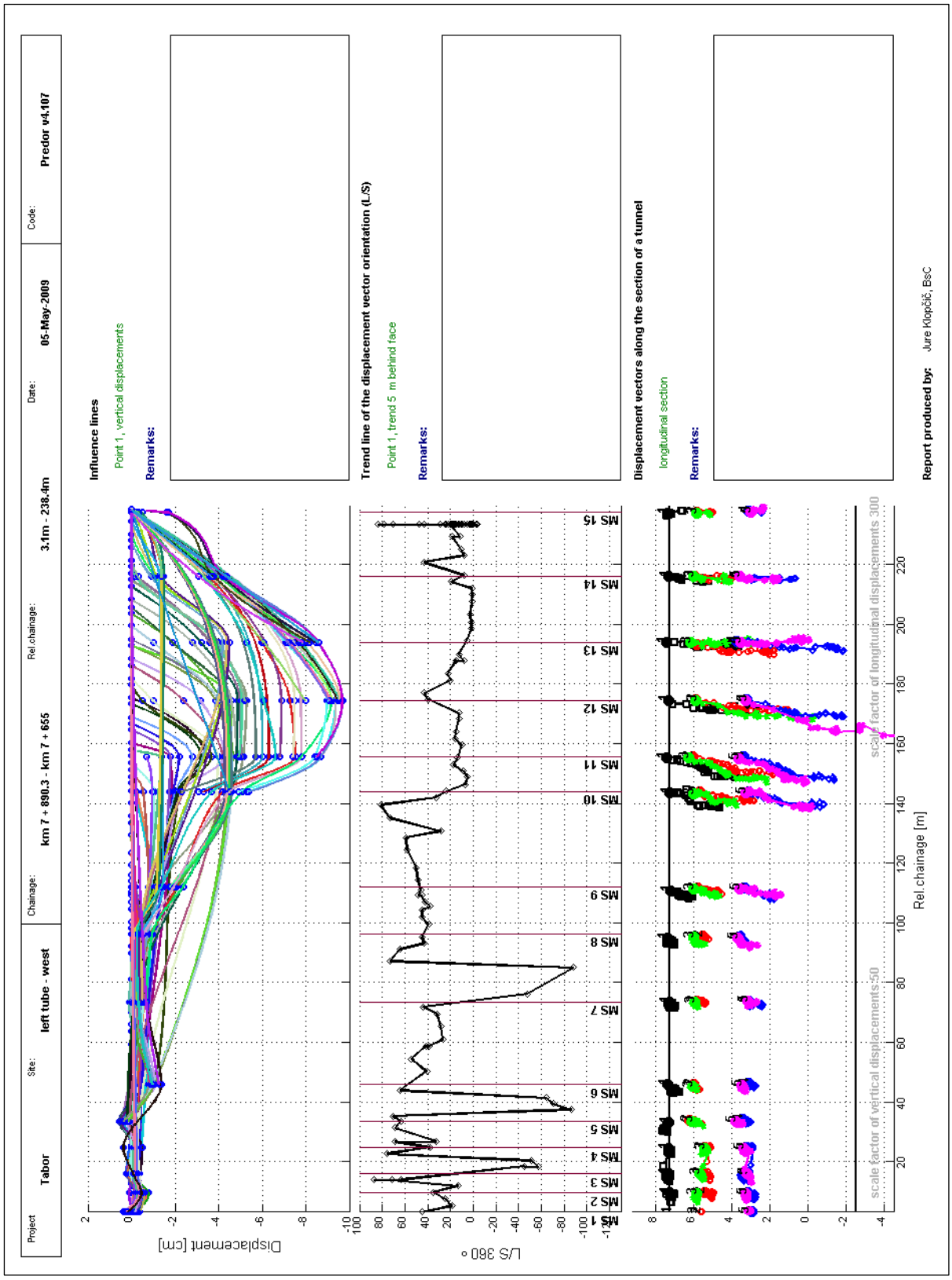

Figure 3-6. Sample of the report page RP2 of the displacements along tunnel axis.

Slika 3-6. Primer poročila RP2 za pomike, izrisane vzdolž predorske cevi.

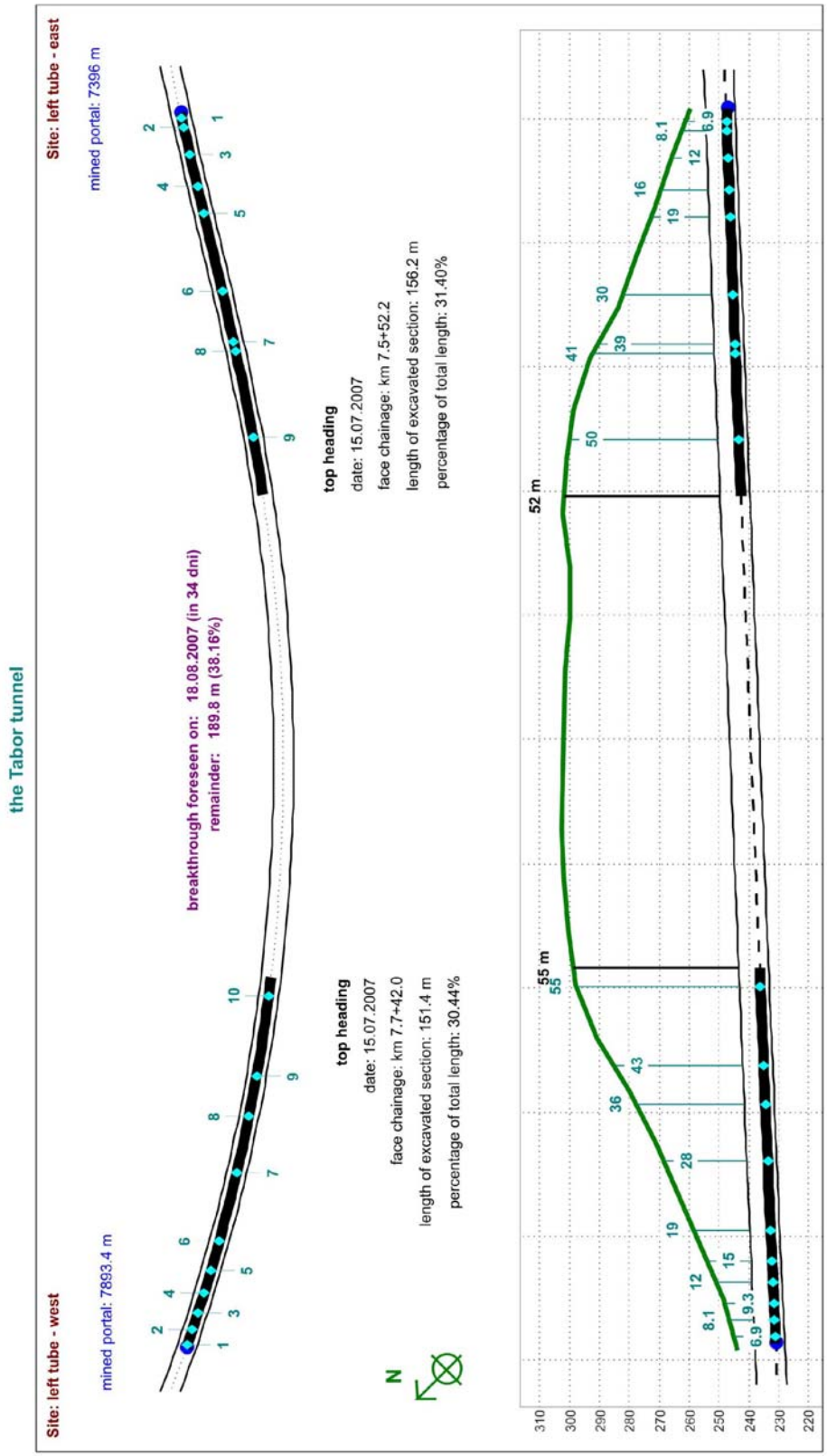

Figure 3-7. Sample of the report page RP3.1 of the situation of construction phases.

Slika 3-7. Primer poročila RP3.1 za situacijo gradnje z izrisom položaja izkopnih čel.

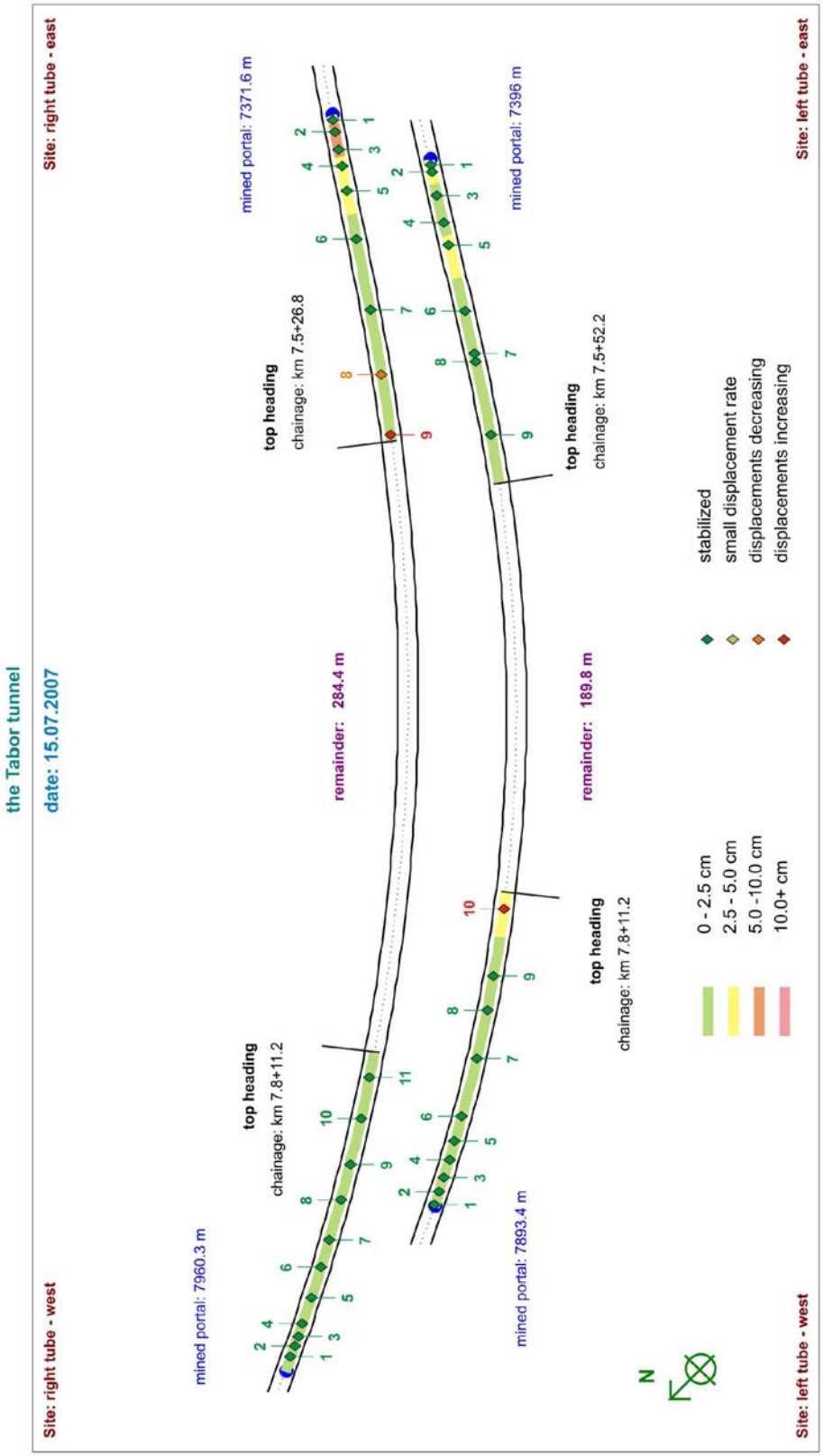

Figure 3-8. Sample of the report page RP3.2 of the situation of measuring sections.

Slika 3-8. Primer poročila RP3.2 za situacijo merskih profilov.

- report page RP3.1 of the situation of construction phases (a sample is shown in Fig. 3-7); the form comprises: (upper plot) a layout of tunnel alignment with marked cross sections and selected excavation faces; data on the mined portal, the length of the excavated section on each of the sites as well as the length of unexcavated section between the sites and a foreseen date of the tunnel breakthrough for selected excavation face are given; (lower plot) a tunnel alignment in the longitudinal section with plotted overburden above the tunnel; data on the overburden above each of the measuring sections and current position of the selected face are given.

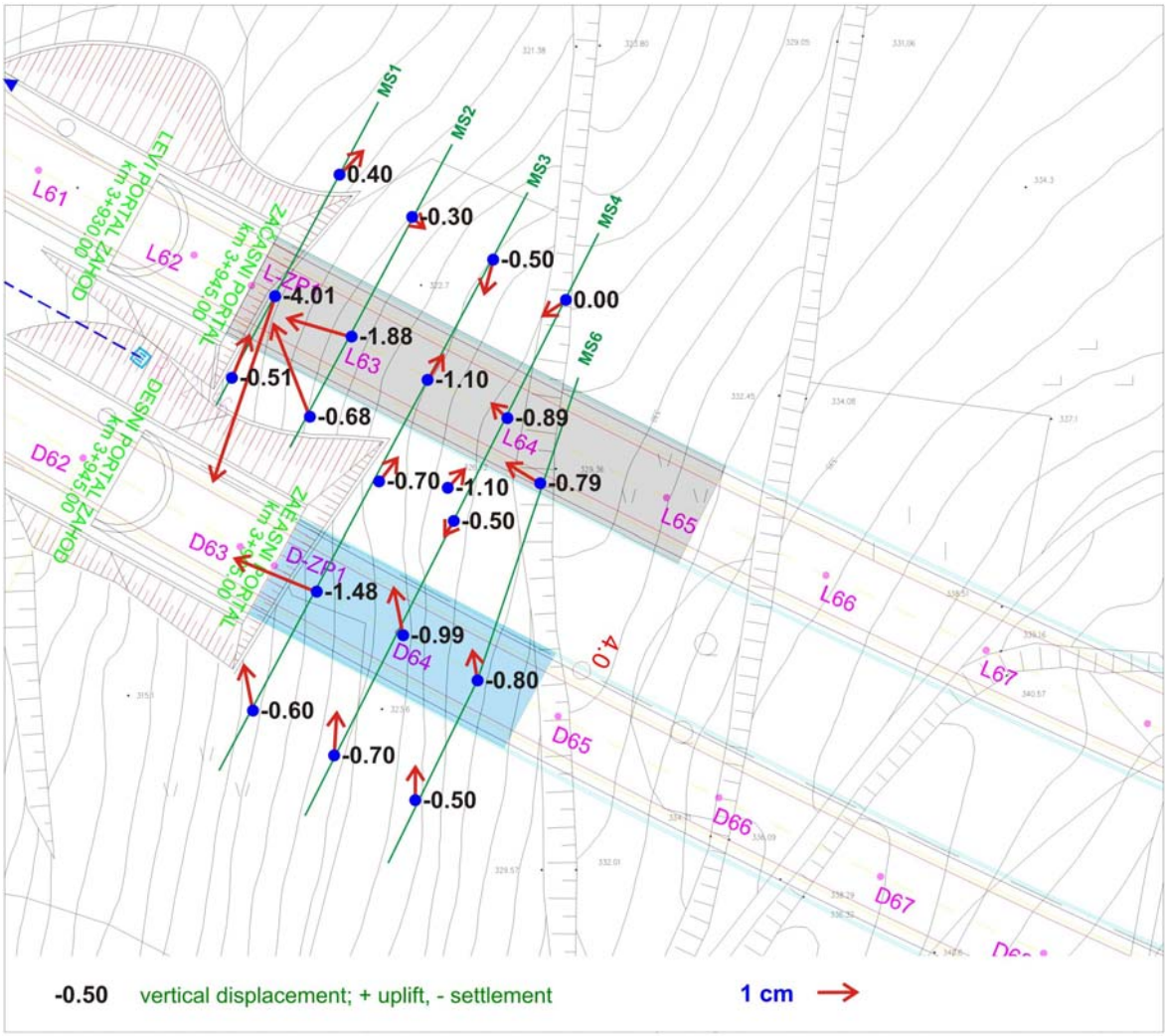

Figure 3-9. Sample of the report page RP3.3 of the situation of surface measuring sections.

Slika 3-9. Primer poročila RP3.3 za situacijo merskih profilov na površini.

- report page RP3.2 of the situation of convergence measuring sections (a sample is shown in Fig. 8); the form comprises a layout of tunnel alignment with marked cross sections and selected excavation faces; lines representing sections of the tunnel are plotted in different colours illustrating

the magnitude of the largest measured displacement with regard to the thresholds, defined with the present tunnelling category; the colour of the markers of convergence measuring sections indicates the displacement trend in each individual measuring section.

- report page RP3.3 of the situation of surface measuring sections (a sample is shown in Fig. 3-9); the form comprises a topographic plot of tunnel alignment with marked cross sections and selected excavation faces; the direction and magnitude of the displacement vectors are illustrated with an arrow of scaled length; settlement of the target settlement is given with a number.

Before starting the automatic system of the project, a template of the Microsoft Word document must be prepared together with a cover page. Automatic system then manipulates this document by inserting text, tables and graphical presentations according to previously selected parameters. The final outcome of the automatic procedure for graphical report preparation is arbitrarily designed Microsoft Word document that can be further on transformed to PDF format.

Reports are in case of only one set of daily convergence measurements produced when the daily monitoring data are received. In case of several sets of measurements per day, the automatic system produces reports according to the preset schedule. Different reports with diverse content (weekly or monthly reports) can also be scheduled in advance.

Completed reports are immediately sent via e-mail to the predefined recipients using SMTP connection. If network allows sending SMS via internet or if a special application for sending SMS is provided, the automatic system informs the operator using SMS service about the current status of the automatic procedure (whether the received data were correctly inserted in the database and reports were produced or not). Automatic system also writes a trace log file of all performed activities to enable the reconstruction of any breakdown events during the operation.

3.3 Application of the automatic system in recent projects

The development of the automatic system started prior to the construction of Barnica and Tabor tunnels to speed up and facilitate the data input and report preparation for these two tunnels that were constructed simultaneously. At the commencement of monitoring of both tunnels the system allowed automatic data input of previously downloaded and checked files, execution of report pages RP1.1 and RP2 (without face log in the plot of the displacement vectors in cross section) and their insertion with manipulation in the Microsoft Word file. To be able to trace easily the construction activities, the report page RP3.1 was developed later on. Originally the system did not include the algorithm for checking the incoming data for gross errors, which caused the system to stop several times. With the

development of this missing algorithm and implementation of an application for downloading files from Microsoft Outlook and for sending e-mails, a fully automatic system was achieved. The complete service enabled recognition of the sender and downloaded files from the Microsoft Outlook inbox, checking of these files for errors, insertion of the data to the database, preparation of daily reports and their sending by e-mail to predefined recipients without an intervention by the operator. Since the reliability and stability of the system had not been previously tested or proved, an intensive superintendence of the operator was inevitable for some weeks to eliminate some smaller errors and upgrade the software to be able to respond to previously unanticipated circumstances. In 8 month period altogether 619 daily and 18 weekly reports were produced by the automatic system for the Barnica tunnel and 594 daily and also 18 weekly reports for the Tabor tunnel. The longest period of continuous operation without intervention by the operator was 40 days. The majority of breakdowns in the monitoring period was due to the inability of the system to establish the SMTP connection or due to computer shutdown. These two problems can not be solved within software.

There was a major issue with the size of the Microsoft Word files that were sent by e-mail (as requested by the client), since several pictures in high resolution JPEG format were inserted. Producing graphical presentations in EMF format significantly decreased the file sizes and maintained high resolution of images.

In the preparatory stage for the Leščevje tunnel construction two new report pages were developed (RP1.2 and RP3.3), since the design foresaw some surface monitoring sections. The system was upgraded to store the incoming sketch forms of the excavation faces for individual sites to the database. Further on, an algorithm was developed, extracting for newly installed measuring section the face log from the closest sketch form of an excavation face and plotting it under the displacement vectors in cross section. Since these forms are drawn by hand in the tunnel and then scanned, they usually lack quality. A part of the algorithm removes noise from the face log and also decreases contrast (Fig. 3-10).

A satisfactory operation in the Barnica and Tabor tunnels proved the reliability of the system. Therefore, no major modifications were applied. 264 reports of the tunnel convergence measurements were sent to the client in 5 months of monitoring the Leščevje tunnel. The longest period of continuous operation without intervention by the operator was somewhat shorter than at the Barnica and Tabor tunnels (34 days), but only 23 stops of the automatic system occurred (recorded in a trace log file) in the total period of monitoring the Leščevje tunnel. The main problem was again the accessibility of the internet connection.

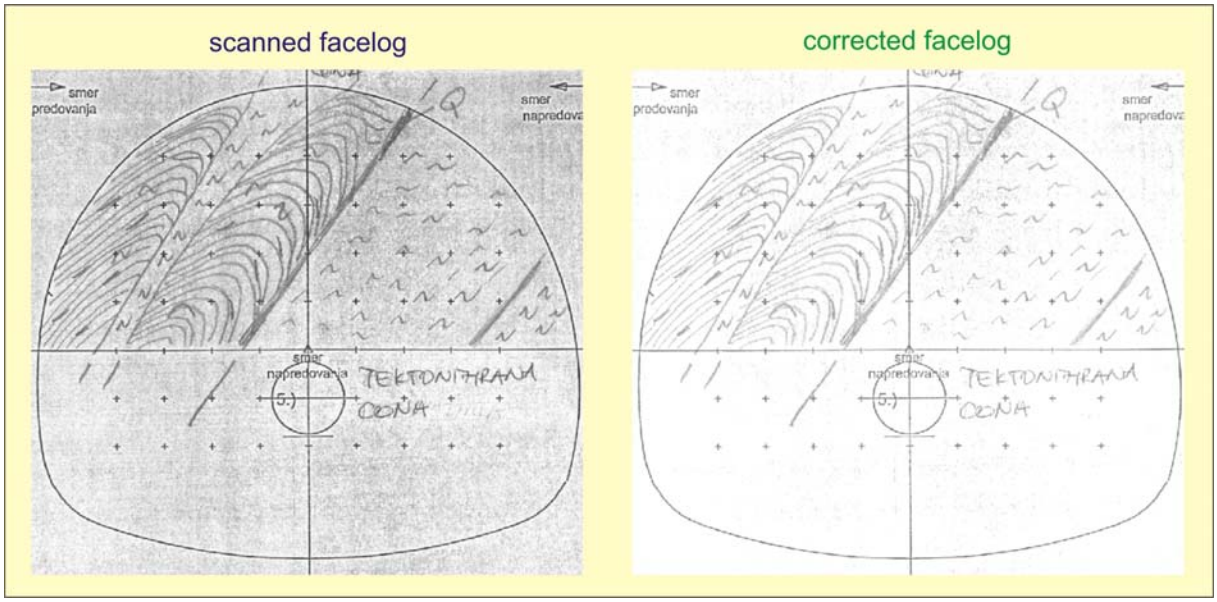

Figure 3-10. Sample of scanned face log (left) and the same face log after correction (right).

Slika 3-10. Primer digitaliziranega geološkega popisa čela (levo) in popravljenega (desno).

The report page RP3.2 allows quick insight in the displacement trends and displacement magnitudes comparing to thresholds of all measuring sections in one project. It has been developed recently and will be operational for the monitoring of the future Markovec tunnel (situated on the highway Koper – Izola). To remind the surveyors of unrecorded measuring sections when scheduled (predefined by the designer), the system will send an e-mail with a list of sections that need to be recorded as soon as possible. A new report form for monitoring the structures above the tunnel will also be developed.

4.0 Influence of the foliation on displacements due to tunnelling

4.1 Literature review

Excavation of a tunnel induces stress re-distribution around the opening and some inward convergence occurs. In case of circular tunnel subjected to hydrostatic stress, the tunnel wall uniformly displaces radial to the circumference (Hoek, 2007). Quite similar displacement pattern is observed when tunnelling in "homogeneous" ground.

Displacement pattern changes significantly in heterogeneous rock mass where stress re-distribution process depends primarily on the stiffness of the surrounding rock. If a zone of softer material is for example located in the vicinity of the left sidewall of a tunnel tube, stress due to tunnel excavation concentrates in stiffer rock mass in-between. This leads to the increase of the tunnel wall displacements close to softer material (Fig. 4-1). Influence of fault zones close to tunnel tube has been thoroughly studied by several authors (Button, 2004b; Moritz et al, 2004; Schubert et al, 2002; Schubert et al, 2005).

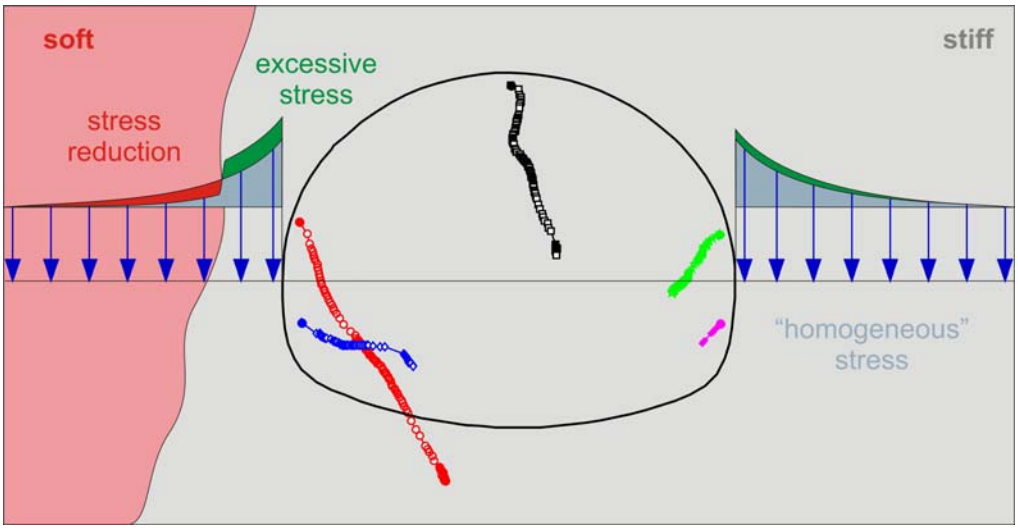

Figure 4-1. Stress state alteration after tunnel excavation close to a soft zone and resulting displacements (measured displacements of MS47 in the southern tube of the Trojane tunnel).

Slika 4-1. Sprememba napetostnega stanja po izkopu predora v bližini mehkejše hribine s pripadajočimi pomiki (prikazani so izmerjeni pomiki merskega profila MS47 v južni cevi predora Trojane).

Even more complex displacement pattern occurs when tunnelling in anisotropic ground conditions. Anisotropy refers to direction-dependent properties of the rock mass (Leitner et al, 2006) that strongly

influence the stress re-distribution and displacements. Usually it is associated with weak planes in rock mass structure (foliation, bedding planes, faults, joints) and leads to higher deformability. The response of the underground structure in case of anisotropic rock conditions thus strongly depends on strength properties and relative orientation of discontinuities to an opening (Wittke, 1990; Solak, 2009). Experience from some projects in foliated rock mass have also showed significant dependence of costs, displacement magnitudes, construction time and quantity of primary support needed for successful tunnelling on different relative orientation of foliation with regard to the tunnel tube (Huber et al, 2005).

The disturbed zone around an opening is a region where the original state of the rock mass has been affected by excavation and notable displacements have occurred or the deviatoric stress has increased significantly (Shen et al, 1997). Three different types of disturbed zone can be distinguished in anisotropic rock masses (Tonon, 2003):

- failure zone, where blocks can separate from the rest of the rock mass and fall into excavated area,
- open zone, where discontinuities open up,
- shear zone, where shear deformation occurs between discontinuities.

In anisotropic rock mass, the resulting magnitude and orientation of the displacement is the combination of the normal displacement that would occur in the isotropic rock mass and additionally from the shear displacements along the discontinuities and from dilatation of the discontinuities. Knowledge of how the tunnel response changes with the relative orientation of the discontinuities is essential in order to properly understand and interpret monitoring results in anisotropic rock mass conditions. A general behaviour can be investigated using two dimensional numerical analyses solely in case where the strike of the discontinuities is parallel to the tunnel axis (Goricki et al, 2005). In all other cases the simplified 2D simulations can not take into account the development of the displacements with approaching and digressing tunnel face and time consuming 3D analyses are necessary.

Nowadays available and widely used numerical methods can be in general classified in two different groups: (1) continuum modelling, where the geometry of the rock mass anisotropy including the behaviour of discontinuities is modelled within direction-dependent constitutive law and (2) discontinuum modelling, where the constitutive law with corresponding material parameters is assigned separately for rock mass and discontinuities; discontinuum model thus consists of blocks that are modelled as continuum and interactions between these blocks. Barton (1996) proposes that

continuum models can be used for rock masses with Q-values less that 0.1 and for massive rock where the spacing of discontinuities is much greater than the scale of the opening (Q-values are more than 100). Use of discontinuum models is thus recommended for the rock masses with Q-values between 0.1 and 100. Similarly, Leitner suggests that decision on suitability of each of the groups for certain problem depends on the dominating deformation mechanism of the rock mass (Leitner et al, 2006). According to the comparison of the numerical results obtained using both methods, the discontinuum model should be selected if the mechanism strongly depends on the spacing of discontinuities and the continuum model if the strength of the rock mass depends on small scale deformation behaviour like for example thin layered schist (Leitner et al, 2006). However, according to experience (Barla, 2000) isotropic continuum modelling is used far more frequently than discontinuum modelling, even in cases where rock exhibits strong anisotropic behaviour.

When modelling anisotropy in numerical models, a distinction can be made between elastic and plastic anisotropy (Brinkgreve et al, 2000). Elastic anisotropy refers to the use of direction-dependent stiffness parameters (usually described with a shear modulus in planes perpendicular to the plane of transverse isotropy and two elastic moduli and Poisson's ratios, one set in the plane of transverse isotropy and one perpendicular to it (Tonon, 2003)). Plastic anisotropy refers to direction dependent strength parameters (shear stresses along discontinuities are limited according to some criterion and plastic shearing occurs when maximum shear stress is reached) and/or kinematic hardening (Brinkgreve et al, 2000).

3D numerical analyses of the influence of elastic anisotropy on tunnel wall displacements performed by Tonon (2002) showed that the foliation direction also affects displacements ahead of the face if the plane of transverse isotropy is not striking parallel to the tunnel axis. Two different cases were analyzed: one with the planes of transverse isotropy dipping in the tunnel (referred to as tunnelling "against dip", as shown in Fig. 4-2) and the other with planes dipping in the excavation direction (referred to as tunnelling "with dip"). Analyses displayed that when tunnelling with dip, over 60% of the total displacements occurs before the section is excavated, while in opposite case only less than 10%. Tonon explained this phenomenon with stiffer rock mass parallel to the plane of anisotropy and more deformable perpendicular to it. When tunnelling with dip, the rock mass is more deformable towards the excavated part of the tunnel and can freely expand. In the opposite case almost no displacements can occur, since the rock mass is more deformable in the non-excavated part of the tunnel and the majority of the convergences occurs after the excavation of a section. The displacement vector in this case tends into the excavation direction.

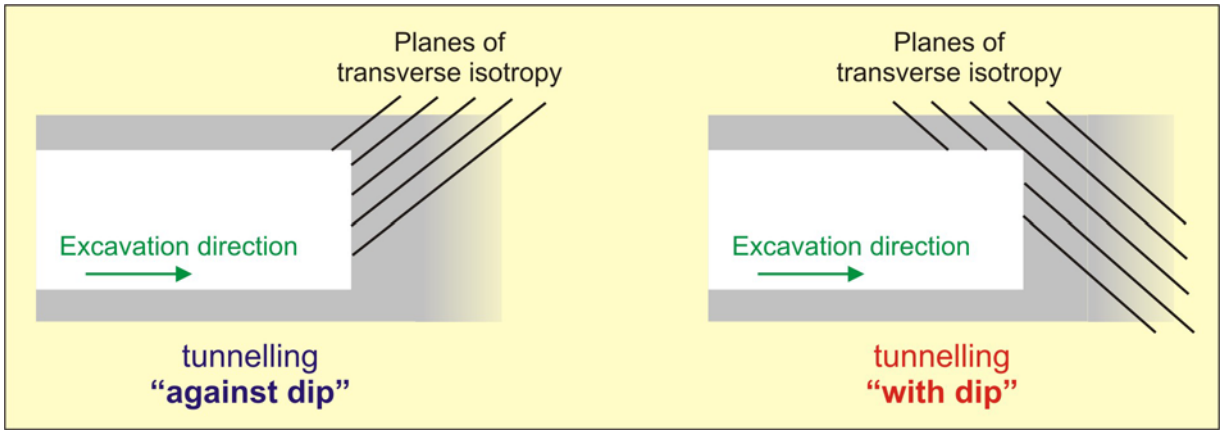

Figure 4-2. Orientation of planes of transverse isotropy when tunnelling "with" and "against dip" (Tonon, 2002).

Slika 4-2. Orientacija ploskev ortotropije pri gradnji predora z ali proti vpadu plasti (Tonon, 2002).

This was, however, not confirmed by Goricki (2005), who also investigated the influence of the variation of the dip of discontinuities on the behaviour of the tunnel with 3D Fast Lagrangian Analyses of Continua (*FLAC 3D*). Calculated displacement vectors of all points behind the face showed a tendency against the excavation direction.

On the other hand, Steindorfer (1998) analyzed monitoring data from two tunnels in Austria constructed in schists and phyllites, where schistosity governed the deformation behaviour. When tunnelling against dip which strikes more or less perpendicular to the tunnel, displacement vectors tended slightly into the excavation direction. A visible tendency in the excavation direction is reported in the case with the same dip, but with strike between an obtuse and an acute angle to the tunnel axis (Steindorfer, 1998).

In tunnel design there are many uncertainties involved in the evaluation of the geological and geomechanical characteristics of rock mass, especially if a tunnel runs through frequently changing ground. In-situ and laboratory tests provide input data for computational methods to predict tunnel behaviour. However, the monitored response often differs from the predicted and input data that have been used in numerical analyses are modified to improve the agreement between the calculated and the monitored response. This procedure is called parameter identification (Sakurai, 1997). In the sequel a quick overview of the outcome of the reported back analysis for parameter identification in three presented projects (Trojane, Šentvid and Golovec) will be given. These tunnels run through soft, densely foliated rock mass and the use of continuum models with orthotropic material constitutive laws would be

appropriate according to Barton (1996) and Leitner (2006). However, at least in the eastern part of the Trojane tunnel and partly in the Golovec tunnel the geological situation can be mainly characterised by what is called "block-in-matrix" rock mass due to intensive tectonics. Nevertheless, despite faulting and folding processes the general dip and strike of the foliation relative to the tunnel tubes can still be determined from the sequence of face logs. Therefore, isotropic as well as anisotropic constitutive models can be used, depending on the location.

In case of the Trojane tunnel laboratory and in-situ tests displayed significant variability of geomechanical properties of each individual lithological unit as a consequence of tectonics and weathering processes. Ranges of measured strength and stiffness parameters for siltstone and claystone, the two prevailing lithological units, are given in Table 4.1 (Likar et al, 1997). Parameters c and φ were according to Likar (Likar et al, 1997) determined based on direct shear and triaxial tests and a stiffness parameter E_{50}^{ref} from triaxial test.

Table 4-1. Measured strength and stiffness parameters for foliated claystone and siltstone in the Trojane tunnel project (Likar et al, 1997).

Preglednica 4-1. Izmerjeni trdnostni in togostni parametri skrilavega glinovca in meljevca v predoru Trojane (Likar et al, 1997).

	claystone	siltstone
E_{50}^{ref} [MPa]	55 - 110	120 - 180
c [kPa]	18 - 54	22 - 58
φ [°]	22 - 28	28 - 33

Based on these parameters, Vukadin (2001) performed back analyses of the retaining walls at both portals using Plaxis 2D code (*Plaxis 2D*) with isotropic Mohr-Coulomb and Hardening soil constitutive models. Using the same software and the Hardening soil constitutive model, Gogala (2001) back calculated strength and stiffness parameters of foliated claystone from pressuremeter tests at the Trojane tunnel. Besides both two abovementioned isotropic constitutive models, Miklavžin (2004) analysed surface settlements induced with tunnelling in two different cross sections close to famous restaurant also with an anisotropic constitutive model (Jointed rock). The best match was obtained with the Hardening soil model. Back calculated parameters of all three authors are presented in Table 4.2 (remark: strength parameters are the same for Mohr-Coulomb (MC) and for Hardening soil (HS) constitutive models and are given only once in Table 4.2).

Back calculated parameters of Vukadin and Miklavžin are evidently quite similar in case of claystone and the Hardening soil model and represent somehow an average value of the measured

parameters. Gogala, on the other hand, obtained much higher stiffness parameters and cohesion, but lower friction angle. Surprising is the value of unloading/reloading modulus (E_{ur}^{ref}), which is only twice as large as the loading modulus.

Table 4-2. Back calculated strength and stiffness parameters for foliated claystone and siltstone in the Trojane tunnel project.

Preglednica 4-2. Izračunani trdnostni in togostni parametri skrilavega glinovca in meljevca v predoru Trojane.

material model:	*author lit.unit*	Vukadin claystone	Miklavžin claystone	Gogala claystone	Vukadin siltstone
HS	E_{50}^{ref} [MPa]	95	72	200	150
	E_{oed}^{ref} [MPa]	75	68	200	130
	E_{ur}^{ref} [MPa]	285	216	400	450
	m	0,8	0,85	0,5	0,8
	c [kPa]	30	30	100	30
	φ [°]	26	27	22	32
MC	E [MPa]	65	150		120

material model:	*author lit.unit*	Miklavžin claystone
JR	E_1 [MPa]	81
	ν_1	0,25
	E_2 [MPa]	78
	ν_2	0,25
	G_2 [MPa]	30
	c [kPa]	23
	φ [°]	17

Somewhat better conditions were encountered in the Golovec tunnel according to 2D numerical analyses performed by Fifer-Bizjak (2004). Back calculated value of elastic modulus for siltstone amounted to 400 MPa, peak cohesion 50 kPa and friction angle 32°. The best fit of the calculated results to measured displacements was at "30-35% of rock relaxation simulating the effect of approaching face" – (Fifer-Bizjak et al, 2004).

Table 4-3. Back calculated strength and stiffness parameters for foliated claystone and siltstone/sandstone in the Šentvid tunnel project.

Preglednica 4-3. S povratnimi anlizami izračunani trdnostni in togostni parametri skrilavega glinovca in meljevca/peščenjaka v predoru Šentvid.

lit.unit	**siltstone/sandstone**		**claystone**	
mat.model	MC	Multilaminate	MC	Multilaminate
E [MPa]	1400	1400	300	300
c [kPa]	214	0	70	0
φ [°]	34	25	19	10
strike [°]		0		0

During 3D numerical analysis of the influence of the exploratory tunnel on the excavation of the Šentvid motorway tunnel, Jemec (2006) checked the design parameters for two prevailing rock mass

types in the Šentvid tunnel: RMT2 with prevailing siltstone/sandstone and RMT3 consisting of foliated claystone. Back calculated parameters for two different constitutive models (isotropic Mohr-Coulomb and anisotropic Multilaminate model) are shown in Table 4.3.

4.2 Displacements in cross section

4.2.1 The Šentvid tunnel

To obtain appropriate initial input parameters for further 3D numerical analyses and at the same time to spend as little time as possible on these preliminary studies, 2D numerical analyses were performed. As outlined earlier, two-dimensional calculations of the anisotropic rock mass are suitable only for sections where discontinuities strike parallel to the tunnel axis. Such sections were among three tunnels in foliated rock mass identified only in the right tube of the Šentvid tunnel. Since the area around the cavern was well investigated with boreholes and the geological structure was well known after the excavation of the cavern, the first calculation was performed in the cross section through the cavern A in the right tube. Simplified geological model was used to create the numerical model that is shown together with excavation sequence in Fig. 4-3. The parameter *ΣMstage* in Plaxis programme was used to select the amount of stresses released before the installation of primary lining in two-dimensional analysis in order to simulate the effect of approaching face in real 3D situation. The *ΣMstage* parameter defines a portion of applied unbalanced forces that result from the tunnel excavation. Selection of the *ΣMstage* value is based on measured displacements ahead of the face of the Šentvid motorway tunnel (detailed description is given in Chapter 5). Rock bolts were substituted with a soil cluster with higher cohesion. The increase in cohesion was calculated using the equation presented at the bottom of Fig. 4-3.

Initial analysis was performed with the isotropic Hardening soil constitutive model, since it had proved to satisfactorily model the tunnel response in Perm-Carboniferous foliated rock mass. The starting stiffness parameters were equivalent to the Mohr-Coulomb parameters back calculated by Jemec. The obtained displacements were significantly underestimated compared to the measured values. Stiffness parameters were reduced in further analyses in order to fit the calculated settlement of the crown of the exploratory tunnel to the measured displacement. Also strength parameters were slightly reduced (Klopčič et al, 2008). Since the calculated displacement of the point in cavern lining was still undersized, only characteristics of the upper layer were decreased. This measure affected only the displacements of the cavern and not the behaviour of the exploratory tunnel. But even with unrealistically low stiffness of the upper layer (E_{50}^{ref} = 50 kPa) the measured displacement could not be reached.

In case of the Šentvid tunnel the encountered geological conditions were rather more favourable than in the Trojane tunnel and several measuring cross sections exhibited anisotropic behaviour as they were located in rock mass with sufficiently uniform foliation. Use of the Jointed rock constitutive model is intended for rock masses where the following three conditions are fulfilled: (1) a discontinuity set (or more of them) can be identified within the rock mass, (2) discontinuities are not filled with fault gouge and (3) spacing between discontinuities has to be small compared to the characteristic dimension of the structure (Brinkgreve, 2001). According to these criteria the Jointed rock constitutive law is suitable for modelling the behaviour of siltstone in the Šentvid tunnel.

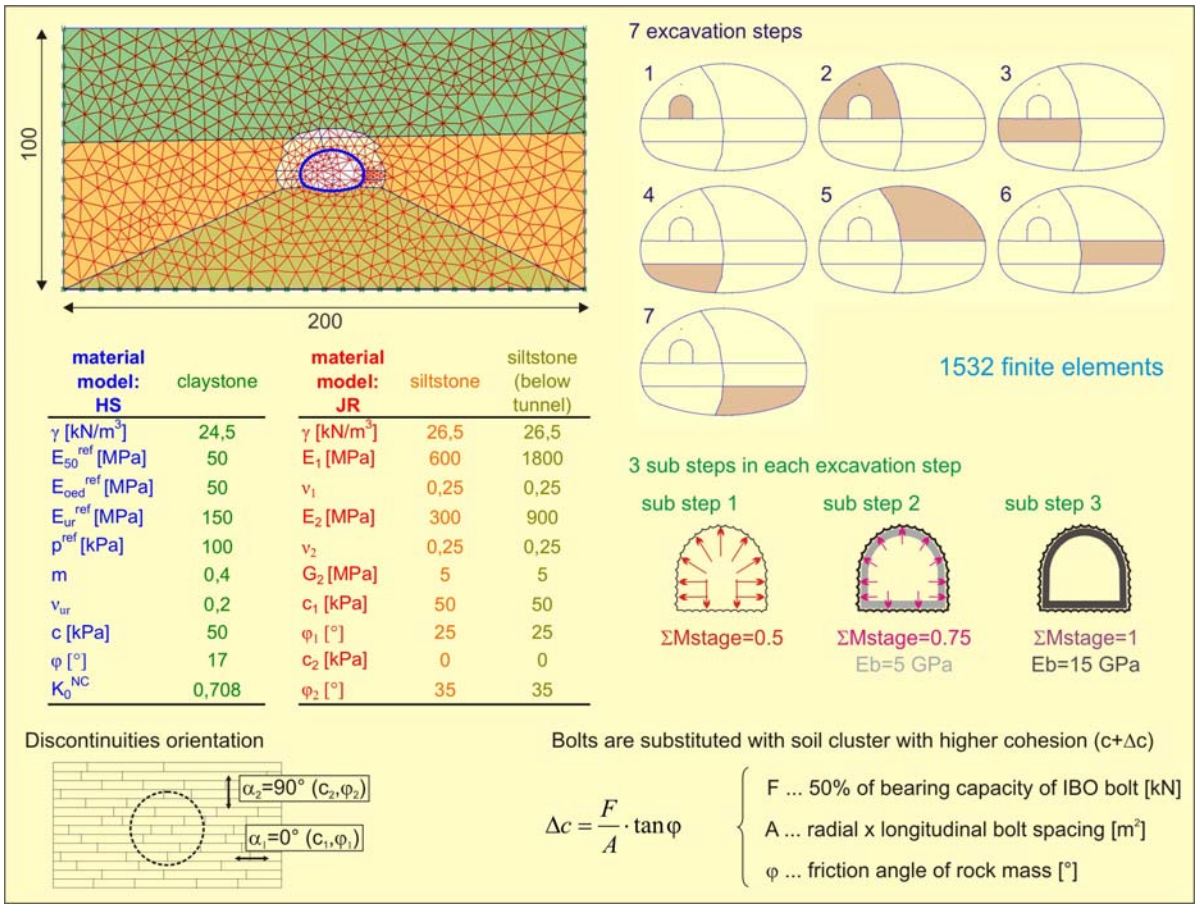

material model: HS	claystone	material model: JR	siltstone	siltstone (below tunnel)
γ [kN/m³]	24,5	γ [kN/m³]	26,5	26,5
E_{50}^{ref} [MPa]	50	E_1 [MPa]	600	1800
E_{oed}^{ref} [MPa]	50	ν_1	0,25	0,25
E_{ur}^{ref} [MPa]	150	E_2 [MPa]	300	900
p^{ref} [kPa]	100	ν_2	0,25	0,25
m	0,4	G_2 [MPa]	5	5
ν_{ur}	0,2	c_1 [kPa]	50	50
c [kPa]	50	φ_1 [°]	25	25
φ [°]	17	c_2 [kPa]	0	0
K_0^{NC}	0,708	φ_2 [°]	35	35

Figure 4-3. Numerical model for back calculation of Jointed rock material parameters in the right cavern of the Šentvid tunnel.

Slika 4-3. Numerični model za povratno analizo materialnih parametrov "Jointed rock" konstitutivnega modela v desni kaverni predora Šentvid.

Two discontinuity sets were identified in this location on the basis of face logs (horizontal foliation and some joints in perpendicular direction to foliation). Since the Jointed rock constitutive model does not distinguish elastic moduli for loading and unloading conditions, the same material but with three

times higher moduli was applied at the bottom of the model to prevent unrealistic uplifts. Several analyses were performed to match the calculated and measured displacement of the point in cavern lining just above the exploratory tunnel. Based on presuremeter tests, back calculations by Jemec (2006) and design parameters back calculated from the exploratory tunnel (Žigon et al, 2005), the value of elastic modulus of isotropic rock mass (E_1) was set to 600 MPa. As the well pronounced displacement pattern normal to foliation planes was often monitored in several sections, the effect was considered with lower characteristics in this direction (lower E_2 modulus with an initial ratio $E_1:E_2 = 2:1$). The foliation planes are rather slickensided, but undulating and uneven. Initial strength parameters were thus estimated on these observations and information from the design. A shear modulus G_2 was applied for fully isotropic conditions, calculated from E_2 ($G_2 = 0.5E_2(1+\upsilon_1) = 120$ MPa).

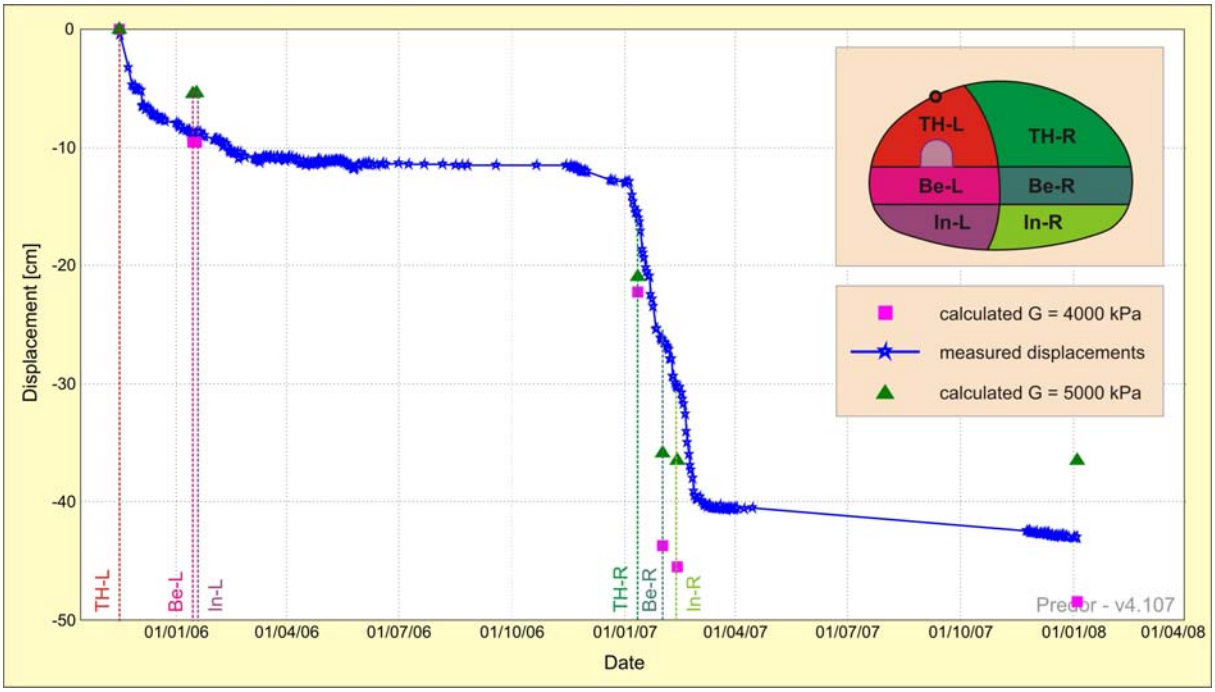

Figure 4-4. The result of back calculation with Jointed rock material parameters in the right cavern of the Šentvid tunnel for the model from Fig. 4-3. Measured displacements in measuring section MS27 at chainage km 1.3+29; target above the exploratory tunnel.

Slika 4-4. Rezultat povratne analize z "Jointed rock" konstitutivnim modelom v desni kaverni predora Šentvid. Merjeni pomiki v merskem profilu MS27 na stacionaži km 1.3+29; točka nad raziskovalnim rovom.

The calculated settlement of the observed point was still underestimated compared to the measured value. For this reason first E_2 together with G_2 was decreased to limit values where the calculation became unstable.

Next, also strength parameters were decreased to limit values, but the calculated response was still undersized. The values of both elastic moduli were kept high in further set of analyses with ratio $E_1:E_2 = 2:1$. Strength parameters were set at the initial values and only value of shear modulus was reduced to investigate the effect of shear deformations along foliation planes on the displacements in vertical direction. Final parameters that gave satisfactory agreement between calculated and measured displacements are shown in Fig. 4-3. Contrary to our expectations, the final value of shear modulus was really low ($G_2 = 5$ MPa) compared to fully isotropic conditions ($G_2 = 120$ MPa).

In Fig. 4-4 a significant dependence of vertical displacements on the shear modulus along the horizontal foliation is presented. The measured displacements of the target in the lining of the cavern just above the exploratory tunnel are plotted with blue line, while the calculated displacements with shear modulus $G_2 = 5$ MPa are shown with green triangles (2D calculation provides only individual points after each excavation step). The difference between the measured and the calculated values during the excavation of the left gallery could be explained by rather different geometry of the right side wall compared to the designed (executed wall convexity was much smaller than the designed and consequently the shape of the temporary tunnel was more unfavourable, which probably caused larger radial displacements). Final calculated displacements with $G_2 = 5$ MPa were somewhat smaller than the measured values. On the other hand, the calculated displacements with shear modulus $G_2 = 4$ MPa match the measured displacements only up to the excavation of the left gallery, and they are overestimated for further excavation steps.

Some additional analyses were performed with the same parameters in other sections with parallel strike of foliation to the tunnel axis to verify the obtained parameters. A section with non-horizontal foliation was selected for the investigation of the influence of low shear modulus also on displacement vectors in cross section. In the area of measuring section MS6, the foliation dips with an angle of about 30° to the left sidewall, as shown in Fig. 4-5. Two models for this cross section were analysed: one comprised soil clusters with increased cohesion for the simulation of bolt effect, in the other one single uniform material was used. Since no distinctive difference in displacements was observed, further analyses were performed using solely basic material.

Monitored displacement vectors reveal anisotropic behaviour of the tunnel tube. Measured displacement vector of the crown point (dark blue line in Fig. 4-5) in the presented measuring section tends to the right side wall almost perpendicular to the foliation. In isotropic conditions displacement vector of the upper right sidewall point (dark green line) would point into the excavated area due to unloading, but was in this case almost vertical and even pointed towards the wall. Only at the end some inward movement occurred. The lower right sidewall point can not be taken into consideration,

since the first measurement was taken later than for the other points. A change in the vector orientation can be noticed also at the lower left sidewall point, although some other factors affected the displacements as well (observed especially in first few days after the first measurement). The alteration of the displacement vector orientation occurred in the influential area ahead of the bench excavation face.

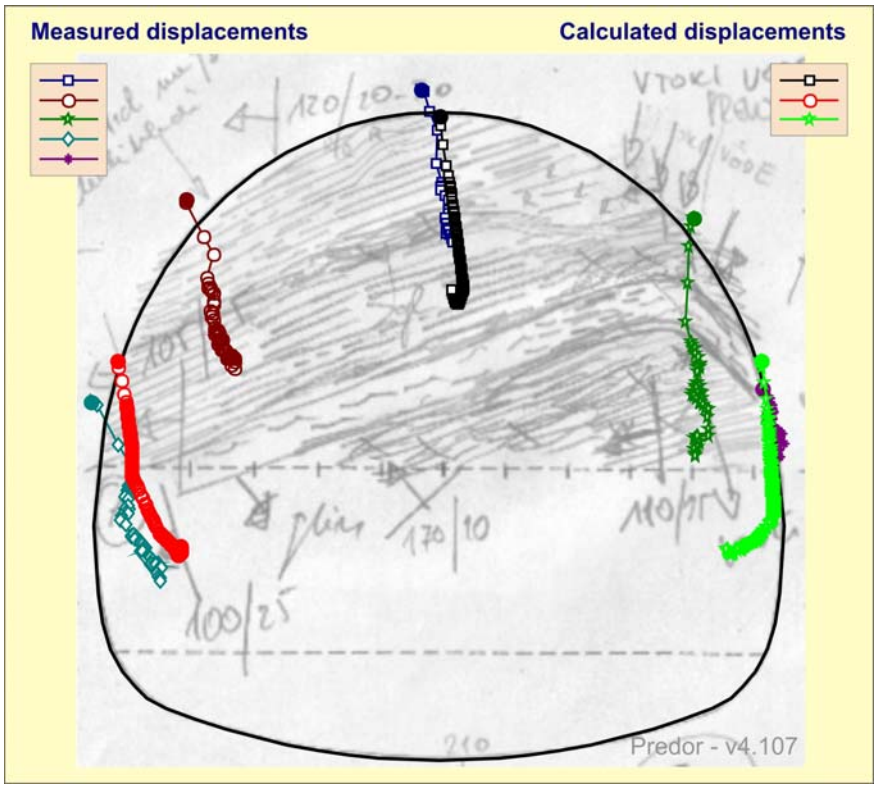

Figure 4-5. Comparison of measured and calculated displacements with Jointed rock parameters from Fig. 4-3 in measuring section MS6 at chainage km 1.1+23.2 in the right tube of the Šentvid tunnel.

Slika 4-5. Primerjava izmerjenih in izračunanih pomikov z "Jointed rock" materialnimi parametri iz slike 4-3 v merskem prerezu MS6 na stacionaži km 1.1+23.2 v desni cevi predora Šentvid.

The calculated displacement vectors satisfactorily match the monitored behaviour, only the displacements along the discontinuity direction after the ring closure are more pronounced for the right sidewall point and also for the crown point where such alteration of the displacement vector orientation was not observed.

4.2.2 The Trojane tunnel

In further analysis the suitability of low value of the shear modulus was studied also for foliated rock mass with worse mechanical characteristics than in the case of the Šentvid tunnel. Since no longer sections with dip parallel to the tunnel axis were mapped either in the Trojane or in the Golovec tunnel, the decision was taken to analyse two cross sections in the Trojane tunnel where local folds in tunnel scale were observed during excavation.

The geological situation is characterized by local kink-fold syncline in case 1 (measuring section MS81 at chainage km 81+957 in the northern tube – excavation from west) and by local kink-fold anticline in case 2 (measuring section MS42 at chainage km 81+957 in the northern tube – excavation from west). Both cases are shown in Fig. 4-6. The orientation of these folds corresponds to the prevailing E-W oriented Sava folds in the area of the Trojane tunnel (Schubert P. et al, 2005), as schematically shown in Fig. 4-6. The axis of the fold dips in both cases from the upper right crown to the lower left invert of the tube and is nearly parallel to the tunnel axis.

Displacement patterns in these two cases are characterized by non-symmetric displacements (direction and magnitude), but having fairly constant direction throughout the construction process. Displacement vector of the crown point tends towards right in the direction of the fold axis in both cases; major difference is the magnitude of displacements on both sidewalls. Based on face logs in the vicinity it was concluded that the south dipping limb of the fold (surface of red colour in Fig. 4-6) is probably weaker then the north dipping limb (surface of green colour), since it was more exposed to shear and extension in the folding process (local faults and quartz veins were far more frequent in the south dipping limb). The north limb lies sub-parallel to the stressing and is thus more exposed to sliding along the discontinuities (Schubert P. et al, 2005). This explains larger displacements of wall points in the south dipping limb.

According to these observations and generally weaker soft foliated rock mass than in the Šentvid tunnel, the strength and stiffness material parameters are lower than in the previously discussed analysis for the Šentvid tunnel. Initial elastic moduli were thus determined as half of the moduli in the Šentvid tunnel (ratio E_1:E_2 was kept at 2:1) and friction angle along the discontinuities was decreased to 15° in case 1 (overburden of about 140 m as seen in Fig. 2-4).

As the Jointed rock constitutive model does not comprise stress dependent stiffness parameters, elastic moduli were additionally decreased in case 2, where the overburden is only 40 m. Reduction of the moduli was assessed on the basis of equation for the calculation of stress dependent elastic

modulus in Hardening soil model (Brinkgreve et al, 2000). For the depth difference of 100 m (from 140 to 40 m) the elastic modulus reduces to 1/3 of the value at the depth of 140 m.

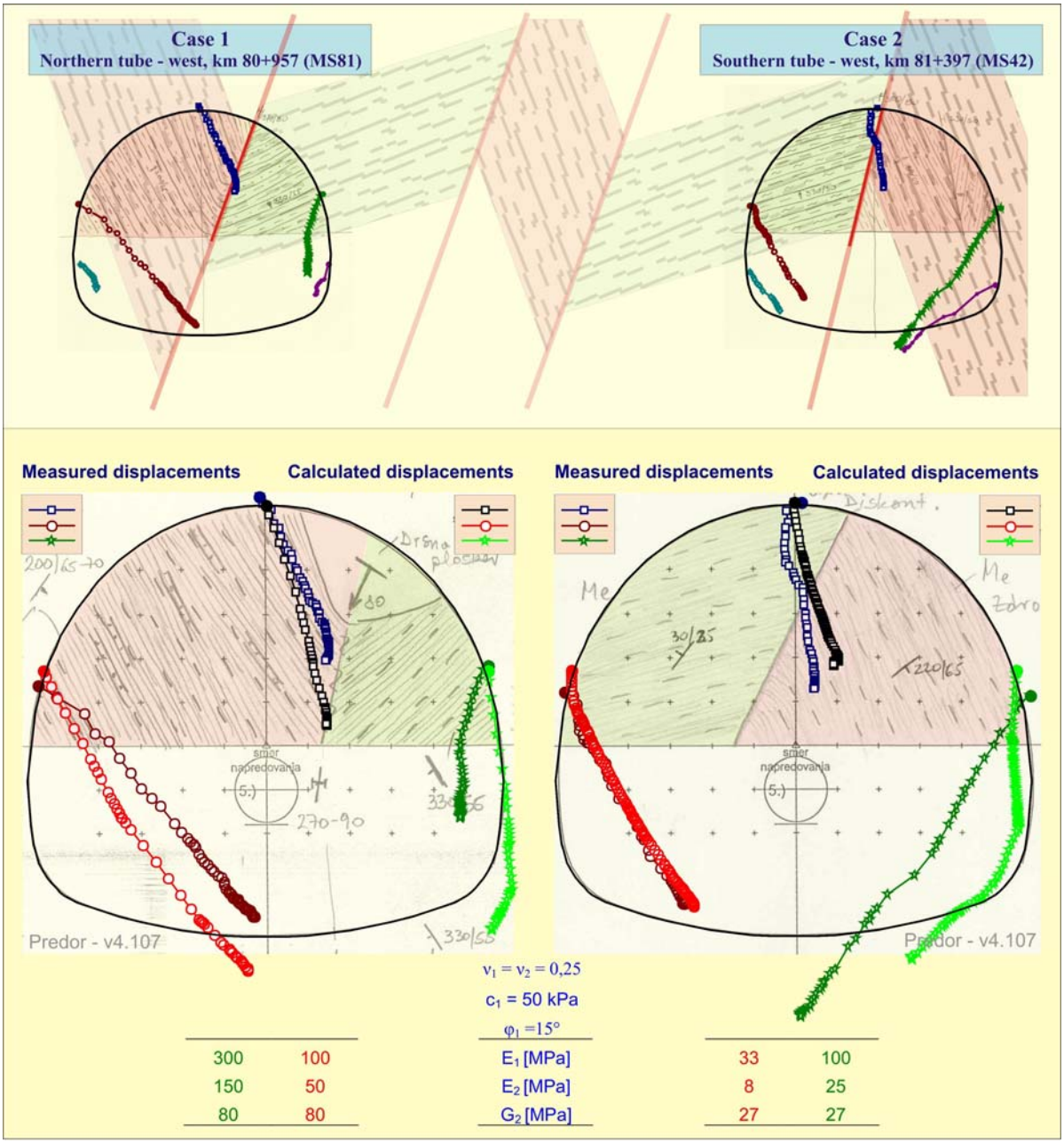

Figure 4-6. Characteristic displacement patterns in the local folds (anticline and syncline) in the top and comparison of measured and calculated displacements with the Jointed rock constitutive model in the Trojane tunnel in the bottom.

Slika 4-6. Karakteristični deformacijski vzorec v primeru lokalnih antiklinalnih in sinklinalnih gub (zgoraj) ter primerjava izmerjenih in izračunanih pomikov z "Jointed rock" konstitutivnim modelom v predoru Trojane (spodaj).

Initial calculations were performed with shear modulus of 5 MPa and the obtained response was rather different from the measured (much larger displacements and irregular displacement vectors). Then shear moduli were increased and finally set to isotropic values as calculated from the elastic modulus E_1 of the north dipping limb to simulate the effect of crushed rock mass to the extent that it behaves almost like an isotropic medium. The calculated response matches satisfactorily the measured displacement vectors in both cases at the left sidewall and in the crown and it differs significantly in direction and magnitude at the right sidewall, especially in case 2. Unlike in the Šentvid tunnel, the geological situation in these two cases is far more complex and it is unrealistic to expect a perfect match. Final back calculated material parameters for Jointed rock constitutive model in the Trojane tunnel are given in the bottom part of Fig. 4-6.

4.2.3 Comments

2D back calculations in the right tube of the Šentvid tunnel showed that the Hardening soil constitutive model, which was successfully applied in several back analysis calculations of cases at the Trojane tunnel (Gogala, 2001; Vukadin, 2001; Miklavžin, 2001), can not model satisfactorily the response in case of the Šentvid tunnel, not even in regions where anisotropic behaviour was not well pronounced. On the other hand, the Jointed rock constitutive model proved to be appropriate. Back calculated values of elastic moduli in both directions are related to measured stiffness parameters, while low value of shear modulus $G_2 = 5$ MPa causes deformation of the rock mass in the foliation direction and enables proper modelling of the tunnel response.

On the other hand, the Trojane tunnel also runs through foliated rock mass, but its mechanical properties are worse due to intensive tectonics and weathering processes, especially in the eastern part, than in the Šentvid tunnel. Although anisotropic behaviour is evident from Fig. 4-6, the best match of the calculated and the measured response was obtained with isotropic value of the shear modulus, which confirms the predominant influence of the "BIMrock" structure rather than the foliation influence on the displacements. However, it should be emphasized that the presented back calculated values can be treated solely as approximate since a two-dimensional analysis was performed in a cross section with a strike which is not parallel to the tunnel axis and thus the effect of the approaching and digressing face was not considered. The intention of the latter analysis was just to investigate the influence of the shear modulus magnitude in different ground conditions.

4.3 Displacements in the longitudinal direction

During the analysis of the measured displacements in the Trojane tunnel, a longer section of the displacements in the excavation direction attracted our attention. The section was situated under a declined

slope towards the valley. Similar situation was observed also for the Golovec tunnel. The change in the displacement vector orientation from »normal« to the excavation direction occurred when the tunnel alignment passed the top of the hill. Large longitudinal displacements in the excavation direction were recognized also in the Jasovnik, Ločica and Podmilj tunnels and in another section in the Trojane tunnel.

4.3.1 Literature review

Unlike the radial displacements, the longitudinal displacements cannot be predicted using analytical functions; their shape and magnitude do not follow the proposed solution. Use of longitudinal displacements in geological – geotechnical interpretation of the tunnel response was neglected for quite a long time.

Since the construction of the railway tunnel Inntaltunnel in Austria more attention has been focused on the longitudinal displacements. While approaching an extensive fault zone, a remarkable variation of the longitudinal displacements was observed by Schubert (1993). Before entering a heavily faulted rock mass, the longitudinal displacements of average magnitude of 80 millimetres with a peak at 170 millimetres in the crown and 100 mm on both sidewalls against the excavation direction were measured. Similar behaviour was observed also in the railway tunnel Galgenberg in Austria while approaching and entering two extensive fault zones (Schubert et al, 1995). The relative increase of the observed longitudinal displacements while approaching fault zones was considerably higher than the relative increase in radial displacements, indicating the area of comparatively low stress ahead of the face.

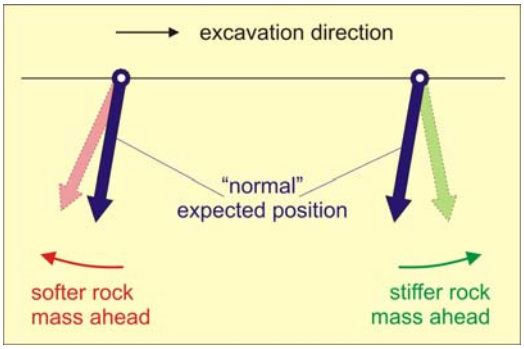

Figure 4-7. Influence of the stiffer or softer rock mass ahead of the tunnel face on the deviation of the spatial displacement vector orientation from the "normal" position

Slika 4-7. Vpliv območja hribine z večjo ali manjšo togostjo pred čelom predora na odklone vektorja pomikov od "normalnega" položaja.

Several numerical simulations were carried out (Steindorfer, 1998) to explain the observed phenomenon and to learn lessons for future projects. Analysis of the performed numerical calculations

showed that the spatial displacement vector orientation (the ratio between longitudinal and radial displacements) is an appropriate indicator for the determination of the discontinuities in the rock mass structure well ahead of the tunnel face. Based on these findings and measured displacements the deviation of the spatial displacement vector orientation of 8°-12° against the excavation direction was defined as "normal" or expected behaviour (Schubert et al, 2002). Other studies defined as "normal" somewhat higher angle of deviation – 15° against the excavation direction (Jeon et al, 2005).

When approaching softer rock mass ahead of the face, the spatial displacement vector orientation deviates from "normal" position even more against the excavation direction, while it deviates from the "normal" position towards the face or even in the excavation direction if approaching the stiffer rock mass as presented in Fig. 4-7. Numerical simulations also indicate that shortly after the excavation of the round length the displacement vectors point in excavation direction, but during further excavation they change to opposite direction (Steindorfer, 1998).

Depending on the primary stress state and the differences in the rock mass stiffness, the analysis of the spatial displacement vector orientation enables the prediction of softer or stiffer material 1 – 2 diameters of the tunnel tube ahead of the face (Steindorfer, 1998; Jeon et al, 2005).

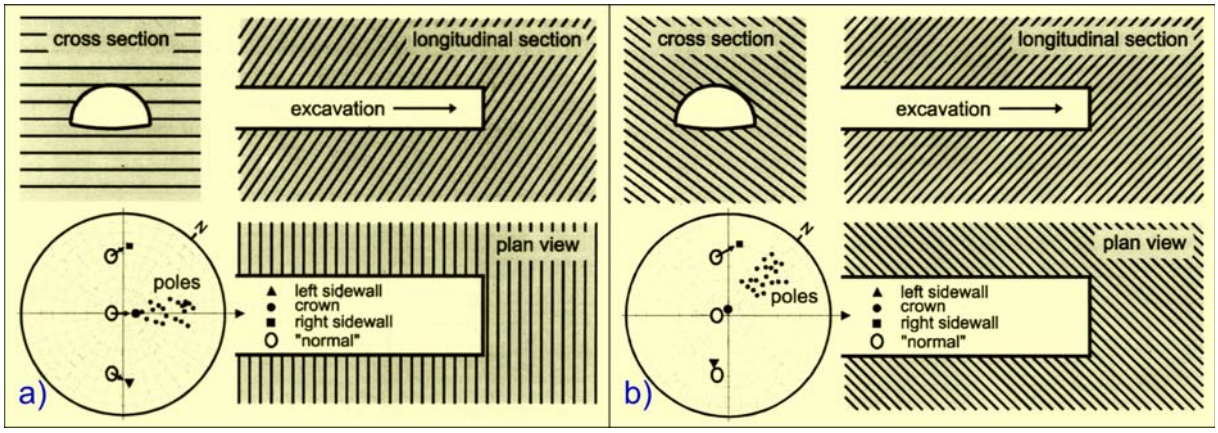

Figure 4-8. Typical development of displacement vector orientations when tunnelling against dip (Steindorfer, 1998); a) discontinuities strike perpendicular to the tunnel axis, b) discontinuities strike from left to right hand side.

Slika 4-8. Značilni deformacijski vzorec orientacije vektorja pomikov pri izkopu predora proti vpadu diskontinuitet (Steindorfer, 1998); a) diskontinuitete vpadajo pravokotno na os predora, b) diskontinuitete vpadajo od leve proti desni strain predora.

Additionally Steindorfer (1998) described in his thesis some typical deformation patterns that were observed in fault zones of the Inntal and Galgenberg tunnels in Austria. Rock mass of these sections

consists of moderately to highly fractured schists and phyllites. Steindorfer observed that in such cases schistosity governs the deformation pattern of the tunnel circumference, while faults, joints and other discontinuities influence the deformation process only locally. As denoted by Steindorfer, "the analyses have to be characterized as preliminary studies only", since only limited amount of data was available at that time. Monitoring data are presented with stereonet (poles of dominating discontinuity planes together with displacement vector orientations of the crown and both sidewall points) for sections with similar dip direction and dip angle of the discontinuities with regard to the tunnel axis.

Typical developments of displacement vector orientations when tunnelling against dip are presented in Fig 4-8 (Steindorfer, 1998). In the left hand side plot discontinuity planes strike more or less perpendicular to the tunnel axis and dips approximately 20° to 70° against the direction of the excavation. The orientation of the displacement vectors of crown and both sidewall points tend to point slightly in the direction of the excavation. In case b) - the right hand side plot - discontinuity planes strike from left to right sidewall with similar dip as in the first presented case.

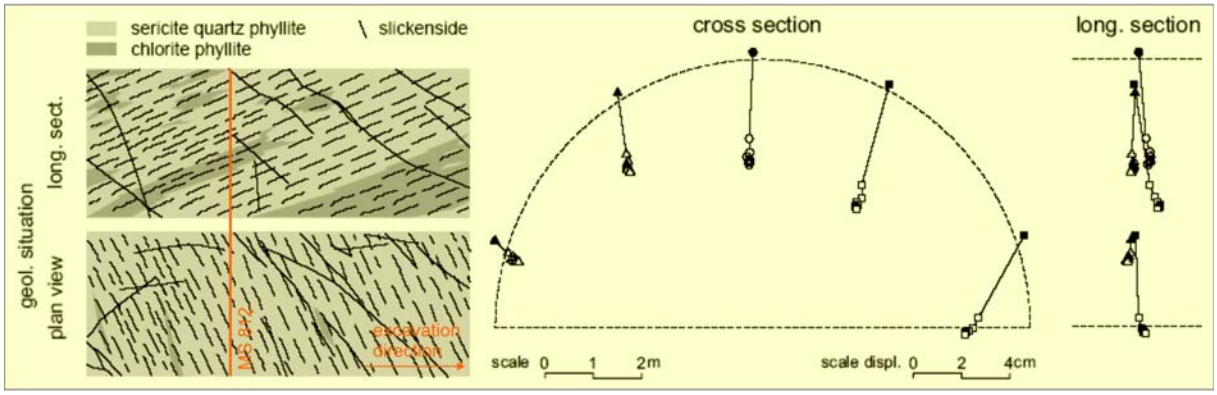

Figure 4-9. Geological situation and displacement vector plot in cross and longitudinal section; Tauerntunnel, heading north, MS 812 (face position 32m ahead) (Grossauer, 2009)

Slika 4-9. Geološka situacija in izris vektorjev pomikov v prečnem in vzdolžnem prerezu; Tauerntunnel, izkop s severa, MS 812 (položaj čela 32 m naprej) (Grossauer, 2009)

The displacement vector of the right sidewall target tends to point visibly in the direction of the excavation (Steindorfer, 1998). The same pattern can also be ascribed to the crown point, but the phenomenon is less pronounced. No magnitudes of the displacements are given in the presented thesis.

The same deformation pattern as in case b) is described also by Grossauer (2009) for the Tauerntunnel (Fig. 4-9) and Wienerwaldtunnel in Austria. In a tunnel section composed of phyllite with a foliation flatly dipping against the excavation direction and striking the tunnel with around 15°

from left to the right, the crown and the right sidewall point moved in the excavation direction. The magnitude of longitudinal displacements in the excavation direction amounts up to 0.5 cm and displacement vector orientation is less than 10° in the excavation direction for all measuring sections in the presented area of the Tauerntunnel (geological situation in the left hand side of Fig. 4-9).

The presented case histories in the Inntal and Galgenberg tunnels (Steindorfer, 1998) and in Tauerntunnel (Grossauer, 2009) show that when tunnelling against dip in anisotropic ground conditions, the displacement vectors can point also slightly in the excavation direction.

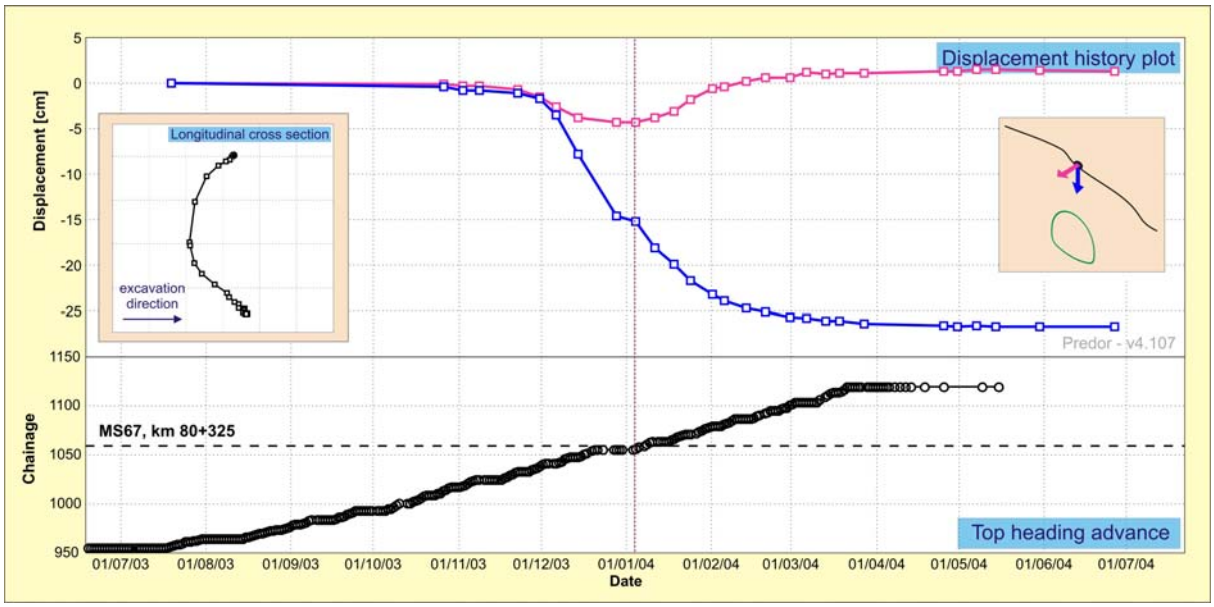

Figure 4-10. Curves of vertical and longitudinal displacement for the point above the left tube axis of the Trojane tunnel (MS67 at chainage km 80+325).

Slika 4-10. Časovni potek vertikalnih in vzdolžnih pomikov merske točke na površini v osi leve cevi predora Trojane (merski profil MS67 na stacionaži km 80+325).

The magnitude of the measured longitudinal displacements in reviewed literature is in the range from a few millimetres to 170 millimetres in the Inntaltunnel against the excavation direction. Only a few reports were found on the longitudinal displacements in the excavation direction; the magnitude of the reported displacements is up to 30 millimetres (Moritz et al, 2002) in the case of the Lainzer tunnel (section was situated in a weak zone with large settlement that occurred according to authors due to the tilting and sinking of the section of the tunnel tube where the ring was not closed due to lack of adequate foundation or ground strength (Moritz et al, 2002)).

In contrast to “normal” behaviour of tunnel points in the longitudinal direction, a “normal” behaviour of the target on the surface exhibits characteristic two-phase response (displacement curve

of pink colour in Fig. 4-10) in case of stable (horizontal) surface above the tunnel. When the tunnel face approaches the measuring section, the displacement vector points in the direction of nearing face and tends vertically down when tunnelling just beneath the monitored target. With further face advance the displacement vector "follows" the excavation direction (Fig. 4-10).

4.3.2 Case studies

4.3.2.1 The Trojane tunnel

The excavation from the western portal started from an unstable slope with heavy retaining walls and continued into a hill with maximum overburden of approximately 45 m (Fig. 4-11). After 300 m the tunnel alignment passes the top of the hill and approaches the Učak valley, which presents a major fault zone striking N – S (Budkovič et al, 2005).

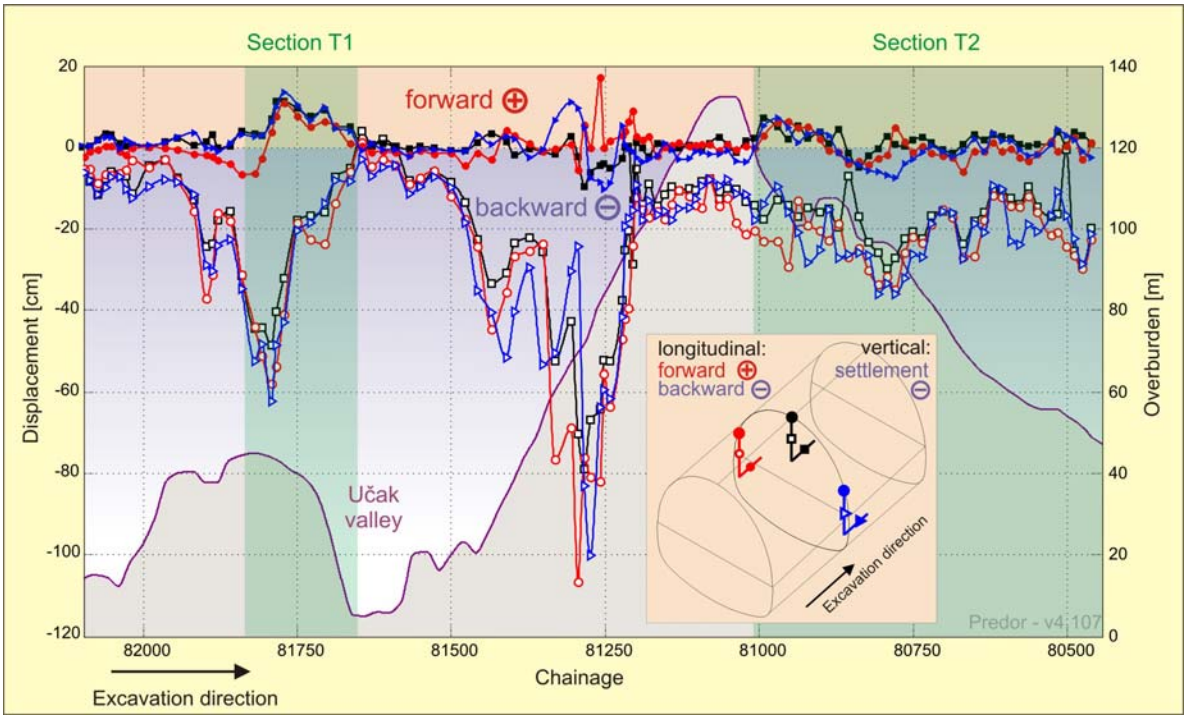

Figure 4-11. Contour of measured vertical and longitudinal displacements in the southern tube of the Trojane tunnel (excavation from western portal) with plotted overburden; sections of the longitudinal displacements pointing in the excavation direction are highlighted in green.

Slika 4-11. Kontura izmerjenih vertikalnih in vzdolžnih pomikov v južni cevi predora Trojane (izkop iz zahoda) z izrisanim nadkritjem; območji izmerjenih vzdolžnih pomikov v smeri napredujočega čela sta obarvani zeleno.

As soon as the excavation face passed the point with maximum overburden, the measured longitudinal displacements of the observation points on the tunnel circumference changed the direction from "normal" into the excavation direction. When tunnelling under the decreasing overburden, the vertical displacements decreased (Fig. 4-11), while in the excavation direction unanticipated magnitudes of the longitudinal displacements were measured: maximum longitudinal displacement of 14.2 cm of the crown point in measuring section MS30 at chainage km 81+674 in northern tube (Fig. 4-12). Spatial displacement vector orientation constantly increased from "normal" position to nearly 40° towards the Učak valley (Fig. 4-13 – last value of L/S of almost 70° in the section T1 is already influenced by the Učak valley – significant longitudinal displacements and almost no settlements). Similar range of the displacement was observed also in the southern tube (Fig. 4-11). Considerable circumferential cracks were registered in the tunnel lining at the beginning of this section (Schubert P. et al, 2005). Longitudinal displacements oriented back to normal in the Učak valley, where the tunnel crown runs only 2 m below the ground and uplift of the measuring points in the tunnel lining of maximum of 2.5 cm was measured.

The described behaviour was observed in both tubes over considerable length (chainage km 81+840 to km 81+660 in southern tube - section length 180 m (green area T1 in Fig. 4-11) and chainage km 81+760 to km 81+615 in northern tube - section length 145 m (green area T1 in Fig. 4-13).

Area of a very stiff rock mass would be expected ahead of the tunnel face according to the reviewed literature, as the displacement vector tends considerably in the direction of further excavation. However, the geological interpretation (Budkovič et al, 2005) does not confirm this. On the contrary: as already stated, the Učak valley presents a major fault zone. The phenomenon could then be explained by the combination of the ground morphology (declining surface towards the Učak valley), the dip and strike of foliation and possible residual stresses due to intense tectonics. Another section with the displacements in the excavation direction in the Trojane tunnel is marked green in Fig. 4-11 and named T2.

After passing the Učak valley, the tunnel runs into a hill with a maximum overburden of 140 m. At chainage km 81+350 the tunnel excavation face of the left tube entered a fault zone where vertical displacements of up to 110 cm were measured (Fig. 4-11). In this section the maximum longitudinal displacement in the Trojane tunnel in the excavation direction was measured: 17.2 cm of the left side wall point in MS50 at chainage km 81+258. Since the measuring points on the right side wall and in the crown in the same MS pointed against the excavation direction with magnitude of up to 10 cm, the

observed behaviour can be explained by rotation of the tunnel walls (Schubert P. et al, 2005), which is influenced by local geological conditions.

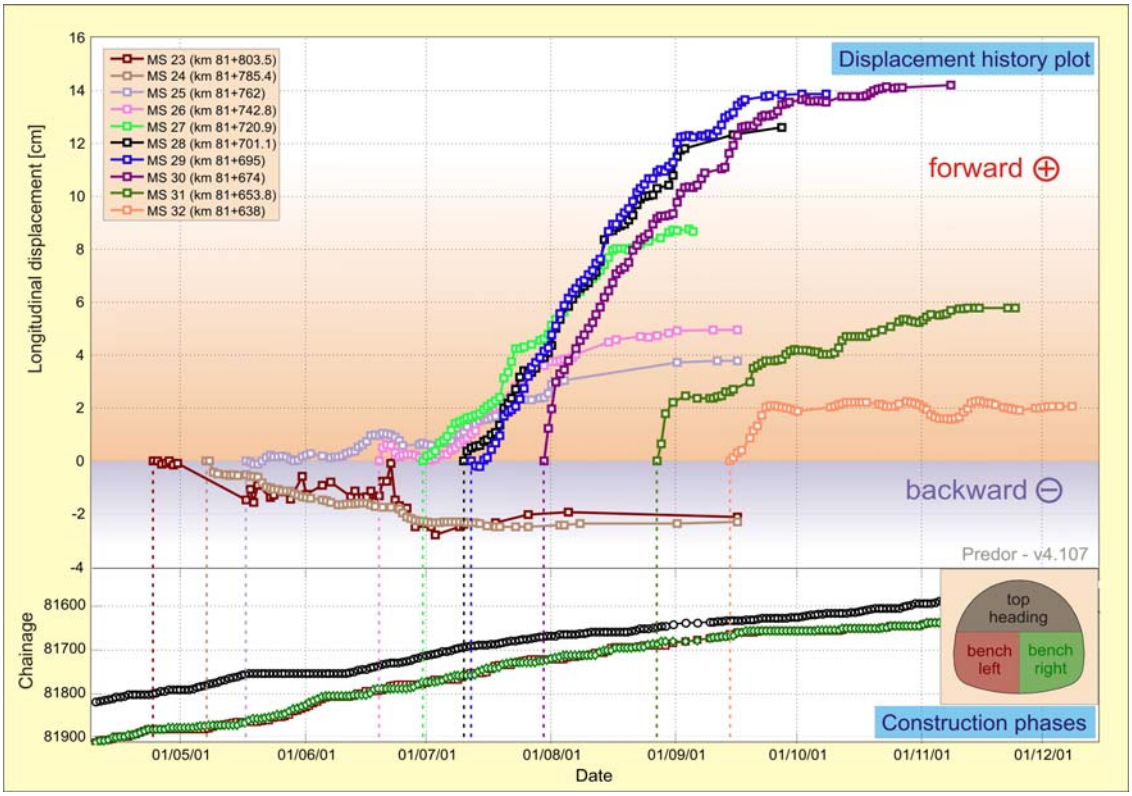

Figure 4-12. Displacement history plot of longitudinal displacements of the crown points in MS23 to MS32 in the northern tube of the Trojane tunnel (plot at the top) and excavation faces advance plot (bottom plot). The location of MS's can be seen from Fig. 4-11.

Slika 4-12. Krivulje časovnega poteka vzdolžnih pomikov stropnih točk v prerezih MS23 do MS32 v severni cevi predora Trojane (izkop iz zahoda) na zgornjem delu slike ter napredki posameznih izkopnih čel na spodnjem delu. Položaj merskih profilov je razviden s slike 4-11.

When the tunnel alignment passed the chainage of the top of the hill (km 81+000), the measured longitudinal displacements again turned into the excavation direction (denoted as section T2 in Fig. 4-13). This alteration occurred at a considerably higher overburden (approximately 135 m) than in section T1. The magnitude of longitudinal displacements in section T2 is lower, up to 7.3 cm. Although individual measuring points in section T2 exhibited longitudinal displacements against the excavation direction, the majority of the points moved in the excavation direction when tunnelling under the decreasing overburden towards the Trojane village. Local geological conditions (fault zones, folds, alterations in the geological structure) most likely caused the oscillations of the longitudinal displacement vector orientation from its general direction into the excavation direction.

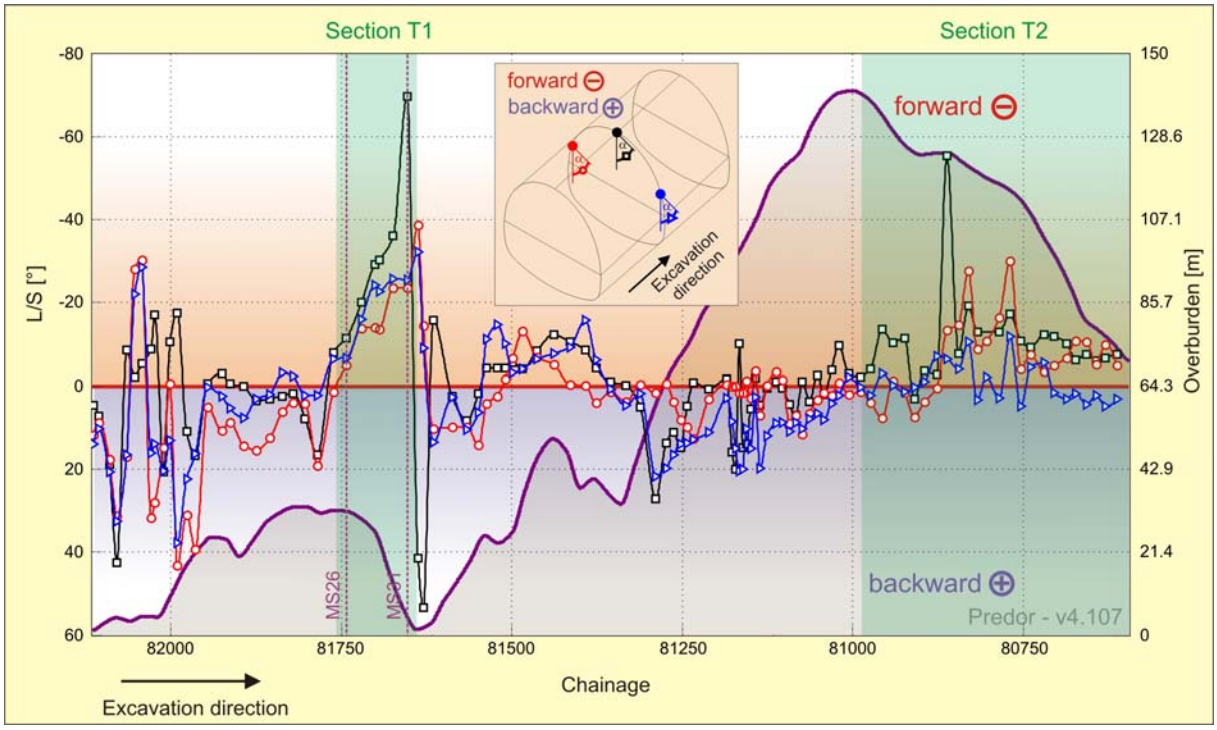

Figure 4-13. Contour of the displacement vector orientation (L/S) in the northern tube of the Trojane tunnel with plotted overburden (excavation from western portal); sections of the longitudinal displacements pointing in the excavation direction are highlighted in green.

Slika 4-13. Kontura orientacije vektorja pomikov (L/S) v severni cevi predora Trojane (izkop iz zahoda) z izrisanim nadkritjem; območja izmerjenih vzdolžnih pomikov v smeri napredujočega čela so obarvana zeleno.

The length of section T2 is approximately 650 m in the southern tube (chainage km 81+050 – km 80+400) and 330 m in the northern tube (chainage km 80+980 – km 80+650). The excavation from western portals was stopped at these chainages.

In Fig. 4-12 an interesting situation is presented with the displacement history plots. No major displacements in the longitudinal direction were measured on monitoring points in MS25 and MS26 until the beginning of July 2001 and small longitudinal displacements against the excavation direction were measured in MS23 and MS24, situated just before section T1. At this time the top heading face was approximately 50 m farther away from MS25 and the bench excavation face was approaching the cross section but was still 20 m away.

The measured longitudinal displacements then started to accelerate, which was not the case in previous measuring sections. Presumably the further top heading excavation well away from these measuring sections influenced their behaviour and also resulted in large longitudinal displacements that were

measured in next 4 measuring sections from MS26 on. Since similar behaviour was noticed in both tubes, excavated in this area almost simultaneously at mutual distance of 40 m, the influence of the excavation of the southern tube can be excluded as the cause for the observed behaviour. The magnitude of the longitudinal and vertical displacements decreased when approaching the Učak valley. Longitudinal as well as vertical displacement rates did not converge to zero for a long time after the ring closure.

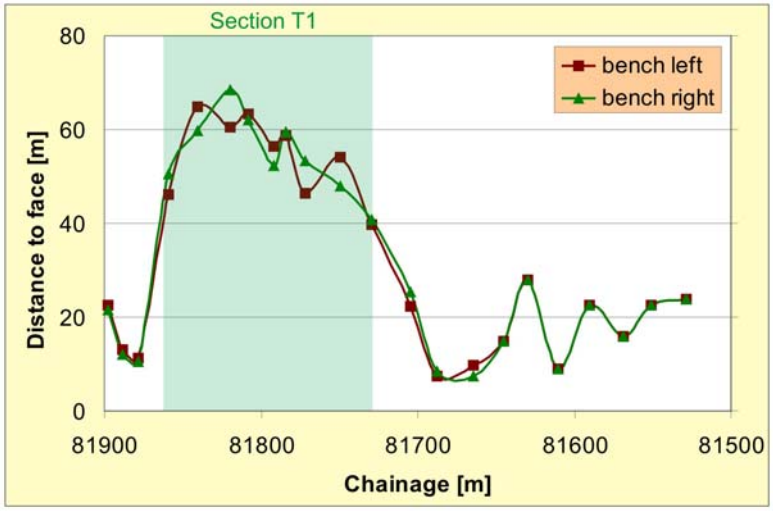

Figure 4-14. Distance between the bench/invert excavation face and measuring section when the latter can be considered as stabilised in the area of section T1 in the southern tube of the Trojane tunnel.

Slika 4-14. Razdalja med točko dokončanja celotnega podpornega obroča in merskim profilom, ko se le-ta lahko smatra za umirjenega, v območju T1 v južni cevi predora Trojane.

When plotting the distance between the bench and the invert excavation face that followed immediately after the bench excavation (ring closure) and the measuring cross section when the measuring section can be considered as stabilised, the distance increased from the range of 10 to 20 m for the measuring sections before section T1 to the range of 50 to 70 m for the measuring sections within section T1 (Fig. 4-14). The mentioned distance decreased again to "normal" values at the measuring sections ahead of section T1. The influence of the construction of the other tube can be excluded for the same reasons as mentioned above. A reason for the described behaviour could be the activation of the complete hill towards the Učak valley, especially if the foliation of the rock mass was parallel to the slope and the displacements would occur due to the sliding in between the foliation planes.

Geological structure in section T1 is rather chaotic. Rock mass is faulted to high extent with fault gouge in faults. Geological situation was somewhat better in section T2. The dominating dip of the

foliation with regard to the tunnel tubes can be assessed and dips in both sections T1 and T2 into the excavated area with approximate angle of 45° as shown in face log in Fig. 4-15. In the excavated top heading faces local folds were frequently observed (Schubert P. et al, 2005).

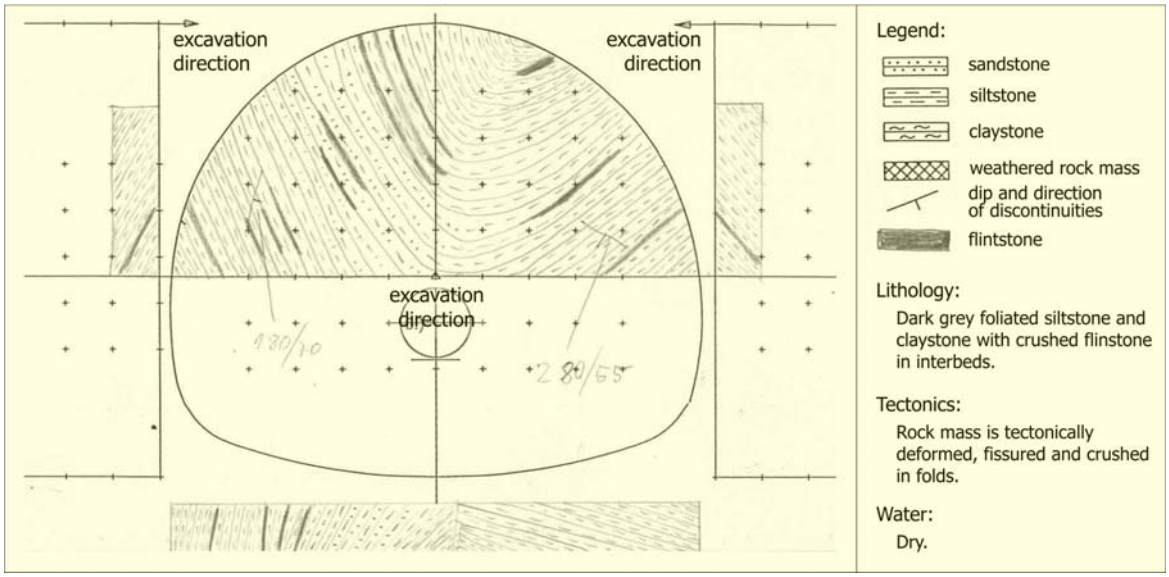

Figure 4-15. Face log at the chainage km 80+947 in the northern tube of the Trojane tunnel (section T2).

Slika 4-15. Geološka skica izkopnega čela kalote na stacionaži km 80+947 v severni cevi predora Trojane (območje T2).

If the complete hill was activated, the displacement downwards the slope could be measured. Since an extensive monitoring scheme of the surface above the tunnel was established, luckily an area above sections T1 and T2 was also partly monitored, though the monitoring of surface displacements was mostly performed in populated regions. One wide cross section with 12 measuring points covering 60 m from each of the tunnel tubes (at chainage km 80+634 and at overburden of 45 to 75m as shown in Fig. 4-16) was installed at the end of section T2 (27 m from the breakthrough point of the northern tube in the direction of western portal).

Measured vertical displacements (green line in the left plot in Fig. 4-16) followed the expected settlement line (the largest settlement above the tunnel tubes – up to 16 cm, settlements decrease with increasing distance from both tunnel tubes and reduce to zero at the most distant points), while the longitudinal displacements (violet line in the left plot in Fig. 4-16) are rather uniform, ranging from 3 to 8.5 cm. The comparison of the displacement history plot of the longitudinal displacements (the upper right plot) with construction phases plot (the lower right plot) indicates that the surface movements were induced by tunnelling.

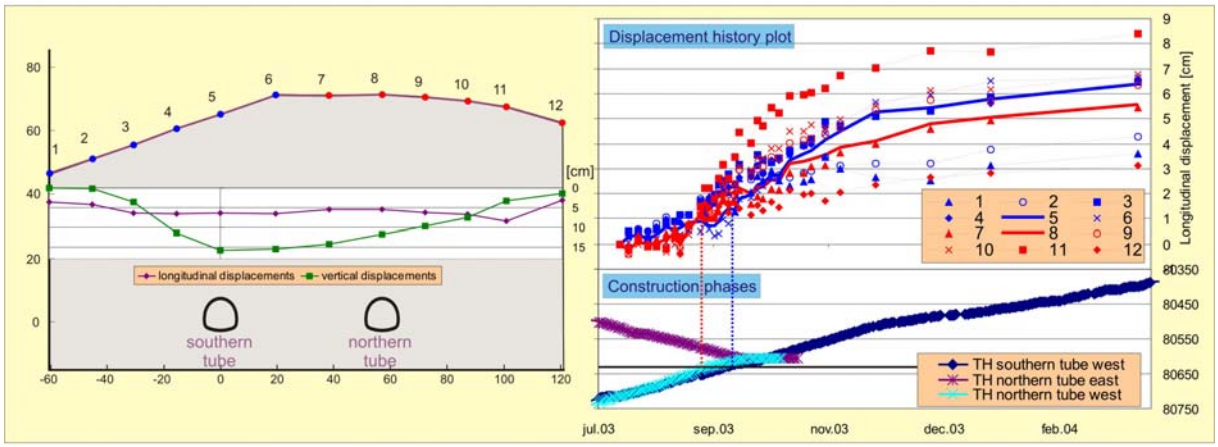

Figure 4-16. Contour of vertical and longitudinal displacements of surface measuring profile in km 80+634 (left); displacement history plot of longitudinal displacements of the same points above the Trojane tunnel with the advance of construction phases (right).

Slika 4-16. Kontura vertikalnih in vzdolžnih pomikov površinskega merskega profila na stacionaži km 80+634 (levo); časovni potek vzdolžnih pomikov točk omenjenega profila z napredkom izkopnih čel (desno).

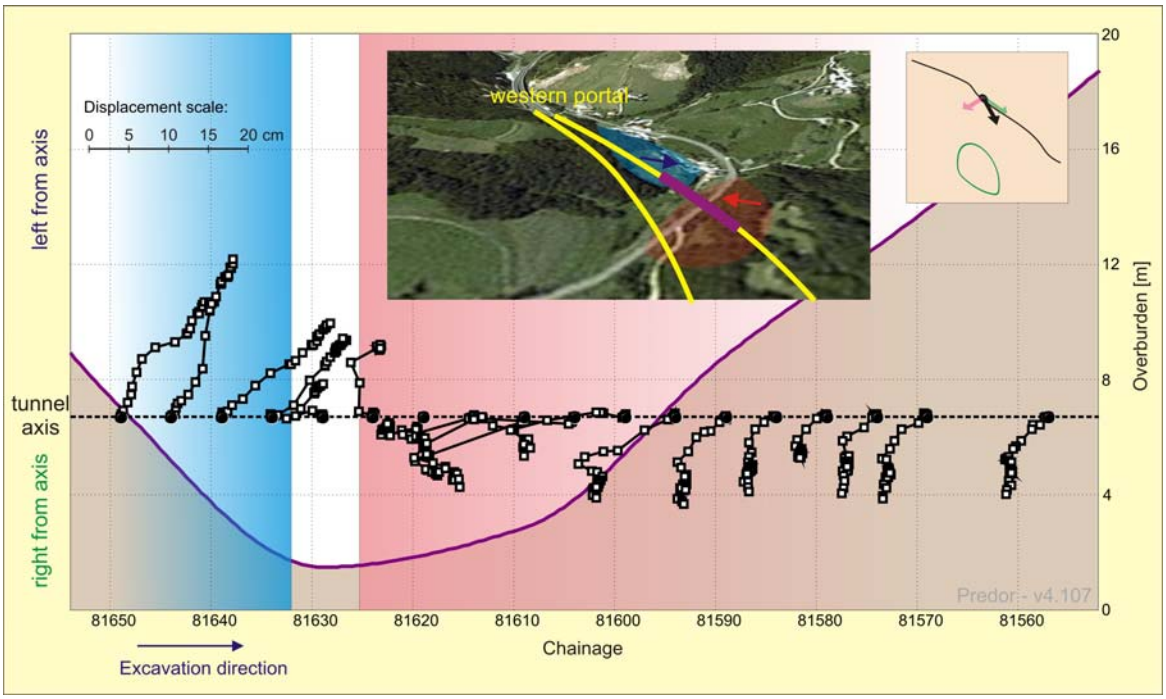

Figure 4-17. Plan view of the displacement vectors of surface points in the axis of the northern tube of the Trojane tunnel in the vicinity of the Učak valley with plotted overburden.

Slika 4-17. Tlorisni izris vektorjev pomikov površinskih točk v osi severne cevi predora Trojane v območju Učaka z izrisanim nadkritjem.

Similar deformation pattern can also be recognized at the area close to the Učak valley. Unfortunately, not the complete section was monitored, only a 100 m long part where the tunnel runs very close to the surface, as shown in Fig. 4-17 for the right tube. The slope before the valley is dipping to north-east (area of blue colour in Fig. 4-17; slope direction is marked with a blue arrow). The displacement vectors pointed in the same direction, which in some way suggests that the sliding of the slope towards the valley occurred due to tunnel excavation. Similar explanation can be suggested for the area onwards of the valley.

4.3.2.2 The Golovec tunnel

During the analysis of the measured displacements of the Golovec tunnel (Šlibar, 2005) quite a long section of longitudinal displacements in the excavation direction was identified.

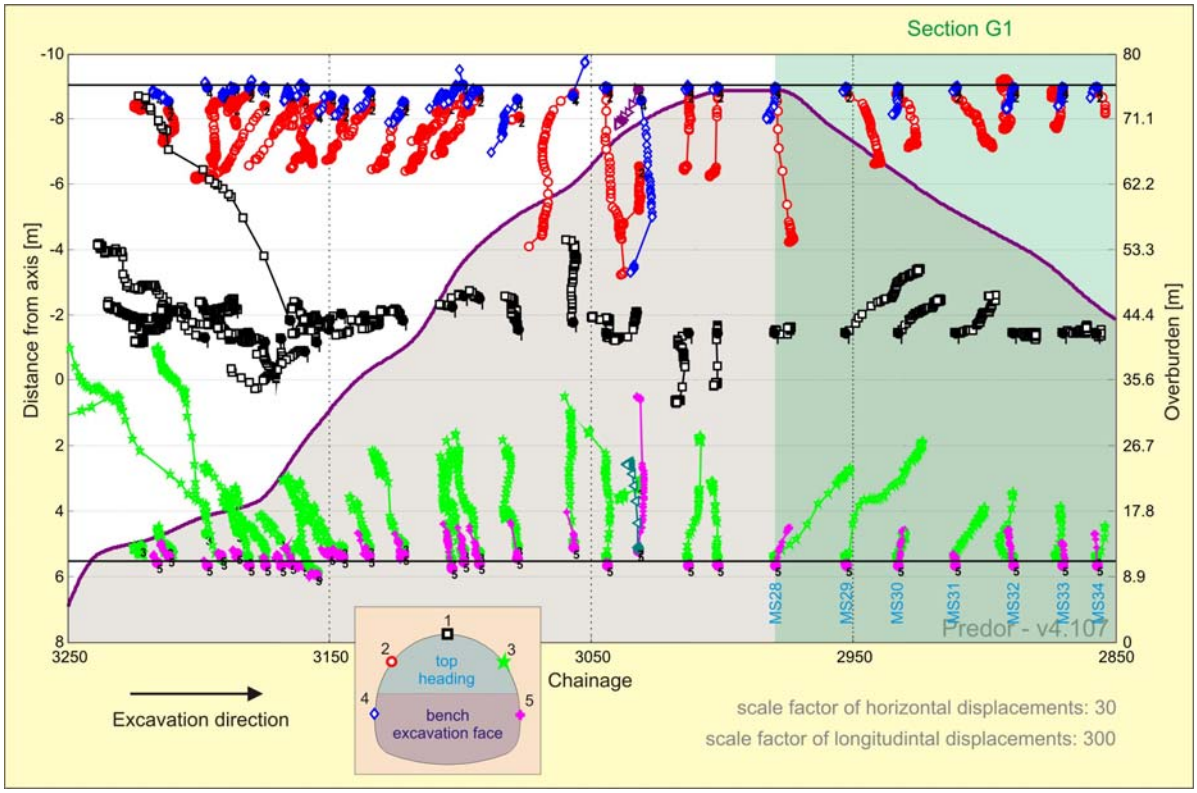

Figure 4-18. Plan view of the displacement vectors (horizontal and longitudinal displacements) in the eastern tube of the Golovec tunnel (excavation from the southern portal) with plotted overburden; section of the longitudinal displacements pointing in the excavation direction is highlighted in green.

Slika 4-18. Situacija vektorjev pomikov (prečni in vzdolžni pomiki) v vzhodni cevi predora Golovec (izkop iz juga) z izrisanim nadkritjem; območje izmerjenih vzdolžnih pomikov v smeri napredujočega čela je obarvano zeleno.

As already mentioned, the excavation of both tunnel tubes started from southern portals with heavy retaining structures that were constructed due to the sliding of the slope above the portals. Sliding and to a high extent tectonized rock mass affected the tunnelling in the first 100 m: a number of roof collapses occurred, large settlements of the tunnel crown up to 80 cm and large longitudinal displacements against the excavation direction up to 23.5 cm were measured, although the excavation of the top heading was split into two side galleries and a core. To overcome these difficulties several measures were undertaken: installation of pipe roof, installation of a temporary invert shortly after the top heading excavation, thicker shotcrete – up to 50 cm instead of the designed 25 cm, shortest possible distance between the top heading excavation face and the ring closure and maintaining face stability with a supporting core and anchors (Popović et al, 2001). These measures reduced displacements to acceptable values and enabled further excavation works.

Approximately 130 m from the southern portals the geological conditions in the area of the tunnel tubes somewhat improved. The alternation of layers of sandstone and siltstone dipping south and southeast with approximate angle of 30° (Fig. 2-14) were observed almost to the northern portal (Beguš et al, 2000). Better geological and geotechnical conditions resulted in smaller vertical as well as longitudinal displacements. When the tunnel alignment passed the top of the Golovec hill, the displacement vectors of the measuring points turned in the excavation direction (Fig. 4-18).

Figure 4-19. Distance between the bench excavation face and the measuring section when the latter can be considered as stabilised in the area of section G1 in the eastern tube of the Golovec tunnel.

Slika 4-19. Razdalja med točko dokončanja celotnega podpornega obroča in merskim profilom, ko se le-ta lahko smatra za umirjenega, v območju G1 v vzhodni cevi predora Golovec.

The length of section G1 with measured longitudinal displacements in the excavation direction is 130 m in the western tube (km 2+970 to km 2+860 – MS29 to MS35) and 140 m in the eastern tube (chainage km 3+000 to km 2+860 – MS28 to MS34). The excavation from the southern portals was finished at the end of these sections. Though the measured longitudinal displacements in the excavation direction were generally smaller than in the Trojane tunnel, the maximum measured longitudinal displacement was nearly the same (14.1 cm for the crown point in MS32 at chainage km 2+897 in the western tube).

Due to unstable slopes the assumption of the movement of the northern slope of the Golovec hill towards the northern portal together with the tunnel tubes would be possible, if the dip of the layers was towards north and some major sliding between these layers occurred. Some surface monitoring points were situated above both tunnel axes and in between in the area from the top of the Golovec hill and the breakthrough point, as shown in Fig. 4-20. The tunnelling induced large settlements up to 40 cm and longitudinal displacements up to 30 cm. Displacements in the slope direction are highest at the end of section G1 (lower part of the monitored slope) and represent the needed deformation for the activation of ground shear resistance in order to reach the new equilibrium state of the surrounding rock mass after the excavation of the tunnel.

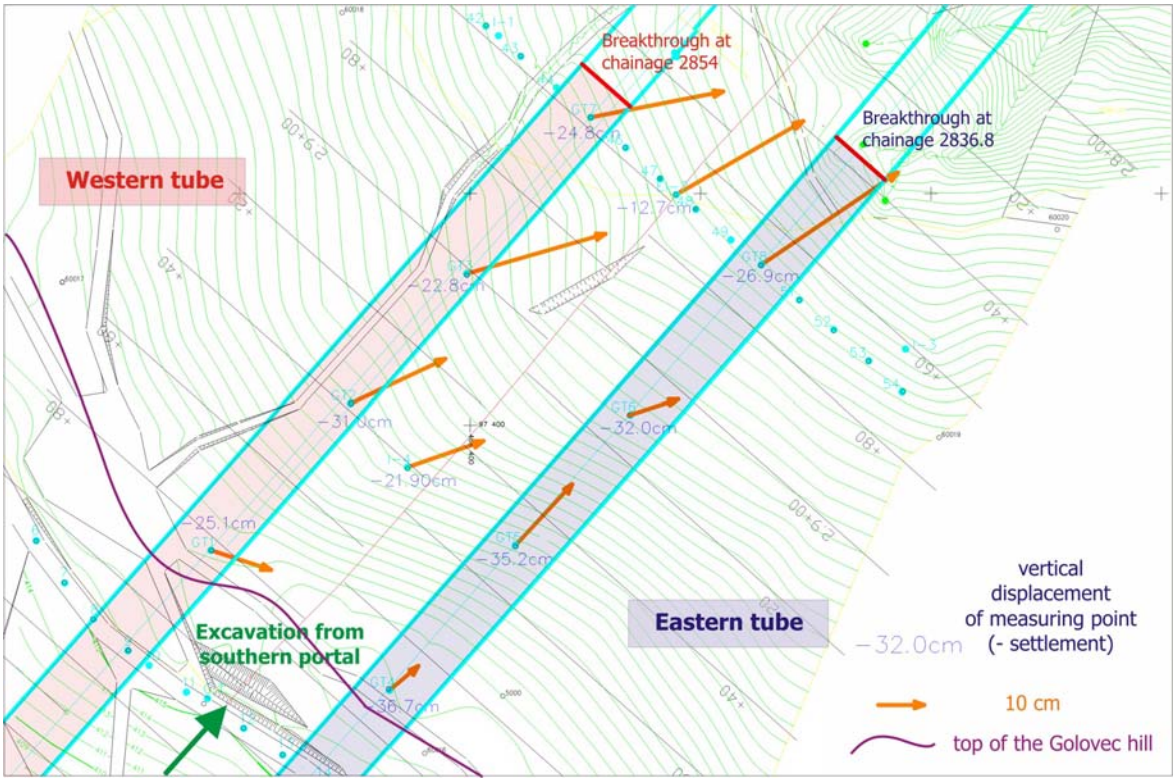

Figure 4-20. Layout of the surface displacements above the Golovec tunnel.

Slika 4-20. Situacija površinskih pomikov nad predorom Golovec.

4.3.2.3 The Jasovnik tunnel

Due to better geological – geotechnical conditions and consequently smaller displacement magnitudes the analysis of the measured displacements in the Jasovnik tunnel was not carried out until the phenomenon of the longitudinal displacements in the excavation direction was recognized at the Trojane and the Golovec tunnel.

Since the first 1000 m from the eastern portal of the tunnel were excavated in dolomite, the measured displacements remained within the margins of the measuring accuracy, i.e. in the range of a few millimetres. Around chainage km 76+400 the top heading excavation face entered the Pseudozilian shales and the measured displacements increased: settlements of up to 35 cm and longitudinal displacements of up to 20 cm in the excavation direction were observed (Fig. 4-21).

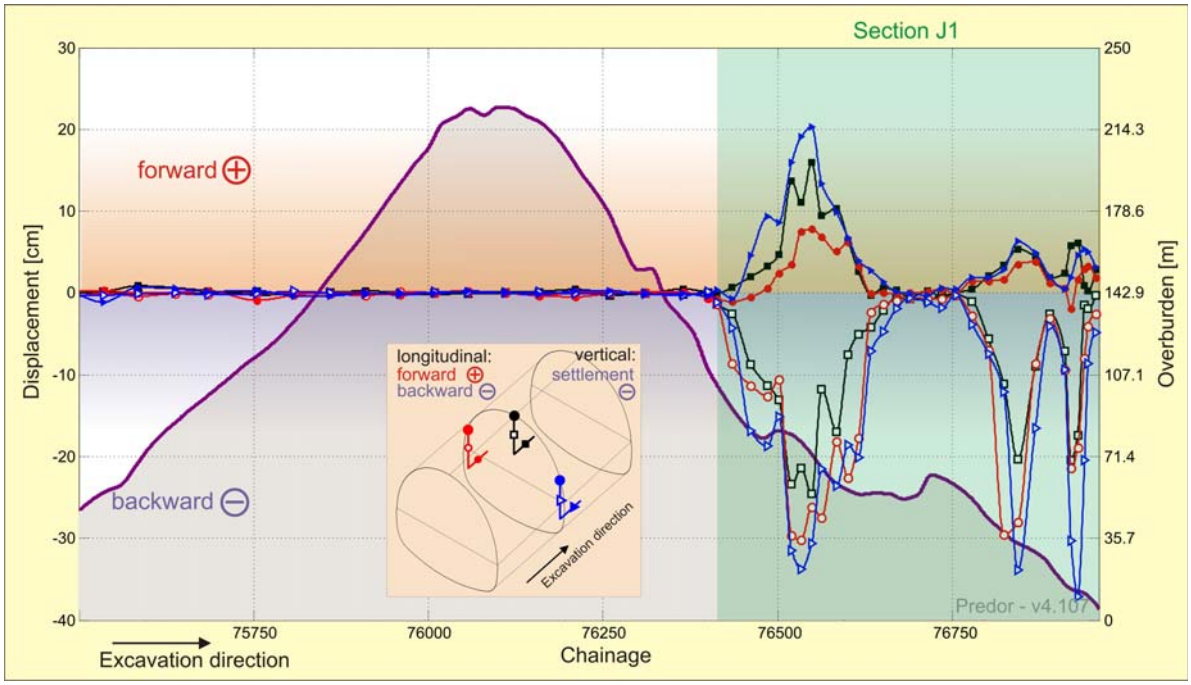

Figure 4-21. Contour of measured vertical and longitudinal displacements in the southern tube of the Jasovnik tunnel with plotted overburden; section of the longitudinal displacements pointing in the excavation direction is highlighted in green.

Slika 4-21. Kontura izmerjenih vertikalnih in vzdolžnih pomikov v južni cevi predora Jasovnik z izrisanim nadkritjem; območje izmerjenih vzdolžnih pomikov v smeri napredujočega čela je obarvano zeleno.

In the section between km 76+650 and km 76+950 the tunnel tubes are situated in prevailing tuff formations of siltstones and sandstones. Due to high stiffness of the surrounding rock mass the

measured displacements were much lower than in the Pseudozilian shales, especially between chainages km 76+650 and km 76+750. However, the orientation of the spatial displacement vector remained the same. Displacements increased again when approaching the western portal, where very colourful lithological structure was found (sediment breccia with rapidly changing content of tuff, claystone, siltstone and sandstone).

The alteration of the displacement vector orientation with the alteration of the slope inclination cannot be confirmed in the case of the Jasovnik tunnel due to very small measured displacements below the region of maximum overburden. However, with the transition to softer rock mass at an overburden of approximately 110 m the longitudinal displacements in the excavation direction were clearly measured and kept the direction up to the western portal. The length of the section with longitudinal displacements in the excavation direction is approximately 500 m in each tube (from chainage km 76+435 at MS23 to km 76+955 at MS52 in southern tube and from km 76+490 at MS24 to km 77+030 at MS54 in northern tube). The maximum measured longitudinal displacement was 20.3 cm of the right side wall point in MS 30 at chainage km 76+563 in the southern tube (Fig. 4-22).

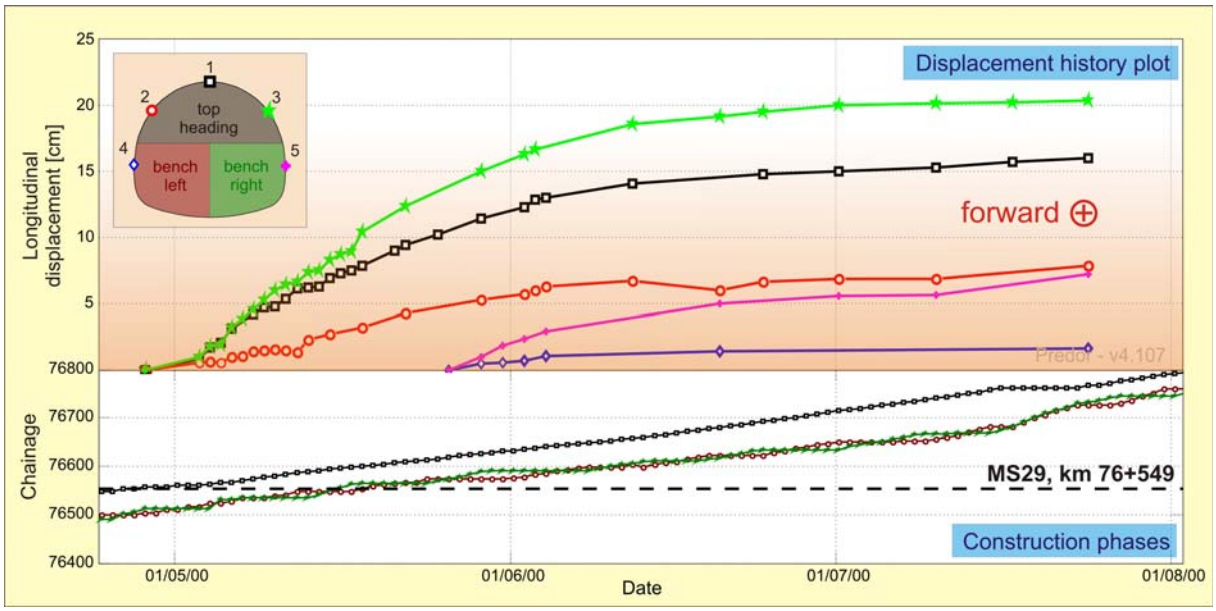

Figure 4-22. Longitudinal displacement history plot with construction phase plot for MS29 at chainage km 76+549 in the southern tube of the Jasovnik tunnel.

Slika 4-22. Krivulje časovnega poteka vzdolžnih pomikov točk v merskem profilu MS29 na stacionaži km 76+549 v južni cevi predora Jasovnik.

Like in the previously described two projects a far-reaching influence of the excavation works was also observed in section J1 of the Jasovnik tunnel, but with unexpected length. The distance from the

ring closure point to the measuring section amounted to 160 m on average, with the peak of up to almost 200 m in the Pseudozilian shales, and it decreased to 70 m when approaching the tuff formations (Fig. 4-23).

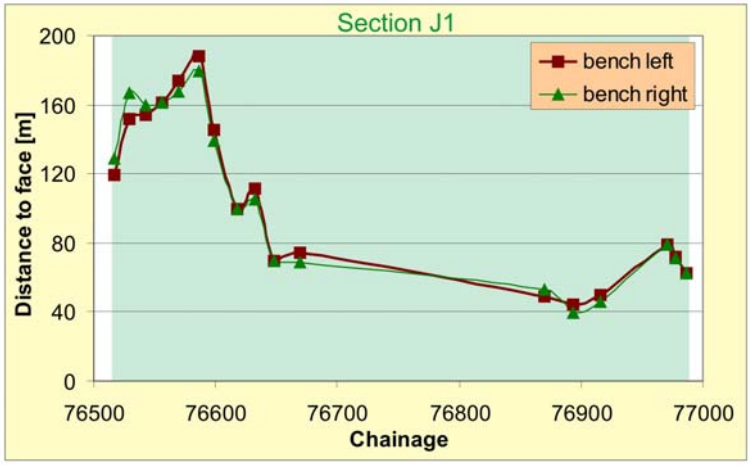

Figure 4-23. Distance between the bench excavation face and the measuring section when the latter can be considered as stabilised in the area of section J1 in the northern tube of the Jasovnik tunnel.

Slika 4-23. Razdalja med točko dokončanja celotnega podpornega obroča in merskim profilom, ko se le-ta lahko smatra za umirjenega, v območju J1 v severni cevi predora Jasovnik.

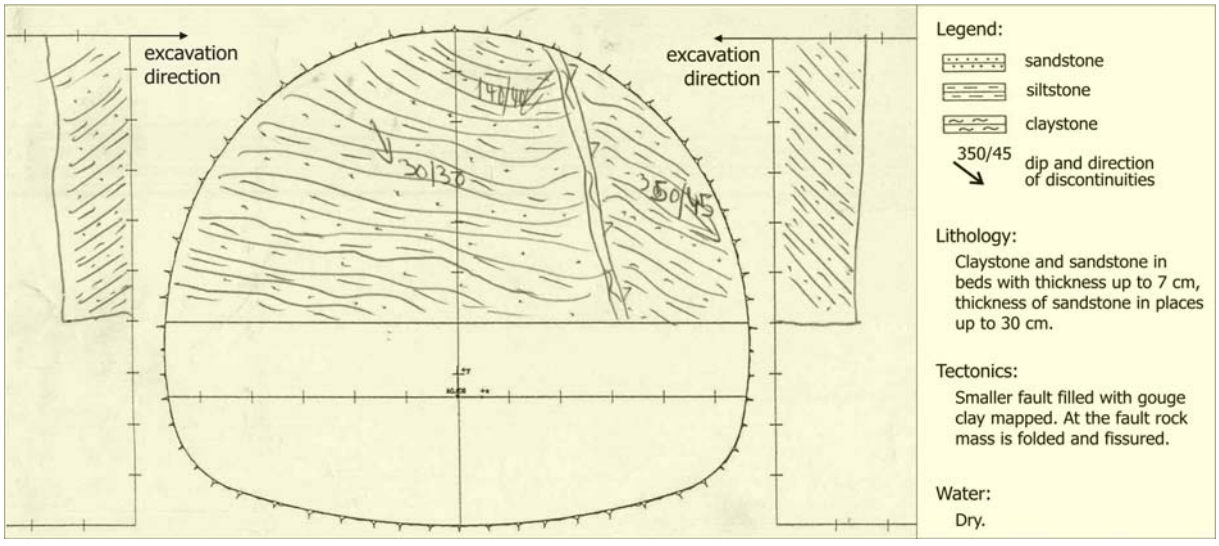

Figure 4-24. Face log at chainage km 76+610.3 in the southern tube of the Jasovnik tunnel (within section J1).

Slika 4-24. Geološka skica izkopnega čela kalote na stacionaži km 76+610.3 v južni cevi predora Jasovnik (območje J1).

In the latter we were not able to reliably asses the point when the observed cross section can be considered as stabilized. At the end of the tuff formation the distance was shorter (40 m) and increased again to 70-80 m further towards the western portal. The "normal" values of the distance from the ring closure point to the measuring section can not be assessed in the case of the Jasovnik tunnel, since the measured displacements in the first 1000 m were negligible, while the overburden above the tubes was increasing.

As seen from the longitudinal cross section of the Jasovnik tunnel (Fig. 2-17) and also from a typical face log from section J1 (Fig. 4-24), the inclination of the layers of the siltstone and sandstone is into the excavated area the same as in the previous two cases. An average dip of the layers is about 45°.

4.3.2.4 The Ločica tunnel

Due to fair tunnelling conditions the magnitude of the measured displacements in the Ločica tunnel was considerably smaller than in previously described projects. Maximum vertical displacement was 12 cm and the displacement measurements were not systematically performed every day.

The portal cuttings of the eastern portal were secured with shotcrete, wire mesh and rock bolts due to the 4 m thick layer of weathered rock on the slopes above the portal. The excavation of both tubes started from eastern portals in PC category according to ÖNORM B 2203 and then continued in category C2 up to chainage km 72+690, where a larger fault zone was encountered in the southern tube (Fig. 2-19). No larger displacements were monitored in this section.

Further excavations were performed in category B2, except in the vicinity of the western portals, where in some shorter sections the C2 and PC categories were used. The measured displacement increased around chainage km 72+800, where the dominating dip of the foliation is oriented into the excavation direction. The maximum vertical displacement was 12 cm and the longitudinal displacement up to 4 cm against the excavation direction.

Just before the top of the hill (at chainage km 73+000) the tunnel alignment entered the Upper Triassic marly limestone section and the measured displacements decreased. Almost no longitudinal displacements occurred. However, when the alignment passed the top of the hill (at chainage km 73+100 in the southern tube as shown in Fig. 4-25), the displacement vectors pointed in the excavation direction. The length of section L1 in the southern tube of the Ločica tunnel was approximately 200 m (from chainage km 73+100 to km 73+300 – MS18 to MS26) and 150 m in the northern tube (from chainage km 73+070 to km 73+200 – MS16 to MS22).

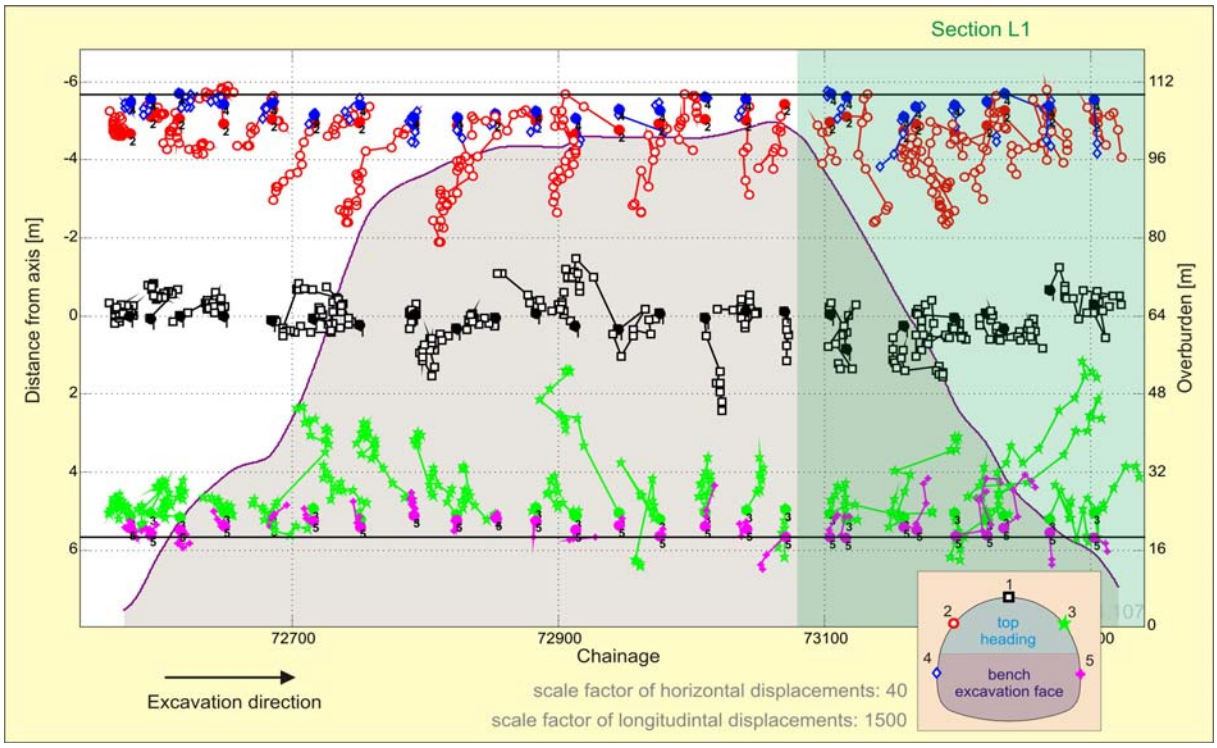

Figure 4-25. Plan view of displacement vectors (horizontal and longitudinal displacements) in the southern tube of the Ločica tunnel; section of longitudinal displacements pointing in the excavation direction is highlighted in green.

Slika 4-25. Situacija vektorjev pomikov (prečni in vzdolžni pomiki) v južni cevi predora Ločica z izrisanim nadkritjem; območje izmerjenih vzdolžnih pomikov v smeri napredujočega čela je obarvano zeleno.

The maximum longitudinal displacement in the excavation direction in section L1 was 5.8 cm at the right side wall point in the MS23 at chainage km 73+221 in the southern tube. The alteration of the slope inclination in the case of the Ločica tunnel occurred at an overburden of approximately 100 m and 85 above the southern and the northern tubes, respectively.

Similar to other three presented projects a prevailing dip of the foliation within section L1 is oriented into the excavated area, i.e. towards the eastern portal (Fig. 4-25). The dip angle is higher compared to other three projects and amounts to around 60°.

As already mentioned, the 3D displacement measurements of the targets on the tunnel circumference were not performed periodically every day. Therefore we were not able to reliably asses the distance of the ring closure point to the measuring section, when it can be considered as stabilized in case of section L1 of the Ločica tunnel.

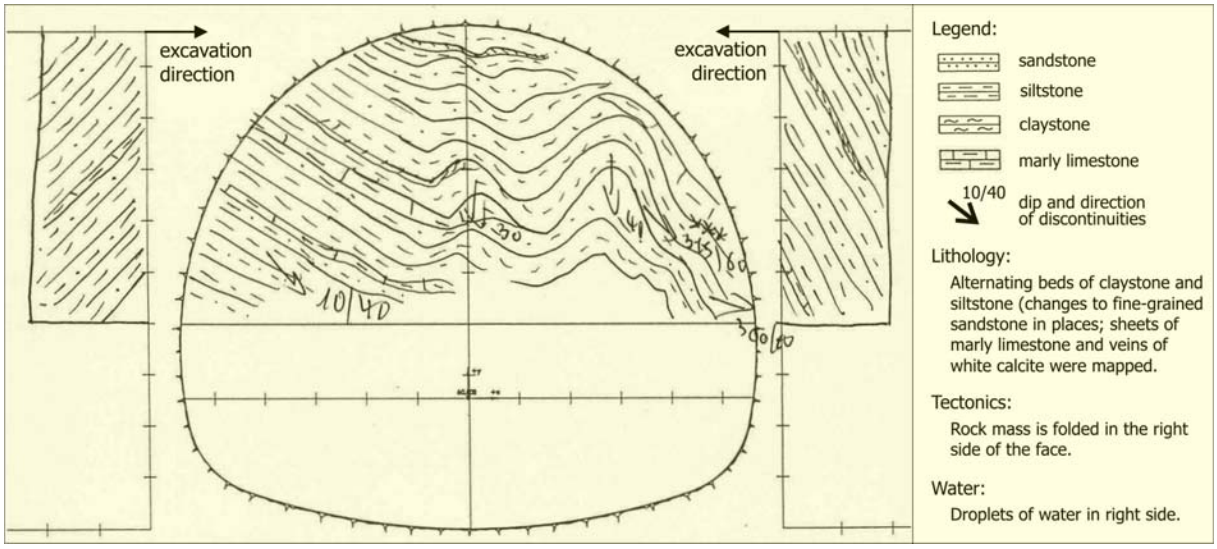

Figure 4-26. Face log at chainage km 73+226 in the southern tube of the Ločica tunnel (within section L1)**.**

Slika 4-26. Geološka skica izkopnega čela kalote na stacionaži km 73+226 v južni cevi predora Ločica (območje L1).

4.3.2.5 The Podmilj tunnel

Among all presented case histories the measured displacements in the Podmilj tunnel were the smallest (maximum vertical displacement of 9.3 cm), since it was constructed in fair geological conditions.

When tunnelling from the eastern portal through dolomite, the monitored convergences on measuring sections to MS9 were insignificant. Displacements increased after passing a fault zone (MS9 and MS10 were located in crushed rock mass). These two measuring sections exhibit "normal" behaviour, i.e. displacement vectors pointed into the excavated area as shown in Fig. 4-27. Further tunnelling took place in Gröden layers, where the largest displacements were measured. After approximately 100 m of excavation in Gröden layers the tunnel alignment passed about 160 m under the top of the hill and similarly to other presented cases the alteration of displacement vector orientation occurred into the excavation direction. The same orientation remained until the end of the site, i.e. to the breakthrough point. Section length was 150 m in the northern tube (chainage km 83+380 to km 83+530) and 180 m in the southern tube (chainage km 83+440 to km 83+620). Unlike other cases the longitudinal displacements in the Podmilj tunnel were much smaller compared to radial displacements (maximum measured longitudinal displacement was only 2.6 cm at the right sidewall point in MS13; the scale factor of longitudinal displacements in Fig. 4-27 is twenty times higher than the scale factor of the vertical displacements).

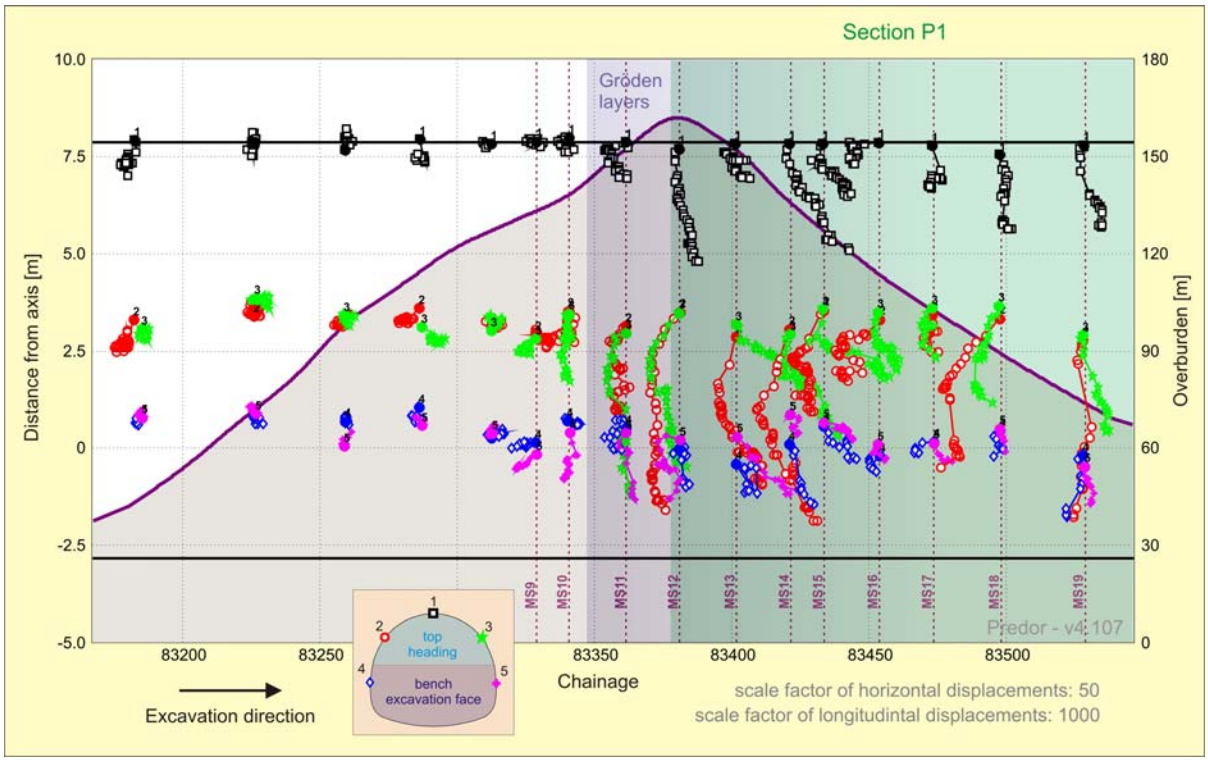

Figure 4-27. Longitudinal section of the displacement vectors (vertical and longitudinal displacements) in part of the northern tube of the Podmilj tunnel (excavation from the eastern portal) with plotted overburden; section of the longitudinal displacements pointing in the excavation direction is highlighted in green.

Slika 4-27. Vzdolžni prerez vektorjev pomikov (vertikalni in vzdolžni pomiki) na odseku severne cevi predora Podmilj (izkop iz vzhoda) z izrisanim nadkritjem; območje izmerjenih vzdolžnih pomikov v smeri napredujočega čela je obarvano zeleno.

Moreover, the orientation of the displacement vectors is not uniform. Especially for both sidewall points it can be noticed that the orientation changed from against the excavation direction soon after the installation of the targets into the excavation direction later on. A final displacement vector of the left sidewall target in some measuring sections (to the end of the section P1) still pointed against the excavation direction, although the orientation changed during the deformation process. Such deformation pattern was even more pronounced in the southern tube.

Like in the Ločica tunnel the convergence measurements were not performed continuously and the distance of the stabilised cross section to the ring closure point can not be reliably assessed. The orientation of the rock mass layers in the case of the Podmilj tunnel somewhat differs from other four

cases and is less pronounced. Prevailing dip is rather horizontal with slight inclination into the excavated area as shown in Fig. 4-28.

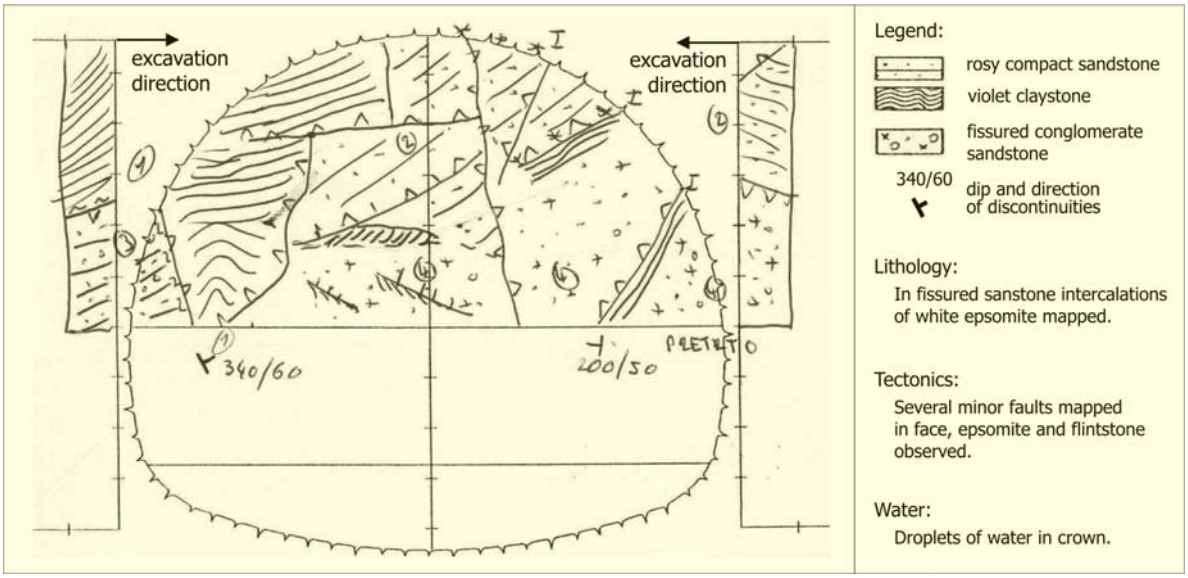

Figure 4-28. Face log at chainage km 83+418.2 in the northern tube of the Podmilj tunnel (within section P1).

Slika 4-28. Geološka skica izkopnega čela kalote na stacionaži km 83+418.2 v severni cevi predora Podmilj (območje P1).

4.3.2.6 Summarized data

The data on the length of sections with the longitudinal displacements in the excavation direction, the overburden when the slope inclination and the displacement vector orientation change, the magnitudes of maximum longitudinal displacements in the excavation direction, the position of the target on the tunnel circumference and the measuring sections these targets belong to are given in Table 4-4.

Table 4-4. Summarized data on the presented projects with longitudinal displacements in the excavation direction.

Preglednica 4-4. Zbrani podatki o projektih predorov, kjer so bili izmerjeni vzdolžni pomiki v smer napredovanja izkopa.

tunnel	tube	section	section length [m]	maximum overburden	maximum longitudinal displacement [cm]	target location
Trojane	northern	T1	145	35	14,2	crown
		T2	370*	130	6,1	left
	southern	T1	180	45	13,7	right
		T2	700*	135	7,3	crown
Golovec	eastern	G1	100**	75	9,7	right
	western	G1	130**	75	14,1	crown
Jasovnik	northern	J1	500	105+	12,8	right
	southern	J1	500	110+	20,3	right
Ločica	northern	L1	150	85	5,1	right
	southern	L1	200	100	5,8	right
Podmilj	northern	P1	150***	160	2,6	right
	southern	P1	180***	145	2,2	right

*the breakthrough was at the end of section T2; the slope was still declining
**the breakthrough was at the end of section G1; the slope was still declining
+overburden, where the measured displacements were not below the range of measuring accuracy
***the breakthrough was at the end of section P1; the slope was still declining

4.3.3 Numerical analysis

Some possible explanations of observed behaviour have already been given in previous chapter. In the case of the Trojane tunnel the slopes above the tunnel are often close to equilibrium limit state and tunnelling induced some sliding. Especially in the case of section T1 the sliding of the complete hill towards the Učak valley would be possible, since the overburden was not high and there was a fault zone ahead of the tunnel face that reduced the stress transfer further along the tunnel axis.

To verify this hypothesis a 3D model was composed in the commercial FEM code Cesar CLEO3D (*Cesar-LCPC CLEO3D*). Some simplifications were applied to keep the model simple. A circular tunnel was modelled instead of a horse-shoe tunnel, the excavated round length was set to 5 m instead of 1m and only the decreasing overburden was taken into account. The excavation was performed in top heading – bench sequence. The model dimensions and initial material characteristics are given in Fig. 4-29. To keep the number of FE at reasonable limits and to omit the influence of the boundary conditions on calculated displacements, an elastic area was added at the boundaries of the model to

decrease the axial stiffness of the primary lining in longitudinal direction. The Mohr-Coulomb model was used for the rock mass.

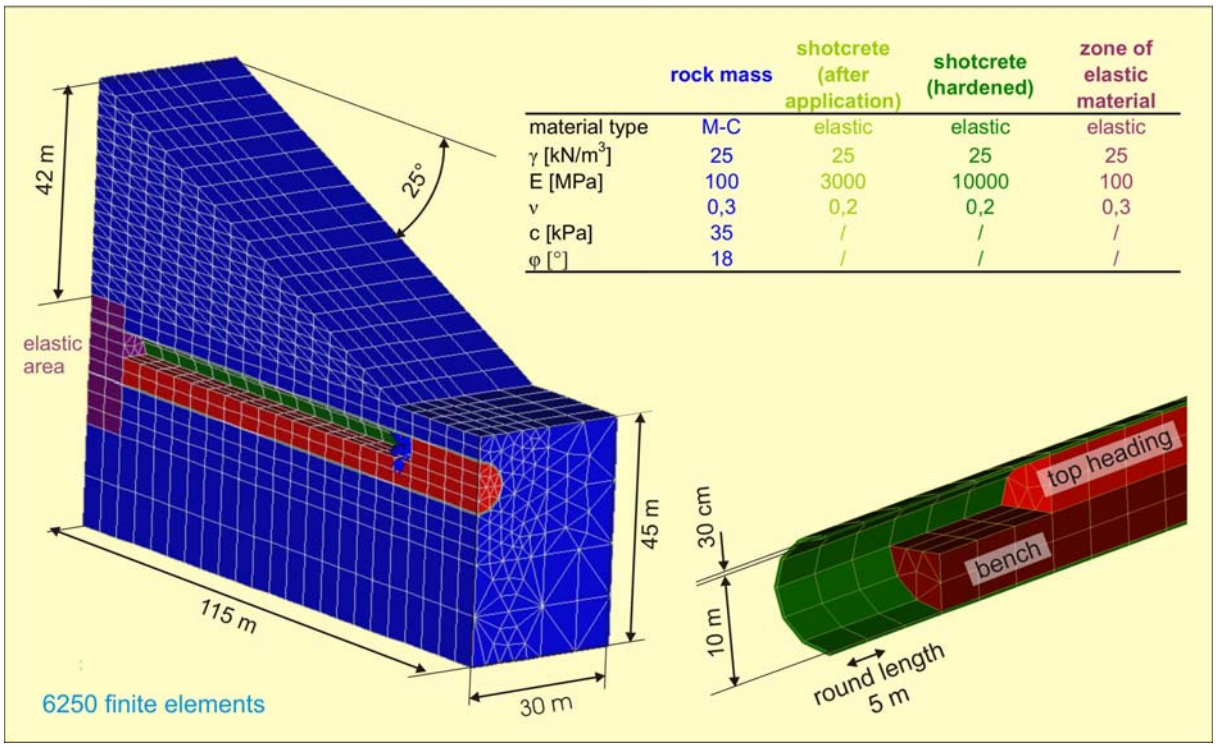

Figure 4-29. Numerical model of section T1 (under declined overburden) in Cesar CLEO3D**.**

Slika 4-29. Numerični model območja T1 (pod padajočim nadkritjem) v programu Cesar CLEO3D.

Despite decreasing characteristics of the rock mass to unrealistically low values the hypothesis could not be confirmed and the calculated longitudinal displacements of the tunnel lining still pointed against the excavation direction (Fig. 4-30). In the area close to the foothill the sliding of the rock mass was initiated by tunnel excavation, but the landslip was not deep enough to influence the tunnel lining. An uplift of complete tunnel tube was calculated in this section. The reason for the calculated response could be the use of the Mohr-Coulomb constitutive model (unrealistic calculated uplifts because of the tunnel excavation).

Since the advanced constitutive models incorporated into the Cesar CLEO3D code are not sufficiently well documented, Plaxis 3D Tunnel (*Plaxis 3D tunnel*) was used for further numerical work. The disadvantage of Plaxis is its inability to model inclined surface, since the code comprises only an extension of the planar section into third dimension. Therefore, the hill needs to be "constructed" either by placing material as a fill or excavation of the redundant material from the

complete block. The solutions differ in the primary stress state of the model. Since most plausible explanation for the valley formation is erosion of the cracked and faulted material, the second case was selected.

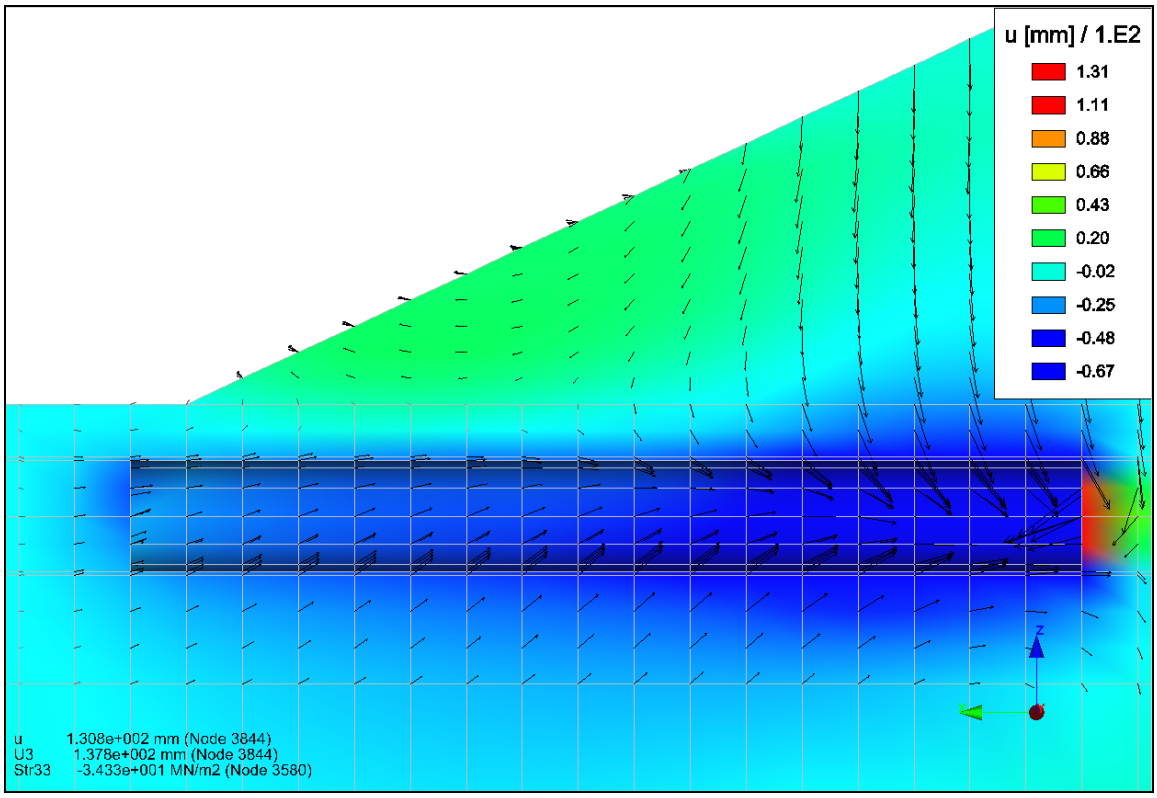

Figure 4-30. Longitudinal displacements in section T1 calculated with Cesar CLEO3D and Mohr-Coulomb material model**.**

Slika 4-30. Vzdolžni pomiki v območju T1 izračunani s programom Cesar CLEO3D in Mohrovim in Coulombovim materialnim modelom.

In order to investigate the influence of increasing as well as decreasing overburden on longitudinal displacements, an extended numerical model was created in Plaxis code. Comprehensive information about dimensions of the model, details about excavation sequence and material parameters for applied constitutive models are presented in Fig. 4-31. The main reason for modelling the behaviour of rock mass with Hardening soil constitutive model was geological structure that is in this section faulted to high extent and it can be described as BIMrock ("block-in-matrix" rock mass). Also the work of Markovič (2009) showed that the observed behaviour of the tunnel lining and the surface above the Trojane tunnel can be satisfactorily modelled by the Hardening soil model. The use of Mohr-Coulomb and Jointed rock models did not adequately reproduce the rock mass behaviour for the Trojane tunnel.

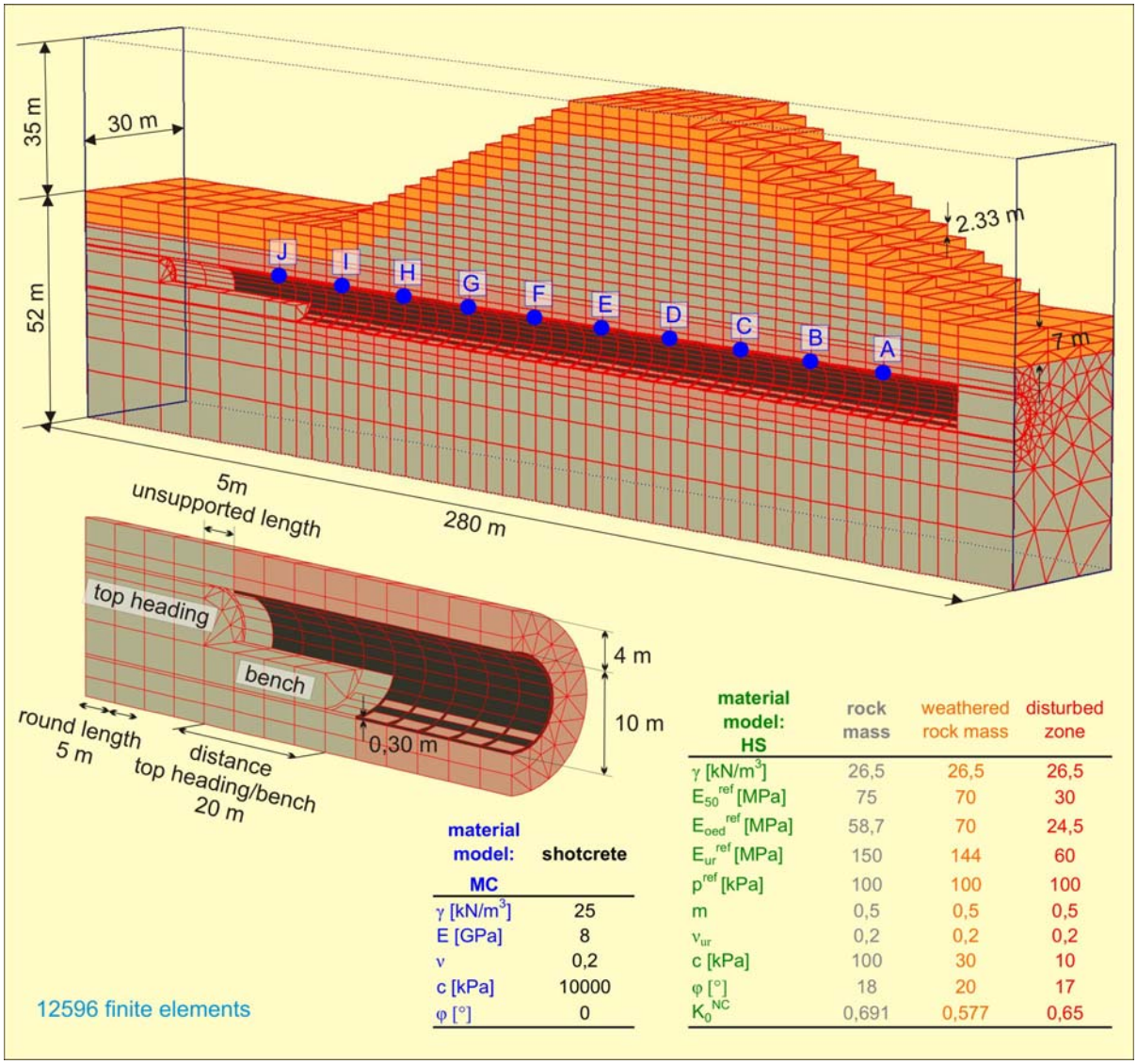

Figure 4-31. Numerical model of section T1 (complete hill) in Plaxis 3D Tunnel**.**

Slika 4-31. Numerični model območja T1 (celotni hrib) v programu Plaxis 3D Tunnel.

The same simplifications of the model as in Cesar CLEO3D were employed. The only exceptions were (1) modelling primary lining with 30 cm tick soil cluster instead of using "beam" elements to obviate large axial stiffness of the "beam" lining and (2) in the 4 m thick disturbed zone around a tunnel, lower stiffness and strength characteristics of the rock mass were applied after the excavation of individual round length. The calculated general deformation pattern was of main interest when performing these analysis and not the magnitude of calculated displacements. Therefore, the use of "homogeneous" material and the excavation round length of 5 m can be justified.

The calculated response is similar to the measured one in section T1 in the Trojane tunnel, as shown in bottom plot of Fig. 4-32. When tunnelling under increasing overburden, the displacement vector pointed in the excavated area (measuring sections MS23 and MS24 in Fig. 4-12 and calculation points A, B and C in Fig. 4-32). At the flat top of the hill almost no longitudinal displacements right after the excavation can be observed in both cases (MS25-26 in bottom plot of Fig. 4-32 and points D and E). Displacements in the excavation direction in these points started to accelerate with further face advance.

When the slope changed from flat to declined, the displacement vectors of the points in tunnel lining tended to the excavation direction right after the excavation. In this section vertical displacements in measured as well as calculated case were still considerable and larger then longitudinal (angle of displacement vector orientation in Fig. 4-13 is well below 30° in this section, magnitude of both displacement vector components can also be seen in Fig. 4-11). Farther points exhibit the trend of decrease of vertical and increase of longitudinal displacements towards the valley (MS27-MS30 26 in bottom plot of Fig. 4-32 and points G-H in middle plot of Fig. 4-32). Uplift of tunnel points close to and inside the valley was again obtained in both cases.

A distinctive deformation pattern can be observed for the longitudinal displacements of the points in front of the excavation face (marked with dashed lines in Fig. 4-32), located under declined overburden. If the point is far ahead of the excavation face, it moves in the slope direction. When the face approaches the observed point, the displacement vector gradually turns against the excavation direction and some large longitudinal displacement occurs. In the last excavation step before the cross section with a point is excavated, the displacement vector alternates again into the excavation direction. Same direction is maintained when the face has already passed this cross section.

The maximum calculated longitudinal displacement of excavated section (preface displacements are not considered) amounted to approximately 2 cm and was much smaller than the largest monitored displacement in section T1. Most probable reason could be an extension of the disturbed zone around the opening. In the presented numerical model the disturbed zone was modelled by reduced rock mass parameters at a thickness of 4 m. The actual extension of softened rock mass and its characteristics are not known and have considerable influence on the values of calculated displacements.

On the basis of performed numerical analysis we can conclude that longitudinal displacements in the excavation direction occurred mainly due to primary stress state rather than due to sliding of the hill, since displacements regularly increase with depth and similarly to the case calculated with Cesar CLEO3D code, only shallow landslip at the foothill was initiated due to tunnelling process.

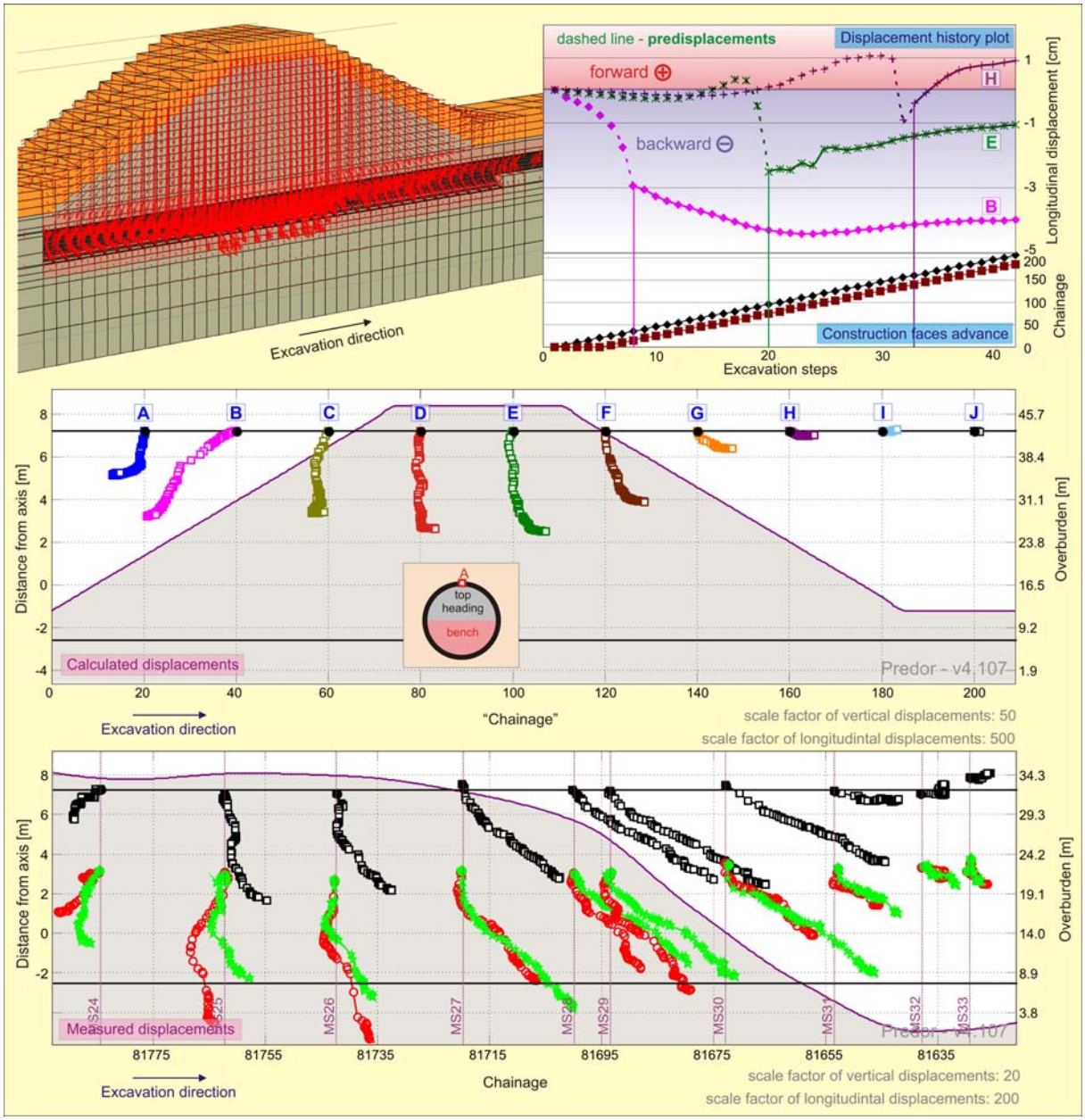

Figure 4-32. Measured (section T1 in the northern tube of the Trojane tunnel - bottom plot) and calculated (middle plot) displacement vectors in longitudinal section, complete longitudinal displacement history plot for selected points (upper right plot) and Plaxis displacement output presented with arrows (Hardening soil constitutive model).

Slika 4-32. Izmerjeni (odsek T1 v severni cevi predora Trojane – spodnji izris) in izračunani (srednji izris) vektorji pomikov v vzdolžnem prerezu (spodnji izris), celoten potek vzdolžnih pomikov za izbrane točke (zgornji desni izris) in prikaz pomikov s puščicami iz programa Plaxis ("Hardening soil" konstitutivni model).

Further on, the influence of foliation on the longitudinal displacements of the tunnel circumference was investigated, since the dominating dip is the same in all five presented case histories. The analysis was performed on numerical model as presented in Fig. 4-31, only rock mass was modelled with the Jointed rock constitutive model. As a base for the definition of the anisotropy direction the Ločica tunnel was selected (geological situation is shown in Fig. 2-18). A simplified geological structure can be characterized as synclinal with fold axis at the centre of the hill was and as such applied to the numerical model. Characteristics of the rock mass and foliation directions are given in Fig. 4-33.

In the bottom part of the numerical model (below the tunnel) rock mass with higher stiffness parameters was applied to obviate unrealistic uplift of the invert. Orthotropic material parameters were also used for the disturbed zone around the opening. Stiffness parameters for the Jointed rock constitutive model were determined on the basis of previously used Hardening soil parameters.

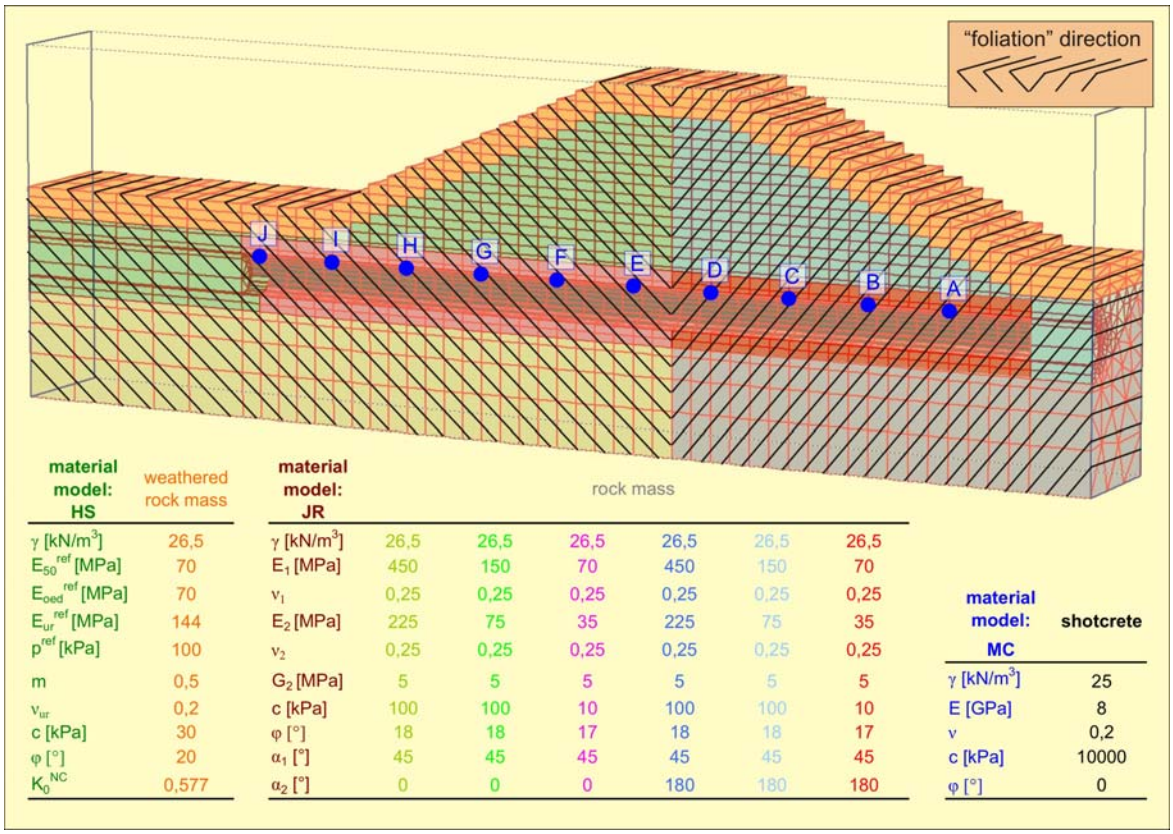

material model: HS	weathered rock mass
γ [kN/m³]	26,5
E_{50}^{ref} [MPa]	70
E_{oed}^{ref} [MPa]	70
E_{ur}^{ref} [MPa]	144
p^{ref} [kPa]	100
m	0,5
ν_{ur}	0,2
c [kPa]	30
φ [°]	20
K_0^{NC}	0,577

material model: JR						
γ [kN/m³]	26,5	26,5	26,5	26,5	26,5	26,5
E_1 [MPa]	450	150	70	450	150	70
ν_1	0,25	0,25	0,25	0,25	0,25	0,25
E_2 [MPa]	225	75	35	225	75	35
ν_2	0,25	0,25	0,25	0,25	0,25	0,25
G_2 [MPa]	5	5	5	5	5	5
c [kPa]	100	100	10	100	100	10
φ [°]	18	18	17	18	18	17
α_1 [°]	45	45	45	45	45	45
α_2 [°]	0	0	0	180	180	180

material model: MC	shotcrete
γ [kN/m³]	25
E [GPa]	8
ν	0,2
c [kPa]	10000
φ [°]	0

Figure 4-33. Numerical model for evaluation of the influence of anisotropy on longitudinal displacements in case of inclined overburden using Jointed rock constitutive model**.**

Slika 4-33. Numerični model za preučevanje vpliva anizotropije na vzdolžne pomike v primeru nagnjenega površja z uporabo "Jointed rock" konstitutivnega modela.

At first sight the calculated displacements (upper left plot in Fig. 4-34) gives the impression that the displacements are symmetrical on both sides of the hill and are pointing against the excavation direction in the section with increasing overburden and in opposite direction under declined slope.

Complete calculated displacements of the comparable points on both sides of the hill are indeed of similar magnitude (largest displacements in the longitudinal direction amounted to approximately 13 cm and the vertical was around 16 cm - upper right plots in Fig. 4-34). Nevertheless, significant difference between both sections arises when only the displacements after the excavation are taken into account. In the section with increasing overburden and tunnelling with dip the majority of longitudinal displacements occurs ahead of the face and merely 2 cm after the excavation (point B), while under decreasing overburden and tunnelling against dip almost entire longitudinal displacement occurs after the excavation (point H). Similar portions can also be observed for vertical displacements.

The obtained response is in excellent agreement with the observations by Tonon (2002). Only percentages of the longitudinal as well as vertical displacements ahead of the face are in the presented case even higher when tunnelling with dip (around 85% of total longitudinal displacements occur ahead of the face and could be explained by significant effect of primary stress state due to inclined slope). On the other hand, only 10% of the total longitudinal displacement occur ahead of the face when tunnelling against dip and under declined slope, which is very similar to numerical results by Tonon (2002).

Unlike in previous analysis with the Hardening soil model, point E (located under the top of the hill) exhibits longitudinal displacement in the excavation direction nearly throughout the complete displacement path. Only just before the excavation of the round length containing point E the displacement vector points into the excavated area. On the other hand, precedent point D exhibited no longitudinal displacements after the excavation. The other two selected points (B and H) move solely in the direction of slope inclination. Interesting is also the magnitude of the displacement vectors in sections with increasing and decreasing overburden. Final displacement values are almost uniform in the first section. In the section with decreasing overburden the largest displacement was calculated for point F at the beginning of this section and displacements then decrease towards the “valley”.

Although the general geological structure in longitudinal section in the latter numerical model follows the structure observed in the Ločica tunnel, the difference of the measured displacement magnitudes when tunnelling with or against dip could not be perceived (Fig. 4-25). Plausible explanation could be different geological conditions in sections of interest (faults, folds, diverse stiffness of the rock mass, etc.).

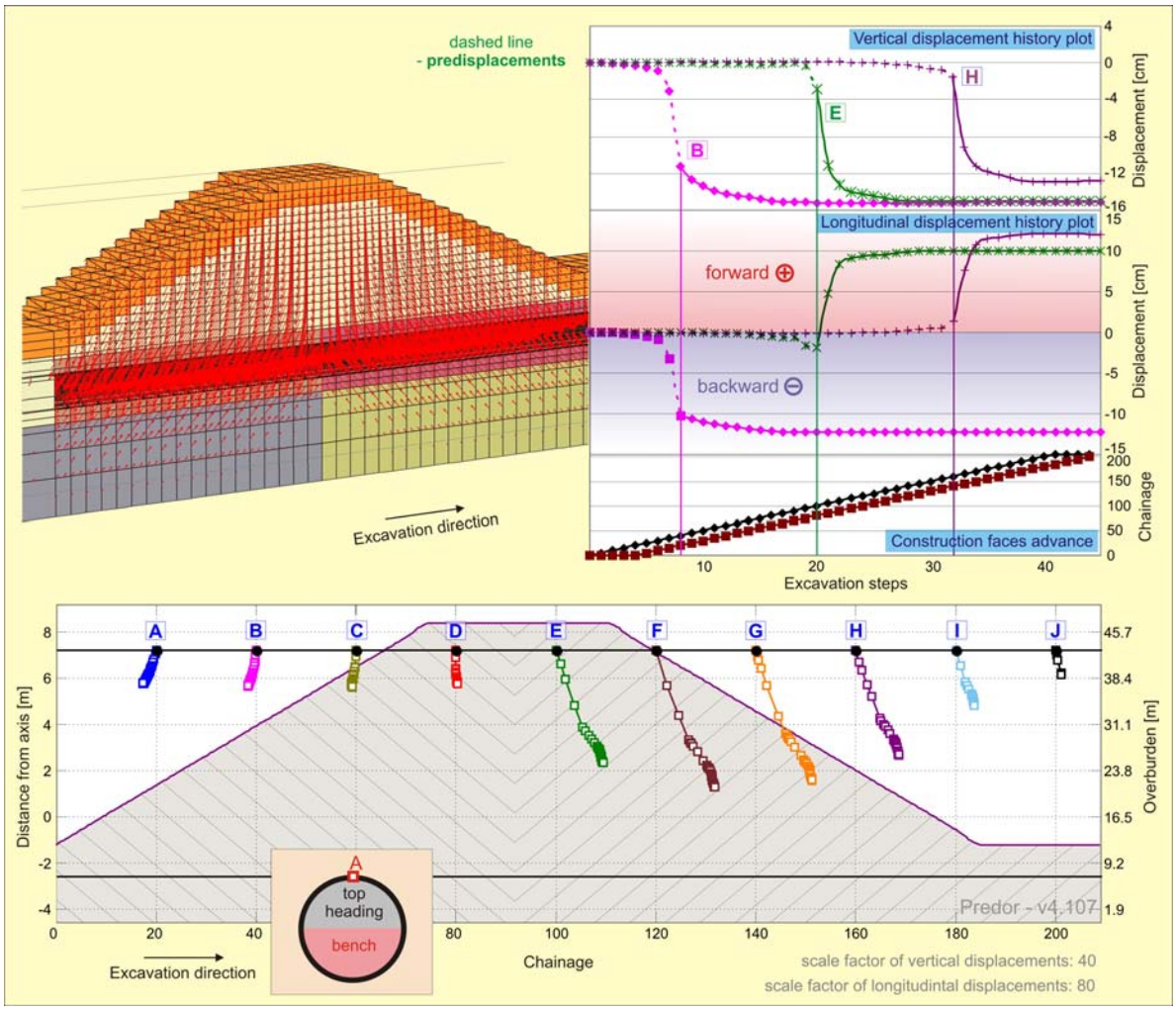

Figure 4-34. Calculated displacement vectors after the excavation in longitudinal section (bottom plot), complete longitudinal and vertical displacement history plot for selected points (upper right plots) and Plaxis displacement output presented with arrows (Jointed rock constitutive model)**.**

Slika 4-34. Izračunani vektorji pomikov po izkopu v vzdolžnem prerezu (spodnji izris), celoten potek vzdolžnih in vertikalnih pomikov za izbrane točke (zgornja desna izrisa) in prikaz pomikov s puščicami iz programa Plaxis ("Jointed rock" konstitutivni model).

The Ločica tunnel is the only of the described projects where different dip orientation with regard to the tunnel driving could be studied. Therefore the only remaining possibility to confirm numerical results would be to investigate the sections close to the breakthrough, if they were executed in rather uniformly foliated rock mass. The only breakthrough section with fairly uniform geological structure and sufficient length to verify the numerically obtained pattern of longitudinal displacements was in the northern tube of the Trojane tunnel.

The geological longitudinal section of the breakthrough area in the northern tube of the Trojane tunnel is presented in Fig. 4-35. The scale in vertical direction was adjusted for more convenient presentation. To get the impression of the true angle of the dip of foliation, two 20 m long divisions were extracted and plotted beneath in true scale.

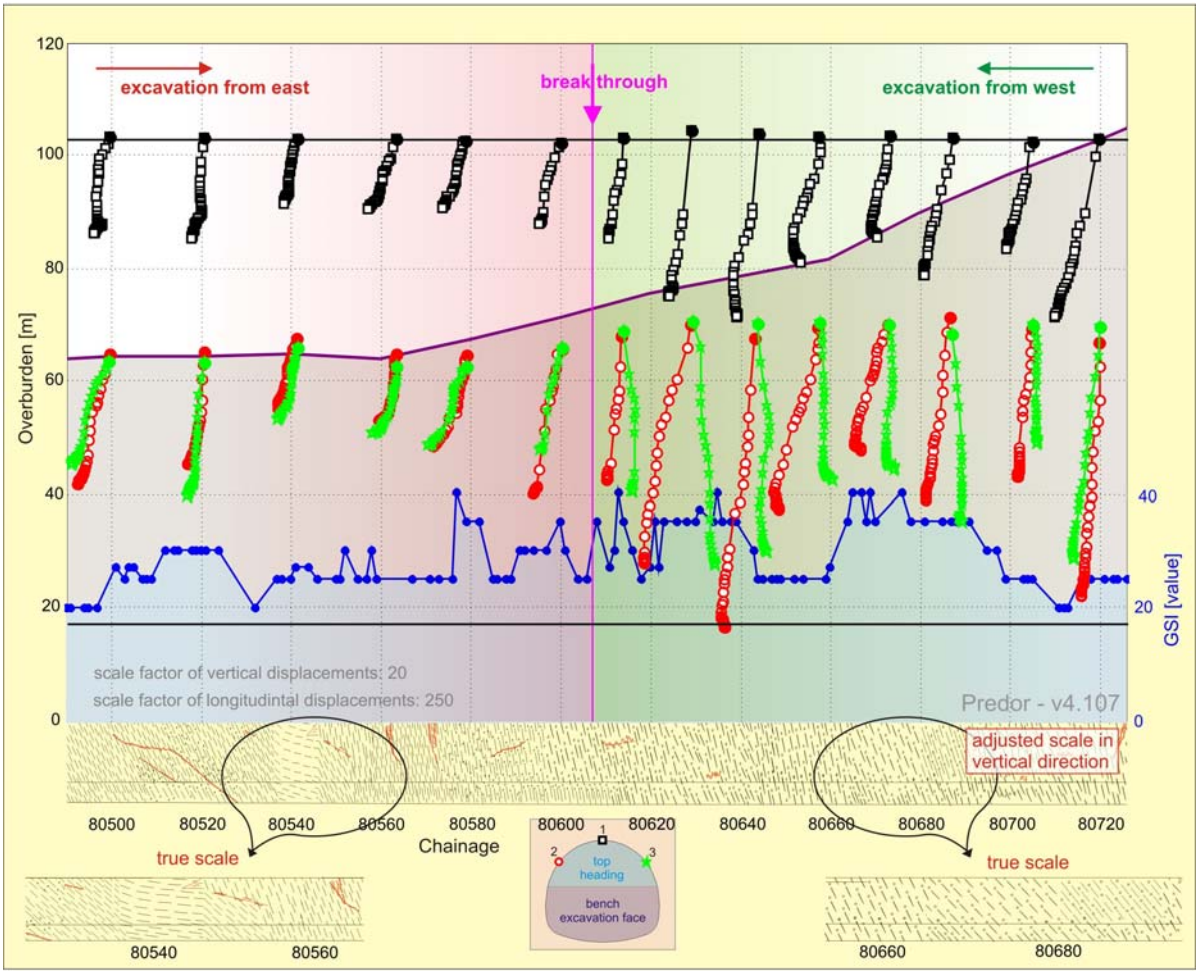

Figure 4-35. Displacement vectors in the longitudinal section in the area of breakthrough in the northern tube of the Trojane tunnel with lined geological longitudinal section (not in scale!) and corresponding GSI value**.**

Slika 4-35. Vektorji pomikov v vzdolžnem prerezu na območje preboja v severni cevi predora Trojane z geološkim vzdolžnim prerezom (ni v merilu!) in pripadajočim GSI.

Rock mass in the western part consists mainly of siltstone alternating with beds of sandstone. The GSI was in the range from 25 to 40 with an average value of 30 to 35 (blue line and surface in Fig. 4-35). In the eastern part siltstone alternates mainly with claystone and subordinately with sandstone. The average value of GSI was lower than in the western part (25 on average). Although some minor

faults and local folds were mapped in the selected section, the geological structure can still be considered as sufficiently uniform with dip angles from 45° to 60° towards west. Dip of the foliation is generally 330° (shown in geological situation in Fig. 4-35).

The measured displacements of approximately 120 m long sections from each heading are presented with the displacement vectors in longitudinal section in Fig. 4-35. The section that was excavated from the western portal is the last part of section T2 and the displacement vectors as already described tended into the excavation direction. In the eastern part the orientation of displacement vectors was "normal" (against the excavation direction). Fairly good agreement of observed and calculated displacement pattern can be seen by comparing figures 4-34 and 4-35. Although more favourable conditions were encountered when tunnelling from west as deduced from GSI values, a significant difference can be observed in the magnitudes of measured vertical displacements (displacements after the excavation). Vertical displacements were considerably larger in the western than in the eastern heading, except for the measuring sections next to the breakthrough point. Due to better geological conditions in the western lot, the difference between displacement magnitudes in both parts is much smaller than at the numerical analysis, but the calculated response can still be proved. In contradiction to the calculated response the measured longitudinal displacements in case of the northern tube of the Trojane tunnel were just slightly higher when tunnelling against dip than with dip.

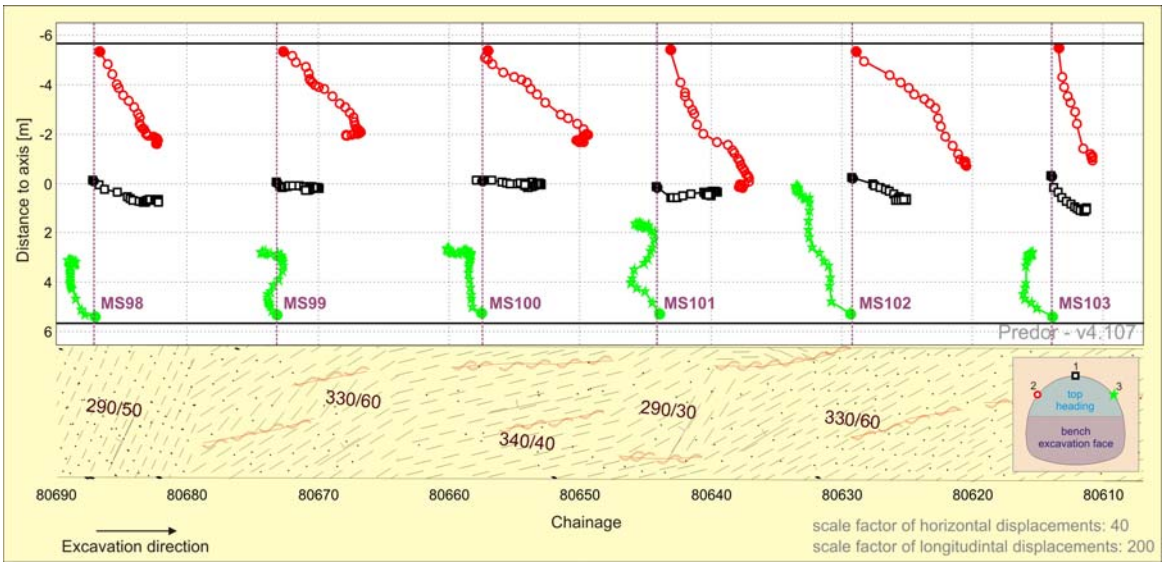

Figure 4-36. Plan view of the displacement vectors (horizontal and longitudinal displacements) in the northern tube of the Trojane tunnel close to the area of breakthrough (excavation from west) with lined geological situation**.**

Slika 4-36. Situacija vektorjev pomikov (prečni in vzdolžni pomiki) v bližini preboja v severni cevi predora Trojane (izkop iz zahoda) s podloženo geološko situacijo.

In western part a distinction between the displacement vector tendencies of both sidewall points is obvious. Left sidewall points and also crown points explicitly displaced in the excavation direction, while displacement vectors of the right sidewall points tended in the opposite direction. The described pattern occurs due to relative orientation of the rock mass foliation to tunnel tube in both sidewalls. Foliation is generally dipping nearly to the north and strikes the tunnel axis at an acute angle. The monitored displacement vectors in both sidewalls thus pointed perpendicularly to the foliation. The crown target somehow followed the same pattern as the left sidewall target, only the longitudinal displacement magnitude was slightly smaller. Similar case history was already presented for the left tube of the Trojane tunnel (Schubert P. et al, 2005). This phenomenon was also mentioned by Steindorfer (1998) and Grossauer (2009).

However, in the presented case the displacement in the longitudinal direction did not occur only because of the mentioned phenomenon. Also the influence of the decreasing overburden can be noticed, especially on right sidewall points. After the excavation the displacement vector pointed perpendicularly to the foliation direction against the direction of excavation. But with diminishing influence of the digressing top heading face vectors started to change orientation moderately in the direction of decreasing overburden. As soon as the support ring had been closed, the displacement vector orientation changed again. This pattern is well pronounced, especially in measuring sections MS99 and MS 101 (see Fig. 4-36). The latter change of the displacement vector orientation can be explained by cessation of stress redistribution process after the ring closure and thus change of the deformation pattern from direction normal to foliation to shearing along discontinuities (more information on this phenomenon is given in Chapter 5.2.1). This response was observed only in the western lot and can be explained by better, i.e. more uniform rock conditions.

In the Trojane, Golovec and Jasovnik tunnels a far reaching influence of the excavation works was noticed in sections with longitudinal displacements in the excavation direction (this can not be displayed for the Podmilj and Ločica tunnels, since convergence measurements of the measuring sections were not performed continuously). The displacement history plot calculated with the Hardening soil constitutive model (Fig. 4-32) indicates long lasting deformation of the surrounding rock mass. The displacement rates of point A as well as point E only slowly converge to 0. In case of point E the distance of the ring closure point to point E amounted to 100 m when the calculation was stopped and the section was still not completely stabilized. On the other hand, the displacements calculated with the Jointed rock constitutive model vanish approximately 60 m away from the ring closure point.

Another case history with well pronounced influence of the rock mass anisotropy on the tunnel wall displacements was observed in the left tube of the Šentvid tunnel. Geological situation is characterized

with local kink-fold syncline with an axis at chainage km 1+565 as shown in geological longitudinal section in Fig 4-37. The tunnelling proceeded with dip in the south dipping limb of the fold and against dip in north dipping limb. When tunnelling with dip the displacement vectors in longitudinal section pointed against the excavation direction (MS54 to MS56), while they pointed in the excavation direction when tunnelling against dip (MS59 to MS61). Major deformation was thus normal to the foliation planes. As the effect of the approaching phase diminished, the deformation resumed in the direction along the discontinuities as evident from displacement vectors in longitudinal section in Fig. 4-37.

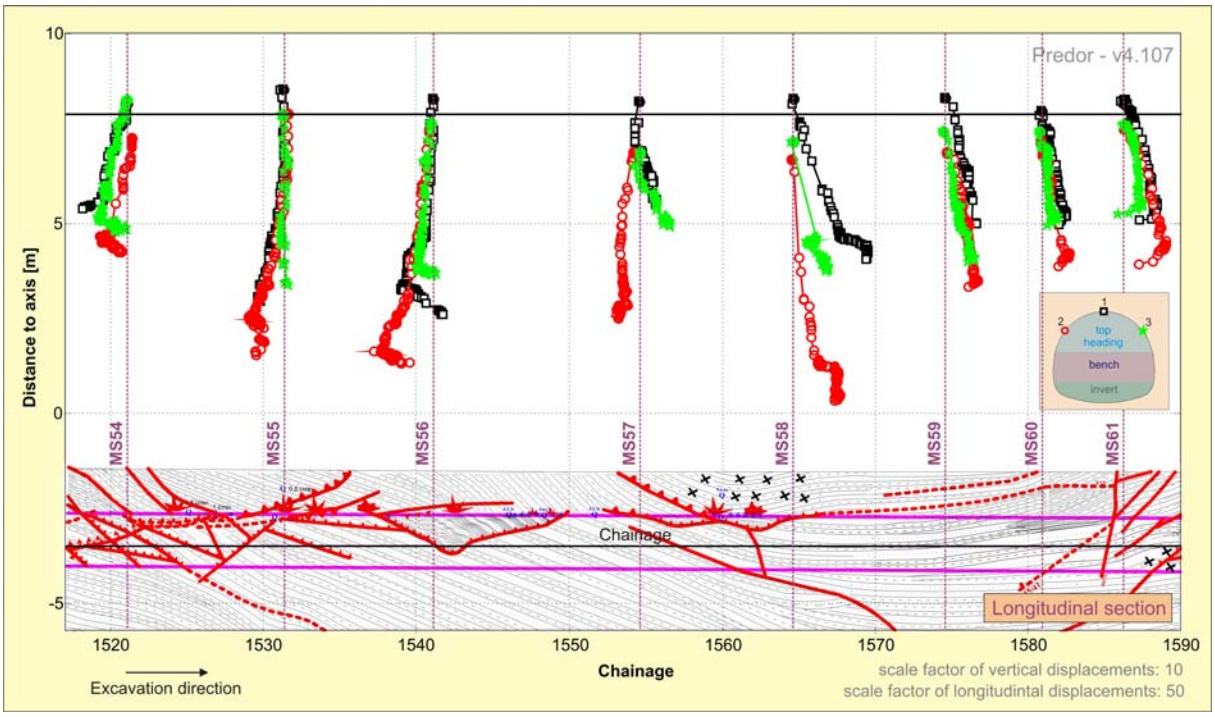

Figure 4-37. Displacement vectors in the longitudinal section (vertical and longitudinal displacements) in the left tube of the Šentvid tunnel (excavation from north) with lined geological longitudinal section**.**

Slika 4-37. Vektorji pomikov v vzdolžnem prerezu (vertikalni in vzdolžni pomiki) leve cevi predora Šentvid (izkop iz severa) s podloženim geološkim vzdolžnim prerezom.

Since the rock mass is cut with several faults that also influence the tunnel response especially in the south dipping limb, the difference in the displacement magnitudes in cases when tunnelling with and against dip can not be observed. Nevertheless, it is obvious that the foliation governs the overall behaviour of the tunnel and worse rock mass conditions caused by faults affect only displacement magnitudes.

4.4 Surface displacements above the tunnel

As already outlined above, tunnelling process inevitably affects existing ground stresses and provokes inward displacement of the tunnel face and convergences of the lining. Further on, these ground movements tend to propagate towards the surface. Their extent and time scale depend on a number of factors like geological and hydro-geological conditions, rock mass properties, size, shape and depth of an opening, excavation method and sequence as well as qualification of the contractor's personnel and site management (ITA WG "Research", 2007). When tunnelling at shallow overburden under populated areas or existing infrastructure, surface movements are of special interest.

On the basis of case histories Peck (1969) showed that the resulting transverse settlement trough can be adequately described by Gaussian distribution curve as

$$s = s_{\max} \exp\left(\frac{-y^2}{2i^2}\right) \qquad \text{Eq. 4-1}$$

s … settlement at certain distance to tunnel centre line

s_{max} ... the maximum displacement on the tunnel centre line

y ... horizontal distance from the centre line

i ... horizontal distance from the centre line to the inflexion point on the settlement trough

For near surface openings O'Reilly et al (1982) ascertained that parameter *i* is approximately linear function of the depth of an opening and can be calculated as

$$i = K \cdot z_0 \qquad \text{Eq. 4-2}$$

K … parameter of the trough width

z_0 ... depth of an opening

Average value of parameter *K* was defined by Mair et al (1996) on the basis of wide range of monitoring data as an average value of 0.5 for tunnels in clays and 0.35 for tunnels in sands and gravels, regardless of tunnel size and construction method.

The proposed procedure for the calculation of settlement trough in case of horizontal layers of sands and clays has become widely used, particularly to assess the potential impact of tunnelling works during the design process (ITA WG "Research", 2007).

According to the given equation a settlement trough in isotropic conditions is symmetric to the tunnel centre line in case of a single tunnel. On the other hand, twin tunnels usually provoke asymmetric trough (Peck, 1969). Also the occurrence of symmetric pattern is unlikely in cases of anisotropic rock mass. Therefore a simple 2D calculation was performed simulating anisotropic conditions to study the influence of the discontinuity orientation on the settlement line above the tunnel.

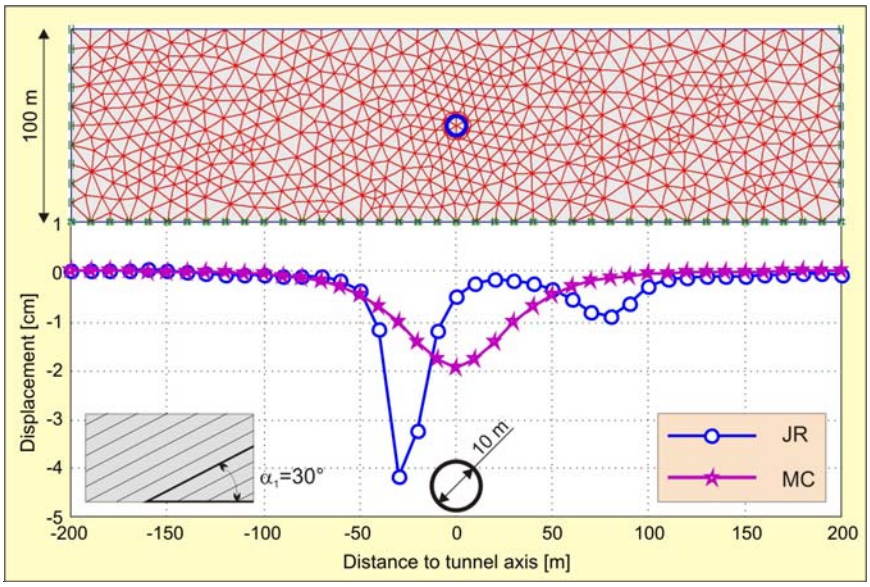

Figure 4-38. Comparison of calculated settlement trough in isotropic and anisotropic material**.**

Slika 4-38. Primerjava izračunanega korita ugrezkov v izotropnem in anizotropnem materialu.

The calculated settlement lines with isotropic Mohr-Coulomb and anisotropic Jointed rock constitutive models are presented in Fig 4-38 (back calculated parameters for the Šentvid tunnel shown in Fig. 4-3 were used for the Jointed rock and corresponding parameters for the Mohr-Coulomb material model, dip of the discontinuities was set at 30°, a circular tunnel with diameter of 10 m was "excavated" in one step). The settlement line is divided into two troughs according to performed calculations in anisotropic conditions: the one with larger magnitude is located left of the tunnel tube and occurs due to deformation normal to discontinuities, while a smaller one occurs mainly due to shearing along the discontinuities. In isotropic media, however, only minor settlement is obtained in the tunnel centre line. The difference can be noticed also in the extension of the influential area. In the area left from the tunnel, i.e. normal to discontinuities, the influence zone is somewhat equal, while on the other side the influence of the shearing along discontinuities reaches significantly farther in the rock mass than in isotropic material. Parametrical study of the influence of different discontinuity orientations and material parameters in the Jointed rock constitutive model on the surface settlements was performed by Markovič (2009).

As described in Chapter 2, a considerable number of cross sections were monitored above the Trojane tunnel and additionally 3 cross sections above the Golovec tunnel. Settlement troughs of the measuring sections with at least 7 continuously monitored targets above the southern tube of the Trojane tunnel are plotted in bottom part of Fig. 4-39. Two wide measuring sections that extended in the expected influential area of both tubes are presented separately in the upper two plots. The maximum settlements in all measuring sections are located in the centre line of the tunnel tube or at least very close to it, just slightly shifted towards the right side. This minor shift and trend alteration in the right side is probably due to the excavation of the northern tube. The location of the right tube is not plotted since it differs from section to section (tunnel tubes were generally set at a distance of 40 m but this distance was increased to 70 m below the Trojane village). Beside visual inspection of the curves no noteworthy analysis could be preformed, since the settlements above the northern tube were not measured and any assessment of the right tube influence would be solely speculation.

A more detailed analysis was, however, performed for the two abovementioned wide cross sections. The left one in Fig. 4-39 (denoted as case TS-1 in Fig. 2-5) was installed just prior to large area of monitored 3D surface displacements in the eastern part of the Trojane tunnel at low overburden of 20 to 40 m. Geological situation is characterized by block of sandstone in the area of the northern tube, while the southern tube passes through soft tectonized claystone, hence significant displacement difference between settlement magnitudes (50 cm above southern tube to 11 cm above northern one). Mapped dominating foliation dip in cross section for both tubes was 30° to the right side wall; distance between tubes amounts 65 m. The other cross section (denoted as case TS-2 in Fig. 2-5) was located close to the northern tube breakthrough point at higher overburden of 45 to 75 m (Fig. 4-16). Foliation dip was 60° to the left side wall in the area of the southern tube and with same angle to the right sidewall in the area of the northern tube. It seems that the tubes are situated in different limbs of a fold. The tubes are situated at a distance of 55 m to each other.

Settlement troughs were calculated for each tube separately according to Eq. 4-1 and then summed to get a total curve. Each of the tubes in case TS-2 affected the settlements of the points between the tubes. Therefore, the settlements due to the influence of the other tube needs to be subtracted from s_{max} when calculating a trough. This value is assessed from the calculated trough of the other tube just above the considered tube. The total trough is determined iteratively so that it fits the measured values in the centre line of both tubes. Applied superposition technique was however different from the one proposed by Suwansawat (2006) who studied the settlements above the twin tunnel due to EPB tunnelling (the settlements of both EPB passes could be distinguished as the second tube was excavated after the settlements due to the first EPB pass ended). In case TS-2 the excavation faces of

three lots affected the targets: excavation faces from the eastern and western portals of the northern tube and excavation faces from the western portal in the southern tube. Application of the superposition technique proposed by Suwansawat was not suitable since the influence of each of the faces could not be distinguished.

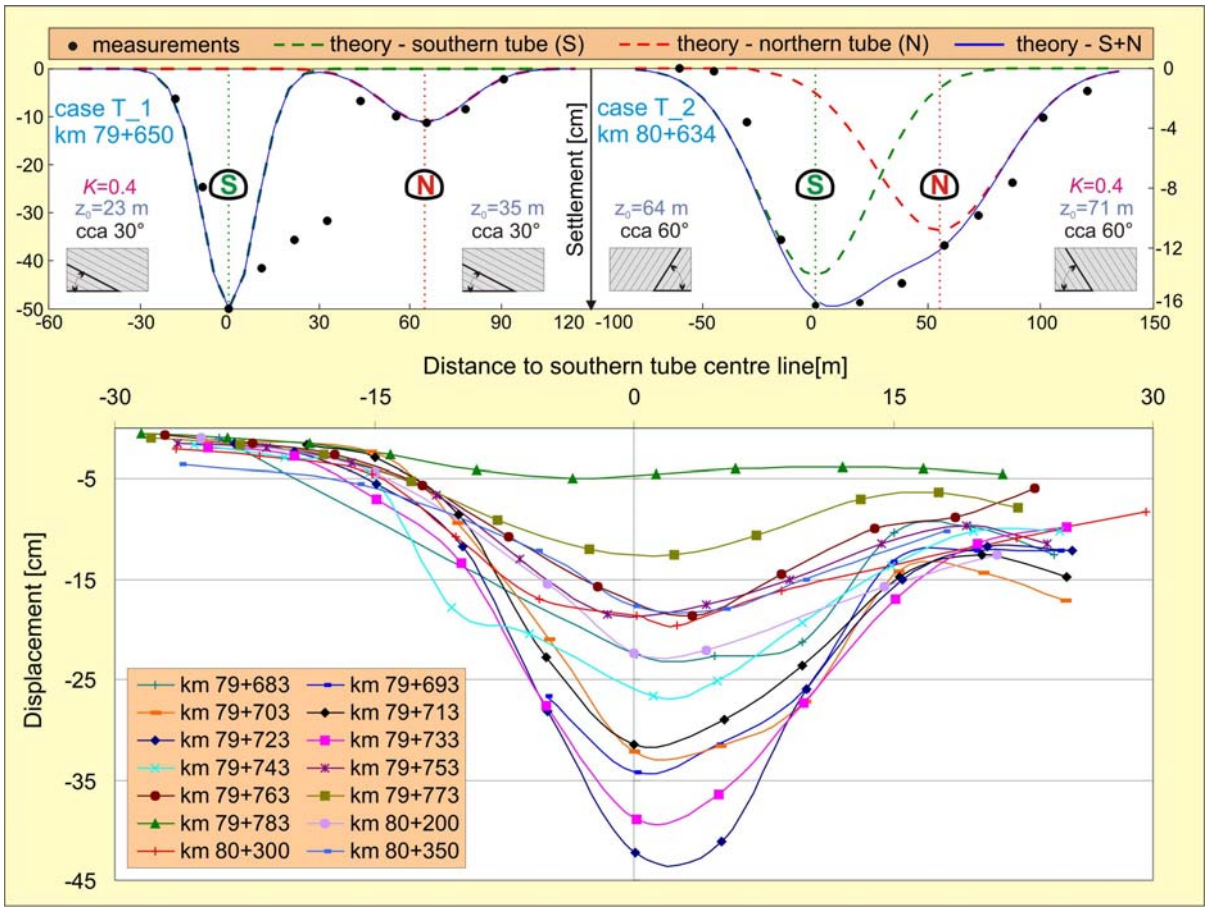

Figure 4-39. Transverse surface settlement troughs at the Trojane tunnel**.**

Slika 4-39. Korita pogrezkov površine prečno na os predora Trojane.

In both cases the calculated trough matches sufficiently well the measured values, only two deviations can be observed in the upper plots of Fig. 4-39. In case TS-1 the measured values significantly deviate in the influential area right from the southern tube, while in case TS-2 they deviate in the area left from the same tube. Smaller displacements in case TS-2 can be explained with lower overburden that declines towards south. No particular reason for the troughs deviation was found in case TS-1 except a large difference in stiffness of the rock mass. Since settlements of the majority of the targets match the calculated curve and especially the maximum of the curves as well as the extensions of influence zone fit, it is obvious that rock mass in the area of the Trojane tunnel in general responded as an isotropic material.

The same analysis was further on performed for two cross sections at the Golovec tunnel: cross section in the area of breakthrough points of both tubes (denoted as case GS-1 in Fig. 2-15) and cross section on a local road (denoted as case GS-2 in Fig. 2-15) - location of both sections is shown in Fig. 2-15. In case GS-1 the foliation uniformly dips with 40° to the right sidewall (Fig. 4-40), as documented by face logs of both tubes. The overburden declines from 55 to 35 m towards east, while it is rather horizontal at approximately 75 m above the tunnel in case GS-2. Foliation in this second case is almost horizontal in the area of the eastern tube and dips with 50° towards right sidewall in the area of the western tube, which is close to the foliation dip in case TS-1.

If just the measured values are taken into account (black dots in Fig. 4-40), it can clearly be seen that the measured settlements above the Golovec tunnel do not follow the same pattern as in the Trojane tunnel – the maximum settlement above the western tube in case GS-1 does not coincide with the centre line of the tube and furthermore the extension of the influential area is different in both cases, although the displacement magnitudes were quite similar. A portion of settlement increase in the area left from the western tube can also be due to higher overburden. Far reaching effect of the tunnelling process can also be noticed in case GS-2 in the same area (west of western tunnel tube) as in case GS-1, which are both characterized by similar dip of foliation.

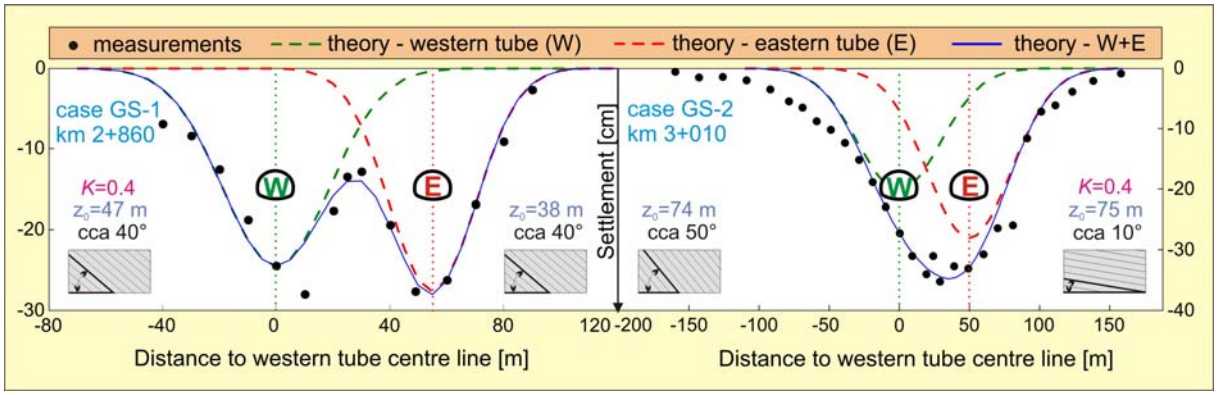

Figure 4-40. Analysis of transverse surface settlement troughs at the Golovec tunnel**.**

Slika 4-40. Analiza korita pogrezkov površine prečno na os predora Golovec.

Comparison of the measured values with the calculated curves expectedly shows deviation from isotropic behaviour in both cases. Based on numerically calculated trough in an anisotropic rock mass (Fig. 4-38), such deviation can be at least for the points above and left from the western tube in case GS-1 mainly attributed to the dip of foliation (the maximum of the settlement curve is shifted in the direction of the foliation dip, while the influence zone is significantly extended in the opposite

direction). Additionally, a maximum shift could be partly influenced by the eastern tube, which was excavated later than the western one beneath section GS-1.

On the basis of simple numerical comparison between the surface settlement trough for isotropic and anisotropic rock mass (Fig. 4-38) and according to the analysis of measured surface settlement troughs in comparison to the well established analytical equation we can conclude that settlement trough in foliated rock mass with better mechanical properties and pronounced anisotropic behaviour (like in Šentvid and Golovec tunnels) differs from the isotropic curve, which can nevertheless be used for the same type of rock mass with worse characteristics, such as in the Trojane tunnel. During studies of the impacts of tunnelling in anisotropic rock masses on the surface a special attention should therefore be focused on the extension of the influence zone as well as the maximum settlement, which is actually larger than the one calculated in isotropic conditions.

5.0 3D displacement measurements ahead of the excavation face in the exploratory tunnel of the Šentvid tunnel

5.1 Introduction

The importance of monitoring and the interpretation of the 3D displacements of tunnel circumference was already presented in previous chapters. However, for complete knowledge on the response of an underground structure one also has to be aware of the magnitude of the displacements that occur ahead of the excavation face and the displacements in the period between the excavation of a section and the first measurement of the target in this section (pre-displacements).

Experimental measurements (Lunardi, 2008) indicate that more than 30% of total ground deformation due to tunnelling process occur ahead of the excavation face. Hoek (2007) suggests that the deformation of the rock mass starts at about one half a tunnel diameter ahead of the tunnel face and that at the face position about one third of the total radial closure has already occurred.

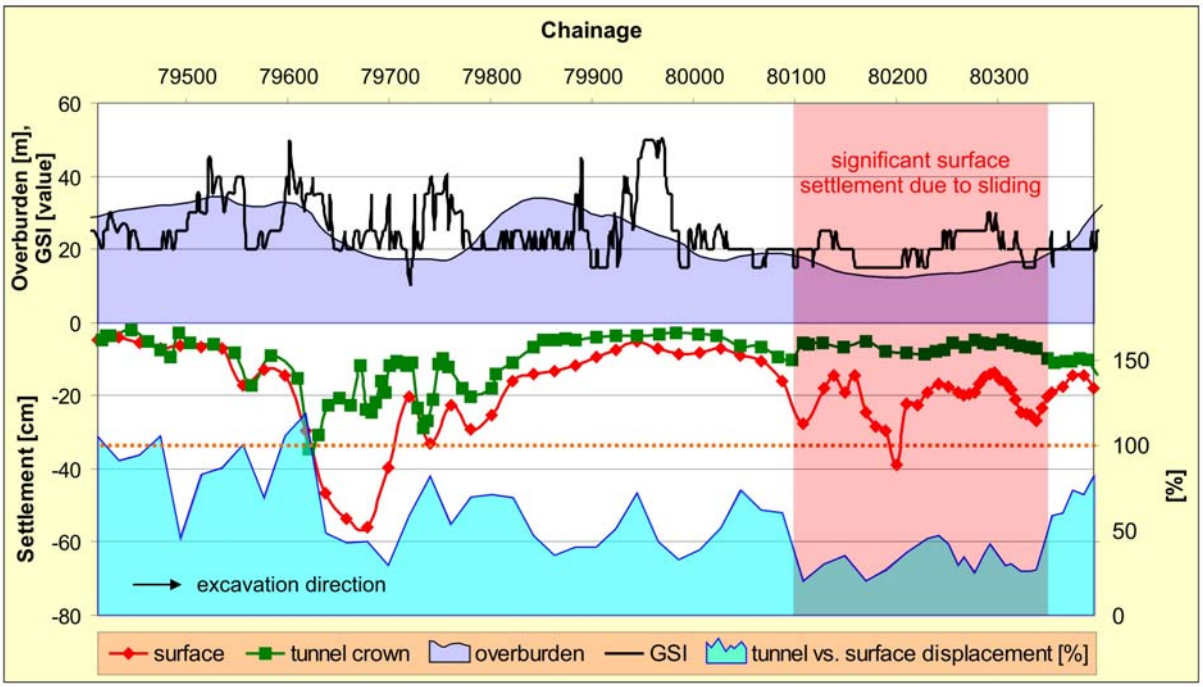

Figure 5-1. Comparison between the displacements of the tunnel crown of the southern tube of the Trojane tunnel (heading Ljubljana) and surface points in the axis of the tunnel.

Slika 5-1. Primerjava pomikov temenske točke v južni cevi predora Trojane (izkop iz vzhoda) ter površinskih točk v osi predora.

Pre-displacements cannot be measured with conventional geodetic equipment. Several geotechnical methods can be/have been used to measure the effect of the face approach to the observed cross section (horizontal inclinometer (Volkmann et al, 2005), multi-point vertical extensometer (Štimulak et al, 2002)). Beside these direct methods the range of pre-displacements can be indirectly estimated also by comparing the measured displacements in the tunnel and the measurements of the surface settlements above the tunnel with shallow overburden. As stated in Chapter 2.2.3 and plotted in Fig. 2-5, surface points in the axis of the tunnel were monitored along considerable length above the eastern part of the Trojane tunnel. In Fig. 5-1 a ratio (blue area) between the displacements of the tunnel crown of the southern tube (green line) and the surface points (red line) is plotted.

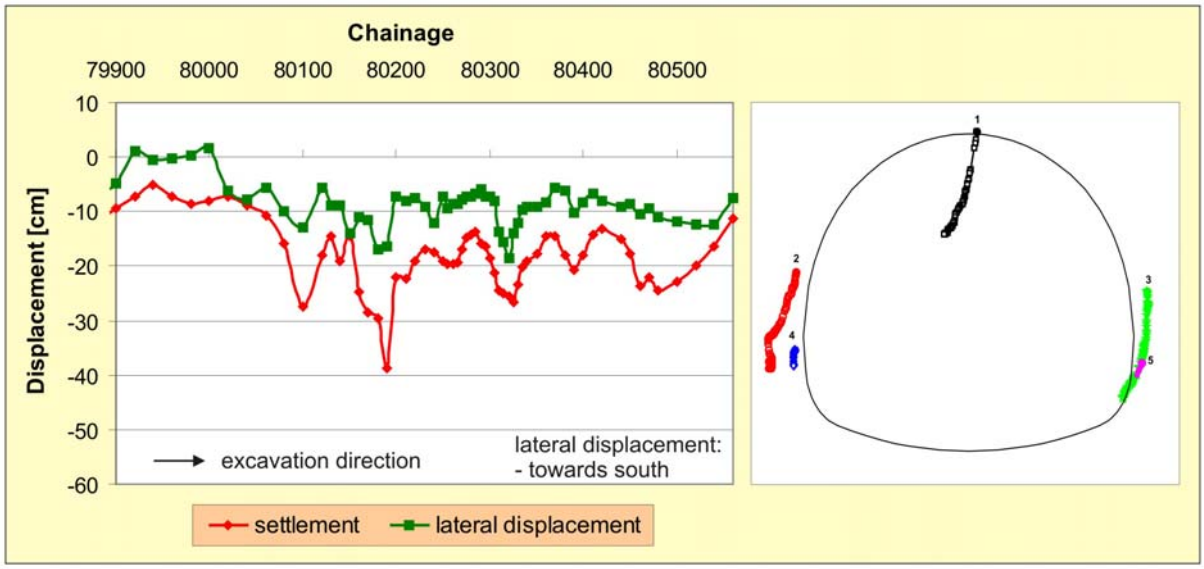

Figure 5-2. Comparison between lateral displacements and settlements of the surface points in the axis of the tunnel and characteristic measuring section in the tunnel in the area of sliding.

Slika 5-2. Primerjava prečnih pomikov in posedkov površinskih točk v osi predora ter karakteristični merski profil predora v območju plazenja.

Measured settlements of the surface points and of the tunnel crown were in the range from 4 to 56 cm and from 2 to 35 cm, respectively. The overburden above the tunnel in the selected section is in the range from 15 to 35 m (area of violet colour) and the GSI value (Marinos et al, 2000) varies from 15 to 50. It can clearly be seen that a portion of the tunnel crown displacements varies between 35% and 115% of the settlements of the surface points; the majority is under 100%. In global this portion is larger in the eastern part and it decreases towards west. The ratio is somewhat correlated to the overburden and the GSI value: in general, the lower the overburden and GSI, the lower the ratio. the lowest ratios can be seen in the western part of the presented section between the chainages km

80+100 and km 80+350, where the settlements of the surface were significantly increased by sliding of the slope towards south (Logar et al, 2004) – measured horizontal displacements were up to 20 cm, sliding affected also the deformation pattern in the tunnel – displacement vectors tend towards the left sidewall as seen in Fig. 5-2.

On the basis of this comparison it can be deduced that except for the first 200 m of the presented section the rock mass around the tunnel was completely activated by tunnelling and a significant portion of volume loss was immediately transferred to the surface. We can also conclude that at least in the case of the Trojane tunnel the measured displacements in the tunnel can amount to as low as 35% of the total displacements induced by tunnelling, if the complete volume loss is transferred to the surface or even less if it is not.

The estimation of the volume loss that is transferred to the surface and more realistic assumption of the magnitude of pre-displacements can be obtained by measuring settlements in different points in the rock mass above the tunnel. This is possible by using multi-point vertical extensometers.

Close to Garni hotel in the Trojane village (shown in Fig. 2-5) a cross section of 7 points was installed at chainage km 79+842 together with a three-point vertical extensometer in the axis of the future southern tube. The surface target was placed 34 m above the tunnel crown. The three extensometer points were situated 4, 8 and 12 m above the crown, as shown in Fig. 5-3. Zero readings of the targets were recorded long before the influence of the tunnel could affect the area.

When the top heading face was approaching the measuring section, positions of the points were taken in regular intervals. As expected, the surface point (blue line) reacted first, while extensometer points reacted quite evenly. When the tunnel surpassed the vertical extensometer, the measuring cross section was installed. Settlements were recorded as long as the rock mass was not stabilized.

If the tunnel crown settlement is compared to the surface settlement, the percentage obtained is quite similar to the values from Fig. 5-1 (about 50%; tunnel crown settlement of 6.8 cm, surface settlement of 13.8 cm). The extensometer anchor at the depth of 30 m, which is 4 m above the crown, settled 19.7 cm or three times the measured settlement of the tunnel crown. If we take the trend of measured settlements of all three extensometer points and extrapolate these measurements (values) to the tunnel crown by taking into account that settlements increase closer to the opening, we can assess the total settlement to around 25 cm. The measured settlements of the crown in this case amount only 27% of the total settlement of the point in the tunnel crown due to tunnelling, if the complete deformation path was measured. These findings indicated that merely the use of stiff primary support to control measured displacements in the tunnel does not necessarily lead to controllable

displacements of the surrounding rock mass, unless proper measures are taken for face stabilization and the pre-face displacements are limited.

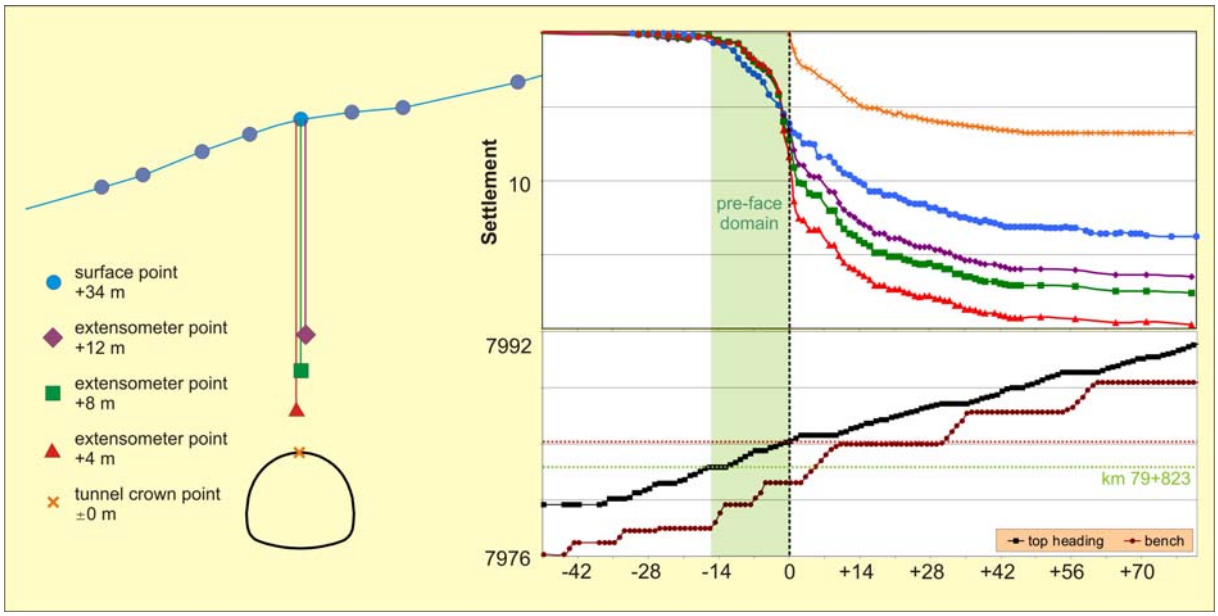

Figure 5-3. Comparison of geodetically measured settlements of the tunnel crown and on the surface and settlements of the rock mass in between, measured by three point vertical extensometer: the Trojane tunnel, southern tube (heading Ljubljana), chainage km 79+842.

Slika 5-3. Primerjava geodetsko izmerjenih posedkov v temenu predora in na površini ter posedkov v hribini, ki so bile izmerjene z vertikalnim ekstenzometrom; Predor Trojane, južna cev (izkop iz vzhoda), stacionaža km 79+842.

Another possibility of assessing the magnitude of pre-displacements is to use horizontal inclinometer above the tunnel crown. To evaluate the utilization of the pipe roof system, four 20 m long in-place horizontal chain inclinometers covering the total length of 80 m (Likar et al, 2004c) were installed in the Trojane tunnel, as shown in Fig. 2-5.

The crown settlements measured by the horizontal inclinometer are shown in the upper plot of Fig. 5-4 with influence lines. Of special interest is chainage km 80+293, where a convergence measuring section was also installed (the displacement history plot of MS83 is shown in the bottom plot of Fig. 5-4). The final measured settlement of the horizontal inclinometer at specified chainage was around 20 cm, while the measured spatial displacement of the convergence measuring section was 4.9 cm. The magnitude of pre-displacements amounts to 15 cm. The measured displacement in the tunnel in this case amounted only to 25% of the complete deformation process due to tunnelling, which is in excellent agreement with the vertical extensometer results.

With both mentioned methods the magnitude of pre-face domain (area ahead of the tunnel face, where the influence of the tunnelling can be observed) can be reliably assessed. If the distance of the deepest vertical extensometer point (4 m above the tunnel crown) is neglected, the pre-face domain measured with the extensometer extends about 20 m ahead of the face. Similarly, in case of horizontal inclinometer the pre-face domain magnitude could be set at 16 m ahead of the face.

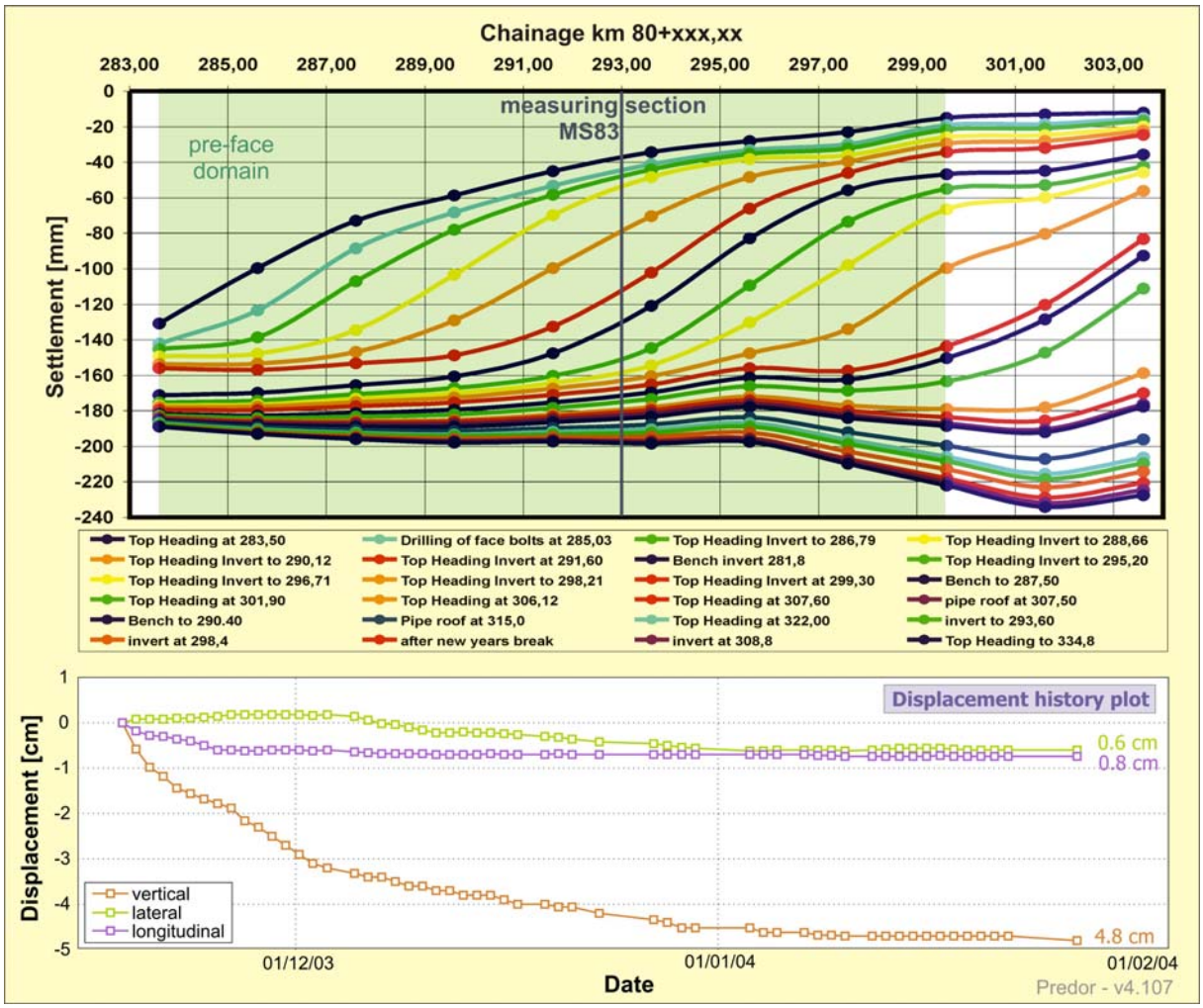

Figure 5-4. Horizontal inclinometer (chain 4) measurement results presented by the influence lines of settlements (Button et al, 2004c) – the upper plot and displacement history plot of MS83 at chainage km 80+293 – the bottom plot.

Slika 5-4. Rezultati meritev horizontalnega inklinometra (4 del), predstavljeni z vplivnicami posedkov (Button et al, 2004c) na zgornji sliki in časovni potek pomikov za merski prerez MS83 na stacionaži km 80+293 na spodnji sliki.

The advantages of measuring displacements ahead of the face with horizontal inclinometer are the accuracy of measurements (0.02 mm of the relative settlement (Likar et al, 2004c)), minimum disturbance of the rock mass and the position of the inclinometer, which allows the direct comparison with the geodetically measured settlement of the crown point. Its major disadvantage is the inability of measuring the 3D displacement. If the onset of the horizontal inclinometer is equipped with geodetic target and is regularly monitored, absolute coordinates can be obtained in addition to the relative ones (Likar et al, 2004c). The longitudinal component of pre-displacement might be additionally measured using deformeters, but no reports on such measurements can be presently found in literature. Similar features, except very high accuracy, are valid for vertical extensometer.

The 3D displacement measurements ahead of the tunnel face can only be obtained by geodetic monitoring, when a small diameter tunnel exists within the alignment of the future tunnel with considerably larger cross section. Such opportunity arose during the construction of the Šentvid tunnel and a comprehensive monitoring scheme was established.

5.2 Experiment description

5.2.1 Scheme of the experiment and equipment

The main goal of the experiment was to observe the rock mass response ahead of the tunnel face due to the tunnel excavation (displacement range, extension of the influence zone, response when approaching a fault zone, effect of installing rock bolts as a stabilization measure of the face, etc.). According to the reviewed literature 3D displacement measurements ahead of the tunnel excavation face had not been performed yet. Therefore, several problems regarding equipment and complete scheme of the experiment needed to be overcome.

Due to risky environment (possibility of overbreaks in the area of the top heading excavation face and consequently possibility of trapping the experiment staff inside the exploratory tunnel) the experiment had to be planned carefully with special focus on safety. A requirement to minimize the number of entries of the personnel into the exploratory tunnel on one hand and the request of high precision 3D measurements of a large number of points on the other hand influenced the decision regarding the type of geodetic equipment.

A total station TCRP 1201R300 produced by Leica Geosystems Inc. fulfilled the abovementioned criteria with its Automatic Target Recognition (ATR) sensor that allowed automatic angle and distance measurements of prisms. Some successfully accomplished projects using automated monitoring systems have already been reported, for example monitoring of structures above the King's

Cross station during the construction of the tunnel connections (Beth et al, 2003), some projects like monitoring of the North/South Metroline in Amsterdam are currently in progress (Netzel et al, 2001). The accuracy of angle measurements of the total station TCRP 1201R300 is ±1" according to the technical data of the instrument, while the accuracy of measuring distances to standard optical prism is ±(2 mm + 2 ppm) and positioning accuracy of the ATR is below ±2 mm (*Leica Geosystems Inc.*). When performing initial measurements of the points, the prism is sighted with the optical sight. After initiating a distance measurement, the instrument sights the prism centre automatically and both angles and the distance are measured to the centre of the prism. When the initial measurements of all planned points are completed, the program is started with the determination of the regular time intervals of the measurements. The monitoring data are stored to an internal memory card. Power supply was in our case provided with an internal battery as well as with an external battery to extend the operating time of the instrument to more than 24 hours.

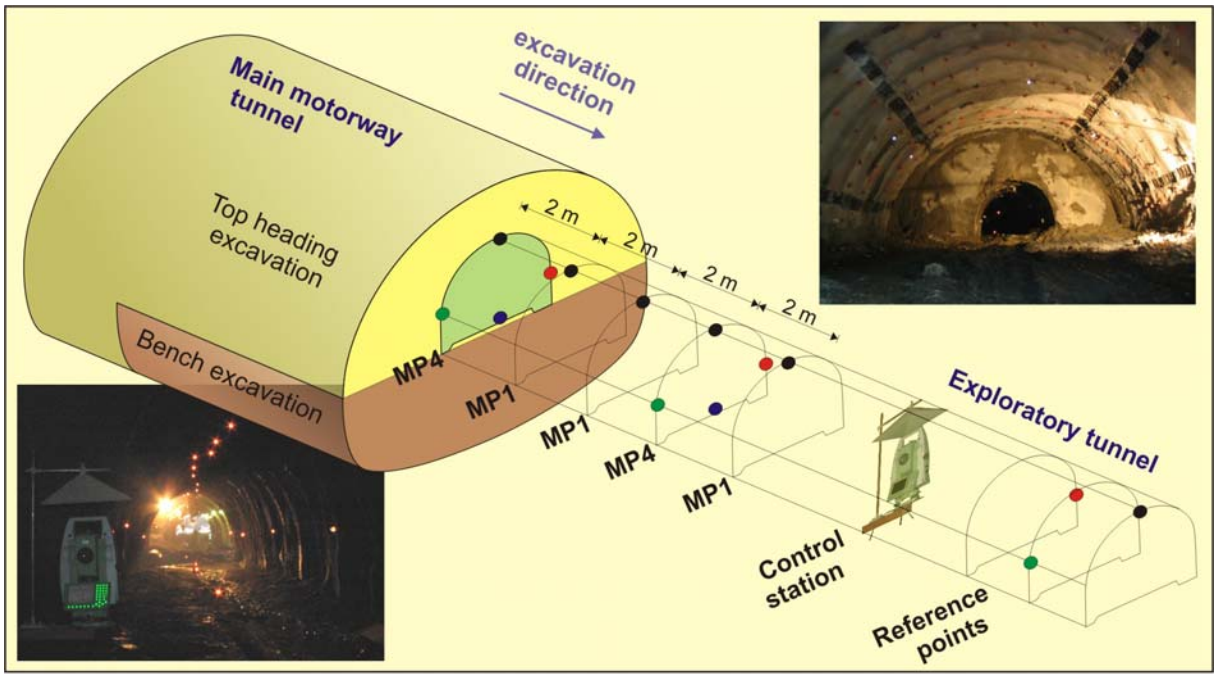

Figure 5-5. Scheme of the experiment.

Slika 5-5. Shema eksperimenta.

To assure high precision measurements, standard optical reflectors had to be mounted on the primary lining of the exploration gallery. The following pattern was selected: optical reflectors were installed every two meters in the crown and every six meters on both side walls and on the ground (Fig. 5-5). A measuring section with single target in the crown was marked with MP1 and the other with 4 targets was marked with MP4. In sections of special interest, such as transition to a fault zone, 3

measuring sections with 8 targets (MP8) were installed (3 on the ground and 5 on the primary lining) to obtain more detailed response of the exploratory tunnel. Also of special interest was the behaviour of the left wall of the cross passage, when the left tube was excavated in the vicinity. Measuring sections with a crown target and additional target on the left side wall were marked with MP2.

Optical reflectors were mounted on rebars with a diameter of 16 mm that had previously been fixed in the primary lining. Since no concrete invert was constructed in the exploratory tunnel, the rebars for the bottom targets were installed directly into the ground and secured with a small amount of concrete.

A distinction of horizontal and/or vertical angles between the targets in the crown would be insufficient for the use of ATR due to small distance from each other (only 2 m) and small diameter of the tunnel if the targets were installed in a straight line exactly in the crown. The position of the "crown" point is therefore somewhat changing along the axis (Fig. 5-4a and Fig. 5-4c), depending on the position of the instrument and the levelness of the tunnel circumference.

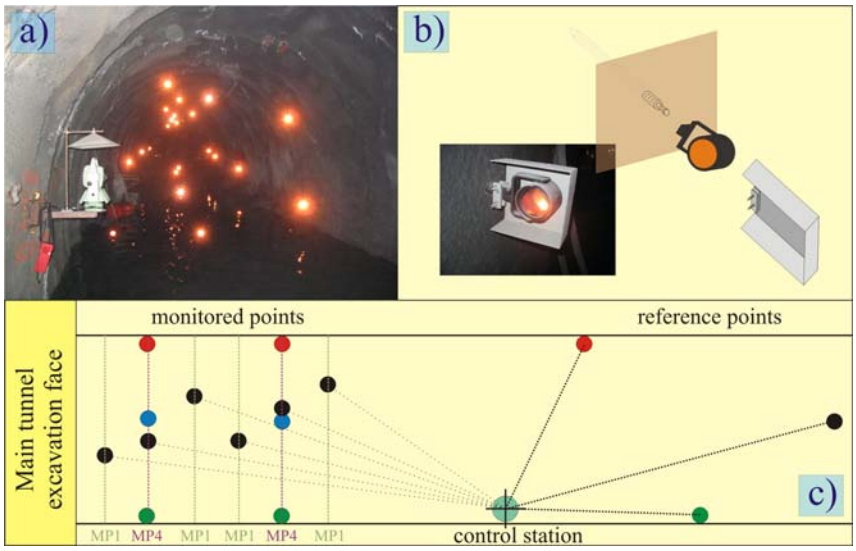

Figure 5-6. (a) Photo of the disposition of the reflectors in the exploratory tunnel. **(b)** Detail of the reflector and its protection. **(c)** Plan view of the monitoring scheme.

Slika 5-6. (a) Fotografija razporeda geodetskih točk v raziskovalnem rovu. **(b)** Detajl geodetske točke in njene zaščite. **(c)** Shematski prikaz eksperimenta v tlorisu.

To cover the expected influence zone due to the excavation of the main motorway tunnel, the monitored area was according to literature (Volkmann et al, 2005; Sellner, 2000; Barlow et al, 1986) and based on analyses of the results of vertical extensometer and horizontal inclinometer measurements primarily determined at 2 diameters of the double lane motorway tunnel ahead of the

top heading face (in our case 20 m with 10 measuring sections and approximately 20 targets). The monitored area was further on re-defined regarding the measured displacements of the targets. Zero readings of the target positions were normally taken when the points were ahead of the influence zone in order to record the entire displacement history of each individual point.

To minimize the risk of instrument damages due to the shotcrete application during the primary lining installation in the main motorway tunnel, the distance of the geodetic instrument to the top heading face was never less than 18 m. The instrument was installed on a steel cantilever beam (Fig. 5-6a) on the left or right side wall of the exploratory tunnel, depending on the visibility of the previously mounted targets and the curvature of the tunnel axis. A steel cover was placed above the instrument (see Fig. 5-5, photo in the bottom left) for protection against possible drops of water and falling pieces of the primary lining in case of larger cracks. The steel cover was placed also on the optical reflectors that were close to the face to prevent any accidental movements or breakage and especially direct application of shotcrete onto the prism (Fig. 5-6b).

One of important issues when planning the experiment was the position of the reference points and the determination of the position of the control station from the known positions of the reference points. According to the previously acquired tunnel surveying experience, three reference points were placed always in the same order: one target on the same side wall as the instrument and one target on the opposite side wall; the distance from these two points to the instrument should be nearly equal and the horizontal angle between the two points as large as possible. The third reference point was installed in the crown deeper in the exploratory tunnel (at a larger distance from the instrument). Initial positions of the first set of reference points were determined from the geodetic network in the main motorway tunnel. Further on, a new set of reference points was determined from the known positions of points monitored at that time. The reference points needed to be installed in a part of the exploration gallery that was not yet influenced by excavation works of the main motorway tunnel top heading excavation face. Such layout of the reference points proved to give optimum results in a given limited space of the exploration gallery (Marjetič et al, 2006).

The position of the control station was determined at the beginning of each set of angles due to the possible movements of the instrument's plinth (the analysis of some control stations in the left tube of the exploration gallery revealed quite large displacements). Another possibility would be to determine the position of the control station only at the beginning of the measurements at each replacement of the batteries or downloading of the monitoring data. This would actually extend the durability of the batteries, but if the instrument was in the influence zone of the excavation works, the obtained measurements of the monitored points would include a systematic error.

According to the original plan the measurements should be performed in 30 minute intervals, but the analysis of the measured displacements indicated that so frequent measurements were unnecessary and the interval was extended to 60 minutes.

All measurements of the monitored points and of the reference points were performed in both faces. Due to safety reasons the reference points were recorded first, so the instrument then stopped in the second face, pointing to the reference points and the measuring lenses faced away from the approaching tunnel face.

The built-in software of the instrument skips the target, if it is removed. If the instrument can not measure its position due to dewy surface of the target or due to dusty environment, the instrument stops during measuring and the intervention of the operator is needed. To enable measurements in aggravating environmental circumstances or measurements of the prisms with not perfectly clear surfaces, the instrument features a low visibility mode.

5.2.2 Execution of the measurements

5.2.2.1 Environmental conditions and safety issues

During the first entry in the exploration gallery the air pollution was checked for methane, carbon dioxide and carbon monoxide, since the exploratory tunnel had no longer been ventilated after its completion. Surprisingly the air in the exploratory tunnel was fresh, even in the most distant parts at the dead end of the exploratory tunnel. On the basis of later observations of the air ventilation we assumed that the temperature differences between the ground (cold water) and the crown of the gallery ran the self ventilation and maintained the air fresh.

An important issue was also a communication with the Contractor. For safety reasons the entrance to the exploration gallery was allowed once a day and only when the excavation step was completed, the primary lining installed and the face stability ensured. Usually we entered the exploratory tunnel during drilling for the rock bolts or during shifts. The Contractor's staff were also requested to remove the optical reflectors and their protection prior to the excavation of the round length with the measuring section.

5.2.2.2 Measurements in the right tube of the exploratory tunnel

At the time of planning the experiment the right tube was excavated in the section with the exploratory tunnel ahead of the face, while the left was not. Consequently, the targets and the instrument were installed in the right tube and the measurements started on September 6th, 2005. In the

first two weeks only one measurement a day was performed to get accustomed to the instrument and to set the exact procedures. Continuous monitoring started on September 22nd.

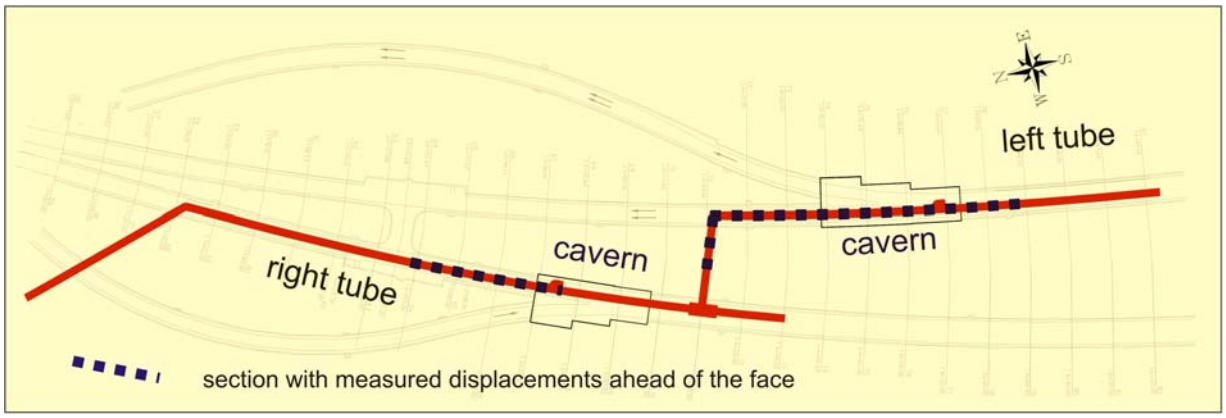

Figure 5-7. Sections of the exploratory tunnel with measured displacements ahead of the motorway face.

Slika 5-7. Odseki v raziskovalnem rovu, kjer so bili merjeni pomiki pred čelom avtocestnega predora.

From measuring sections P1 to P9 (chainage km 1.2+54 to km 1.2+73) the main motorway tunnel was constructed in faulted rock mass and large displacements were measured ahead of the face (vertical displacement 9.3 cm and longitudinal displacement 13.3 cm in the excavation direction).

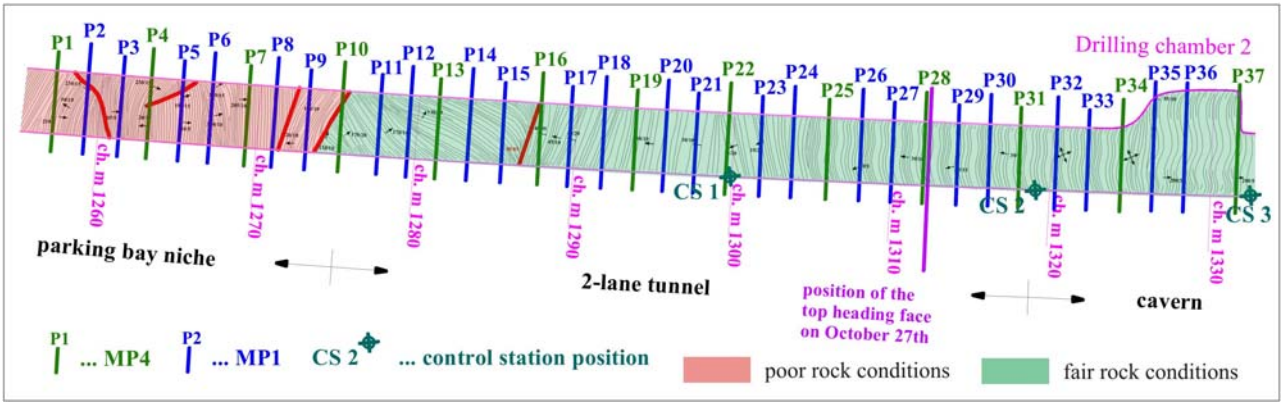

Figure 5-8. Disposition of the measuring cross sections and control station positions in the right tube of the exploratory tunnel with lined geological layout.

Slika 5-8. Razpored merskih profilov in položajev merskega instrumenta v desni cevi raziskovalnega rova; podložena geološka situacija.

When the fault zone was passed and the top heading excavation face approached the merging cavern and entered the block of sandstone with very good geological and geotechnical characteristics, the measured displacements decreased significantly to less than 1 cm and remained in the range of the measuring accuracy of 2 mm (Marjetič et al, 2006) during further excavation in the cavern. Therefore, the continuous monitoring in the right tube ahead of the excavation face stopped on October 27th and the instrument was moved into the left tube that entered the section with the exploratory tunnel ahead of the top heading face.

The length of the monitored section in the right tube amounted to 75 m (from chainage km 1.2+57 to km 1.3+32 – the section is plotted with blue dotted line in Fig. 5-7) and included 37 measuring sections (Fig. 5-8). The first 28 out of 37 measuring sections were monitored on complete deformation path (from the time the measuring section got into the influence zone ahead of the face to the excavation of the round length with the measuring section).

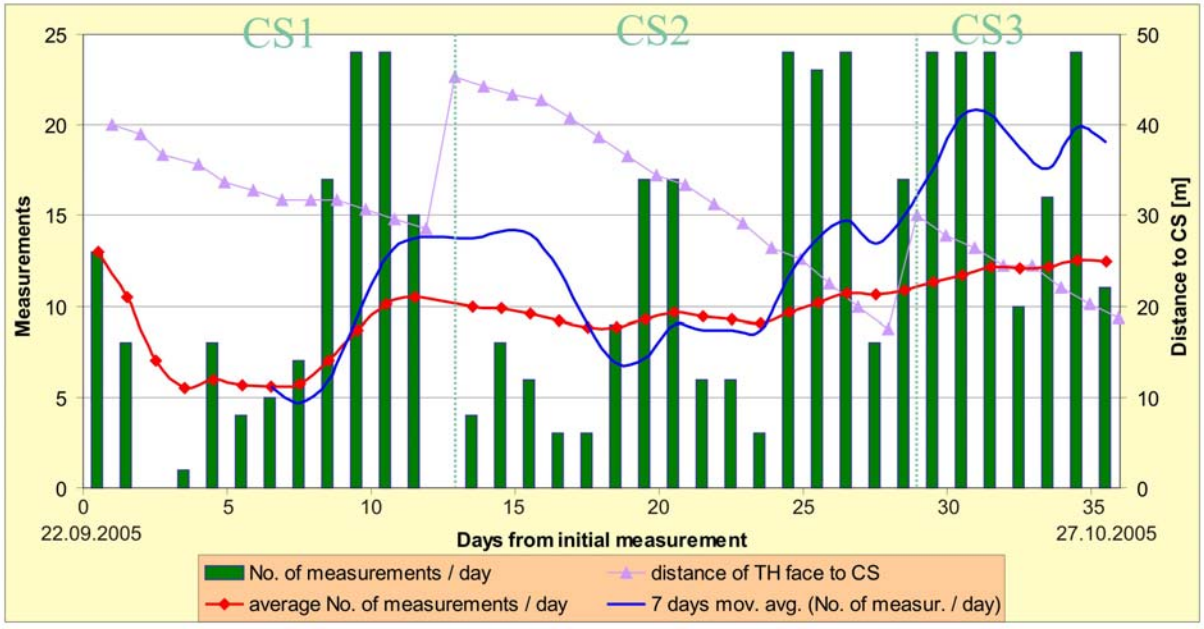

Figure 5-9. Number of daily performed measurements in the right tube of the exploratory tunnel with plotted average measurement rate and distance of the control station to the top heading excavation face of the main motorway tunnel.

Slika 5-9. Število dnevno izvedenih meritev v desni cevi raziskovalnega rova z izrisanim povprečjem ter razdaljo merskega instrumenta od izkopnega čela kalote avtocestnega predora.

Due to fair tunnelling conditions and only minor quantities of water no major problems were encountered during continuous monitoring in the right tube. In 35 days of continuous monitoring 437

sets of measurements were performed or 12.5 measurements per day on average. The number of daily performed measurements through the monitoring period is given in Fig. 5-9.

To avoid accidental damage of the instrument, the first total station position was set at a large distance from the first measuring section (42 meters). With further experience this distance was decreased, since due to the dust caused by the excavation works, the instrument was not able to define the position of the monitored points and thus stopped. Since the entrance to the exploratory tunnel was due to safety and logistic reasons limited to once a day, only some sets of measurements were performed a day if the instrument stopped. The instrument was put in operation again on the next day. The dependence of the number of executed measurements on the distance of the instrument from the face can be observed in Fig. 5-9 and it clearly shows that the number of the measurements performed per day was in general increasing with decreasing distance from the control station to the face.

5.2.2.3 Measurements in the cross passage of the exploratory tunnel

As the excavation of the left tube of the motorway tunnel approached the intersection of the cross passage and the beginning of the left tube of the exploratory tunnel, large cracks developed in the primary lining of the exploratory tunnel. Some individual measurements were executed in this area during the continuous monitoring in the right tube.

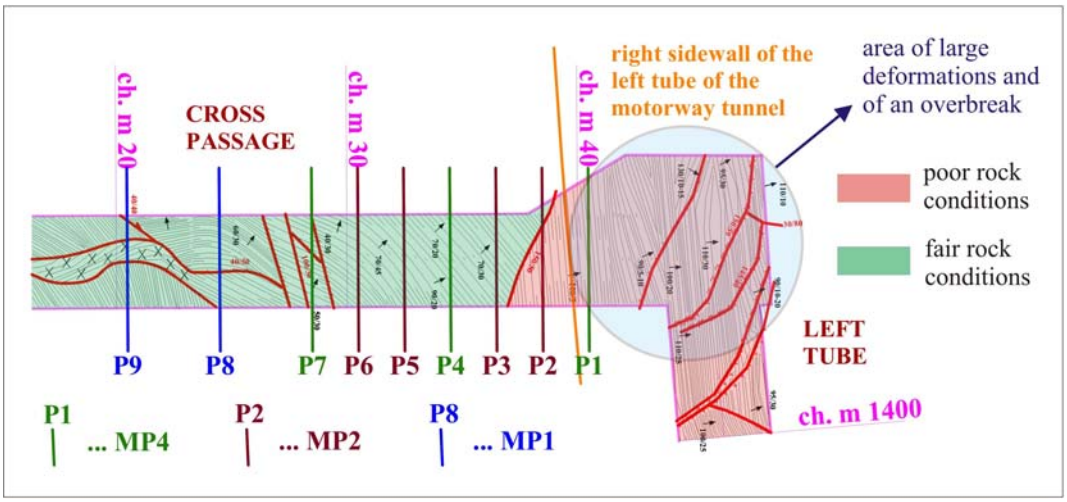

Figure 5-10. Disposition of the measuring cross sections in cross passage of the exploratory tunnel with lined geological layout.

Slika 5-10. Razpored merskih profilov v prečniku raziskovalnega rova; podložena geološka situacija.

To observe the response of the rock mass to excavation also perpendicular to the tunnel axis, 3D displacement measurements were performed in the cross passage. The measurements started on October 7th, when the distance of the intersection to the excavation face of the left tube was 11 m. According to the mapped deformation of the primary lining it is obvious that some deformation was missed. The measured displacements were somewhat smaller than in the right tube (maximum vertical displacement 2.7 cm, horizontal 1.3 cm and longitudinal 1.8 cm) due to the geological structure. The cross passage is situated in a block of firm, horizontally foliated sandstone and siltstone.

Altogether 9 measuring cross sections were installed in 20 meter long section in the cross passage, as shown in Fig. 5-10. To minimize the number of measurements on one hand and to cover the expected influence zone on the other, the distance between measuring sections P7 and P8 was 4 meters, while between individual measuring sections from P1 to P7 it was 2 meters. The control station was placed in the intersection of the right tube and the cross passage and its position was determined on the basis of the reference points in the right tube of the exploratory tunnel. The measurements were performed once a day till October 20th, when the face was 8.6 m ahead of the cross passage. The contractor then reprofiled the entrance to the cross passage. This was an additional contribution to rock mass deformation, as the effects of reprofiling and further excavation of the left tunnel tube acted simultaneously. The original plan to use the cross passage for the observation of the displacements in the perpendicular direction to the advancing tunnel excavation was therefore no longer possible. Thus, the monitoring was stopped.

5.2.2.4 Measurements in the left tube of the exploratory tunnel

Simultaneously with the measurements in cross passage the monitoring of measuring sections P1 to P13 started also in the left tube of the exploratory tunnel. But only two sets of measurements were executed (October 7th and 10th) because of increased influence of the approaching excavation face of the main motorway tunnel and consequently large cracks in primary lining of the exploration gallery. On October 13th an overbreak of approximately 50 m^3 occurred in this area and the entrance to the left tube of the exploration gallery was temporarily closed. Till October 25th no entry to the exploratory tunnel in the left tube was allowed. Continuous monitoring thus started on October 27th, 2005.

The expected as well as the encountered geological conditions in the left tube were considerably worse than in the right tube. Consequently, the monitored deformations were by a magnitude larger (maximum vertical displacement 26.5 cm, horizontal 16.3 cm and longitudinal 29.3 cm against the excavation direction).

A 147 meter long section from chainage km 1.3+97 to km 1.5+44 was equipped with 72 measuring sections, as seen in Fig. 5-11. A complete deformation path of measuring sections from P1 to P66 was obtained. The monitoring of the 3D positions of the targets in the left tube of the exploratory tunnel (and generally ahead of the excavation face in the Šentvid tunnel) finished on April 24th 2006 due to the worsening of the geological conditions that caused complete deterioration of the primary lining in the exploratory tunnel. 2,040 sets of measurements were performed in 179 days of continuous monitoring in the left tube of the exploration gallery ahead of the excavation face or 11.4 measurements per day on average (the number of performed measurements per day during complete period is plotted in Fig. 5-12).

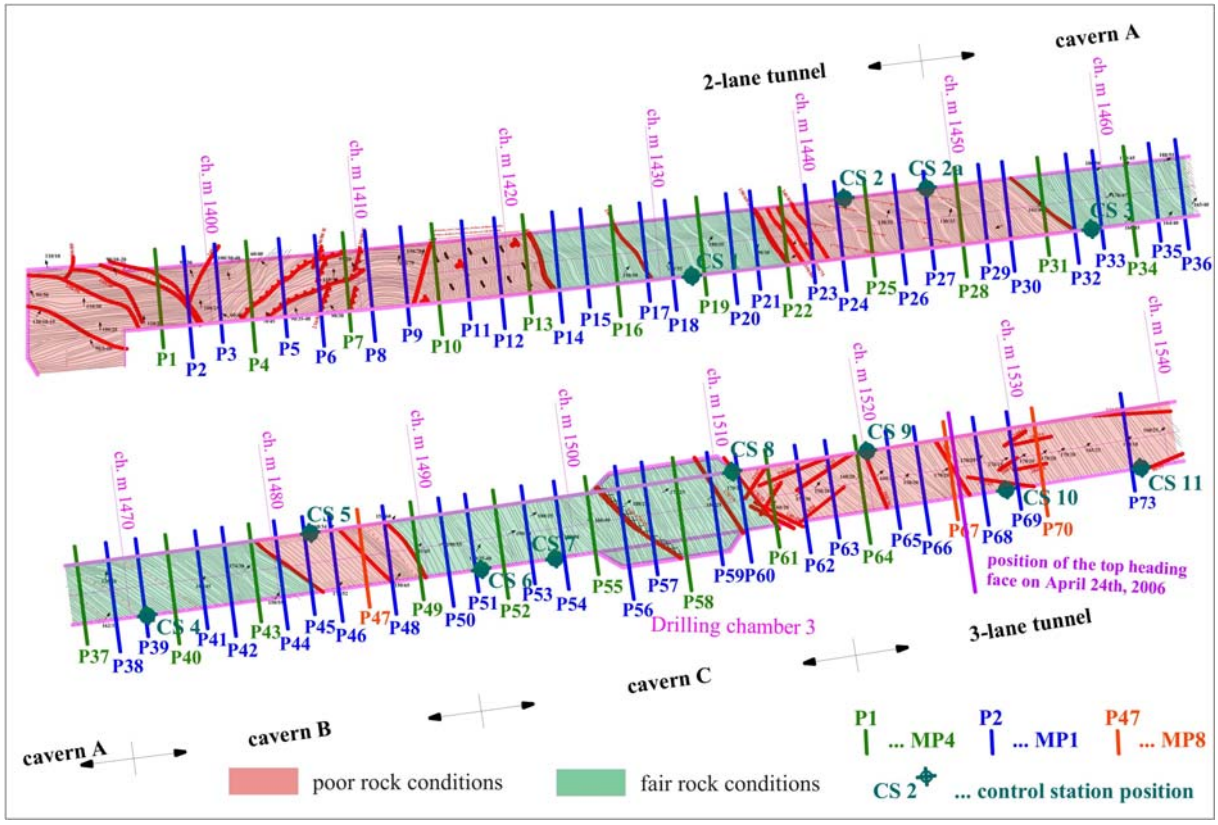

Figure 5-11. Disposition of the measuring cross sections and control station positions in the left tube of the exploratory tunnel with lined geological layout.

Slika 5-11. Razpored merskih profilov in položajev merskega instrumenta v levi cevi raziskovalnega rova; podložena geološka situacija.

Unlike the right tube, where dust turned out to be the main problem of the monitoring and only minor quantities of water flowed out of the exploration gallery, in the left tube water and humidity were a major issue. The monitoring in the right tube took place in early autumn with pleasant weather

conditions and air that was pumped in the tunnel through the ventilation system was warm and dry. As the outside temperatures decreased in the beginning of December 2005 (black line in Fig. 5-12), the humidity in the tunnel increased and condensed on the optical reflectors, which became wet and were covered with droplets of water. The laser beam of the instrument was able to detect a pre-recorded target, but could not measure its position, probably due to the dispersion of laser beam on the water droplets. Thus, it stopped while measuring. The number of executed measurements per day was drastically reduced, as plotted in Fig. 5-12.

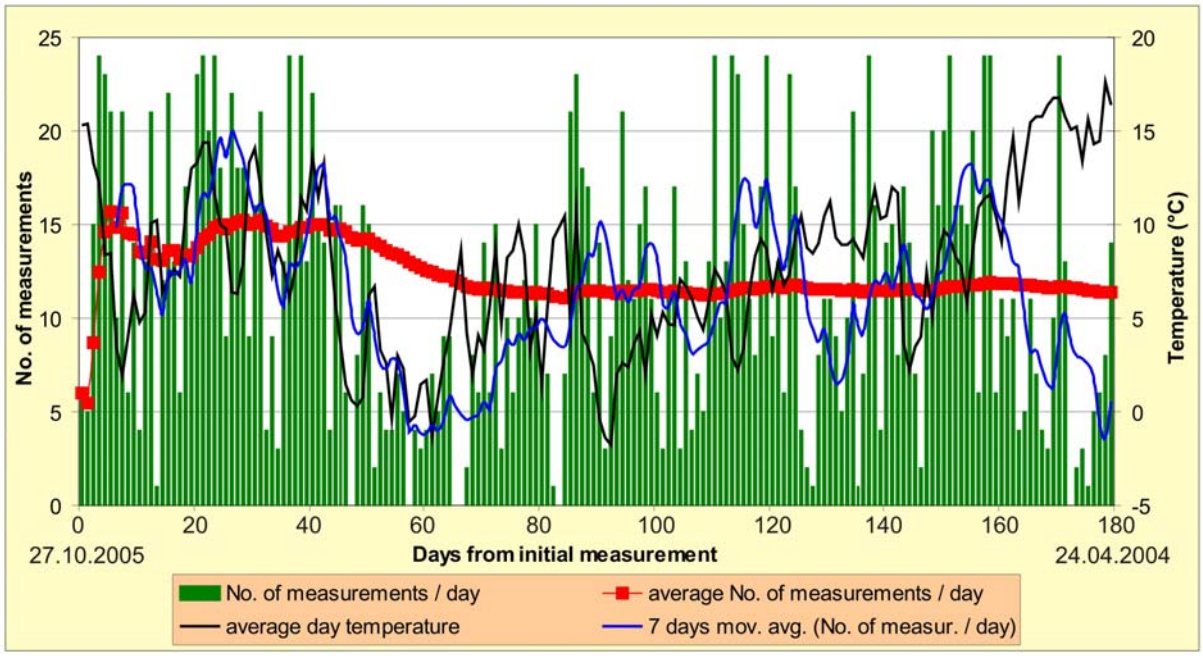

Figure 5-12. Number of daily performed measurements in the left tube of the exploratory tunnel with plotted average measurement rate and average day temperature in Ljubljana.

Slika 5-12. Število dnevno izvedenih meritev v desni cevi raziskovalnega rova z izrisanim povprečjem ter povprečno dnevno temperaturo v Ljubljani.

The conditions in the tunnel even impaired from December 20th to January 4th, when the construction works were stopped and the construction machinery was not heating the air in the tunnel while running. The optical reflectors were wiped off at every entrance into the exploration gallery, but indispensably became wet again in a few hours. Several hydrophobic liquids and/or procedures to prevent dewy surface of the targets were unsuccessfully applied. The only procedure that worked with limited effect was watering of the prisms and thus making a uniform water film on the surface. The droplets of water arose later and after January 5th a few more sets of measurements were performed daily, as seen in Fig. 5-12.

To increase the number of daily performed measurements the low visibility mode was implemented on January 18th, but was switched off 6 days later due to rather lower accuracy of the acquired position of monitoring and reference points. Larger scatter up to 3 mm at the determination of the control station position from January 18th onwards can be seen in Fig. 5-13. From the scatter of measurements in Figure 5-10 before January 18th the inaccuracy in determining the control station position without low visibility function can be estimated in the range of 1 mm (more precise calculation is given in (Marjetič et al, 2006)).

Another problem was related to water damming at the entrance to the exploratory tunnel. The estimated volume of water flowing out of the exploratory tunnel was about 2 L/s (the majority flowed out from the drilling holes in drilling chamber 3 – Fig. 5-11). Due to unfavourable tunnelling conditions the excavation works of the top heading face were divided in several smaller steps and usually required several hours to complete. In the time the water was dammed in the exploratory tunnel, it flooded the bottom targets and the instrument stopped if more than half but not the whole of the prism was submerged. The entry to the exploratory tunnel was impossible until the excavated material was removed and the water was drained out.

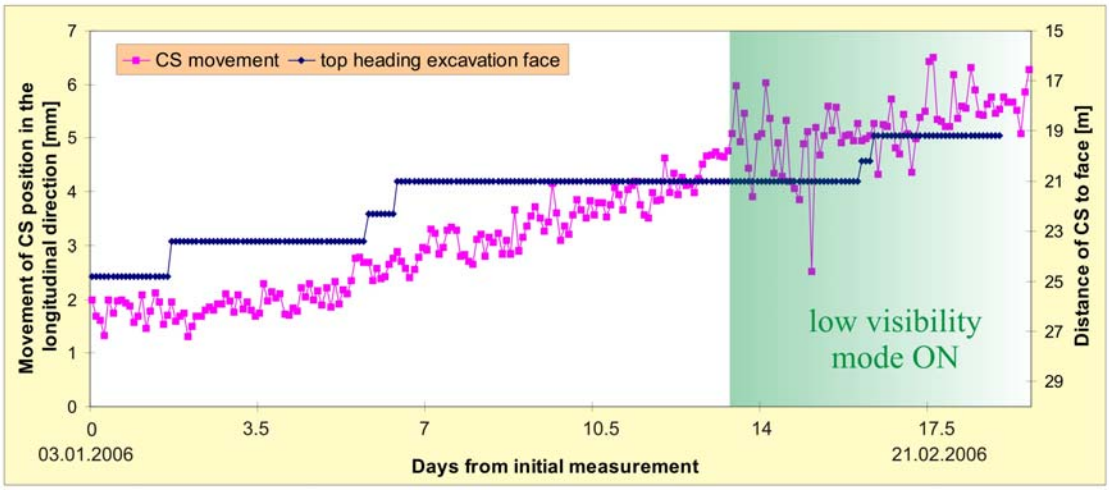

Figure 5-13. Movement of the position of the control station CS6 in longitudinal direction with plotted distance from control station to the top heading excavation face.

Slika 5-13. Pomik merskega mesta CS6 vzdolž predorske osi z izrisano razdaljo do izkopnega čela kalote.

As outlined earlier, the tunnelling conditions in the left tube of the Šentvid tunnel were considerably more demanding and the displacements larger than in the right tube. The measurements of the monitoring points also indicated more extensive influence zone ahead of the excavation face and the instrument was situated inside this zone (usually at a distance of 20-30 m from the excavation

face). The displacement of the instrument on the cantilever beam was primarily noticed on the circular level of the instrument and further analysis confirmed movement of the control station as seen in Fig. 5-14. In this case the decision to determine the position of the control station in each set of angles proved to be appropriate. When the influence zone extended to up to 45 m (Klopčič et al, 2006), the reference points were also exposed to movements. A correct procedure in this case would be to move the instrument further into the exploration gallery, but due to the levelness and small diameter of the constructed exploratory tunnel this would cause problems with Automatic Target Recognition.

On the basis of the performed measurements we concluded that due to the geological structure the reference point on left side wall would move prior to the point on the opposite wall and the analysis of the control station position confirmed it. In Fig. 5-14 the position of CS8 in east-west direction of Gauss-Krueger coordinate system as calculated from different combinations of the reference points is plotted with time, since known positions of two targets are required for the calculation of the position of the third point. The calculated position with the combination crown point – right sidewall point and left sidewall point – right sidewall point is nearly identical, while the combination crown point – left side wall point secedes. In this case only crown point and right side wall point were employed in the calculation of the control station position.

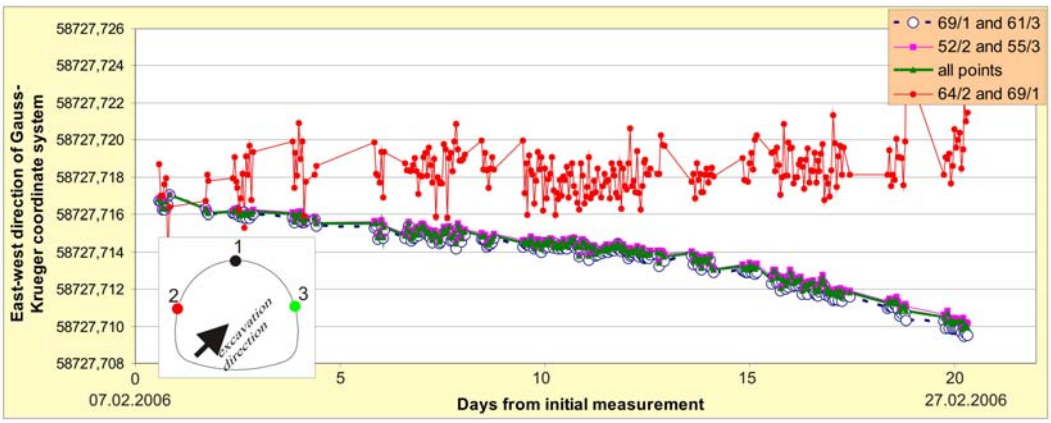

Figure 5-14. Movement of the position of the control station CS8 in east-west direction of Gauss-Krueger coordinate system as calculated from different combinations of the reference points.

Slika 5-14. Sprememba položaja merskega mesta CS8 v smeri vzhod-zahod Gauss-Kruegerjevega koordinatnega sistema, izračunan iz različnih kombinacij danih točk.

At the end of continuous monitoring in the exploratory tunnel ahead of the excavation face of the left tube the position of the latter reference points was measured again from the geodetic network in

the main motorway tunnel. After 6 months, during which time 147 m of the exploration gallery were monitored and the control station position was changed twelve times, the accumulated difference between the position of the reference points, measured from the main motorway tunnel and from local geodetic network in the exploratory tunnel, amounted to 8.5 cm towards west and 3.5 cm towards north. The accumulated height difference was 2 cm.

Table 5-1. Summary of performed 3D displacement measurements in the exploratory tunnel.

Preglednica 5-1. Povzetek izvedenih 3D meritev pomikov v raziskovalnem rovu.

	Chainage	Section length [m]	No. of meas. sections	Monitoring days	Sets of meas.	Avg. No of sets of meas. / day
Right tube	km 1.2+57 – km 1.3+32	75	37	35	437	12.5
Cross passage	km 0+20 – km 0+40	20	9	11	11	1
Left tube	km 1.3+97 – km 1.5+44	147	72	179	2400	11.4
Total		242	118	225	2488	11.7

5.2.3 Sulphate corrosion of shotcrete in the exploratory tunnel

As already stated, the construction of the exploratory tunnel started in spring of 2004, almost a year before the main tunnel execution (at the beginning of 2005). Within daily entrances to the exploratory tunnel deteriorated shotcrete of the primary lining and large quantities of brown precipitate attracted our attention. Shotcrete was of yellow colour with micro cracks on the surface (Fig. 5-15) and of low compression strength. Bigger grains of aggregate were easily separated from the cement matrix (Klopčič et al, 2005). Compression strength measured with concrete test hammer (Schmidt hammer) was well below 10 MPa.

Water from the exploratory boreholes contained particles of brown colour, which precipitated on the ground below the boreholes (Fig. 5-16). Chemical analysis revealed the presence of ferric hydroxide (Petkovšek, 2006), which is the final product of pyrite oxidation. In the surrounding rock mass pyrite in the form of powder or larger pieces (up to 1 cm^3) was observed (Fig. 5-17).

Pyrite is unstable when exposed to oxygen in presence of water and tends to oxidize to form a sulphuric acid (Eq. 5-1) that reacts with the cement matrix and forms sulphates, mostly gypsum ($CaSO_4$ x $2H_2O$) – (Petkovšek, 2006).

$$FeS_2 + 15/4O_2+7/2H_2O = Fe(OH)_3 + \mathbf{2\ H_2SO_4} \quad \text{Eq. 5-1}$$

Figure 5-15. Deteriorated shotcrete with micro cracks.

Slika 5-15. Brizgani beton slabše nosilnosti z mikro razpokami.

Figure 5-16. Ferric hydroxide in tunnel waters.

Slika 5-16. Oborina železovega hidroksida v vodi iz vrtine.

Sulphates are the source of sulphate ions that can initiate the sulphate reaction of the shotcrete and consequently the formation of new, highly expansive minerals like ettringite (Eq. 5-2 – Petkovšek et al, 2005) and thaumasite (Eq. 5-3 - Bensted, 1999) that can expand the volume up to 250%.

$$CaSO_4 \,.\, 2H_2O \text{ x } Ca_3(AlO_3)_2 + 30H_2O = CaO.\ Al_2O_3.\ CaSO_4 \,.\, 32H_2O \quad \text{Eq. 5-2}$$

$$Ca_3Si_2O_7 \text{ x } 3H_2O + 2\{CaSO_4 \,.\, 2H_2O\} + CaCO_3 + CO_2 + 23H_2O = \quad \text{Eq. 5-3}$$

$$CaSiO_3.\ CaCO_3.\ CaSO_4 \,.\, 24H_2O$$

To explore the reason for deteriorated shotcrete a Scanning Electron Microscopy (SEM) analysis of the samples taken from the exploratory tunnel was performed and proved the presence of the

secondary ettringite in the cement matrix (Fig. 5-18). On the basis of these findings samples from the primary lining of the main motorway tunnel were taken. The analysis showed the formation of secondary ettringite in some of the samples. Therefore precaution measures for further construction were undertaken (use of sulphate resistant cement for bolt grouting and reinforcement of the secondary lining). The latter measure was used for the first time in Slovenia.

Figure 5-17. Siltstone, containing larger pieces of pyrite.

Slika 5-17. Meljevec z večjimi kristali pirita.

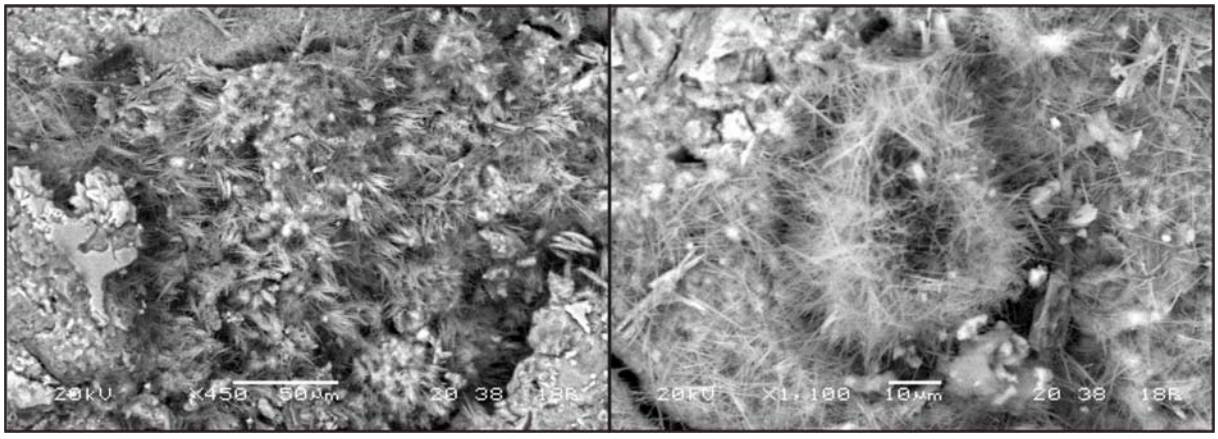

Figure 5-18. SEM scans of shotcrete samples from the exploration gallery (Petkovšek et al, 2005).

Slika 5-18. SEM sliki brizganega betona iz raziskovalnega rova (Petkovšek et al, 2005).

5.3 Results

Monitoring data from the experiment presented were daily processed and inserted in the database. From research point of view the right tube is less interesting than the left one, since the displacements were along a considerable section insignificant, close to the right cavern that is situated in firm sandstone even negligible (Fig. 5-19). Although the monitoring of the right tube started in a fault zone where the first 9 measuring sections with considerable displacements measurements were located, the positions of these targets were not recorded continuously and no particular conclusions can be made.

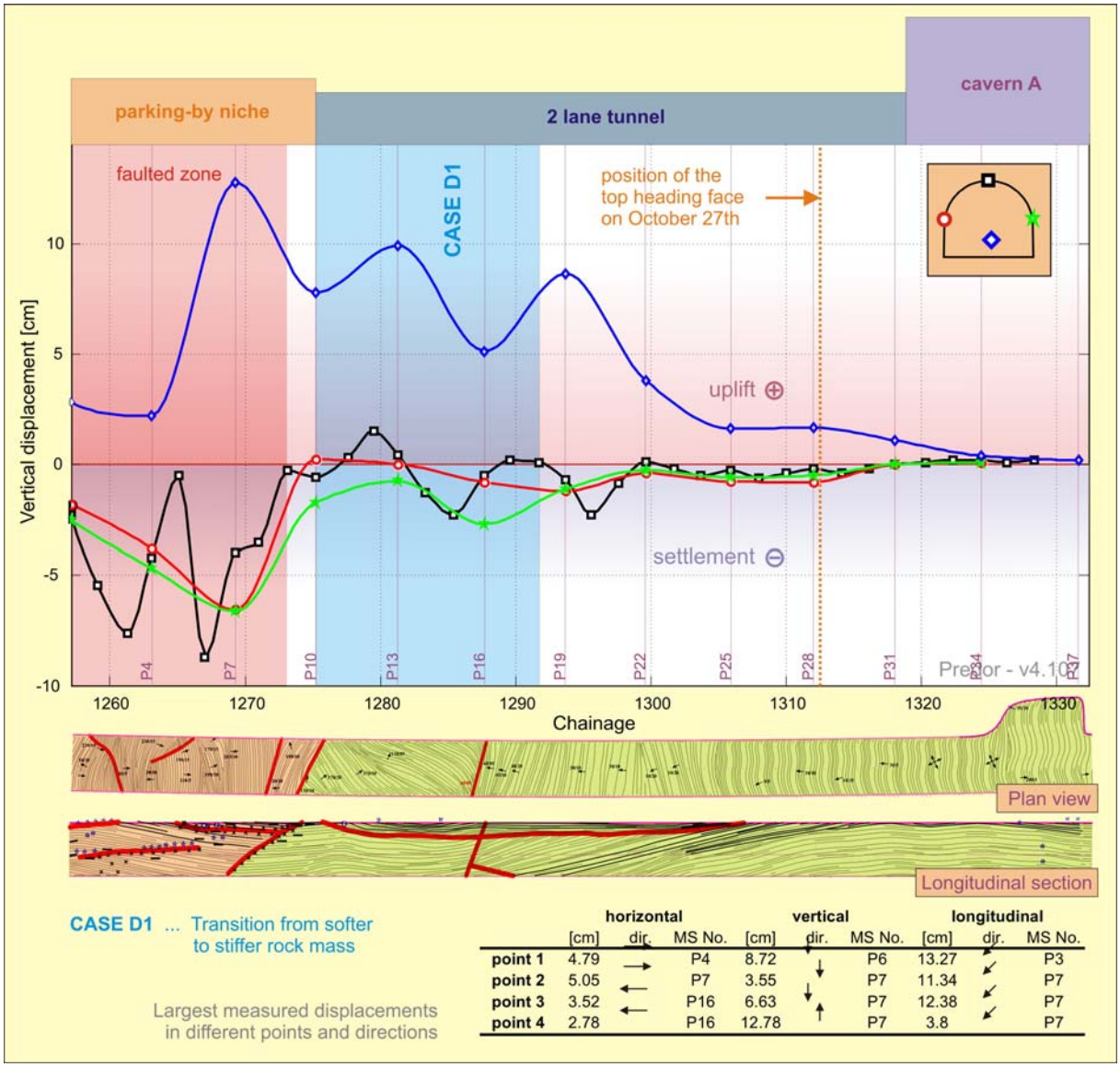

Figure 5-19. Contour of vertical displacements of all 4 points along the complete monitored section in the right tube.

Slika 5-19. Kontura vertikalnih pomikov točk na celotnem merjenem območju desne cevi.

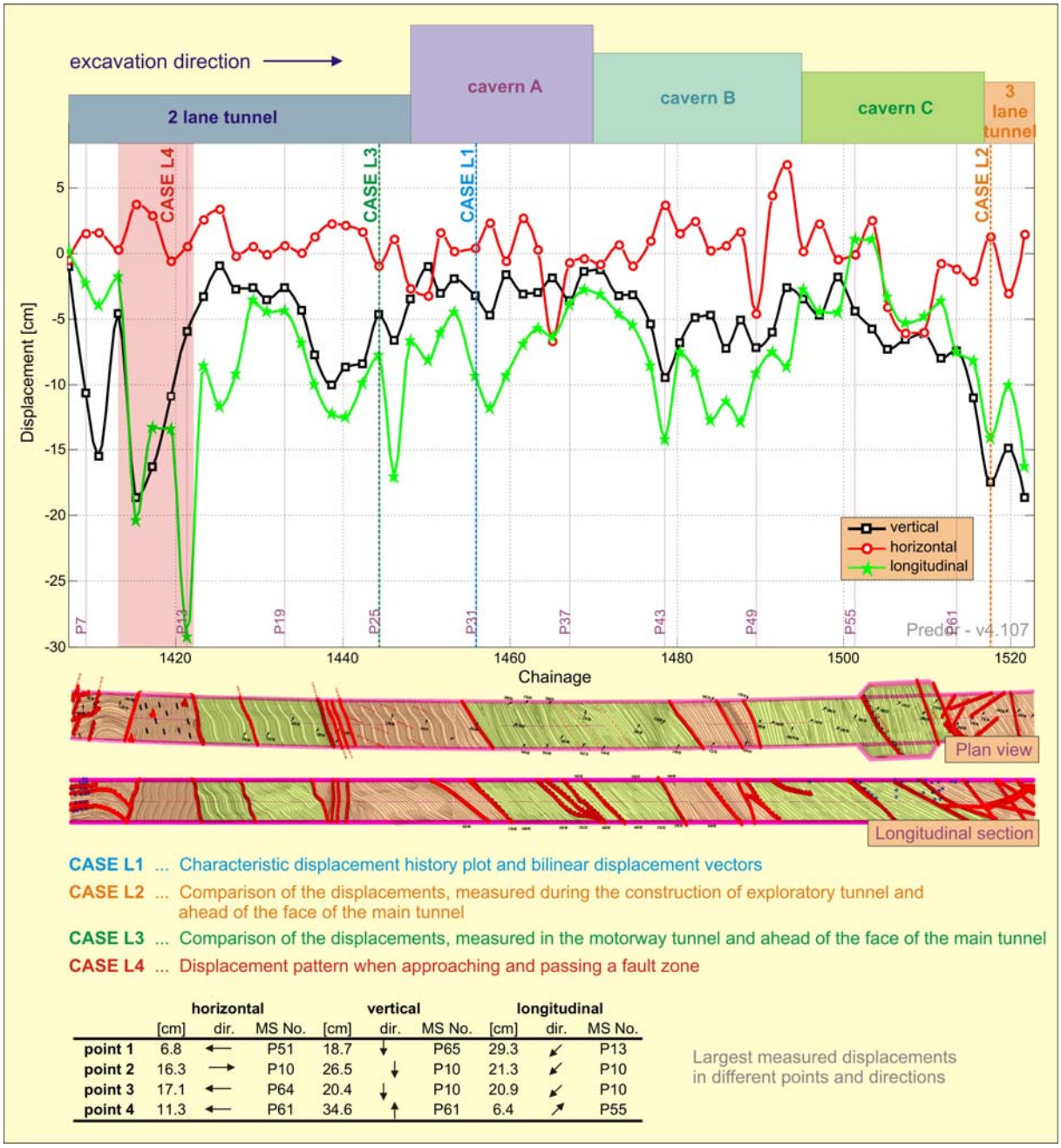

	horizontal			vertical			longitudinal		
	[cm]	dir.	MS No.	[cm]	dir.	MS No.	[cm]	dir.	MS No.
point 1	6.8	←	P51	18.7	↓	P65	29.3	↙	P13
point 2	16.3	→	P10	26.5	↓	P10	21.3	↙	P10
point 3	17.1	←	P64	20.4	↓	P10	20.9	↙	P10
point 4	11.3	←	P61	34.6	↑	P61	6.4	↗	P55

Figure 5-20. Vertical, horizontal and longitudinal displacement contours of the crown point along the monitored section of the left tube of the exploratory tunnel (only monitoring cross sections with total displacement path monitored are shown).

Slika 5-20. Vertikalni, horizontalni in vzdolžni pomiki stropne točke vzdolž opazovanega območja leve cevi raziskovalnega rova (prikazani so samo merski profili, kjer je bila merjena celotna krivulja pomikov).

The only interesting case was noticed on measuring sections just after the fault zone, where two transitions in stiffness of the rock mass were encountered (from fault zone to folded siltstone and further to firm sandstone). A detailed description of the observed behaviour is given in the sequel.

For research purposes the left tube is more promising. A part of the monitored section was located in the 2-lane tunnel, the majority in the merging cavern and the last small part in the 3-lane tunnel. Significant displacements in all three directions (Fig. 5-20) were observed, some measuring sections were located in fault zones and some in sections of "homogeneous" material., Far reaching influence of the tunnel face advance was also perceived on the instrument and on the cracks of the primary lining. When installing rebars for the target bases, a special attention was paid to place the MP4 measuring sections close to measuring sections that were monitored during the exploratory tunnel construction. The comparison of both measured displacements will be shown, as well as the comparison of the displacements in the motorway tunnel and ahead of the face. Measurements of the response ahead of the face also allowed the evaluation of the effect of grouted rock bolts as an active preface support measure on limiting preface displacements.

5.3.1 Characteristic behaviour (case L1)

A simple 3D displacement history plot of a target ahead of the approaching motorway tunnel excavation face is the basic outcome of the presented experiment.

A characteristic 3D displacement history plot of a MP4 measuring section is shown in Fig. 5-21. This measuring section was located in the beginning of cavern A, where the top heading excavation cross section gradually enlarges from 56 m^2 in the 2-lane tunnel to 93 m^2 in cavern A. The first measurement of the bottom target was performed when the distance of the measuring section to the face amounted to around 40 m. The initial positions of other three targets in the primary lining were recorded several days later at the distance to the face of approximately 30 m. The first measurements of the targets at such large distances to the face were inevitable in order to be able to precisely assess the extension of the influence zone ahead of the approaching face. Some extra measurements of the bottom target were performed afterwards because from previously acquired experience we had learned that deformation of the ground starts prior to deformation of the shotcrete lining. When the continuous measurement of the cross section started approximately 20 m ahead of the top heading face, the obtained positions were just slightly different than zero readings of the targets, except for the ground target where about 0.8 cm of spatial displacement was recorded.

With approaching excavation the first measured deformation of the lining of the exploratory tunnel ahead of the face was generally in radial direction, later on longitudinal deformation occurred.

Possible cause could be the axial stiffness of the primary lining ahead of the face. As expected, the longitudinal deformation was towards approaching face, only the displacement vector of the bottom target pointed in the opposite direction. This deviation could be explained by the rotation of the target's base that was fixed into the ground due to ground uplift.

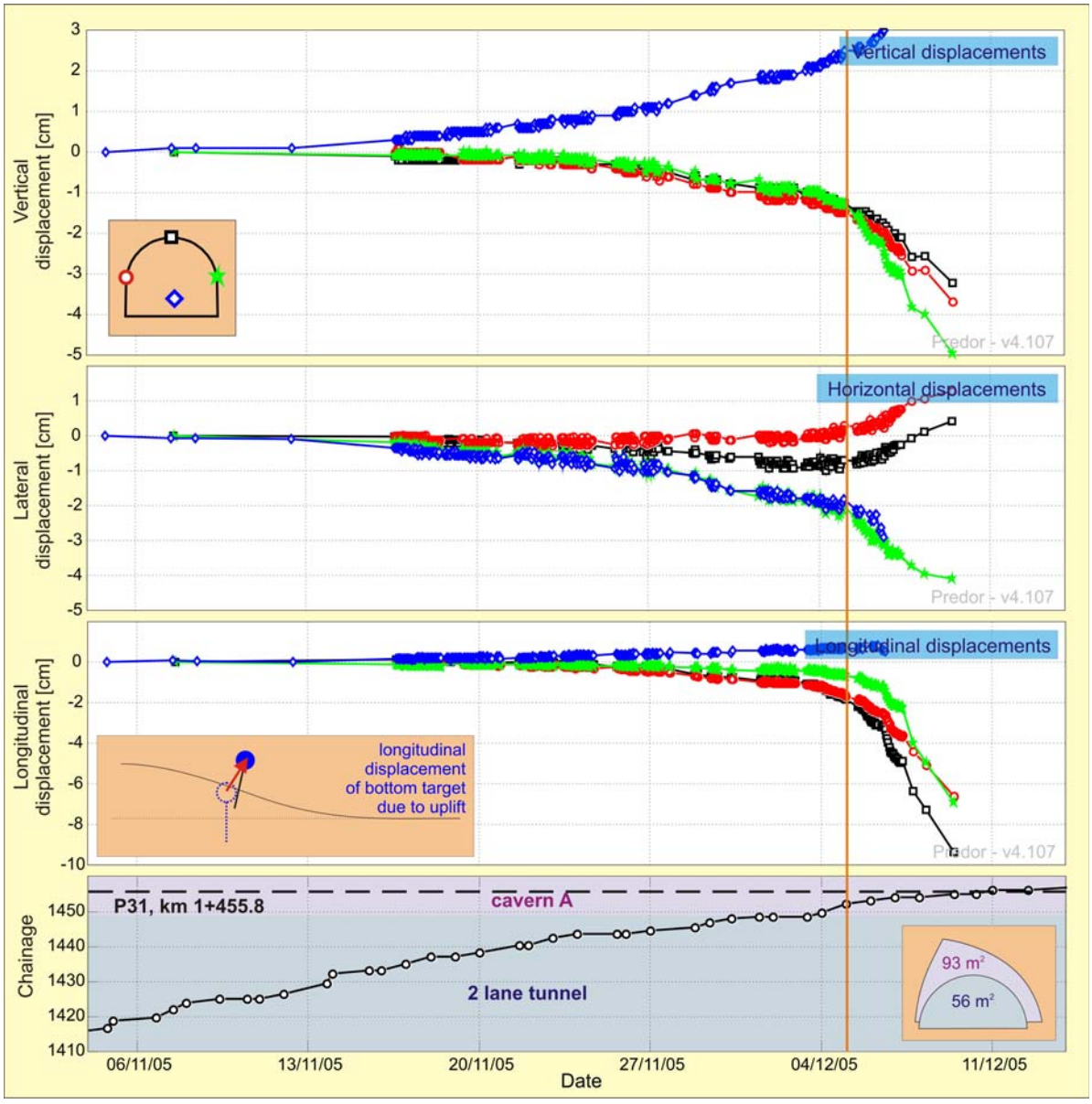

Figure 5-21. Spatial displacement history plot of four monitored points in measuring cross section P31 at chainage km 1.4+55.8 in the left tube of the exploratory tunnel and plot of the top heading advance.

Slika 5-21. Časovni potek vseh treh komponent vektorja pomikov štirih merskih točk v merskem prerezu P31 na stacionaži km 1.4+55.8 v levi cevi raziskovalnega rova skupaj z izrisom približevanja izkopnega čela kalote.

From the displacement curves in Fig. 5-21 it is evident that at some point the displacement rates started to accelerate, especially the longitudinal displacement increased significantly (from about 2 cm to almost 10 cm for the crown point). This happened when the face was some meters away from the measuring section. Large displacements in this area often caused cracking of the shotcrete and some pieces could drop down.

If the measuring section was close to the excavation face, the contractor's staff were requested to remove the targets in the exploratory tunnel before the excavation of the round length to avoid the damages to the optical reflectors. During the excavation the displacements were increasing, since the measuring section was very close to the excavation face, but had not been excavated yet. When the experiment staff entered the exploratory tunnel, the optical reflectors were placed again to the target bases and single measurements of this measuring section were performed to obtain the position of these targets until the measuring section was finally excavated. The reflectors were then removed. Large displacement difference between the last 4 values of the displacement curves in Fig. 5-21 is thus the consequence of missing measurements in the crucial moment, when the displacement rate is highest.

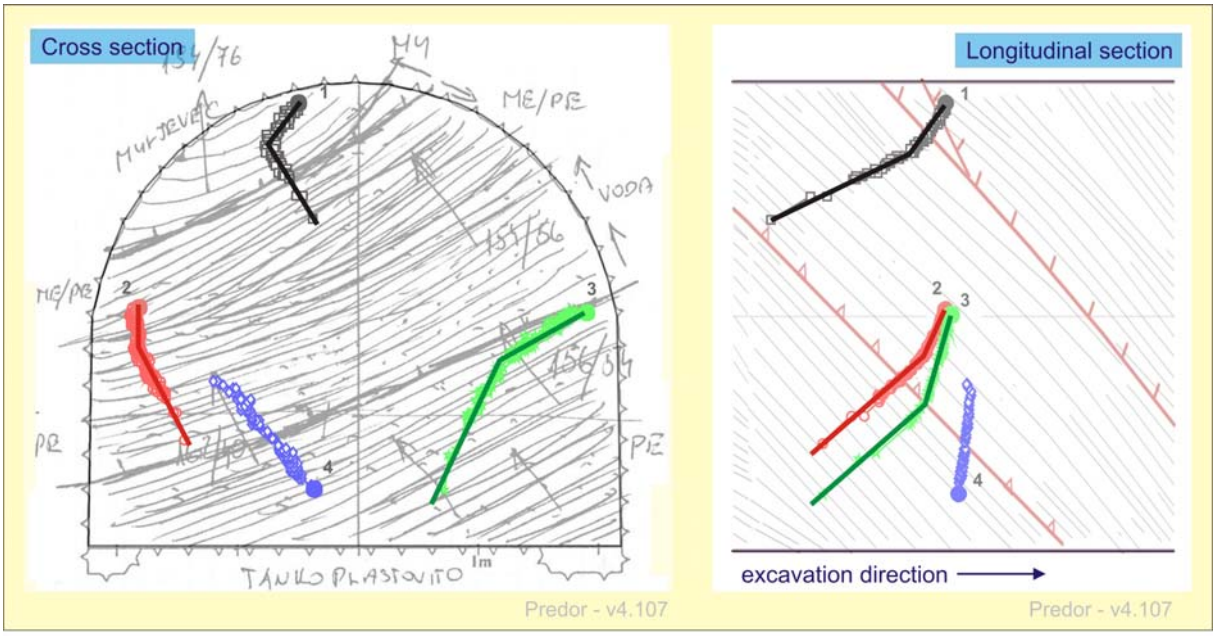

Figure 5-22. Bilinear displacement vectors in cross section and in longitudinal section in the left tube of the exploratory tunnel at chainage km 1.4+55.8

Slika 5-22. Bilinearni potek vektorjev pomikov v prečnem in vzdolžnem prerezu v merskem profilu na stacionaži km 1.4+55.8 v levi cevi raziskovalnega rova.

The obtained curve is in vertical and longitudinal direction of parabolic shape as presumed by Barlow (1986) on the basis of numerical calculations. The displacement curve in the horizontal direction is somewhat exceptional, but can be explained with the effect of the foliation of surrounding rock mass.

Prevailing geological scheme in the monitored section of the left tube is characterized by sub-horizontal foliation in cross section with slight inclination towards the left side of the tunnel and steeply inclined foliation into the excavation direction in longitudinal section. Dip angle of the foliation is approximately 55° with relative dip direction with respect to the tunnel axis of 25° to the left.

To study the influence of the foliation of the rock mass to the exploratory tunnel, response displacement vectors of presented measuring section plotted in cross and longitudinal section provide the most valuable information. The distinctive bilinear deformation pattern can be observed in Fig. 5-22 and is evident in longitudinal as well as in cross section.

The displacement vectors in cross section of the exploratory tunnel followed the direction of the rock mass foliation towards the left sidewall of the tunnel when the excavation face was far away from the observed cross section. In this first deformation phase the additional rock mass pressure onto the primary lining was small and the sliding mechanism along the foliation dominated over the radial deformation due to rock mass pressure. For this reason the left sidewall point tended vertically down and not in the radial direction. Similar explanation can be given for the longitudinal section.

As the tunnel face approached the observed cross section, the displacements due to the rock mass pressure became significantly larger than the sliding displacements along the foliation and consequently the displacement vectors changed their orientation.

The deformation mechanism changed from sliding along the foliation in the first phase to the bending of the foliation planes (deformation perpendicular to the foliation planes) in the second phase when the influence of the excavation face to the monitored cross section was intensified. On the basis of several monitored cross sections with similar deformation patterns we can conclude that the rock mass – support system behaviour well ahead of the face is mainly governed by the orientation of the rock mass discontinuities. Similar findings, but for the monitored or calculated displacements in the excavated tunnel, are presented in Chapter 4 and have been published by several authors (Wittke, 1990; Button et al, 2004b; Goricki et al, 2005).

The displacement vector orientation change occurred suddenly and a turn point happened at a certain distance between the monitored section and the approaching face of the top heading. For easier and more reliable determination of the turn point distance from the face and the portion of the total displacement that occurs before and after this point, the displacement-distance curve was formed by plotting the percentage of the final measured displacement against the distance from the top heading excavation face (Fig. 5-23). The obtained curve is for the majority of analysed cross sections also bilinear and can be simply divided in two parts. For the presented measuring section in Fig. 5-23 the turn point occurred 5.5 m ahead of the two lane tunnel excavation face and at 45 % of the final displacement.

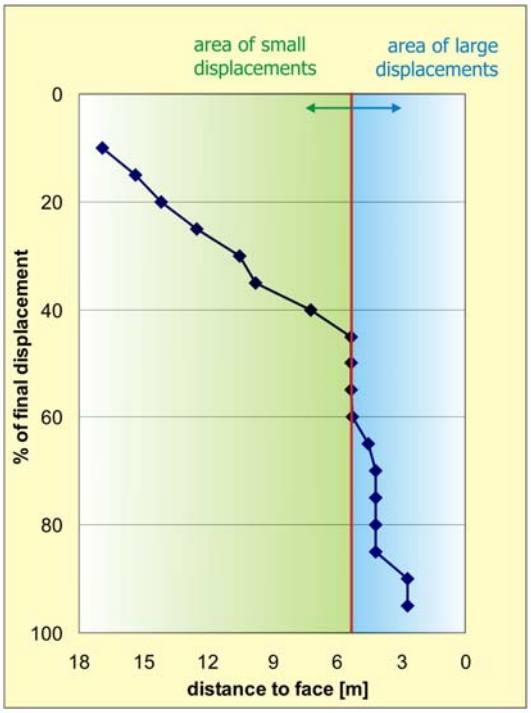

Figure 5-23. Relative vertical displacement of the crown point in exploratory gallery vs. distance to the top heading excavation face.

Slika 5-23. Delež vertikalnega pomika stropne točke v raziskovalnem rovu v odvisnosti od oddaljenosti od izkopnega čela kalote.

The displacement-distance curve was formed for all measuring sections with measured complete deformation path in the monitored part of the left tube of the exploratory tunnel (Fig. 5-24). Turn points were assessed manually. A statistical analysis indicates that the turn point occurs at about 5 m, i.e. one half of an equivalent tunnel diameter in front of the top heading face at 35-50% of the final displacement. This observation coincides with the analyses of the horizontal inclinometer results (Likar, 2004b). The area between the measuring section and the approaching face of the top heading at

the moment when the diagram in Fig. 5-23 exhibits the turn point is referred to as the area of large displacements. The area further away from the tunnel face in the excavation direction can be referred to as the area of small displacements.

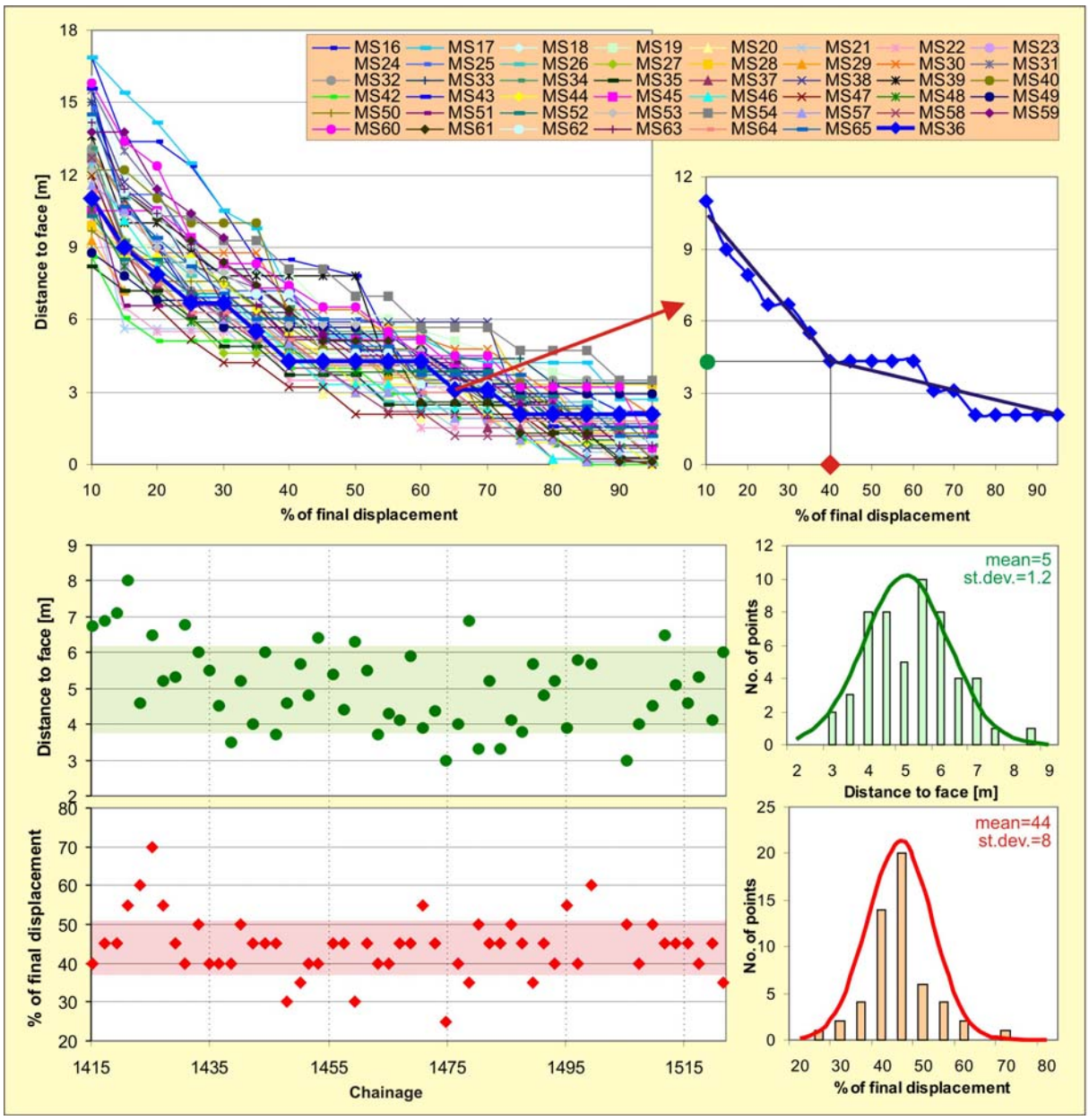

Figure 5-24. Relative vertical displacement of all crown points in exploratory gallery vs. distance to the top heading excavation face with plots of distances of the turn point to excavation face and the belonging percentage of final displacement.

Slika 5-24. Delež izmerjenega pomika vseh stropnih točk v raziskovalnem rovu v odvisnosti od oddaljenosti izkopnega čela kalote skupaj z izrisom razdalje prevojne točke do čela s pripadajočim deležem končnega izmerjenega pomika.

The observed structural damage of the primary lining coincided well with the measured displacements. In the area of small displacements only micro cracks were noticed, while in the section closer to the tunnel face up to 25 cm wide cracks were registered (Fig. 5-25). These large cracks were formed mainly due to large longitudinal displacements in the area of large displacements. In some sections the primary lining was completely damaged.

In some cross sections only minor vertical displacements were observed in the second deformation phase, sometimes even heaving was registered (noticed usually after the transition from soft to stiff rock mass).

Figure 5-25. Photo of large crack in primary lining of the right tube of the exploration gallery due to excessive longitudinal displacements.

Slika 5-25. Nazoren prikaz velikosti razpoke v primarni podgradnji desne cevi raziskovalnega rova zaradi velikih vzdolžnih pomikov.

The beginning of the area of small displacements at the far end from the main tunnel face was determined at a 3 mm displacement of a particular measuring point to eliminate the measurement error (the inaccuracy of determining the position of measuring points was less than 2 millimetres (Marjetič et al, 2006)). In Fig. 5-26 the distances from the excavation face to the measuring points at which the measured vertical displacements of the bottom and crown points reached 3 mm and 1 cm, respectively,

are plotted along the monitored section of the left tube of the exploratory tunnel. It can be observed that the bottom points always moved prior to the crown points. A rather stiff primary lining, where the crown point was installed on one hand and no invert at the bottom of the exploratory tunnel on the other, can explain such behaviour. Area of recognizable displacements as observed on bottom points reached the length of about 18 – 25 m (2 - 2.5 equivalent tunnel diameters) for a 3 mm displacement and 10 – 20 m (1 – 2 diameters) for a 1 cm displacement in front of the face of the two-lane tunnel. Similar behaviour was observed for the crown points as well, only the distances to the face were considerably smaller (10 – 20 m for a 3 mm displacement and 5 – 12 m for a 1 cm displacement in front of the two-lane tunnel).

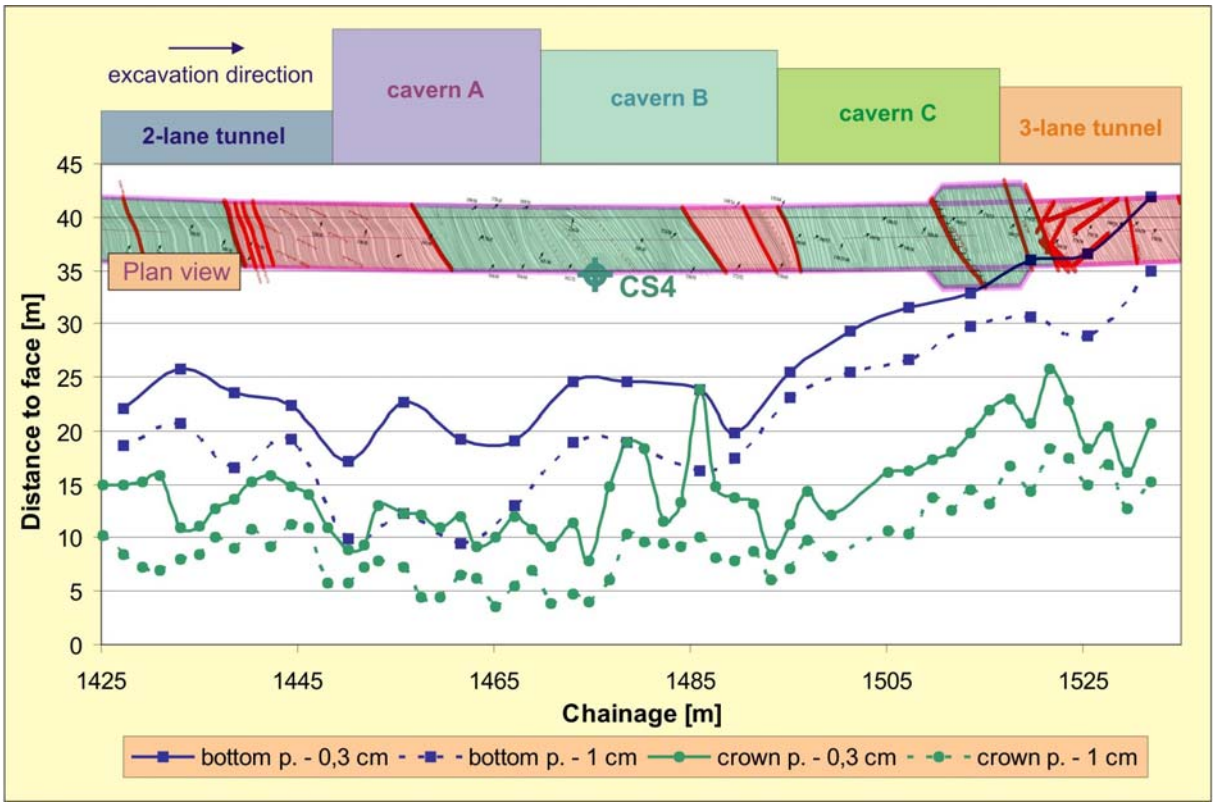

Figure 5-26. Distance of measuring points to the top heading face when the vertical displacement of the bottom and crown points reached 3 mm and 1 cm, respectively, plotted along the left tube of the exploratory tunnel.

Slika 5-26. Oddaljenost merske točke od izkopnega čela kalote, ko vertikalni pomik talne in stropne merske točke doseže 3 mm oz. 1 cm; izris vzdolž osi raziskovalnega rova v levi cevi.

It was however expected that the influential area ahead of the face would be extended when tunnelling in the cavern with larger excavation cross section, but generally up to chainage km 1.4+95

no such effect could be noticed. The extension of the influence zone for the 3 mm displacement of the crown point was even reduced. Farther along the axis the uplift of the bottom was registered at larger distances from the top heading face, probably due to a section of poor rock mass ahead (starting at chainage km 1.5+20). Stress was therefore concentrated in the area of stiffer rock mass in between two faulted regions and resulted in displacement at a large distance from the face, which was increasing towards the mentioned faulted zone. A small amount of stress that was transferred to the faulted area caused noticeable displacement far ahead of the face only on the ground target. The maximum distance to the excavation face, where the measured vertical displacement of the bottom point exceeded 3 mm, reached 42 m. Nevertheless, the influential area as observed on lining points decreased for the points located in the faulted area. Similar pattern but in smaller scale was observed before the section of poor rock mass conditions at the end of cavern B, as seen from Fig. 5-26. A significant increase was monitored especially on the crown points.

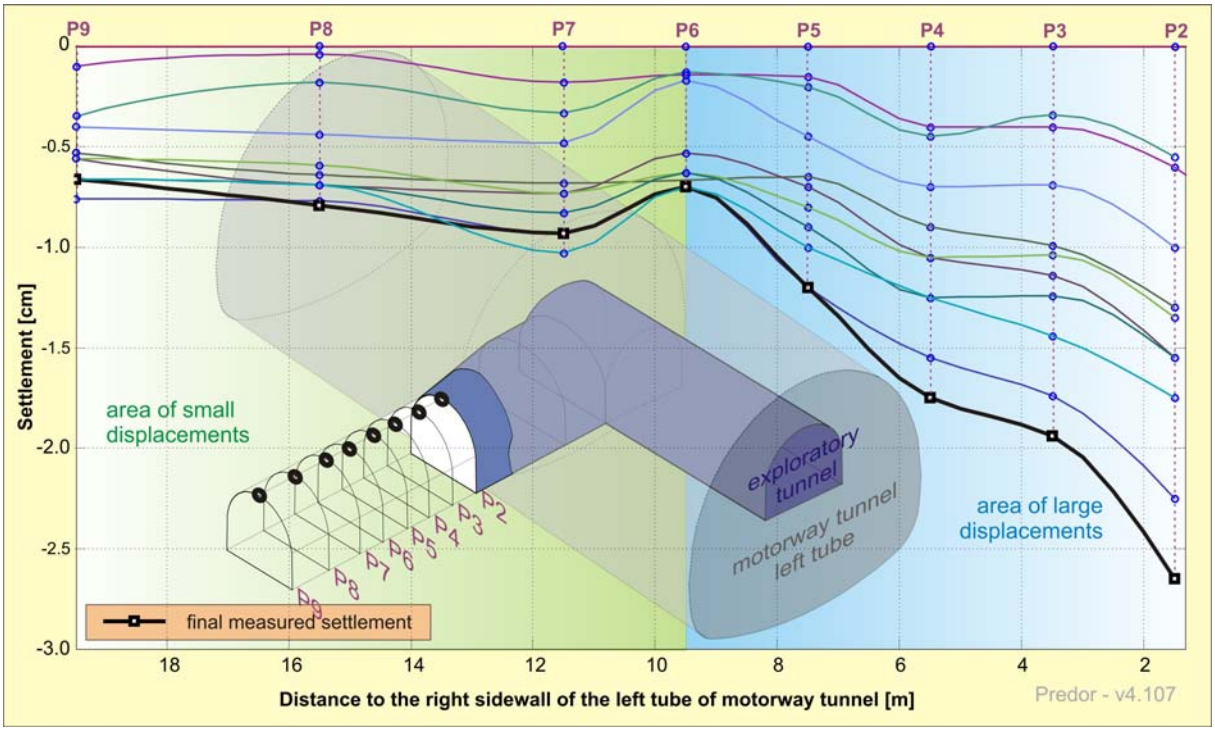

Figure 5-27. Influence lines of vertical displacements of the crown points in the cross passage of the exploratory tunnel.

Slika 5-27. Vplivnice vertikalnih pomikov stropnih točk v prečniku raziskovalnega rova.

The same response was expected also in the cross passage between the right and the left tube when the left tube of the motorway tunnel passed by. The area of large displacements is somewhat larger than ahead of the face and reaches almost 10 m from the right sidewall of the motorway tunnel, as

shown in Fig. 5-27 (as a boundary between areas of large and small displacements a measuring section P6 was selected). Unfortunately, the area of small displacements perpendicular to the excavation face advance extended farther than the target in cross section P9 where still 6 mm of settlement of the crown point were recorded. If the influence line of the final measured settlement (line of black colour in Fig. 5-27) is extrapolated on the basis of experience from monitoring ahead of the face deeper in the cross passage, we can deduce that the influence could be perceived about 25-30 m from the right sidewall of the motorway tunnel.

As outlined in Chapter 5.2.2.4, the influence area ahead of the face was also detected during the analysis of the stability of the control station that was fixed in the sidewall of the exploratory tunnel. Movement of the position of the control station CS4 (lateral displacement is presented in Fig. 5-28 and its position in Fig. 5-26) started already approximately 30 m ahead of the face with insignificant displacement towards the right sidewall. At a distance of 27 m to the face an acceleration of the lateral displacement rate as a consequence of a rapid approach of the face to the measuring section can be observed in small scale well ahead of the face.

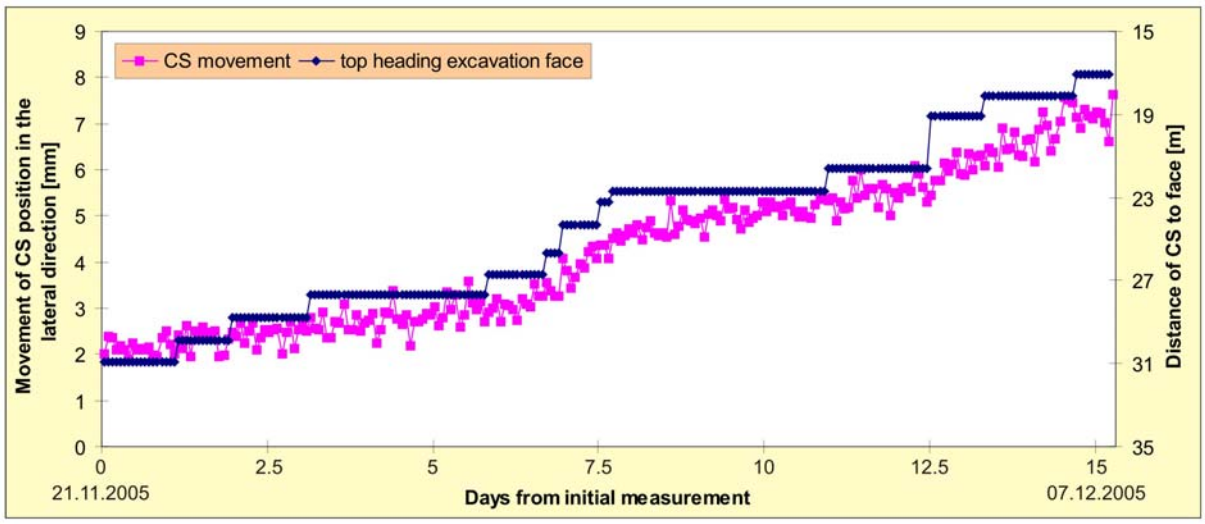

Figure 5-28. Movement of the position of the control station CS4 in lateral direction with plotted distance from control station to the top heading excavation face.

Slika 5-28. Pomik merskega mesta CS4 prečno na predorsko os z izrisano razdaljo do izkopnega čela kalote.

5.3.2 Comparison of the displacements in the exploratory tunnel measured during the exploratory tunnel construction with the displacements measured during the main tunnel construction (case L2)

Previously it was shown that the rock mass behaviour in the exploratory tunnel ahead of the face during the main tunnel construction is mainly governed by the orientation of the foliation. Similar dependence can also be observed at the displacements measured during the exploratory tunnel construction. Fig. 5-29 shows different behaviour of the exploratory tunnel due to two different construction activities (construction of the exploratory tunnel and construction of the main tunnel) and consequently two different load cases.

When the exploratory tunnel was under construction, the stress change rate due to the excavation was the highest in the area of the excavation face. As the excavation continued, the stress change rate around the same cross section was reduced. Consequently, the displacement rates were high during the initial phase and were close to zero later on. The displacement vector of the crown point tended perpendicularly to the foliation during the initial phase (in the area of large displacements –blue line marked with letter L in Fig. 5-29) and parallel to the foliation in the second deformation phase (the area of small displacements –purple line marked with letter S). Bilinear displacement pattern can only be seen to a limited extent, because the absolute values of measured displacements are small. This phenomenon became more evident from the displacement measurements ahead of the main tunnel excavation face, since the measured displacements were considerably larger in this case due to:

- Larger cross section of the main tunnel compared to the exploration gallery.
- In the latter case more or less entire displacement history was measured (some displacement was sometimes missed close to motorway tunnel since the targets were removed as described in Chapter 5.3.1).
- Another possible reason could be also the phenomenon of different amount of pre-displacements in case of different foliation dip with respect to excavation direction (described in 4.2.3.). Left tube of the exploratory tunnel was dominantly excavated with dip as shown in longitudinal geological section in Fig. 5-20 and thus also in the vicinity of the presented measuring section. According to Tonon (2002), performed numerical calculations (Fig. 4-32) and further on from observations in the Trojane tunnel (indirect deduction from the range of measured displacements when tunnelling with and against dip in Fig. 4-33) the pre-displacement magnitude in such conditions is much larger than the displacements of the excavated area.

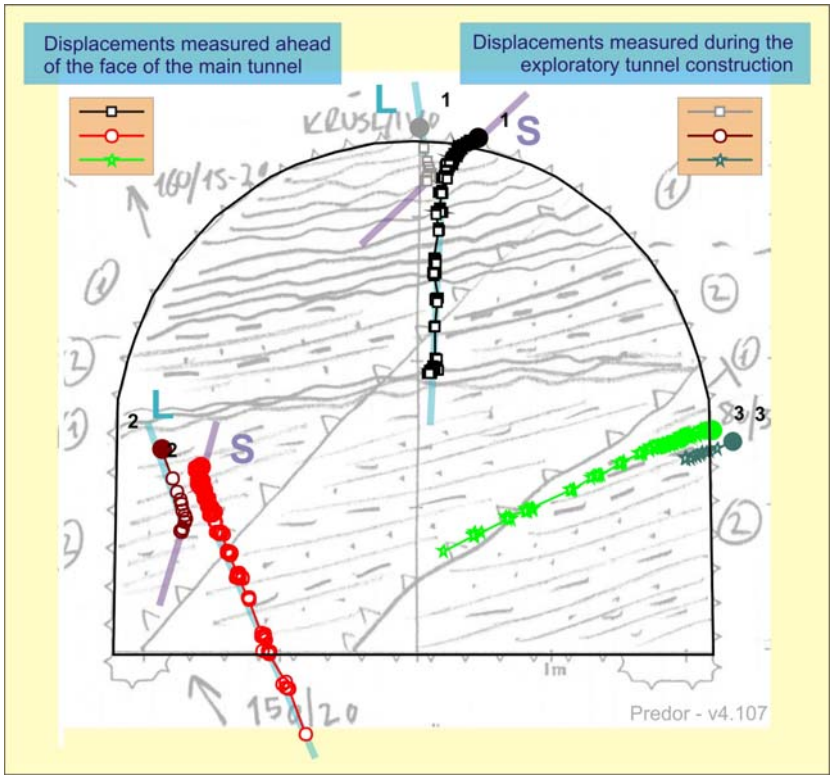

Figure 5-29. Comparison of the displacements measured during the execution of the exploration gallery and the displacements measured during the main tunnel construction in the left tube at the chainage km 1.5+17 – cross section together with a face log.

Slika 5-29. Primerjava pomikov, izmerjenih med gradnjo raziskovalnega rova in pred čelom avtocestnega predora na stacionaži km 1.5+17– vektorji pomikov v prečnem prerezu s podloženim popisom čela.

The behaviour ahead of the main tunnel excavation face was just the opposite of the behaviour, observed during the excavation of the exploratory tunnel. The directions of displacement vectors in both cases coincided well when the displacement rates were small (letter S in Fig. 5-29) and were similar in the area of large displacement rates (letter L in Fig. 5-29). A hypothesis is proposed that the displacements parallel to the foliation dominate when stress change rates are small, while radial displacements govern the behaviour when stress change rates are high.

5.3.3 Comparison of the displacements ahead of the face and the displacements within the main tunnel due to the main tunnel construction (case L3)

The comparison of the measured displacements ahead of the face of the main tunnel with the displacements of the main tunnel at the same chainages along the tunnel axis allows the estimation of

the portion of the pre-face displacements in total measured displacements and the influence of the orientation of foliation on the orientation of the displacement vectors.

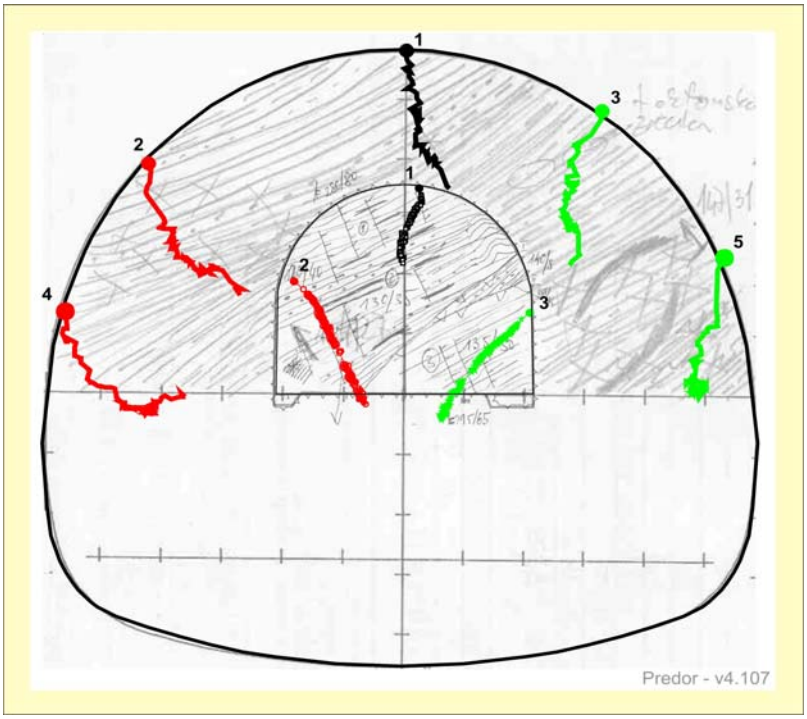

Figure 5-30. Comparison of the displacements ahead of the face and the displacements after the excavation of the motorway tunnel at chainage km 1.4+44 in the left tube of the Šentvid tunnel – displacement vectors in cross section with face log.

Slika 5-30. Primerjava pomikov pred čelom avtocestnega predora in pomikov po njegovem izkopu na stacionaži km 1.4+44 v levi cevi predora Šentvid – vektorji pomikov v prečnem prerezu s podloženim popisom čela.

The displacement vectors of the exploration gallery and of the main tunnel, caused by the execution of the main tunnel, are plotted in Fig. 5-30. Similar displacement patterns as described in the previous chapter can be seen. The displacement rates of the monitored cross section were largest some meters ahead (measured on the lining of the exploration gallery) and behind the top heading excavation face (measured on the lining of the main tunnel). Hence, the crown and the left sidewall point's displacement vectors tended perpendicularly to the rock mass foliation. The orientation of the displacement vectors changed when the excavation face was far enough from the observed cross section (ahead or behind the face) and the rate of displacements diminished.

The magnitudes of the vertical and horizontal displacements of both sidewall points in the exploratory tunnel were approximately the same as the displacements of the sidewall points in the

primary lining of the double lane tunnel. The vertical displacement of the crown point was somewhat smaller in the exploration gallery than the vertical displacement of the crown point target in the main tunnel and reached about 35% of total measured displacement (marked with a red square in Fig. 5-31 for the cross section shown). Total measured displacement refers to the sum of displacements measured ahead of and behind the face of the main tunnel. The displacements caused by the exploration gallery execution are neglected. It should also be noted that the targets, where the displacements were summed and compared, were not installed at the same places in the observed cross section, as can be seen in Fig. 5-30. The influence of these simplifications on the assessment of the pre-face portion of total displacements was studied by numerical analyses and will be presented in Chapter 5.4. The numerical study performed by Jemec (2006) showed that the presence of the exploration gallery had limited effect on the behaviour of the main tunnel.

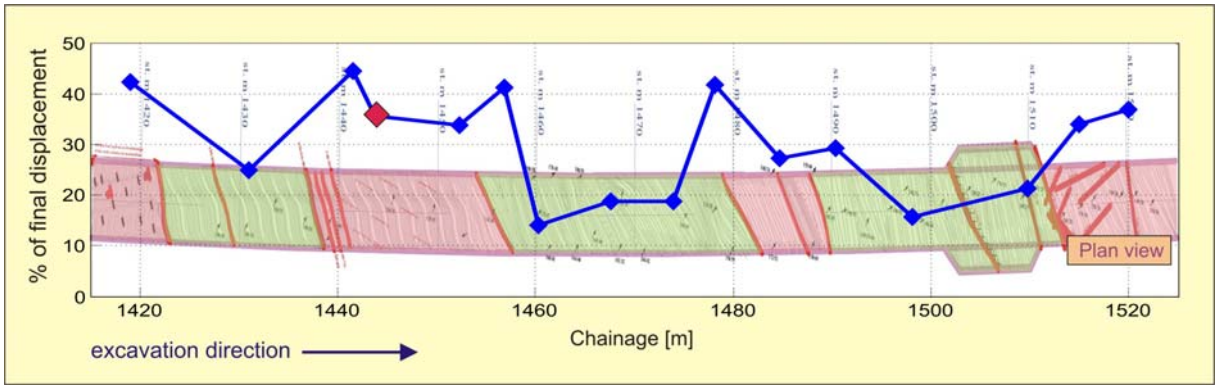

Figure 5-31. The portion of the vertical displacements that occurred ahead of the face for the crown point in the exploratory tunnel and for a point in the main tunnel situated above the exploration gallery.

Slika 5-31. Delež posedkov stropne točke v raziskovalnem rovu, ki se zgodijo pred čelom avtocestnega predora glede na celoten izmerjen posedkov te točke in točke v avtocestnem predoru, ki se nahaja nad raziskovalnim rovom.

In the monitored section of the left tube of the Šentvid tunnel the measured displacements ahead of the face amounted to between 15% and 45% of the total measured displacements in the same cross section (Fig. 5-31). A lower portion of the pre-face displacements was observed in stiffer and non-folded rock mass or folded to smaller extent (regions of green and yellow colour in Fig. 5-31), while in more deformable or intensively folded rock mass (regions of red colour) the percentage of the pre-face displacements was considerably higher. A possible explanation for such displacement pattern could be stability problems during top heading excavation in soft regions, where the excavation of one round length was actually divided in several smaller steps of some square metres (up to 16 excavation steps

in top heading as reported by Popit (2006)) due to high risk of face overbreak. Each individual excavated part of the face was immediately stabilized with shotcrete, wire mesh and rock bolts, while only limited amount of the shotcrete was applied to the unsupported circumference of the tunnel. Not earlier than the excavation of the round length had been finished, primary lining was installed also at the circumference. Such step-by-step excavation took several hours to complete. In the meantime quite some convergences of the unsupported region occurred and smaller portion of the displacement curve was thus measured on the installed target. In stiffer rock mass the excavation and support installation sequence demanded less time and the first measurement of the target was performed in short time after the excavation of the round.

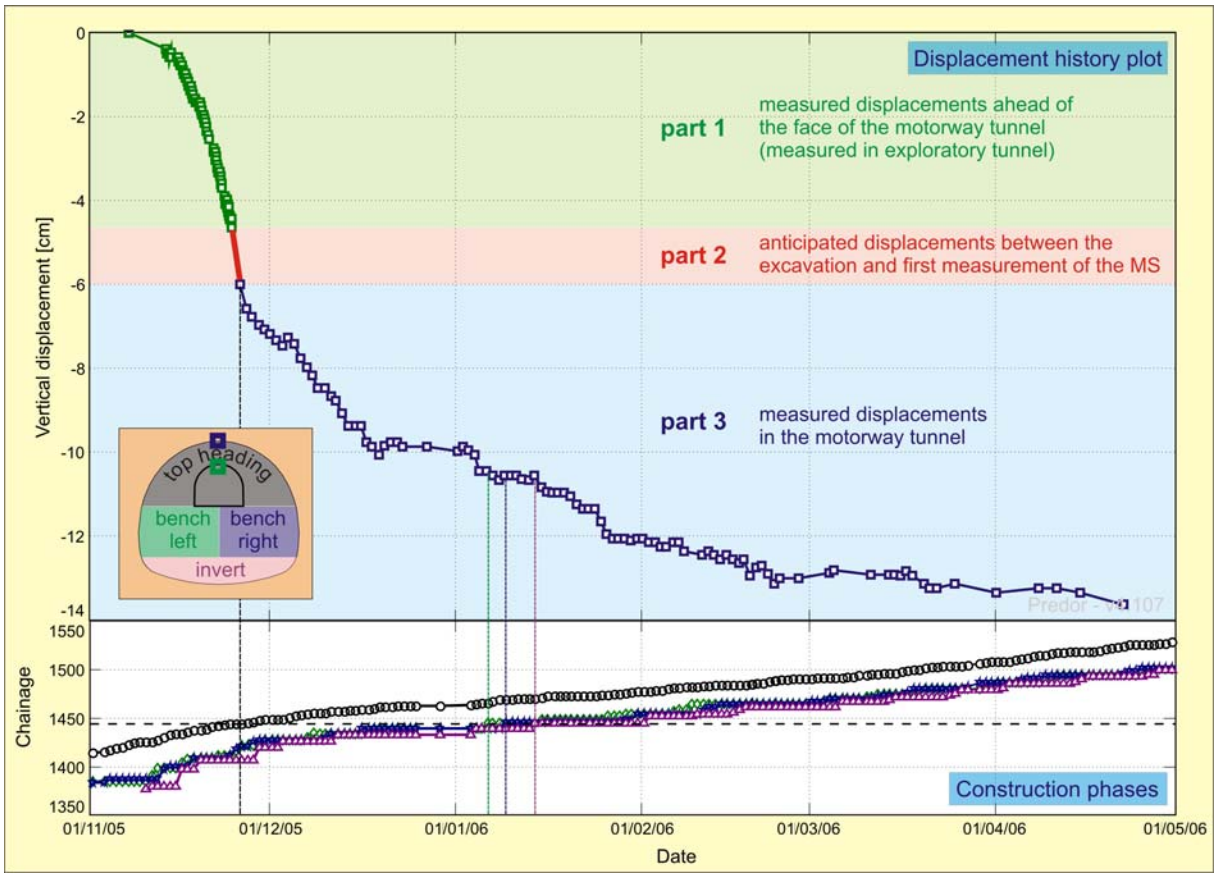

Figure 5-32. Complete displacement history plot of the crown point in the cross section at chainage km 1.4+44.

Slika 5-32. Celoten potek pomikov za stropno točko v merskem prerezu na stacionaži km 1.4+44.

Nevertheless, the above stated percentage does not take into account the displacement that occurred between the last measurement in the exploratory tunnel before the excavation and the first

measurement of the newly installed measuring section in the main tunnel (part 2). The displacement rates in this phase are the highest because of unsupported rock mass immediately after the excavation and low stiffness of the installed support before the shotcrete hardens and before the rock bolts are installed.

On the basis of the displacement's tangent slope close to the excavation face (some days before and after the excavation of the cross section under consideration) and time delay between the excavation and the first measurement, we can anticipate the course and the magnitude of the second part of the displacement function's curve (Fig. 5-32). The estimated portion of the displacements in part 2 is in the range from 10% – 25% of the total displacements, again related to the stiffness of the rock mass due to excavation problems as described above.

From the presented cases we can deduce that 25% - 70% of the displacement occurs before the first measurement of the observed cross section, depending mainly on the stiffness of the surrounding rock mass, construction sequence and the time delay of the first measurement. The upper percentage that was deduced for unfavourable geological conditions is close to previously presented percentages measured with vertical extensometer and horizontal inclinometer at the Trojane tunnel that were also installed in poor rock mass conditions.

5.3.4 Detected rock mass behaviour ahead of the face when the top heading face approaches and passes a fault zone (cases L4 and D1)

5.3.4.1 Left tube (case L4)

Between chainages km 1.4+14 and km 1.4+22 in the left tube of the exploration gallery a 7.5 m thick fault zone was mapped during the excavation of the exploratory tunnel (region of red colour in Fig. 5-33). Before and behind the observed fault zone a section of better rock mass was mapped, especially from chainage km 1.4+22 further onwards in the excavation direction (region of green colour).

When the top heading excavation face approached the fault zone, vertical and longitudinal displacements of the rock mass in the vicinity of the fault zone increased due to the stresses that could not be transferred over the zone of weaker material. In this area vertical displacements were considerably larger than longitudinal ones (Fig. 5-33).

In the measuring sections at the beginning of the fault zone longitudinal displacements increased from 3-4 cm before chainage km 1.4+14 to 20 cm at the first measuring cross section within the fault

zone. This indicates possible failure of the tunnel face when entering the soft rock mass. Support installed ahead of the face is of great importance to prevent the failure of the face in such situation.

Measuring cross sections in the fault zone registered various rock mass response patterns due to the approaching excavation face, depending on the position of the cross section within the fault zone. At the beginning of the fault zone almost no longitudinal displacements occurred in the area of small displacements, while vertical displacements were large compared to longitudinal ones.

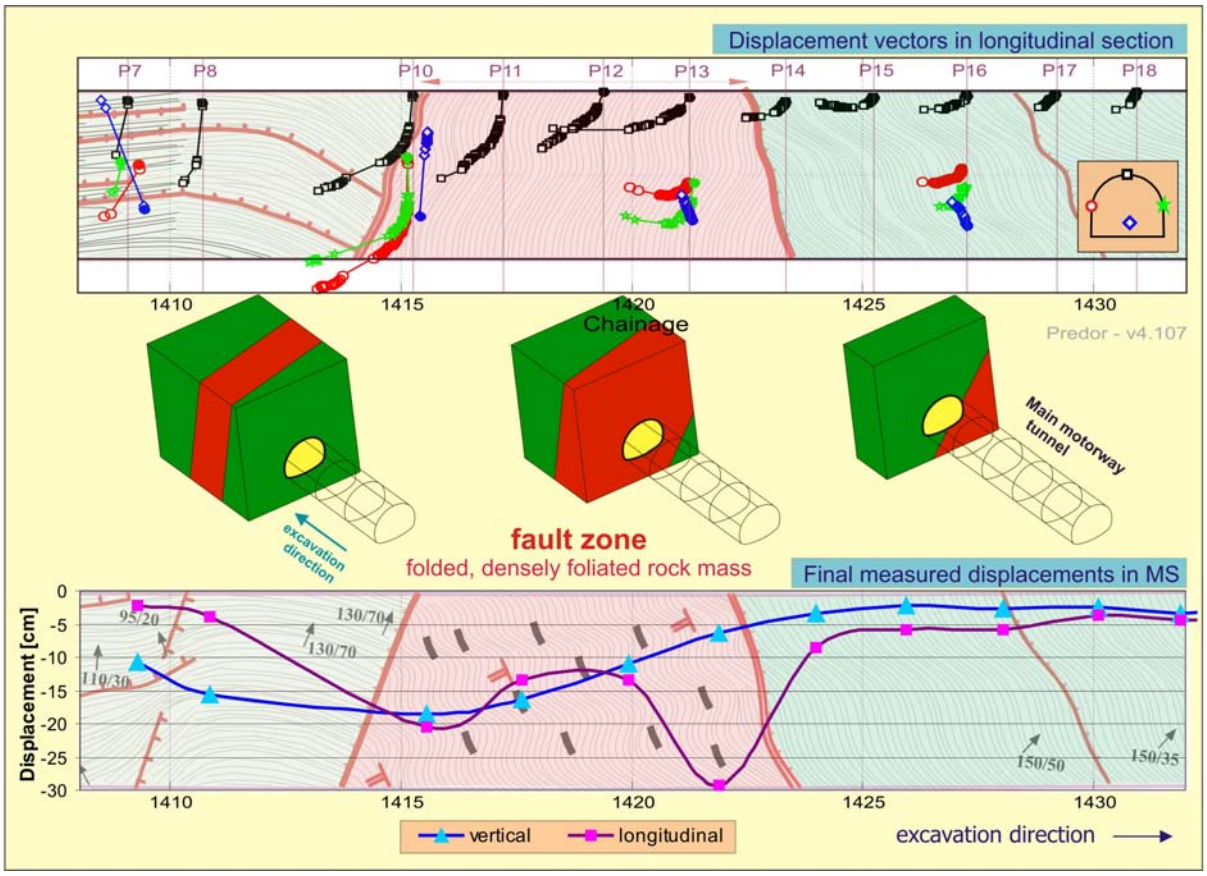

Figure 5-33. Rock mass behaviour when top heading excavation face approached and entered the fault zone between chainages km 1.4+14 and km 1.4+22 in the left tube of the exploratory tunnel; plot of displacement vectors in longitudinal section with geology (top); final measured displacements of crown point in measuring cross sections in longitudinal and vertical direction with plan view of geological structure of the section (bottom).

Slika 5-33. Odziv hribinske mase pri približevanju in prečenju tektonske cone med stacionažama km 1.4+14 in km 1.4+22 v levi cevi raziskovalnega rova; vektorji pomikov v vzdolžnem prerezu s podloženo geološko skico (zgoraj); kontura končnih izmerjenih vertikalnih in vzdolžnih pomikov stropne točke prečnih prerezov z geološko situacijo (spodaj).

Throughout the fault zone vertical displacements decreased from 18 to 6 cm at the end of the fault zone, whereas the monitored longitudinal displacements were the largest recorded during whole period of 3D displacement measurements ahead of the face of the Šentvid tunnel (29.3 cm). The observed response can lead to the separation of the block of faulted rock from stiffer rock further ahead in the excavation direction and consequently to an overbreak in the face region in case of inadequate face support.

In the area of large displacements no vertical displacement of a crown point or even upward movement of both sidewall targets was recorded in the last measuring cross section within the fault zone (upper plot in Fig. 5-33); only significant longitudinal displacements were observed. Similar behaviour of displacement vectors was also observed at the next three measuring sections farther down the tunnel axis. From the end of the fault zone onwards along the tunnel axis the longitudinal displacements in the monitored cross sections were larger than vertical displacements up to the chainage km 1.5+00 as shown in Fig. 5-20). At this point the top heading excavation face reached the vicinity of another, even larger fault zone and the rock mass response changed to similar as described above (larger vertical than longitudinal displacements).

5.3.4.2 Right tube (case D1)

Upward movement was also noticed in several cross sections in the right tube ahead of the motorway tunnel. As seen from Fig. 5-19, the monitoring of the right tube started in a fault zone as outlined earlier. The faulted section (section of red colour in Fig. 5-34) extended to chainage km 1.2+75, where stiffer rock mass was encountered (folded siltstone – section of light green colour). The next transition in the rock mass stiffness was mapped at chainage km 1.2+87 (from folded siltstone to the firm sandstone - section of dark green colour in Fig. 5-34).

During tunnelling in the fault zone the targets ahead of the faulted section settled as expected (final measured vertical displacements are shown in the bottom plot of Fig. 5-34). As soon as the top heading face entered stiffer rock mass ahead of the face, all the targets in this section started to lift and the maximum uplift of 1.5 cm was recorded at the crown target in P12 (displacement curve of violet colour in the upper plot in Fig. 5-34). Further targets onwards from P13 also heaved a bit, but when the transition to the stiff rock mass was approached, the targets in measuring sections P14 to P16 settled (the largest vertical displacement was recorded just before the transition at P15). The crown point in P17 was located already in sandstone and no settlement occurred, as seen from the displacement curve of orange colour. Further targets (especially from P19 onwards the tunnel axis) exhibited expected behaviour, although the displacements were negligible.

Small settlements when tunnelling through the fault zone and then comparably large uplift of the targets just ahead of the fault zone indicate the highly stressed stiffer rock mass close to the fault zone, where the majority of the stress was transferred due to top heading excavation face advance. Uplift occurred due to the stress reduction as soon as the excavation face entered stiffer rock mass. Similar pattern repeated at the next transition, only in a smaller scale.

Figure 5-34. Transition from soft to stiff rock mass and observed displacement pattern ahead of the tunnel face in the right tube of the exploratory tunnel.

Slika 5-34. Deformacijski vzorec pred čelom predora ob spremembi togosti hribinske mase iz mehke v togo v desni cevi raziskovalnega rova.

Stress distribution in the vicinity of the fault zone and its influence on the displacement vector orientation of the tunnel points was already thoroughly studied by Steindorfer (1998) and Schubert et al (2002). As mentioned in Chapter 4.2.1, the orientation of the displacement vector strongly depends on the rock mass stiffness. It deviates from "normal" orientation (approximately 10° in the excavated area) backward when rock mass of lower stiffness is approached and tends more to excavation direction from "normal" orientation when stiffer rock mass is ahead of the face. Orientation of the displacement vector for the left tube of the motorway tunnel is plotted with orange line in Fig. 5-35.

Stiffness of the rock mass governs also the displacement vector orientations ahead of the face, but the pattern observed was somewhat opposite to the one, described by Steindorfer and Schubert. The trend line of the displacement vector orientation 3 m ahead of the top heading face is presented with blue line in Fig. 5-35 together with geological situation for the monitored section in the left tube of the exploratory tunnel. It is obvious that the alterations in the trend line coincided with the transitions in the rock mass stiffness. In sections of weaker rock mass the trend line of the displacement vector increased to maximum angle of up to 75°, while in stiffer rock mass conditions it decreased to as low as 10°. Since the rock mass stiffness changes frequently and thus no longer section of "uniform" stiffness was monitored, the "normal" displacement vector orientation could not be identified.

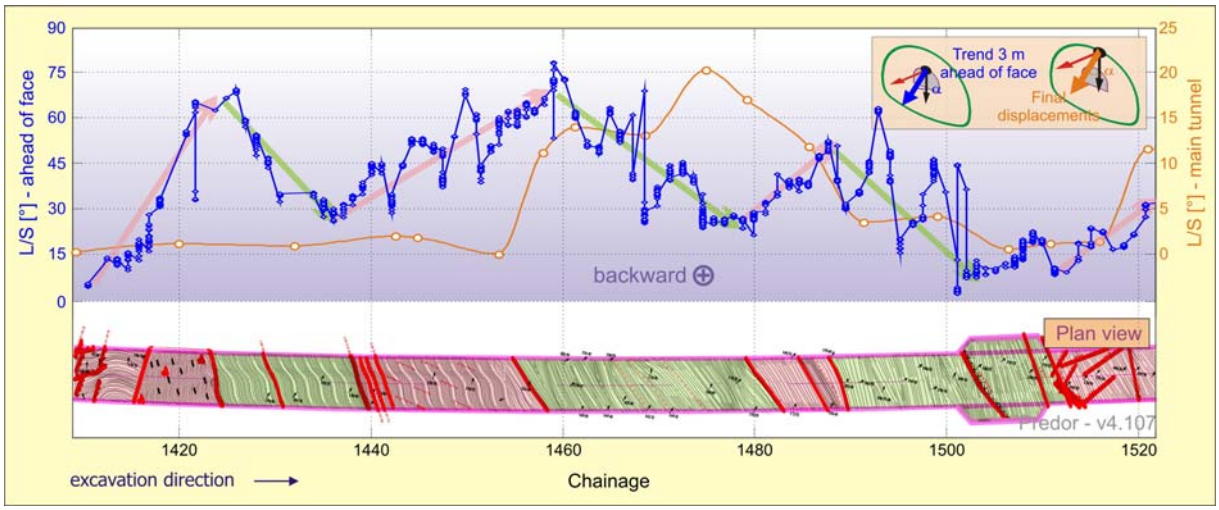

Figure 5-35. Displacement vector orientation L/S ahead of and behind the excavation face in the left tube of the Šentvid tunnel.

Slika 5-35. Orientacija vektorja pomikov L/S pred in za izkopnim čelom v levi cevi predora Šentvid.

5.3.5 Evaluation of the effect of grouted rock bolts on preface displacements

Since the Šentvid tunnel was mainly constructed in poor rock mass conditions, maintaining stability of the excavation face was an important issue. Preface support consisted of shotcrete reinforced with wire mesh and systematic rock bolting as an active face support measure for limiting preface displacements and thus preventing loosening of the rock mass ahead of the face.

Comparison of the measured longitudinal displacements in the exploratory tunnel ahead of the motorway tunnel face and the amount of grouted rock bolts with respect to geological situation allows the evaluation of preface support efficiency. Influence lines of longitudinal displacements for crown

points along the complete monitored section of the left tube are shown in Fig. 5-36. Also contours of final vertical and longitudinal displacements are presented in addition to plan view of geological situation. Positions and lengths of IBO rock bolts (bearing capacity of 250 kN) are plotted in scale (different colours of rock bolts and their 3 m long parts serve only for better representation of the length of individual sets of anchors).

A fast overview of the quantity and disposition of rock bolts gives an impression that complete monitored section was somewhat satisfactorily covered, except between chainages km 1.4+32 to km 1.4+35 where no rock bolts were installed. The amount of rock bolts was smaller in the first part to chainage km 1.4+50, but was further on increased. For example at chainage km 1.4+60 all together 68 rock bolts of different lengths were installed ahead of the face.

To get a measure for bearing strength of the bolts at each meter of monitored section, an index was calculated and will be further on referred to as face bolts index (FBIn).

In the Trojane tunnel some complex measuring sections including multipoint extensometers, convergence targets and bolts equipped with strain gauges at different distances from the opening were installed to obtain comprehensive insight in the rock mass – structure response. A distribution of axial force along 6 and 9 m long bolts and their position with regard to the tunnel in such measuring section at chainage km 80+424 in the left tube of the Trojane tunnel is shown in the upper left plot in Fig. 5-36. On the basis of measured distribution of the bearing capacity along the rock bolt, experience of Contractor's personnel in the tunnel and extension of the area of large displacements, normalized bearing capacity curve of each individual rock bolt was produced (upper right plot in Fig. 5-36) and will be further on referred to as individual face bolt index (FBI_i). Due to large displacements in last few meters ahead of the face where grout is probably cracked to high extent or even disintegrated and due to oral reports of the Contractor's personnel that about 3 m long bolt can be easily pulled out from the face with excavator, the bearing capacity of 3 m long rock bolts was neglected. In the next 4 m the bearing capacity was supposed to linearly increase from 0 to 1 and remains 1 for longer bolts (Eq. 5-4).

$$FBI_i = \begin{cases} 0, & l \le 3 \\ 0.25 \cdot (l-3), & 3 < l \le 7 \\ 1, & l > 7 \end{cases} \quad l \text{ ... length of a bolt ahead of the face} \qquad \text{Eq. 5-4}$$

For each meter of the monitored section the individual face bolt index (FBI_i) was calculated for each of the rock bolts ahead of the face with regard to its length. A face bolts index (FBIn) is obtained as the total sum of face bolt indexes divided by the normalized cross section area of the top heading

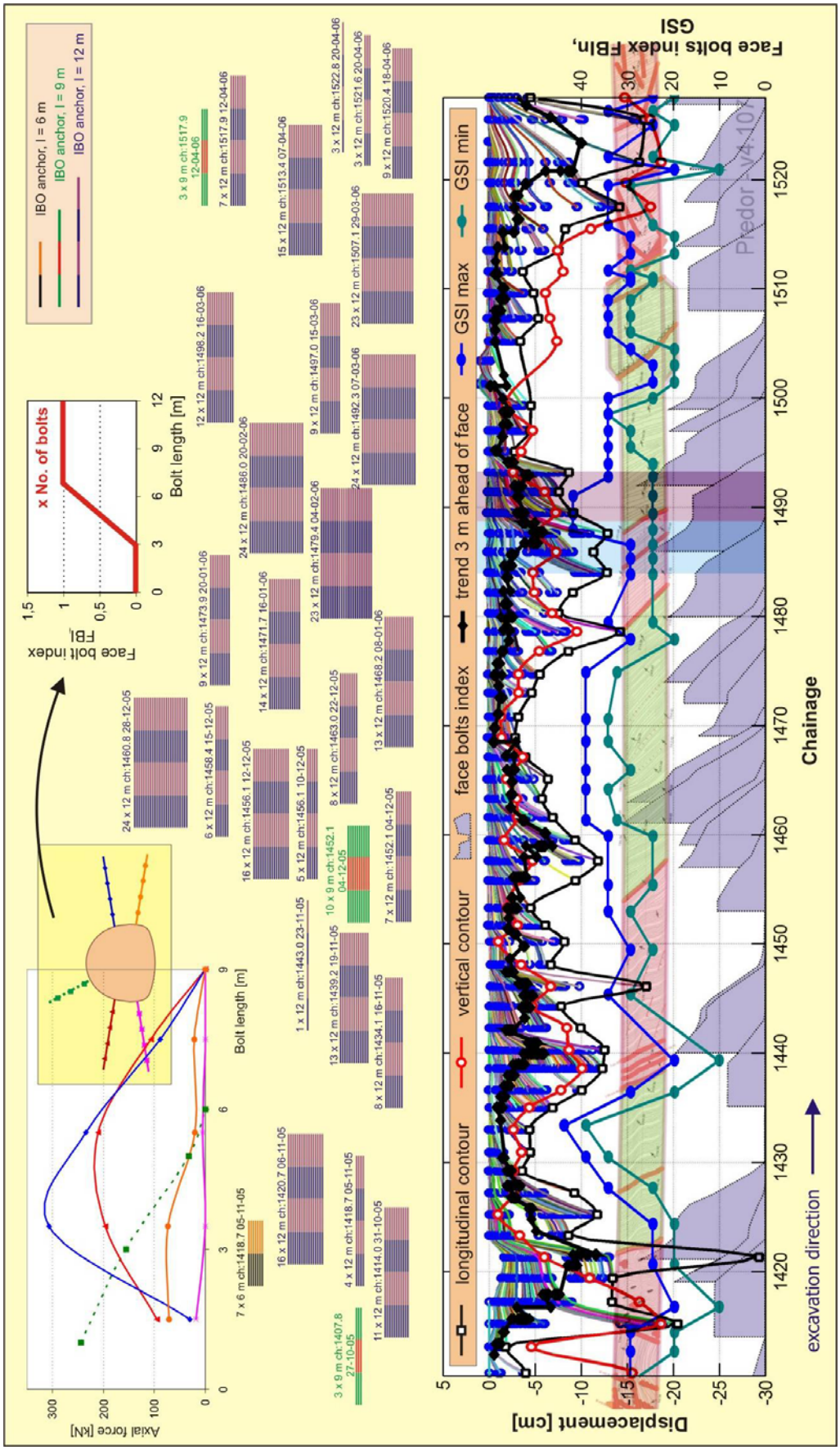

Figure 5-36. Influence lines of crown points in longitudinal direction with plotted contour of final measured vertical and longitudinal displacements and geological plan view in the left tube of exploratory tunnel. Positions and lengths of rock bolts are plotted in scale.

Slika 5-36. Vplivnice v vzdolžni smeri za stropne točke s poudarjenima konturama vertikalnih in vzdolžnih pomikov ter podloženo geološko situacijo v levi cevi raziskovalnega rova. Položaj in dolžina pasivnih sider je izrisana v merilu.

excavation face f_a (Eq. 5-5), since the monitored section was located in part of the tunnel with changing geometry of cross section (2- and 3-lane tunnel, cavern A, B and C – Fig. 5-20).

$$FBIn = \frac{\left(\sum_{i=1}^{n} FBI_i\right)}{f_a}, \; n \text{ ... number of bolts ahead of the face} \qquad \text{Eq. 5-5}$$

$f_a = 1$, 2-lane tunnel (56 m^2)
$f_a = 1.66$, cavern A (93 m^2)
$f_a = 1.54$, cavern B (86 m^2)
$f_a = 1.39$, cavern C (78 m^2)
$f_a = 1.43$, 3-lane tunnel (80 m^2)

Normalized cross section area f_a is calculated from each individual area of the top heading excavation face and is set to 1 for the two-lane tunnel top heading excavation face.

A distribution of face bolts index (FBIn) along the monitored section in the left tube is presented with an area of violet colour in the lower plot in Fig. 5-36 (additional curves at this area represent the effect of the existing bolts before installation of a new set). To allow a direct comparison of the FBIn to measured longitudinal displacements, a trend line 3 m ahead of the face was added to the plot, since the final longitudinal displacement measurements (presented as a contour of longitudinal displacements) were not taken at the same distance to the face.

As already described in previous chapter, longitudinal displacements significantly increased at the end of the fault zone at chainage km 1.4+22. Closer inspection of the trend line reveals similar longitudinal displacement pattern that occurs at almost every transition in stiffness of the rock mass, either from softer to stiffer or from stiffer to softer. In the latter case the magnitude of the measured displacement was smaller.

Although quite a number of anchors were applied in the area of fault zone between chainages km 1.4+15 and km 1.4+22, the face bolts index was relatively low since some six meter long bolts were installed. As seen from Fig. 5-35, the trend line showed an increasing displacement tendency over several readings. Just before the transition to stiffer material a larger set of 12 m long bolts was installed, but significant final longitudinal displacements of the adjoining measuring section were not prevented. The displacement trend decreased together with simultaneous transition to stiffer material and no particular estimation of bolting effect can be adopted. Further excavation was performed in fair conditions (especially chainage km 1.4+28 to km 1.4+35 where average value of GSI index reached

40 – Fig. 5-35) and only minor longitudinal displacement ahead of the face were measured, although no face bolts were installed. Other sections with very low FBIn and no larger monitored displacement change were (1) around chainage km 1.4+50 where only minor change in the trend line occurred but also coincided with a variation of GSI and (2) around chainage km 1.5+06 where no change in the trend line was observed, although a section of faulted rock mass was encountered. On the other hand, the effect of large amount of face stabilization measures can be observed in the reduction of the displacements ahead of chainage km 1.4+60.

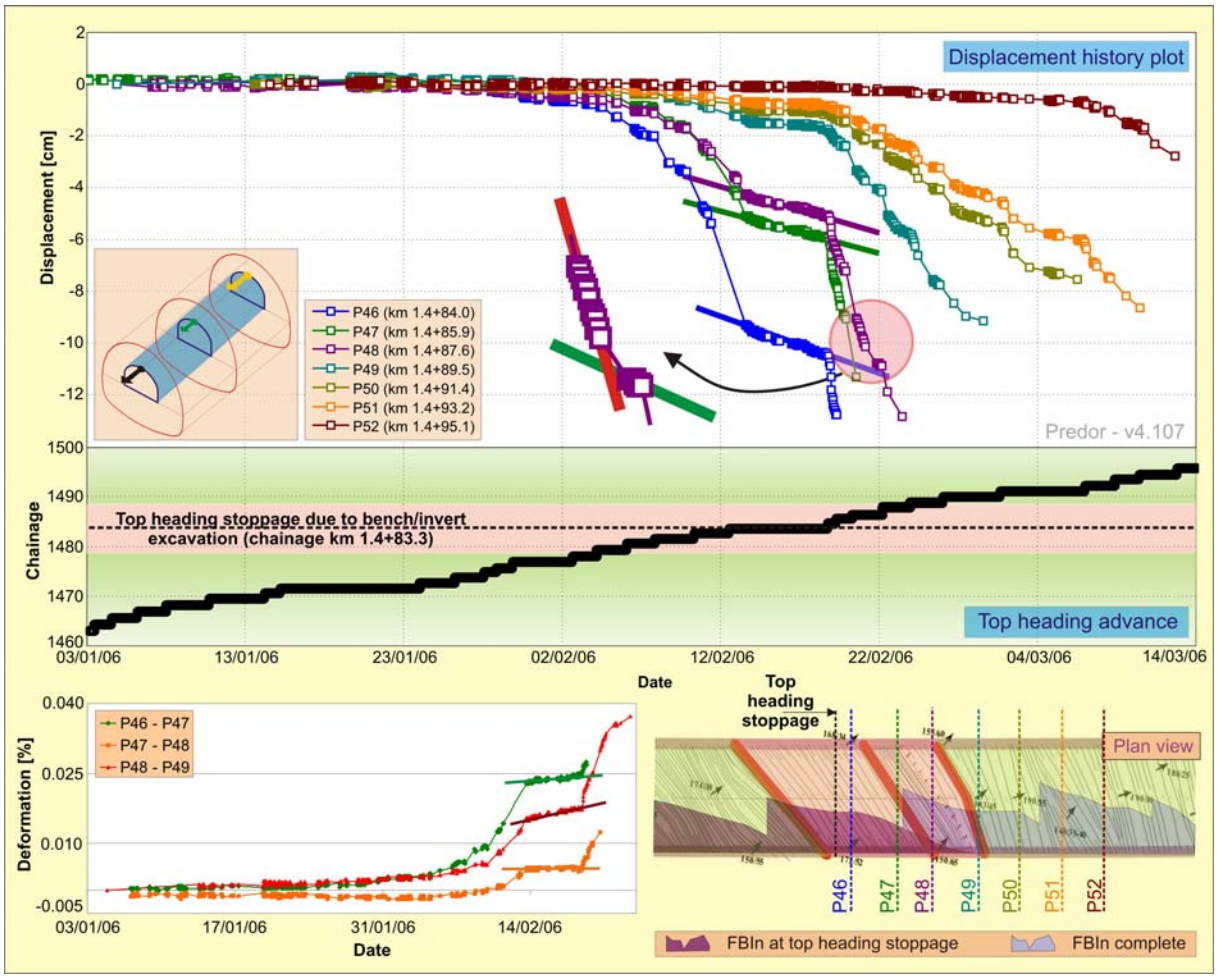

Figure 5-37. Longitudinal displacement pattern ahead of the face in case of inadequate face support (chainage km 1.4+83 – km 1.4+96 in the left tube of the exploratory tunnel).

Slika 5-37. Deformacijski vzorec pred čelom predora v primeru nezadostnega podpiranja čela (stacionaža km 1.4+83 – km 1.4+96 v levi cevi raziskovalnega rova).

A general impression after the comparison of measured longitudinal displacements, geological situation and preface support in large scale suggests that systematic rock bolting has certain influence

on limiting preface displacements. However, a significant influence cannot be proved due to rapid alternations of stiffer and softer rock mass and its dominating influence on the longitudinal displacements. Nevertheless, the effect of face bolt installation can be more explicitly determined in smaller scale. Direct influence of rock bolts on the trends of longitudinal displacements was observed along a section between chainages km 1.4+84 and km 1.4+95 (areas of blue and pink colour in Fig. 5-36, measuring sections P46 to P52). Area of blue colour is located inside faulted rock mass (measuring sections P46 to P48) and area of pink colour in somewhat better tunnelling conditions (P49 to P51 and especially P52), as seen in larger scale in Fig. 5-37 (bottom right plot).

The excavation of the top heading was stopped at chainage km 1.4+83.3 due to the excavation of the bench and invert (because of large dimensions of the cavern simultaneous advance of top heading and bench/invert excavation faces was unfeasible). According to previous observations in similar cases, deformation rates of the rock mass ahead of the face decreased to zero two or three days after the face was stopped (depending also on the distance to face). In the presented case the closest three measuring sections exhibited almost linearly increasing longitudinal displacements in contrast to the next three sections where no displacements were measured two days after the face stopped. Obvious deformation between crown point in P48 and P49 can be seen from bottom left plot in Fig. 5-37 (red curve). No deformation occurred between points in P47 and P48 and only minor deformation between points in P46 and P47.

Further advance of the top heading face provoked significant displacement rates (upper plot in Fig. 5-37) that was also reflected through circumferential cracks of the primary lining. Slopes of the displacement curves were especially for P47 to P49 much steeper than before the top heading face was stopped. This effect reflected also on measuring sections P50 to P51, but in smaller scale. The observed response can be explained by separation of the block of faulted rock due to inadequacy of the installed face support. Although 23 rock bolts were applied ahead of the face, their length was not sufficient, since they hardly reached stiffer rock mass ahead (theoretically they ended just in front of P50).

On the basis of the measured displacements ahead of the face, additional set of 24 bolts was installed when the top heading face was at km 1.4+86. In magnified part of the displacement curve of P48 in the upper plot of Fig. 5-37 two trends are evident (trend before the face bolt installation is emphasized with red line and trend after the installation of new set of rock bolts with green line). The latter line is less steep. Installation of the rock bolts thus decreased the displacement rate. The same effect can be noticed also in measuring sections P49 – P51. Unfortunately, the positions of the targets were not recorded continuously and the time needed for the grout to harden and thus to activate bearing capacity of the bolts could not be assessed.

5.4 Numerical study of the influence of exploratory tunnel

As already outlined earlier, displacements ahead of the face cannot be monitored using conventional geodetic equipment. Therefore some device has to be installed there, which alters the boundary conditions and primary stress state. In those cases where the horizontal inclinometer casings were installed above the crown of the tunnel, the disturbance of the rock mass was small. If the tunnel with small diameter is constructed prior to the construction of larger diameter tunnel inside its cross section, the disturbance is definitely higher than that caused by the installation of the inclinometer casing. Furthermore, rock mass ahead of the tunnel face responds differently during main tunnel excavation if even a small diameter tunnel is located there or not.

Some numerical analyses on the influence of the exploratory tunnel on the construction of the motorway tunnel were already performed by Jemec (2006) and proved that the exploratory tunnel diameter was sufficiently small, so the influence on the internal forces and displacements of the primary lining of the motorway tunnel was negligible. Additional analysis was performed within numerical simulations of this work and confirmed observations by Jemec.

Further 3D analysis using Plaxis software were executed to investigate the influence of the exploratory tunnel on the displacements of the rock mass ahead of the face. The main reason was the evaluation of the measured 3D displacements in the exploratory tunnel by comparing the calculated displacements with an opening (case 2) and without any rock mass disturbance ahead of the face (case 1). Additionally, a micro location of the exploratory tunnel was changed; in case 3 the crown of the exploratory tunnel coincided with the crown of the motorway tunnel. Detailed information about the numerical model is given in Fig. 5-38. The same model with identical mesh was used in cases 1 and 2. In case 2 the exploratory tunnel was “excavated” first and only later the main tunnel (when the exploratory tunnel was finished through complete model in order to track each excavation phase effects separately), while in case 1 only the excavation of the main tunnel was modelled. Displacements were in both cases tracked in the same point in the crown of the exploratory tunnel at “chainage” 77 m of the model.

To obtain a wide range of possible results in anisotropic as well as in isotropic conditions, calculations of cases 1 and 2 were repeated with 4 different sets of material parameters, one with Hardening soil, two with Jointed rock and one according to the Mohr-Coulomb constitutive model. Back calculated stiffness and strength parameters from Chapter 4.1 were applied (shown in Fig. 5-38). The reason for two sets of Jointed rock parameters is different dominating dip and strike of the discontinuities in each of the tubes. Dominant dip in the right tube is nearly horizontal and strikes parallel to the axis (mark JR1), while the dip direction of discontinuities in the left tube point

approximately towards south, i.e. in the excavation direction (mark JR2) with average dip of 34° (acquired geological data are presented with Fisher concentrations and poles plot in Fig. 5-38). Shotcrete was modelled with cluster element like in Chapter 4.2.3 to avoid unrealistic axial stiffness of the "beam" elements in longitudinal direction as experienced in the preliminary studies of the exploratory tunnel influence.

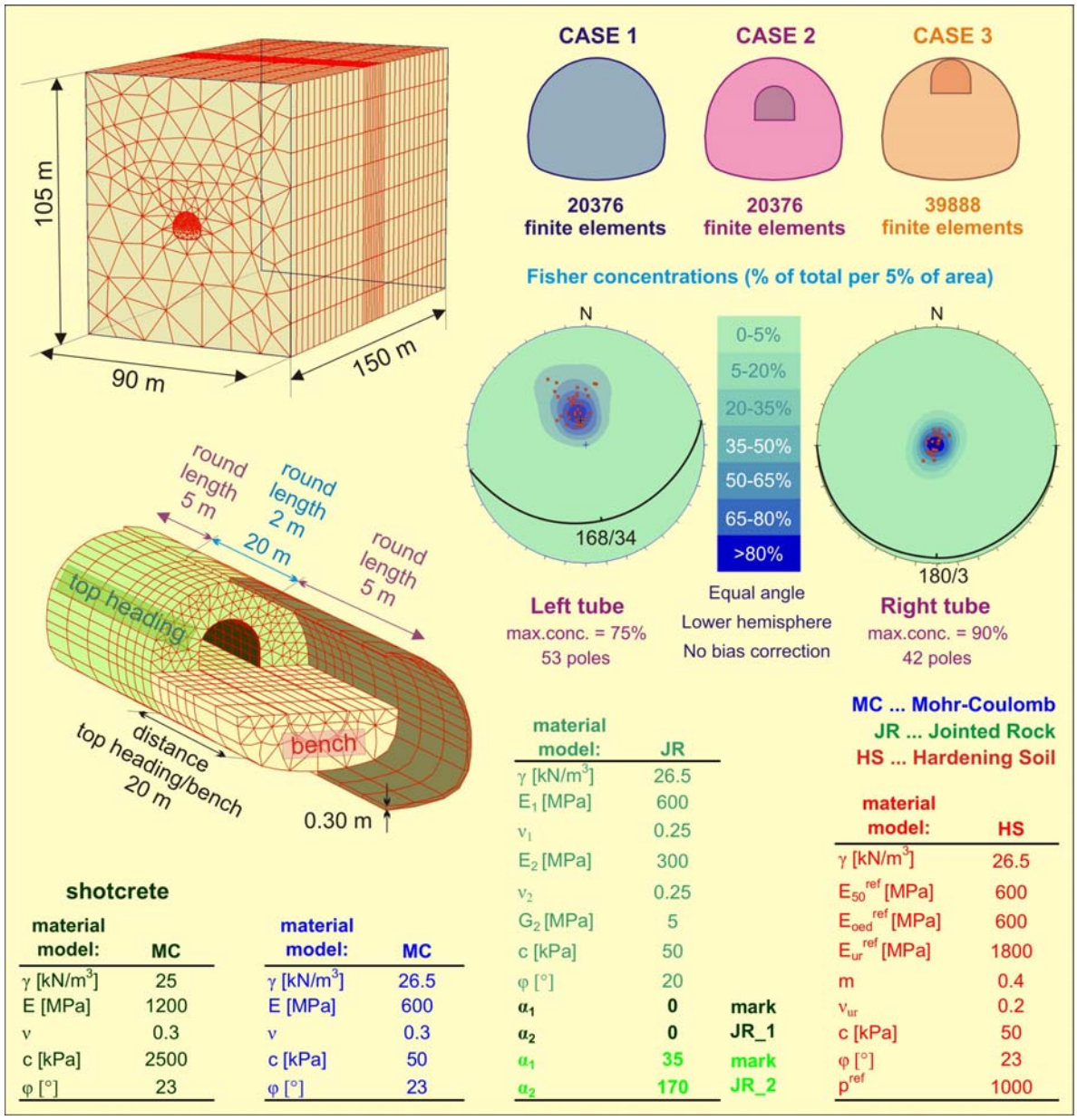

Figure 5-38. Numerical model to analyse the influence of the position of the exploratory tunnel regarding the motorway tunnel.

Slika 5-38. Numerični model za analizo vpliva položaja raziskovalnega rova glede na avtocestni predor.

Since the shotcrete of the exploratory tunnel, especially in the left tube, was partly disintegrated due to sulphate corrosion and cracked to high extent (no wire mesh or rock bolts were installed, shotcrete was only micro reinforced), lower elastic modulus as suggested by Pottler (1990) and lower strength parameters were adopted for the primary lining, as seen from Fig. 5-38. As the Jointed rock constitutive model does not distinguish elastic moduli for loading and unloading conditions, the same material but with three times higher moduli was applied at the bench excavation to prevent unrealistic uplifts.

Calculated response for cases 1 and 2 is presented in Fig. 5-39 with displacement history plots of vertical and longitudinal displacements and displacement vectors in longitudinal section to allow direct comparison between both cases. As expected, based on experience from 2D back analysis (described in Chapter 4.1) the displacements calculated with isotropic models are in general significantly smaller compared to those calculated with the anisotropic model.

Both isotropic models exhibit similar displacement pattern with the distinct two-phase response. When approaching the observation point, only vertical displacements occur, while minor longitudinal displacements point in the excavation direction in cases 1 and 2. Displacement pattern changes at a distance of 6 m from the top heading face to the observation point. Longitudinal displacements start to increase, unlike the vertical displacements that decrease in this second phase; in case 2 even an uplift occurs in the last step. This pattern occurs due to arching effect that compresses the section ahead of the face and it diminishes when the face is excavated in the vicinity and rock mass displaces towards the face. Such displacement pattern was not observed in "homogeneous" conditions (transitions in the stiffness of the rock mass are excluded) at monitoring sections ahead of the excavation face in the Šentvid tunnel. Isotropic constitutive models were therefore not used in further calculations.

On the other hand, the calculated response with Jointed rock constitutive model is very similar to the monitored patterns for both discontinuity orientations in case 2. The final magnitudes of vertical displacements were larger and also started to develop prior to the longitudinal ones for orientation JR1 (uniform orientation of the displacement vector with minor longitudinal displacements was both measured and calculated). Only minor longitudinal displacement can be explained by the foliation orientation (rock mass is more deformable normal to foliation than in parallel direction). The same explanation stands also for orientation JR2, which caused larger magnitudes of final longitudinal displacements than vertical. Bilinear displacement vectors in longitudinal section were again measured (Fig. 5-39) and observed (Fig. 5-22). Hence, the comparison of displacement patterns and also of the stress states (Fig. 5-40) of cases 1 and 2 can give some measure about the value of the performed 3D displacement measurements ahead of the face in the Šentvid tunnel.

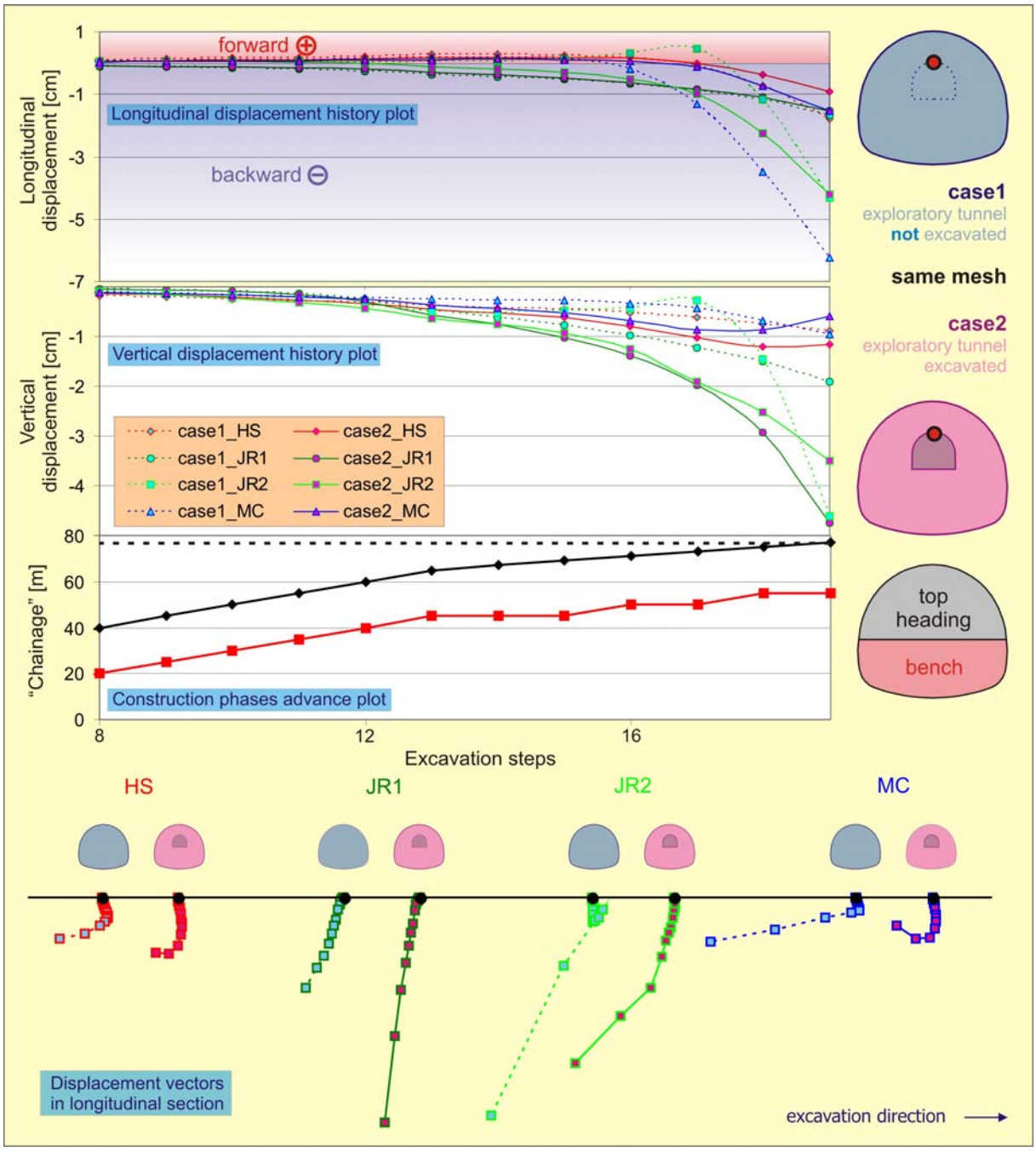

Figure 5-39. Calculated vertical and longitudinal displacements of the crown point in the exploratory tunnel together with displacement vectors in longitudinal section for cases 1 and 2.

Slika 5-39. Izračunani vertikalni in vzdolžni pomiki stropne točke raziskovalnega rova skupaj z vektorji pomikov v vzdolžnem prerezu za primera 1 in 2.

Calculated vertical displacements with the Jointed rock constitutive models as well as with both isotropic models are in general larger in case 2 compared to case 1, since the lining of the exploratory

tunnel is not stiff and allows deformation of the rock mass in the excavated area. On the other hand, longitudinal displacements are larger in case 1. The observation on the ratio of both components of the displacement vector somehow confirms the assumption that the exploratory tunnel acted like a reinforcement and limited significant longitudinal displacements.

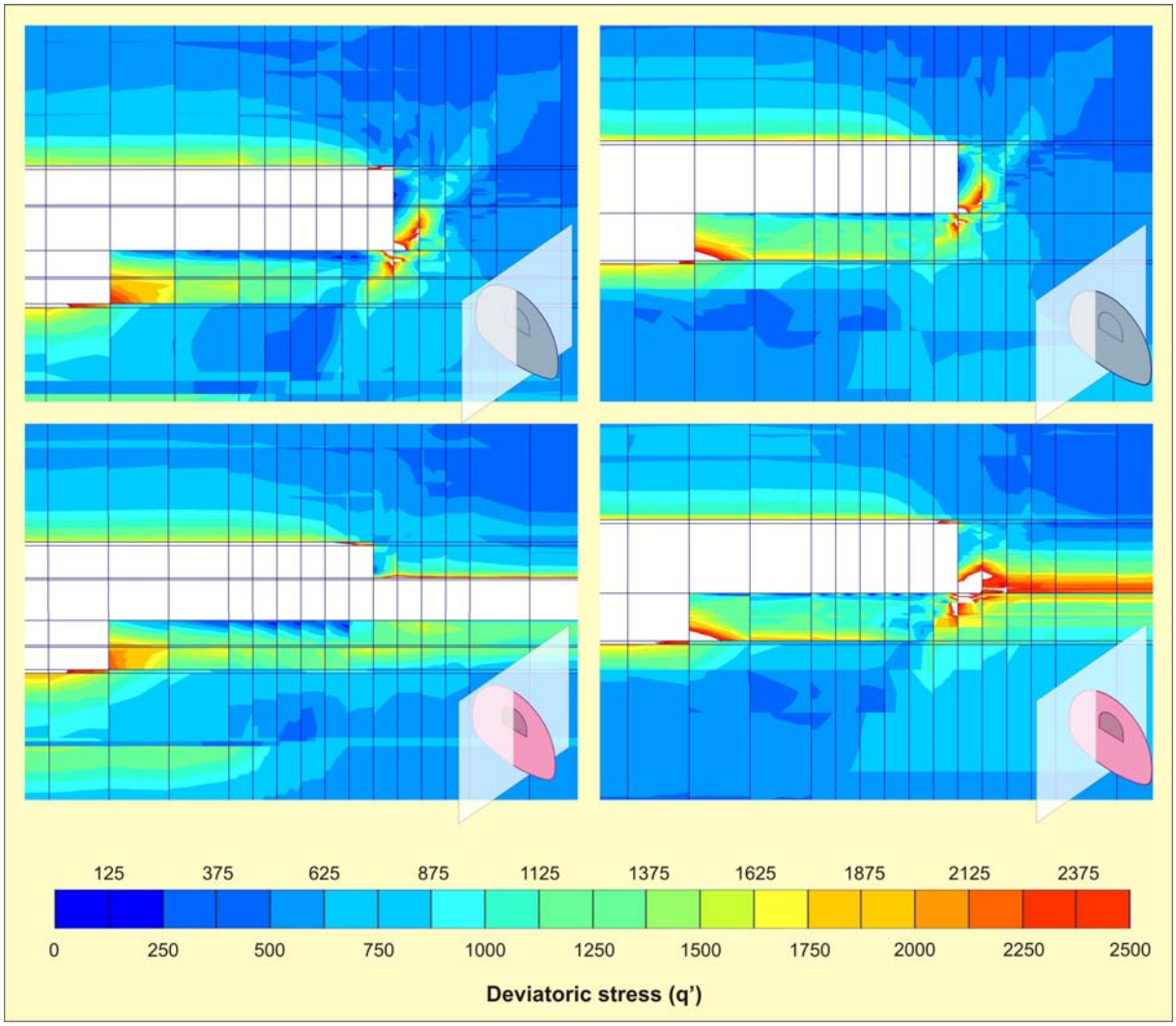

Figure 5-40. Deviatoric stress state of the model in cases 1 and 2 (longitudinal section through the crown (left images) and close to the left sidewall of the exploratory tunnel (right images)) – foliation dip JR2.

Slika 5-40. Deviatorično napetostno stanje modela v primerih 1 in 2 (vzdolžni prerez čez teme (levi sliki) in tik ob levem boku raziskovalnega rova (desni sliki)) – vpad skrilavosti JR2.

This assumption arose during the evaluation of the effect of face rock bolts on limiting the pre-face displacements, where no major difference in the longitudinal displacement pattern was observed in sections without or lots of rock bolts. Smaller longitudinal displacements in case 2 can be further on

explained also with relaxation of stresses transferred ahead of the face in radial direction normal to the circumference of the exploratory tunnel. Without the opening ahead of the face the only possible deformation is towards the excavation face.

For discontinuity orientation JR1 the longitudinal displacement curves have the same course in both cases, while the vertical displacements are larger in case 2 due to previously mentioned reason. The explanation for the discontinuity orientation JR2 is more complicated. Some 6 to 8 meters ahead of the face an uplift and longitudinal displacement in the excavation direction occur as seen in Fig. 5-39. As the face was 4 m to the observation point, the trend changed and the increase of stresses resulted in significant vertical and longitudinal displacement. The deformation pattern is further explained in Chapter 5.5.1.

Case 3 was investigated at the assumed best possible position of the exploratory tunnel for the performance of 3D displacement measurements ahead of the tunnel face. The reason is the theoretical coincidence of its crown with the main tunnel crown. Results of case 3 and comparison of longitudinal and vertical displacements to case 1 are given in Fig. 5-41. As already observed in case 2, the displacements in case 3 also start prior to case 1, which is the consequence of the opening ahead of the face. Longitudinal displacements for discontinuity orientation JR2 started about 17 m ahead, while in case 1 only 6 m. Nevertheless, final vertical displacements were almost of the same magnitude. For orientation JR1 longitudinal displacements are generally smaller than for JR2 due to horizontal foliation, but for case 3 actually no longitudinal displacements occur due to comparably larger axial stiffness of the lining with regard to the stiffness of the surrounding rock (the observation point is numerically attached to the same lining throughout the simulation of complete excavation process). Unlike longitudinal, vertical displacements are more similar in both presented cases regarding magnitude as well as the course of the displacement curves, especially for discontinuity orientation JR1.

A comparison of deviatoric stresses of cases 1 and 3 confirms that unlike in case 2, in case 3 a previously excavated exploratory tunnel would affect the stresses within the rock mass above the future main tunnel. A portion of stresses would thus be relaxed and the measured displacements in the main tunnel would decrease. Compared to case 2 a larger area at the sidewalls of the exploratory tunnel ahead of the face is highly stressed and reaches in parts the area of the future main tunnel lining.

The position of the exploratory tunnel where its crown coincided with the main tunnel crown would be from the research point of view (for the performance of 3D measurements ahead of the face) more appropriate, but on the other hand it would unavoidably affect the behaviour of the main tunnel.

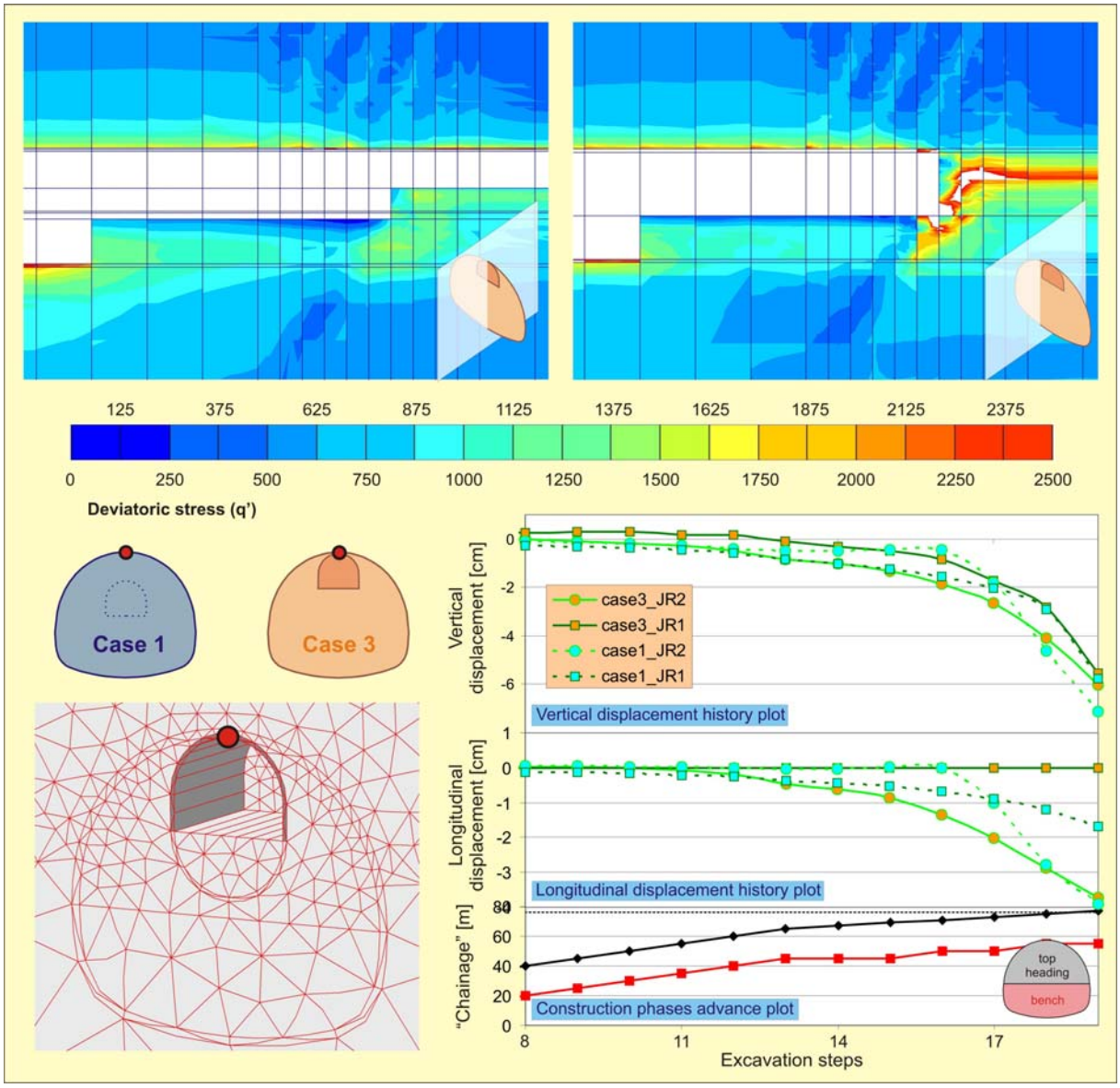

Figure 5-41. Deviatoric stress state in the model in case 3 (foliation dip JR2) and comparison of longitudinal and vertical displacements of cases 1 and 3.

Slika 5-41. Deviatorično napetostno stanje modela v primeru 3 (vpad skrilavosti JR2) in primerjava vzdolžnih in vertikalnih pomikov za primera 1 in 3.

5.5 Numerical study of monitored behaviour and phenomena

5.5.1 General behaviour

For the analysis of general behaviour of the rock mass – support and other observed phenomena ahead of the face of the main tunnel – the same model was used as for the investigation of exploratory

tunnel influence on the displacements ahead of the face (shown in Fig. 5-38). General behaviour was studied only for the left tube of the exploratory tunnel, therefore foliation type JR2 was applied. The calculated response of the crown point mainly matches the observed displacement pattern when comparing the displacement history plots in Fig. 5-42 and Fig. 5-21. The main difference presents the absence of lateral displacements along the foliation when the face was far from measuring section, i.e. in the area of small displacements. As opposed to was monitored, the calculated displacement vector in cross section surprisingly does not exhibit bilinear displacement pattern, which was however obtained in 2D calculation (Fig. 4-5).

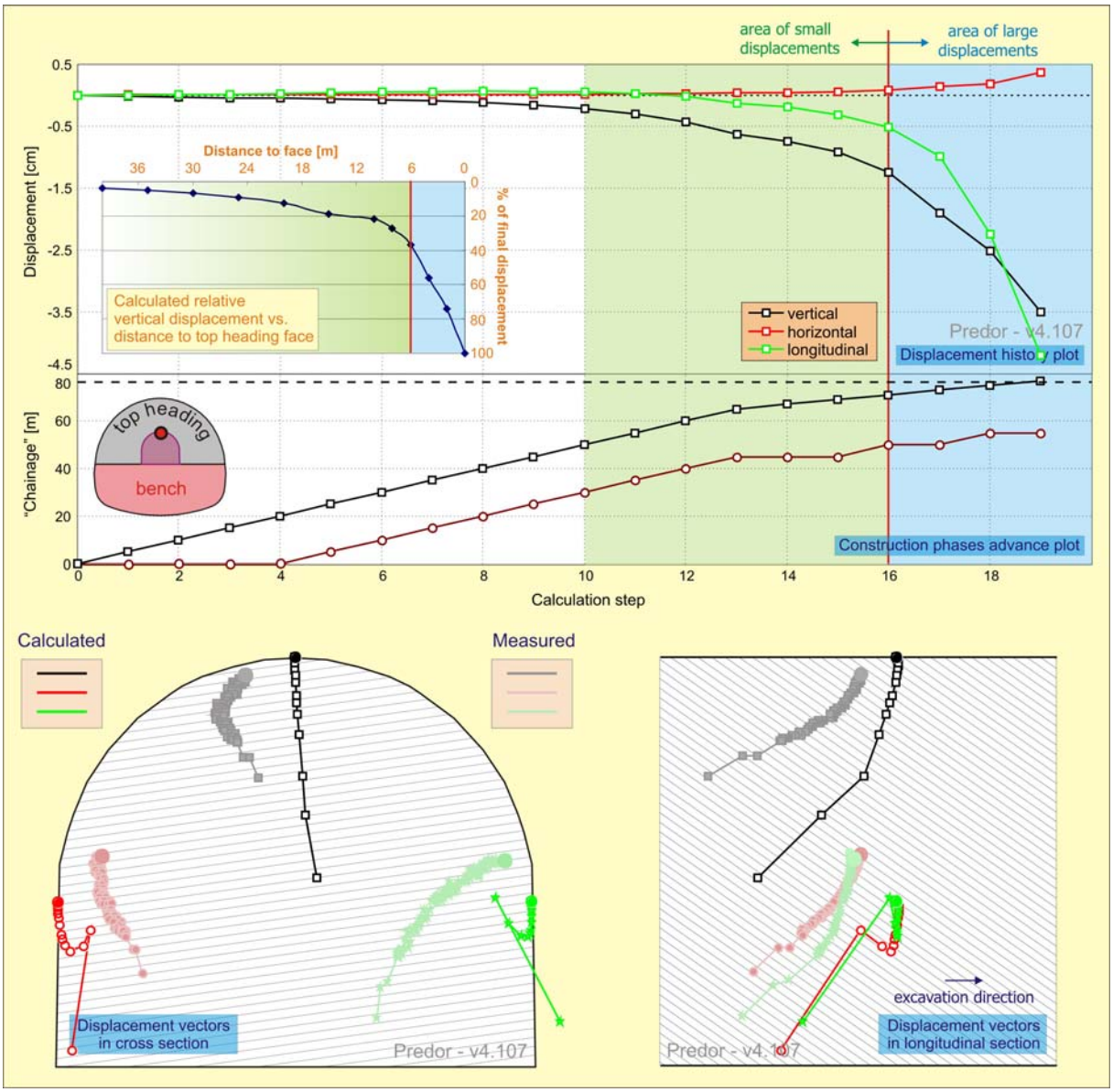

Figure 5-42. Calculated behaviour ahead of the main tunnel face – foliation type JR2.

Slika 5-42. Izračunani odziv pred čelom glavnega predora – vpad skrilavosti JR2.

On the other hand, such pattern can be seen in the longitudinal direction for the crown point as shown in the lower right plot in Fig. 5-42. Initially it was assumed that the absence of the bilinear displacement pattern in the cross section occurred due to the particular discontinuity orientation JR2 as used in the calculation with gradual dip in the cross section. Therefore another calculation was performed with the discontinuity orientation 150°/50°, as shown in lined face log in Fig. 5-22. The calculated horizontal displacement in this case was of larger magnitude, but again uniform without any change in the orientation of the displacement vector.

Except for bilinear displacement vector in cross section, other calculated displacement characteristics are similar to the observed ones. The stress redistribution due to approaching tunnel face reflected in the increase of vertical displacement of the crown point much earlier than of longitudinal or horizontal displacements. The beginning of the area of small displacements (3 mm displacement of the point) can be set at 30 m ahead of the face, which is rather larger extent than it was monitored. The displacement history plot in Fig. 5-42 displays that the deformation actually starts 60 m ahead of the face. We believe that this is small strain stiffness problem and that the calculated extent of influential area would be considerably smaller and would probably be in the range of monitored values if the Jointed rock model comprised the small strain behaviour.

The turn point between the area of large and small displacements is defined as the point where the relative vertical displacement plot versus distance to the excavation face changes the trend significantly (described in Chapter 5.3.1 and shown in Fig. 23). The turn point of the calculated vertical displacements of the crown points occurs at a distance of 6 m to the face as seen in small plot in Fig. 5-42 and is at the upper bound of the monitored values, while approximately 40% of the final vertical displacement at the occurrence of the turn point are at the lower bound. Longitudinal displacements of the crown point considerably accelerate in the area of large displacements and their final magnitude is larger than that of vertical displacements, as also monitored (shown in Fig. 5-21).

Unlike for the crown point, the calculated response of both sidewall points was significantly different from the monitored pattern. The most apparent is the uplift in the area of large displacements and then significant settlement in the last excavation step (displacement vectors in cross section in Fig. 5-42 display even deformation towards the rock mass in this step). This deviation can be explained by inability of applying different stiffness parameters for loading and unloading conditions in the Jointed rock constitutive model. The calculated uplifts at the bottom of the exploratory tunnel are therefore significantly overestimated and unrealistic. Uplift of the rock mass was calculated under the exploratory tunnel as well as beside both sidewalls almost to the half of the height of the exploratory tunnel as seen from phase displacements 4 m away of the observation point (upper plot in Fig. 5-43).

In order to limit the uplifts, a rock mass with higher stiffness parameters and cohesion was applied at the bottom of the model and in the bench section. The calculated displacements with both models are shown in Fig. 5-43 (dashed lines represent the displacements of the model with higher stiffness parameters).

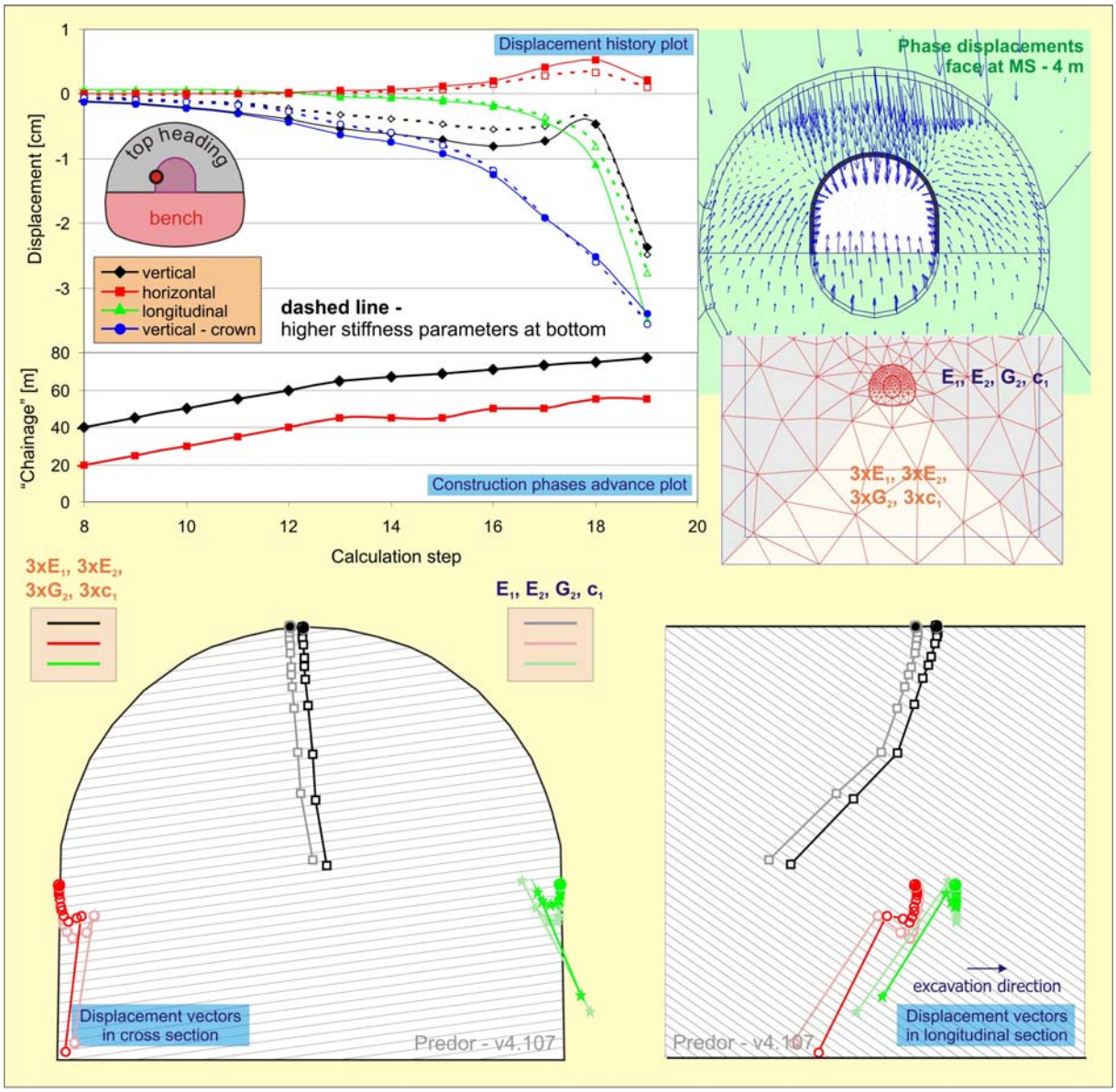

Figure 5-43. Comparison of calculated displacements ahead of the face with and without stiffer rock mass beneath the tunnel.

Slika 5-43. Primerjava izračunanih pomikov pred čelom glavnega predora z in brez bolj togega materiala pod predorom.

Comparison of both vertical displacement curves of the crown point (blue line) shows no larger impact of the applied measure, while the uplift of the sidewall point and the deformation towards the rock mass in the last excavation step are significantly smaller. We believe that the calculated response would be even more comparable to the measured displacements if the Jointed rock constitutive model comprised different stiffness parameters in loading/unloading conditions. Due to model dependant problems, sidewall points were not analyzed in further work.

5.5.2 Influence of rock mass stiffness on the displacement proportions ahead of and behind tunnel face

With respect to the observed dependence of the portion of pre-displacements on the stiffness of the rock mass (Chapter 5.3.3), additional calculations were performed on the same model as before with three different parameter set (back calculated parameters were used as basic parameter set – marked with "E" in Fig. 5-44; soft rock was modelled with 1/3 of basic stiffness parameters and lower strength parameters (marked with 1/3x"E"), while very stiff rock mass was modelled with three times higher elastic moduli than basic parameters and high values of cohesion and friction angle along the discontinuities (marked with 3x"E")).

5.5.2.1 Comparison of displacements ahead of and behind the face of the main tunnel

Two different points were tracked: in the crown of the exploratory tunnel and in the crown of the motorway tunnel to allow the comparison with the measured results. Displacement curve of the crown point in the exploratory tunnel ahead of the main tunnel face was then combined with the displacement curve of the motorway tunnel crown point after the excavation of the round length with the observation point. Composed vertical displacement history plots for all three parameter sets are presented in Fig. 5-44. Due to large differences in the displacement magnitudes the curves of parameter sets 1/3x"E" and 3x"E" in Fig. 5-44 are normalized to set "E" for more convenient presentation (final displacements of the motorway tunnel crown point were matched).

Normalized calculated displacement curves ahead of the face exhibit almost no difference in the magnitude with regard to various stiffnesses of the rock mass. Around 45% of the total vertical displacement occurs before the section is excavated. The stated percentage fits the measured portion of pre-displacements in the soft rock mass. In Chapter 5.3.3 we proposed the assumption that the lower portion of the measured displacements behind the face in soft rock is the consequence of the long lasting excavation sequence of one round length, which causes late instalation af the measuring point and considerable amount of displacement is not measured (denoted as part 2 in Fig. 5-44). The performed calculations show, however, that the maximum displacement that can be missed by

measurements (i.e. displacement that results from the excavation of a single round length) can not explain the observed range of pre-displacement portion of 15% to 45% as observed by measurements in the rock mass with different stiffnesses (See Fig. 5-31).

Another possible cause for the difference in pre-face portion of the measured displacements in various rock mass conditions could also be a small equivalent diameter of the exploratory tunnel compared to the main motorway tunnel and the size of the geological structure (the sequence of softer and stiffer rock mass alternates each 10 to 15 m as seen from Fig. 5-20). The exploratory tunnel is sufficiently small to be located in somewhat uniform rock mass and thus its response depends only on local conditions if the influential area of 1 to 2 diameters is taken into account. On the other hand, the equivalent diameter of the main motorway tunnel is of similar size as the rock mass structure units and the displacements of the main tunnel circumference were probably affected by different lithological units.

Further on the numerical calculation was re-run for the isotropic value of shear modulus G_2 and similar displacement curve was obtained. As it will be shown later on in Chapter 6, the portion of pre-displacements for such orientation (dip direction close to 0°, dip angle of 30°) is only slightly dependent on the material properties. The dependence thus drastically increases for steeper dip angles and is more sensitive to variation of the elastic moduli ratio E_1:E_2 than to the variation of shear modulus.

The first step of the displacement curve that belongs to the motorway tunnel crown point (denoted as part 3 and presented with the area of orange colour in the vertical displacement history plot in Fig. 5-44) includes also the displacements occurring in the virtual tunnel between the excavation of the cross section and its first measurement – denoted as part 2. This portion depends on the execution of works and performance of measurements and can not be assessed from calculated displacements.

5.5.2.2 Comparison of displacements ahead of the face of the main tunnel and displacements due to the exploratory tunnel construction

The same fact stands also when comparing the calculated displacements caused by the construction of the exploratory tunnel (displacements after excavation of the round length – displacement vectors in longitudinal section of cyan colour in upper plot of Fig. 5-44) to the displacements that occur ahead of the top heading face of the main motorway tunnel (violet colour). No major difference except for the poor rock mass conditions, i.e. 1/3x"E", can be noticed at first sight as it would be expected based on the measured response (described in Chapter 5.3.2 and presented in Fig. 5-29). Nevertheless, a large portion of spatial displacement in the initial step after the excavation can be attributed to part 2 of the

displacement curve. If this amount is subtracted from the displacement during the exploratory tunnel construction, the difference between these displacements and the displacements ahead of the face of the main tunnel is close to the measured one.

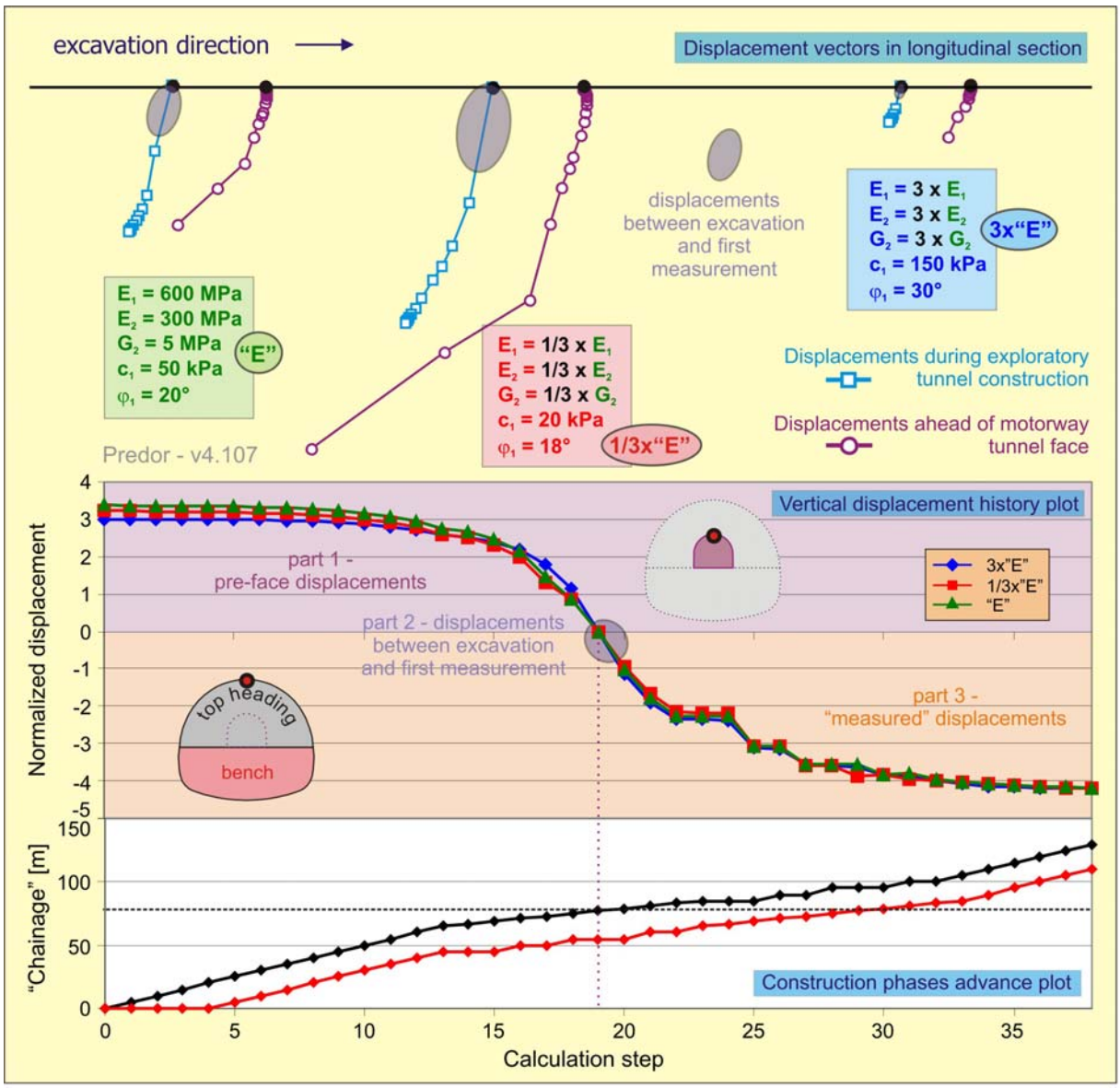

Figure 5-44. Comparison of calculated displacements ahead of the face with displacements, measured during the construction of the exploratory tunnel and the main motorway tunnel (displacement history plots are normalized with final displacement obtained for parameter set "E"!).

Slika 5-44. Primerjava izračunanih pomikov pred čelom glavnega predora s pomiki, izmerjenimi med gradnjo raziskovalnega rova ter avtocestnega predora (krivulje časovnega poteka pomikov so normalizirane s končnim pomikom za niz materialnih parametrov "E"!).

The calculated displacements ahead of the face of the exploratory tunnel during its excavation were significantly larger than the "measured" displacements behind the face. This observation as well as the comparison of the measured and calculated displacements during the exploratory tunnel construction to the displacements ahead of the face of the main tunnel confirm again the assumption that the large portion of measured pre-displacements in the Šentvid tunnel arises from the orientation of geological structure (tunnelling with dip).

5.5.3 Displacement pattern when approaching and digressing from transitions in the rock mass stiffness

For the same model as in previous cases the influence of the transitions in rock mass stiffness (from soft to stiff and from stiff to soft) on the displacement pattern ahead of the tunnel face was studied. The Jointed rock model was used in all calculations. Basic material parameter set was assigned to the stiff material and four times lower elastic moduli with same strength parameters were initially assigned to the soft material. Crown points of the exploratory tunnel in denser part of the mesh were considered in the analysis ("chainage" 67 to 85 m, stiffness transition was set at "chainage" 75 m). Since transition cases were observed in both tubes, calculations were performed for prevailing discontinuity orientations JR1 and JR2. The calculated response is presented in Fig. 5-45 with displacement vectors in longitudinal section for both discontinuity orientations and additionally with trend line of displacement vector orientation L/S 3 m ahead of the face and with contours of final vertical and longitudinal displacements for the discontinuity orientation JR2.

In both transition cases for the discontinuity orientation JR2 the major change in the deformation pattern always occurs at the observation points that are situated between the face and the transition as the displacement vectors farther of transition are almost identical and also final vertical and longitudinal displacements display hardly any change in displacement magnitudes. A more detailed description will be provided for the soft to stiff transition, since it can be directly compared to the observed pattern presented in Fig. 5-33.

The calculated response for the observation points between the face and the transition is characterized by uniform decrease of vertical as well as longitudinal displacements, which were in the soft rock much larger than the vertical, as seen from bottom plot of Fig. 5-45. At first sight this differs from the measured response, but if the last two measurements of the measuring section P13 (shown with displacement vectors in longitudinal section in the upper plot in Fig. 5-33) are neglected as they were taken when the section was within the supporting core and the rock mass around was already excavated, the obtained plot would be quite similar to the calculated displacements.

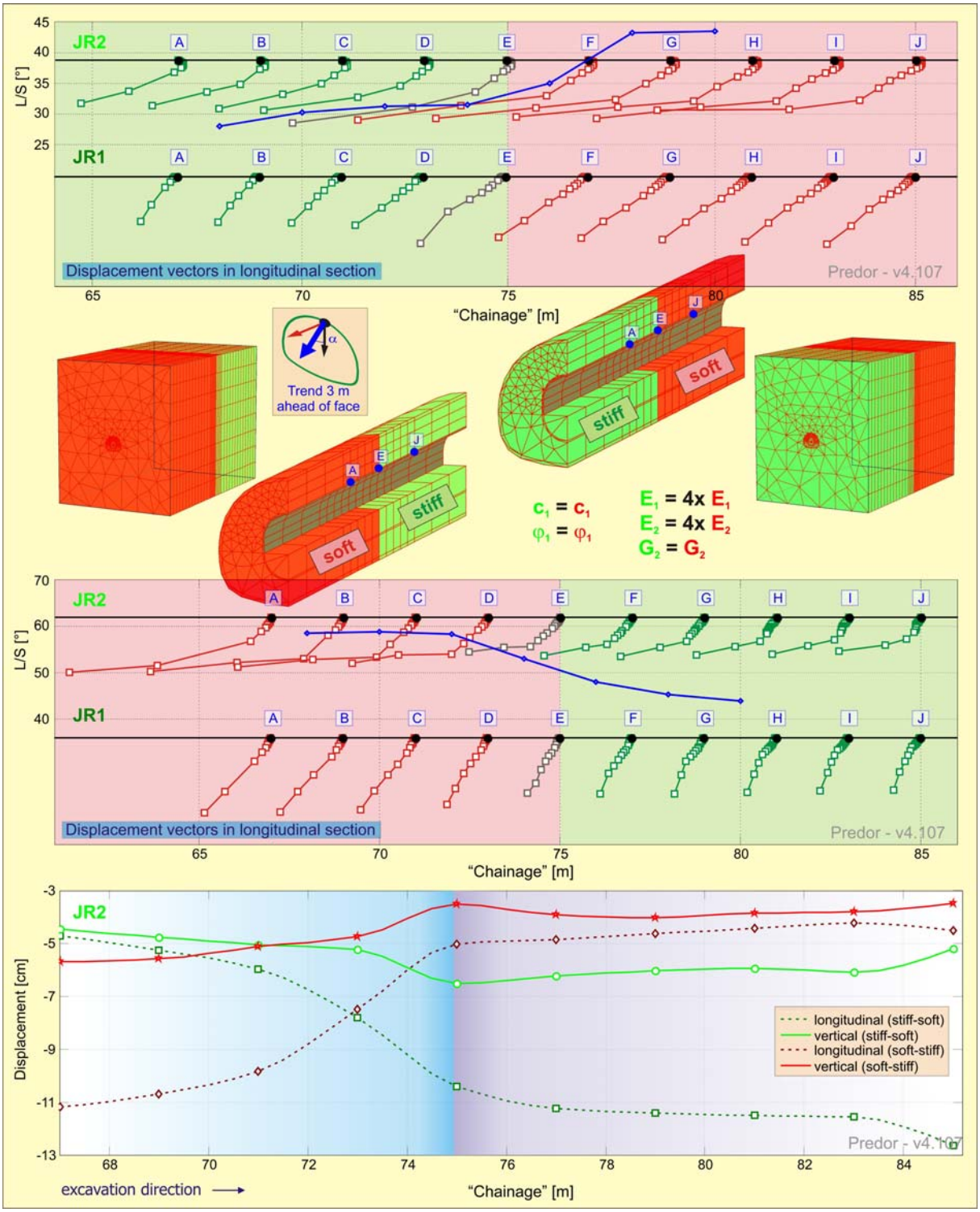

Figure 5-45. Calculated behaviour ahead of the face when approaching and digressing from the transition of the rock mass stiffness.

Slika 5-45. Računski odziv pred čelom glavnega predora pri približevanju spremembi v togosti hribinske mase in oddaljevanju od nje.

With further excavation in stiff rock the magnitude difference between final longitudinal and vertical displacements was much smaller and constant in the measured as well as in the calculated case. The major distinction between both cases is the magnitude of final vertical vs. final longitudinal displacements in the soft ground. This could be explained by quite short section of soft material on site and thus the influence of the previous (stiff to soft) transition. However, the simulated stiff to soft transition did not display larger increase of vertical with regard to longitudinal displacements when approaching the soft zone ahead, as it was observed in two cases in the Šentvid tunnel.

The analysis of calculated displacement vector orientation L/S (trend line of blue colour in Fig. 5-45) shows significantly smaller variation of the orientation angle than observed (measured vector L/S is shown in Fig. 5-35). When tunnelling from stiff to soft the angle of around 30° is obtained for points in stiffer zone and the angle increase to 45° in the softer material. When tunnelling from soft to stiff the L/S angle decreases from around 60° in soft zone to 45° in stiff ground. The trend line exhibits the tendency of further decrease of the L/S angle. For further investigation of the displacement vector orientation to identify the "normal" orientation in both transition cases, a longer numerical model is required.

If the calculated trend lines are compared to the measured one, some parallels can be drawn. In both cases the change in the trend occurs at the transition in rock mass stiffness; the L/S angle increases when the soft zone is entered and decreases in case of stiff zone. Also the angle values are comparable: the initial value of the L/S angle amounts to around 60° in softer rock and around 30° in stiffer rock, which is close to values where some L/S trend alternations occurred.

Much smaller difference between the displacement vectors can be observed for the discontinuity set JR1. The displacement vectors of points A, B and C are almost identical when approaching stiffer rock mass, as shown in Fig. 5-45. Longitudinal displacement started to increase just 2 m before the transition. Further excavation in the soft rock resulted in identical vectors of points F to J. Similar behaviour can be observed when tunnelling from soft to stiff ground. Such deformation pattern is not even close to the monitored one (shown in Fig. 5-34). No uplift occurs in the model in stiffer rock mass when tunnelling in soft rock mass and approaching the transition.

5.5.4 Influence of face rock bolts

To study the influence of the rock bolts on pre-face displacements, three sets of 25 twelve meter long bolts were "installed" in the dense part of the mesh around the exploratory tunnel. Bolts were modelled with 20 cm wide "geogrid" elements of adequate strength.

Almost no distinction can be seen between the calculated vertical and longitudinal displacement curves of the crown point at "chainage" 75 m with and without bolts, as presented in Fig. 5-46. It was however expected that some important difference would occur at least close to the tunnel face and that the bolting effect could be seen in more homogeneous displacement pattern of the bolted section ahead of the tunnel face. Absence of plastic deformation, i.e. elastic behaviour, of the modelled rock mass due to low shear modulus on one hand and rather high strength parameters on the other is a possible explanation of the obtained response. Nevertheless, the analysis of the measured displacements ahead of the face and their comparison to the face bolts index (presented in Chapter 5.3.5) also indicates that due to the relaxation effect of the exploratory tunnel face bolts had only limited effect on limiting pre-face displacements.

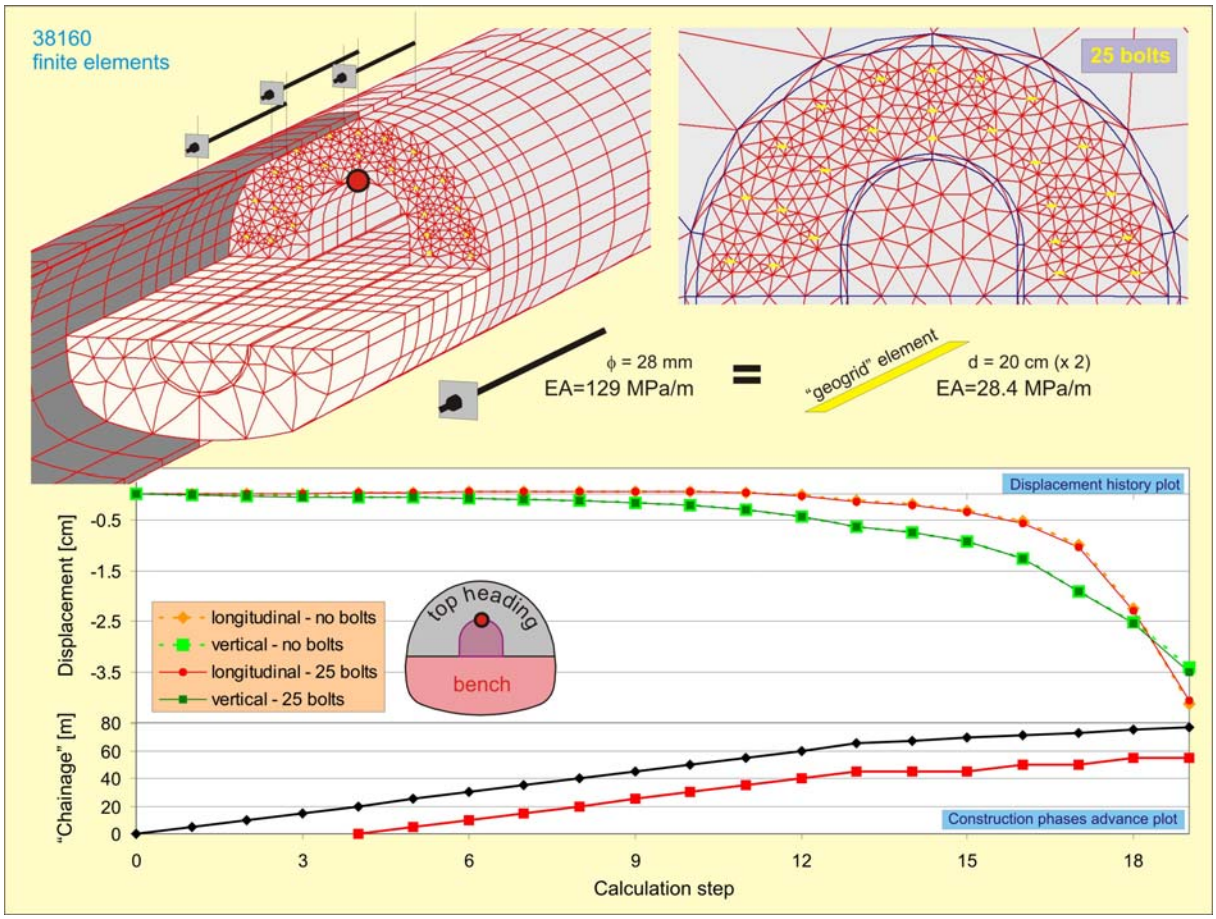

Figure 5-46. Calculated influence of rock bolts on limiting pre-face displacements.

Slika 5-46. Računski vpliv sider na zmanjševanje pomikov pred čelom.

6.0 Application of the displacement function in foliated soft rock

As the tunnel circumference converges inwards due to stress redistribution, the overexcavation of the profile is required with regard to the expected deformation. Assessment of the magnitude of these deformations is one of the most demanding tasks of the geotechnical engineer in the underground construction process since it is influenced by several factors. The stress redistribution causes elastic deformation, time dependent deformation (creeping of the rock mass) and plastic deformation if yielding of the rock mass occurs (Barlow, 1986). The deformation of an opening thus depends on the interplay of these factors and also on the stiffness properties of the lining. It is, however, an unfeasible task to take into account all of these factors when modelling the tunnel response. Further on, it is a toilful task to determine reliable and representative material characteristics of the rock mass, especially in heterogeneous or anisotropic ground where properties vary widely within the rock mass. Unreliable estimation of the convergence magnitude leads to underexcavation or overexcavation of the profile and to further costs when reprofiling in the first case and filling the void with concrete in the second case.

The amount of overexcavation for tunnels in Slovenia is determined on the basis of numerical calculations and experience from projects in similar ground conditions for each of the expected tunnelling categories along the tunnel axis. However, a proper procedure by the site engineer would be to evaluate the displacement monitoring data and to determine the amount of overexcavation according to expected geological conditions and displacements. Nevertheless, there are only a few methods available for such task. 3D numerical analyses are time consuming and therefore not suitable for use on a day-to-day basis. Additionally some simplifications are applied: complex geological structures cannot be modelled in detail, material parameters of the rock mass as input parameters are usually unreliable and the primary stress state is unknown. Even more simplifications of the stress and rock mass conditions with limitations to two dimensional and time independent problems are involved in analytical methods (Sellner, 2000). To overcome these deficiencies a simple but accurate method was developed by Guenot et al (1985), extended by Barlow (1986) and further on modified by Sellner (2000). The proposed method focuses solely on radial displacements, since they are the most easily obtainable and universally measured and describe the displacement behaviour of the rock mass and support in radial direction as a function of excavation advance and time dependent response of the rock mass (Barlow, 1986). Semi-empirical function of hyperbolic shape is fitted to the displacement measurements by adjusting what we call function's parameters. These parameters describe the response of the rock mass and support, taking into account the sequentially staged construction.

6.1 Basics of the displacement function

The original proposal for the convergence equation was given by Guenot et al (1985). This analytical function describes the displacements within a cross section of a circular tunnel with full face excavation without the installation of the support. These displacements are caused by face advance effect and time-dependent effects of the rock mass. In order to overcome the limitations of the convergence equation, Barlow (1986) extended the displacement function for more realistic description of the conditions during tunnelling, especially in soft rock mass. Barlow added to displacement function a pre-displacement part of the curve to account for the sequential excavation. Displacements related to individual excavation steps were simply superposed. Further on, Barlow introduced support by adding only one additional parameter to the displacement function and thus considered the effect of support installation on displacements of the excavated area as well as on displacements ahead of the face. Further modifications of the displacement function were introduced by Sellner (2000). Parameter that describes the influence of the support was on the basis of numerical calculations modified for more realistic representation of the support effect. Instead of just superposing the effects for each excavation step, Sellner suggests that the time dependent part of the displacement function is considered only once and introduced an extension for additional support that is installed at a certain distance to face. Since the proposed procedure did not reliably describe the behaviour ahead of the top heading face, Sellner further on proposed a new iterative procedure for the calculation of pre-displacements ahead of the top heading excavation that does not depend on the estimation of the pre-face domain. This final displacement function was used in the framework of this thesis and is expressed by the following three equations:

- the displacement that occurs ahead of the face - part 1:

$$C(x,t) = \left[Q_1 \cdot C_{pf}(x) - Q_k \cdot P_k^+(x)\right] \cdot \left[C_{x\infty} + A \cdot C_2(t)\right] \qquad \text{Eq.6-1}$$

- the displacement that occurs between the excavation and the installation of support - part 2:

$$C(x,t) = \left[Q_1 + Q_2 \cdot C_1(x) - Q_k \cdot P_k^+(x)\right] \cdot \left[C_{x\infty} + A \cdot C_2(t)\right] \qquad \text{Eq.6-2}$$

- the displacement that occurs after the installation of support - part 3:

$$C(x,t) = \frac{\left[Q_1 + Q_2 \cdot C_1(x) + K \cdot C_s - Q_k \cdot P_k^-(x)\right]}{\left[1 + K \cdot \left(C_{x\infty} + A \cdot C_2(t)\right)\right]} \cdot \left[C_{x\infty} + A \cdot C_2(t)\right] \qquad \text{Eq.6-3}$$

where

$C_1(x)$ ... time independent function (loading function)
$C_2(t)$ ... time dependent function
x ... distance between observed cross section and excavation face
t ... time elapsed between excavation and observation time
X ... curve fitting parameter describing the shape of $C_1(x)$
T ... curve fitting parameter describing the shape of $C_2(t)$
$C_{x\infty}$ ... curve fitting parameter describing ultimate time independent displacement
A ... curve fitting parameter describing ultimate time dependent displacement
Q_1 ... proportion of the total stress change due to the tunnel excavation that occurs ahead of the face
Q_2 ... proportion of the total stress change due to the tunnel excavation that occurs after the excavation face passes the monitored cross section ($Q_1 + Q_2 = 1$)
$Q_k \cdot P_k^+(x)$ and $Q_k \cdot P_k^-(x)$ … functions that distribute the effect of the support installation on the displacements ahead and behind the face, respectively
C_s ... displacement at the time of support installation
K … the parameter of the support (original by Barlow, modified by Sellner).

The main objective of this work is related to the pre-face displacements described by Eq. 6-4, which includes the loading function ahead of the face (C_{pf}) defined as:

$$C_{pf} = \left[\frac{X}{X + (x_f - x)} \right]^{1.2} \qquad \text{Eq.6-4}$$

where

x_f ... the length of the pre-face domain (influential area ahead of the excavation face).

A simple algorithm that enables fast and reliable assessment of the stabilization process and the displacement magnitude in the observed measuring section (Sellner, 2000) are the major advantages of the use of the displacement function if compared to other methods described above. Unlike the analytical methods the displacement function takes account of time effects and 3D effects of the tunnel excavation. Additionally, the displacement function is a much more time-effective method than the numerical calculations and does not require a large amount of parameters, the determination of which would demand a lot of costly and time-consuming laboratory tests. These advantages make the displacement function suitable for the use on a day-to-day basis on construction sites (Sellner, 2000).

While part 3 of the displacement function (after the excavation face passed the observed cross section - Eq. 6-3) is very well defined by fitting the curve to the measured displacements, the first two parts (ahead of the face (part 1) and between the excavation and the support installation (part 2)) are determined on the basis of numerical simulations and rely on the parameters that depend on the rock mass behaviour ahead of the tunnel face: Q_1 and x_f. Barlow found out that the value Q_1 amounts to 0.27 for elastic conditions and that it increases for non-elastic conditions and with the increasing extent of the plastic zone (it can reach the value of 0.6 for plastic zone of two times the tunnel radius).

Barlow also claims that the magnitude of the displacements ahead of the face reflects the amount of the stress change that occurs ahead of the face. Analysis of results of vertical extensometer, horizontal inclinometer and 3D displacement measurements (presented in Chapters 5.1 and 5.3) indicate that with regard to the stiffness of the rock mass the displacements ahead of the face amounted to up to 75% of the total displacement of the measurement point.

The magnitude of the displacements of the exploratory tunnel primary lining in the Šentvid tunnel due to the main tunnel construction and its portion in all the measured displacements is strongly correlated to the stiffness of the rock mass. The comparison of the displacements ahead of the face with the displacements after the excavation of the main tunnel indicates that 15-45% of the measured displacements occur ahead of the face (less displacement in stiff rock mass that was not folded and more in worse geological – geotechnical conditions). On the basis of the measured displacements in different rock mass types we can assume the strong dependence of the portion of the stress state alternation ahead of the face (parameter Q_1) on the stiffness of the rock mass.

The geological structure ahead of the face affects the influence area ahead of the face due to the excavation face advance or what is called pre-face domain. The analysis of the measured displacements shows that a small displacement domain can be observed approximately 2 equivalent diameters of the tube ahead of the face (observations with vertical extensometer and horizontal inclinometer at the Trojane tunnel displayed the same magnitude of pre-face domain) and the majority of the displacements occur within a half of an equivalent tube diameter from the face.

6.2 Numerical calculation of the anisotropy orientation effect on parameters Q_1 and x_f

As shown in Chapter 4.2.3 for the breakthrough area of the northern tube of the Trojane tunnel and from performed numerical simulations we can assume a large effect of the relative orientation of discontinuities to the tunnel axis on the portion of the displacements that occur ahead of and behind the tunnel face. As observed, more deformation occurs ahead of the face when tunnelling with dip than when

tunnelling against dip in the same rock mass conditions. To investigate the influence of the relative discontinuity orientation and different ground conditions on parameters Q_1 and x_f, a large number of numerical calculations was performed in the Plaxis 3D Tunnel code using anisotropic Jointed rock constitutive model. Details of numerical model and material parameters are presented in Fig. 6-1.

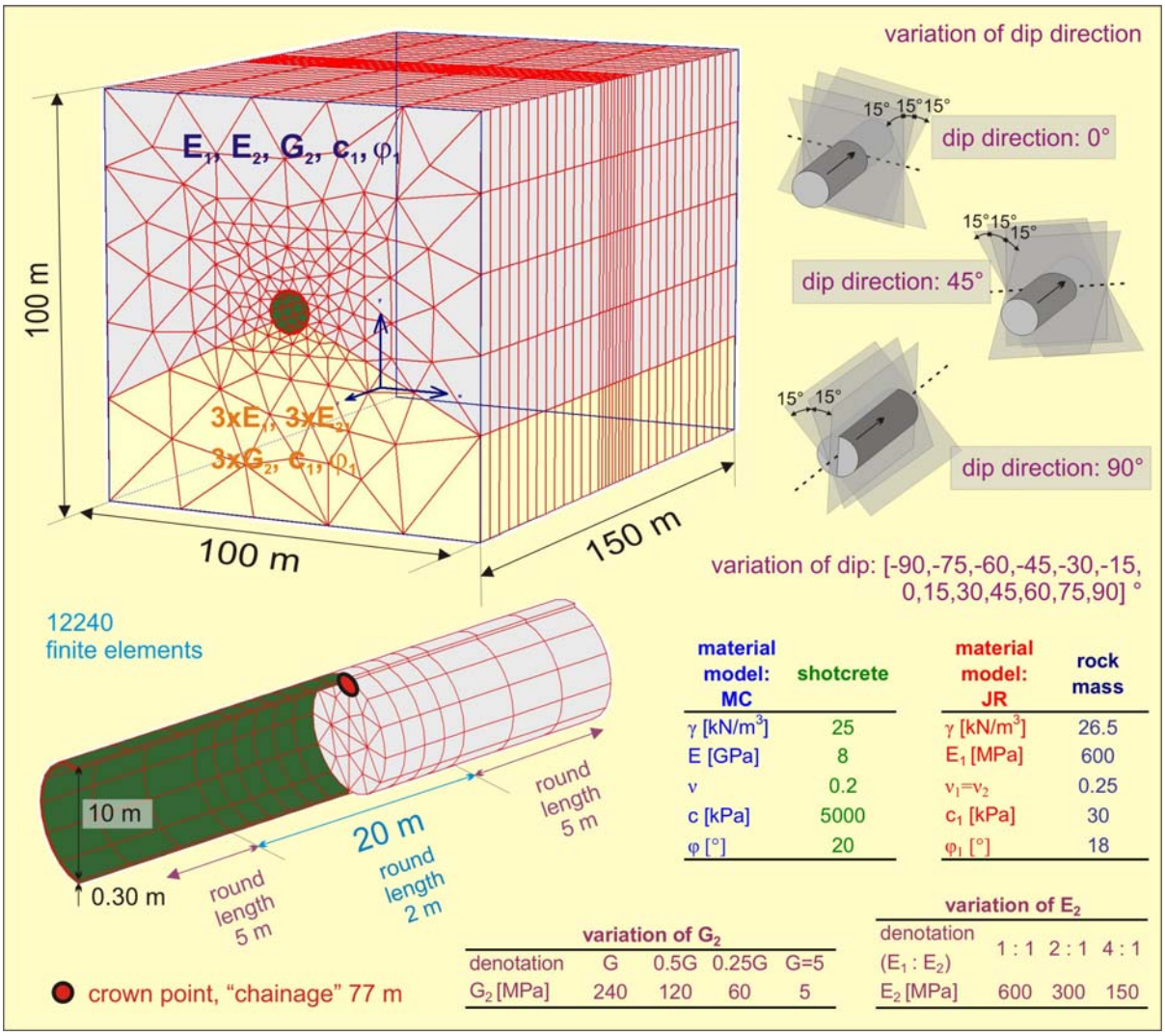

Figure 6-1. Numerical model for the calculation of parameters Q_1 and x_f using anisotropic Jointed rock constitutive model.

Slika 6-1. Numerični model za izračun parametrov Q_1 in x_f z uporabo anizotropnega "Jointed rock" konstitutivnega modela.

Three dip directions were applied:

(1) 0° - strike perpendicular to the tunnel axis (α_2 = 0° and α_2 = 180° in Plaxis since dip has to be applied in range [0°,90°]),

(2) 45° - strike at angle 45° to the tunnel axis (α_2 = 135° and α_2 = -45° in Plaxis) and

(3) 90° - strike is parallel to the tunnel axis (α_2 = 90° in Plaxis).

For each of these dip directions dip was varied in range [-90°,90°] with a step of 15°. Further on, three different ratios E_1:E_2 and four different values of shear modulus G_2 were investigated as shown in Fig. 6-1 (denotation G is given to the isotropic value of shear modulus G_2). As a reference, calculations were performed also with elastic parameters ($E = E_1$, $v = v_1$) and Hardening soil constitutive model ($E_{50}^{ref} = E_{oed}^{ref} = E_1$, $E_{ur}^{ref} = 3E_1$, $c = c_1$, $\varphi = \varphi_1$, $m = 0.5$, $K_0^{NC} = 0.691$, $v_{ur} = 0.2$, $p_{ref} = 1050\ kPa$). To reduce the unrealistic uplift, material with three times higher stiffness parameters was applied at the bottom of the numerical model for elastic parameters and Jointed rock constitutive model. In total 350 3D numerical calculations were performed.

According to Barlow, parameter Q_1 is defined as a pre-face portion of the total displacement magnitude of a single point. In our case vertical displacement of the crown point at "chainage" 77 m was tracked in all cases. Curves of parameter Q_1 for different material characteristics are shown for each of the three dip directions separately in the left three plots in Fig. 6-3; curve is formed by linking the values of Q_1 for all dip angles and a single combination of dip direction, shear modulus and E_1:E_2 ratio. For more convenient presentation the area of the obtained results is highlighted in green (curves for $G_2 = 5\ MPa$ are plotted with dashed lines and are not included in the highlighted area, since so low value of the shear modulus is generally unrealistic; nevertheless, even these curves follow the general response, only the maximum and minimum values are more extreme). In figures and table showing results, negative values of dip angles stand for tunnelling with dip and positive values for tunnelling against dip.

The curves of parameter Q_1 as a function of dip can be for dip directions 0° and 45° roughly approximated with a curve of sinusoidal shape with two maxima (the largest values of Q_1 were obtained around dip angle of -45° and the second maximum at dip angle of 75°) and two minima (at dip angle of 15° and -75° to -90°). A large scatter of Q_1 values can be observed when tunnelling with dip, especially for steeper discontinuity inclinations (dip angles 45°, 60° and 75°). On the other hand, the scatter is small for dip angles 30°, 45°, 60° and 75° when tunnelling against dip and reveals very limited dependence of the pre-face portion of total displacements on the material parameters of the surrounding rock mass. Similarly, the curves for dip direction 90° can be approximated with sinusoidal shaped curve with extreme values at dip angle of 0° and 90° (maximum and minimum value depends on the material parameters).

As expected, the upper boundary of the highlighted area when tunnelling with dip and the lower boundary when tunnelling against dip are both defined with a curve, calculated with the ratio E_1:E_2 =

4:1 and shear modulus of 25% of isotropic G_2 (the worst material parameters taken into account if the curves calculated with $G_2 = 5\ MPa$ are excluded). On the other hand, the lower boundary of the highlighted area when tunnelling with dip and the upper boundary when tunnelling against dip are defined with a curve, calculated with the ratio $E_1:E_2 = 1:1$ and isotropic shear modulus (best material parameters that were taken into account). Maximum value of Q_1 amounts to 0.91 for dip direction 0° and 0.68 for dip direction 45° at dip angle of 45° when using realistic material parameters, while minimum value amounts to 0.36 at dip angle 0° for both cases. The latter value is close to the value of Q_1 as calculated with elastic parameters (0.32), while Q_1 calculated with the Hardening soil constitutive model (0.47) is close to the highest calculated Q_1 value (0.48) at dip angle of 0°. Scatter of Q_1 values for strike parallel to the tunnel axis is the largest for sub-horizontal discontinuity orientations and decreases for steeper dip angles. As expected, the influence of the material parameters and different dip angles for dip direction 0° on the portion of pre-displacements is limited. As seen from Table 6.1, the Q_1 values are in the latter case in range [0.30, 0.48], i.e. close to the values calculated with isotropic constitutive models.

Three right hand side plots in Fig. 6-2 present the calculated magnitude of pre-face domain, i.e. parameter x_f. The beginning of the influential area ahead of the face is determined at 3% of the pre-face displacement. This limit was set due to the observations in Chapter 5.5 that the calculated influential area ahead of the face due to tunnelling process is probably larger than it would be measured due to small strain stiffness phenomenon which is not implemented in the Jointed rock constitutive model. Therefore, the calculated extent of pre-face domain can serve only as an orientation value and should be reduced if used in further calculations. Nevertheless, all performed calculations include the same systematic error.

Like in the plots of parameter Q_1, the area of the obtained x_f values is highlighted in blue colour (curves for $G_2 = 5\ MPa$ are again excluded). In general, the extent of the pre-face domain is inversely proportional to the calculated curves of parameter Q_1 (the maximum area of one parameter somewhat coincides with the minimum of another). The extent is in the range from 12 to 42 m (the diameter of the tunnel was 10 m) for dip directions 0° and 45°, with minima at dip angles of -45° and 75° and maxima at dip angles of -75° and 0°. Unlike in case of parameter Q_1, the upper and lower bounds are not simply related to the curve calculated with the worst or best material characteristics. Thus, no general conclusion can be adopted. Also in this case extreme values of parameter x_f were calculated with $G_2 = 5\ MPa$. For dip direction 90° the extent of pre-face domain is almost independent of the dip angle for higher values of shear modulus G_2 (G, 0.50G) and is in the range from 32 to 42 m. It varies from 22 to 42 m for lower values of shear modulus (0.25G, G=5).

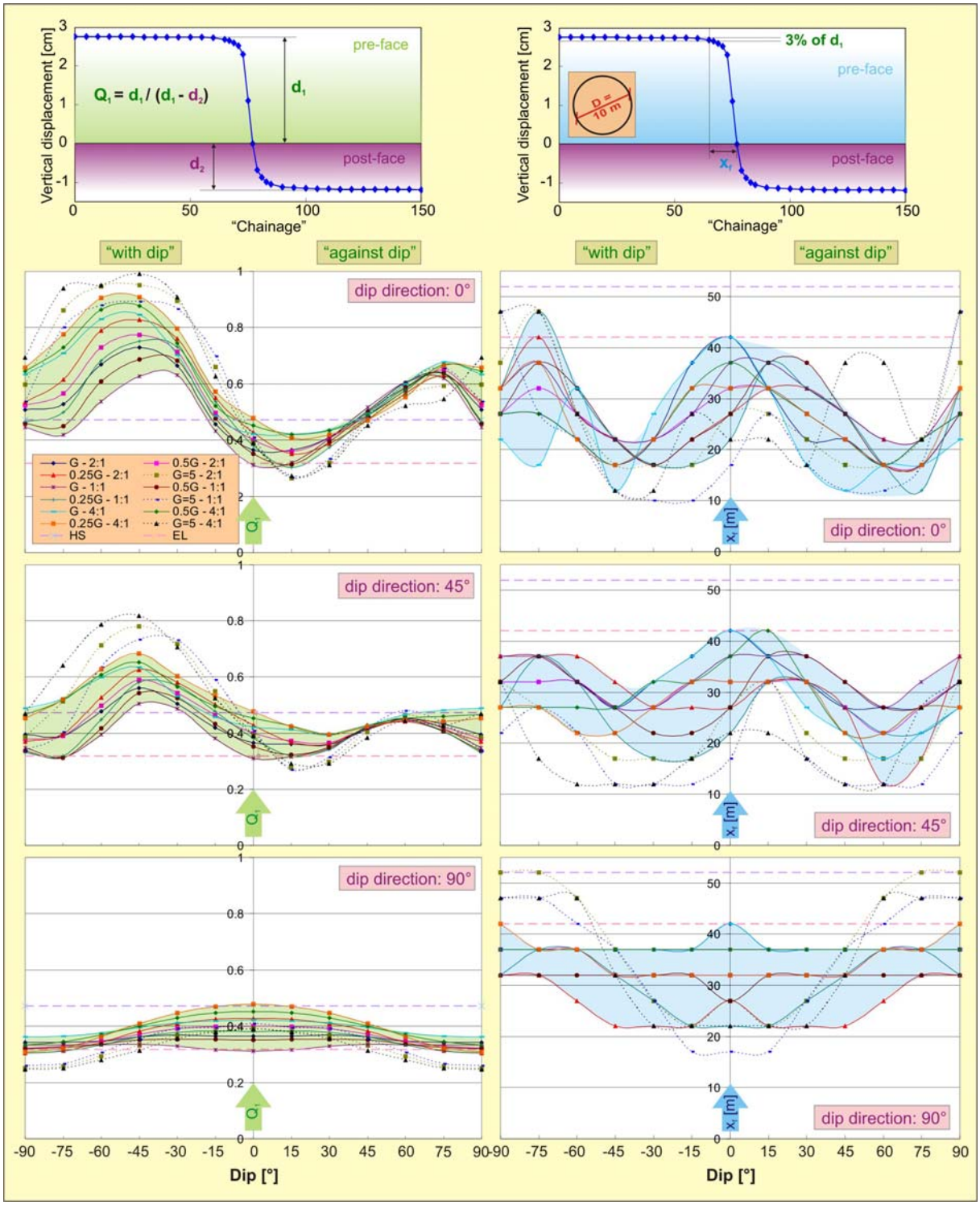

Figure 6-2. Calculated parameters Q_1 and x_f for the combination of three different dip directions and E_1:E_2 ratios, four different shear modulus values and 12 different dip angles.

Slika 6-2. Izračunani parametri Q_1 in x_f za kombinacije treh razmerij E_1:E_2 in azimutov diskontinuitet, štirih različnih vrednosti strižnega modula in 12 različnih vpadov diskontinuitet.

Further on, it was noticed that the total displacement varies for different dip angles and directions, calculated with the same material properties. To compare all total displacements regardless their values, the curves were normalized to the curve at 0°/0°, which is common to all dip directions. Results of normalized total displacements (further on denoted as $|d|$) are presented in the left three plots in Fig. 6-3. Like in previous two cases, the area of obtained values is highlighted in orange colour for more convenient presentation. The magnitude of normalized total displacements is strongly correlated to the ratio $E_1:E_2$ and dip angle and only slightly to the shear modulus, especially in the case of dip direction 90°. Dependence on shear modulus increases for dip direction 45° and is even more pronounced for dip direction 0°. The highlighted areas of calculated results are rather symmetric with regard to the ordinate of the coordinate system for dip directions 45° and 90°. The total normalized displacement magnitudes $|d|$ uniformly decrease from 1 to approximately 0.6 with increasing of dip angle for ratios $E_1:E_2 = 2:1$ and $E_1:E_2 = 4:1$; the largest difference is for ratio $E_1:E_2 = 1:1$. The total displacements for different dip angles and $E_1:E_2$ ratios thus vary from 60% up to 110% of the total displacement at the discontinuity orientation 0°/0°. The same observation stands for dip direction 0° when tunnelling against dip, only the range of $|d|$ is larger. On the other hand, normalized displacements significantly deviate from the described pattern when tunnelling with dip for dip direction 0°, where $|d|$ is mainly higher than 1 except for the dip angle of 75°. The total normalized displacements for different dip directions, dip angles and $E_1:E_2$ ratios were calculated in the range from 50% to 120% of the total displacement at the discontinuity orientation 0°/0°.

Some excerpts of the parameter Q_1 curves are presented in the right hand side plots in Fig. 6-3. The upper plot displays the dependence of parameter Q_1 on the variation of the shear modulus. When tunnelling against dip, this variation has nearly no effect, since the rock mass is more deformable in the direction towards face, where only limited deformation can occur. Similar conclusion can be adopted for the ratio $E_1:E_2$, except for dip angle of 15° and 90°. On the other hand, both variations have significant influence when tunnelling with dip. The decrease of shear modulus results in linear increase of parameter Q_1, while the decrease of elastic modulus E_2 also increases parameter Q_1 but shifts the maximum to steeper dip angles as seen in the middle plot on the right in Fig. 6-3. Variation of dip directions from 0° to 90° results in flatter curves and decreases the portion of pre-displacements in total displacements.

To facilitate a more direct comparison of the effect of tunnelling with or against dip on the tunnel wall displacements, the normalized displacement that occurs behind the face Q_2* was calculated for each of the combinations according to the equation in Fig. 6-4. The area covered with the obtained curves is highlighted in red. For dip direction 90° and material properties closer to isotropic conditions ($E_1:E_2 = 1:1$ and isotropic value of G_2), Q_2* is almost independent of the dip angle; variation of Q_2* in

the range [-90°,90°] is only 0.05. The major influencing factor in this case is the ratio E_1:E_2, while the largest difference (0.20) is obtained for the curve calculated with ratio the E_1:E_2 = *4:1* and isotropic value of G_2. A scatter of the values Q_2* is about 0.25 for different combinations of soil characteristics. Value of Q_2* calculated with the Hardening soil model presents almost a mean value.

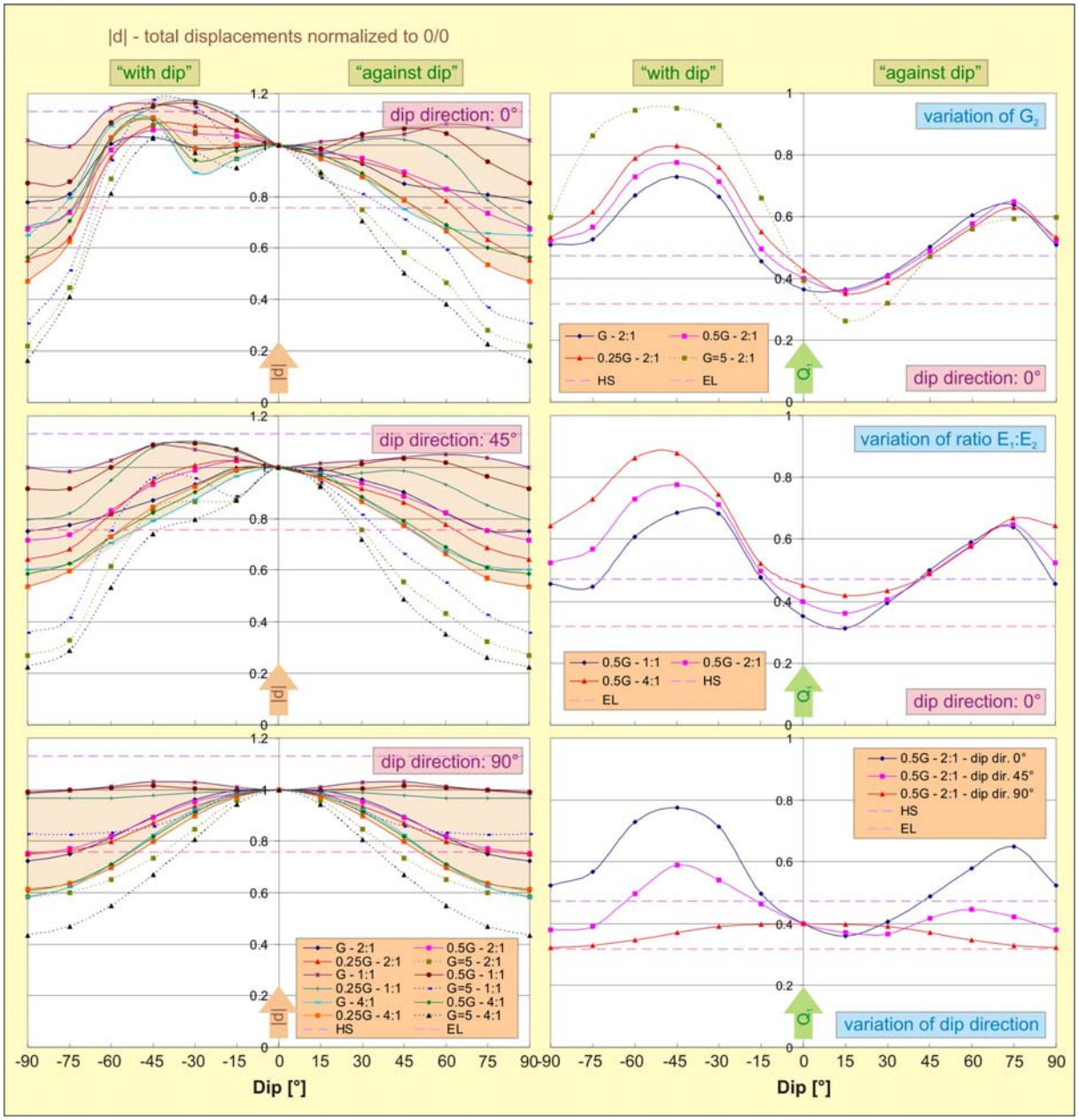

Figure 6-3. Normalized total displacements to total displacement at 0°/0° and excerpt of Q_1 plots for different E_1:E_2 ratios, shear moduli and dip directions.

Slika 6-3. Normalizirani celotni pomiki glede na celotni pomik pri 0°/0° in izvlečki grafov Q_1 za različna razmerja E_1:E_2, različne vrednosti strižnega modula in azimutov diskontinuitet.

		$E_1:E_2$ = 2:1												$E_1:E_2$ = 1:1												$E_1:E_2$ = 4:1											
		Q_1				x_f				|d|				Q_1				x_f				|d|				Q_1				x_f				|d|			
dip dir.	dip	G1	G2	G3	G4	G1	G2	G3	G4	G1	G2	G3	G4	G1	G2	G3	G4	G1	G2	G3	G4	G1	G2	G3	G4	G1	G2	G3	G4	G1	G2	G3	G4	G1	G2	G3	G4
0° with dip	-90	0.51	0.52	0.53	0.60	27	27	32	37	0.78	0.67	0.55	0.22	0.45	0.46	0.47	0.54	32	27	32	47	1.02	0.85	0.68	0.31	0.63	0.64	0.66	0.69	22	27	32	47	0.65	0.56	0.47	0.16
	-75	0.53	0.57	0.62	0.86	27	32	42	47	0.81	0.74	0.64	0.45	0.42	0.45	0.50	0.80	37	37	47	27	0.99	0.86	0.75	0.51	0.71	0.73	0.78	0.94	17	27	37	47	0.79	0.71	0.63	0.41
	-60	0.67	0.73	0.79	0.95	22	27	27	27	1.01	0.98	0.95	0.87	0.54	0.61	0.68	0.88	27	32	32	22	1.14	1.09	1.03	0.94	0.83	0.86	0.91	0.95	32	22	22	27	1.07	1.02	1.03	0.81
	-45	0.73	0.77	0.83	0.95	17	22	22	17	1.03	1.06	1.08	1.08	0.63	0.69	0.75	0.89	22	22	22	12	1.16	1.15	1.15	1.18	0.85	0.88	0.91	0.99	12	17	17	12	1.10	1.10	1.11	1.03
	-30	0.66	0.71	0.76	0.90	22	22	17	17	0.99	1.04	1.07	1.05	0.63	0.68	0.73	0.87	22	17	17	10	1.13	1.16	1.17	1.15	0.70	0.74	0.80	0.91	27	22	22	12	0.89	0.94	0.99	0.97
	-15	0.46	0.50	0.55	0.66	37	27	22	17	0.99	1.03	1.06	0.95	0.43	0.48	0.54	0.70	27	22	17	10	1.06	1.10	1.12	1.00	0.48	0.52	0.57	0.63	37	32	32	27	0.95	0.98	1.00	0.91
	0	0.36	0.40	0.43	0.39	42	32	27	27	1.00	1.00	1.00	1.00	0.31	0.35	0.38	0.41	37	27	22	17	1.00	1.00	1.00	1.00	0.42	0.45	0.48	0.39	42	37	32	22	1.00	1.00	1.00	1.00
	15	0.36	0.36	0.35	0.26	32	32	32	27	0.98	0.97	0.96	0.88	0.32	0.31	0.30	0.27	37	37	37	27	1.01	0.99	0.96	0.87	0.42	0.42	0.41	0.27	32	32	32	22	0.96	0.96	0.94	0.89
	30	0.41	0.41	0.39	0.32	22	27	32	22	0.93	0.95	0.94	0.75	0.41	0.39	0.37	0.33	32	37	32	17	1.03	1.04	1.02	0.81	0.44	0.43	0.42	0.31	17	27	27	17	0.88	0.89	0.88	0.71
	45	0.50	0.49	0.47	0.47	22	22	27	17	0.85	0.90	0.88	0.58	0.52	0.50	0.49	0.48	27	27	27	12	1.04	1.06	1.02	0.71	0.49	0.49	0.47	0.45	12	22	22	37	0.75	0.79	0.79	0.50
	60	0.60	0.58	0.57	0.56	17	17	22	17	0.83	0.83	0.78	0.47	0.60	0.59	0.58	0.60	22	17	17	12	1.08	1.04	0.96	0.59	0.60	0.58	0.55	0.52	17	17	17	37	0.68	0.69	0.67	0.38
	75	0.64	0.65	0.63	0.59	22	17	22	22	0.81	0.73	0.63	0.28	0.62	0.64	0.64	0.66	22	17	12	17	1.07	0.94	0.79	0.37	0.68	0.67	0.66	0.55	17	22	17	22	0.66	0.60	0.53	0.23
	90	0.51	0.52	0.53	0.60	27	27	32	37	0.78	0.67	0.55	0.22	0.45	0.46	0.47	0.54	32	27	32	47	1.02	0.85	0.68	0.31	0.63	0.64	0.66	0.69	22	27	32	47	0.65	0.56	0.47	0.16
45° with dip	-90	0.39	0.38	0.37	0.39	32	32	37	32	0.75	0.72	0.64	0.27	0.35	0.34	0.33	0.34	37	32	27	22	1.00	0.92	0.80	0.36	0.49	0.47	0.45	0.47	27	27	27	32	0.60	0.59	0.54	0.23
	-75	0.39	0.39	0.40	0.51	32	32	37	27	0.77	0.74	0.68	0.33	0.31	0.31	0.32	0.40	37	37	37	27	0.98	0.92	0.82	0.42	0.52	0.52	0.52	0.64	27	27	27	17	0.63	0.63	0.60	0.29
	-60	0.48	0.50	0.53	0.71	32	32	37	22	0.82	0.83	0.82	0.61	0.39	0.42	0.45	0.63	32	32	32	22	1.03	1.00	0.95	0.75	0.60	0.61	0.63	0.79	27	27	22	12	0.70	0.73	0.73	0.54
	-45	0.56	0.59	0.62	0.78	27	27	32	17	0.87	0.93	0.95	0.84	0.50	0.54	0.58	0.73	27	27	22	12	1.09	1.09	1.08	0.96	0.63	0.65	0.68	0.82	27	27	22	12	0.79	0.82	0.84	0.74
	-30	0.51	0.54	0.58	0.72	32	27	27	17	0.93	0.99	1.01	0.87	0.49	0.52	0.57	0.73	27	22	17	12	1.07	1.09	1.10	0.96	0.53	0.57	0.60	0.71	32	32	27	12	0.87	0.90	0.93	0.80
	-15	0.42	0.46	0.50	0.55	37	32	27	17	1.00	1.03	1.03	0.87	0.38	0.43	0.48	0.59	32	22	17	12	1.04	1.07	1.06	0.89	0.46	0.50	0.53	0.52	37	32	32	17	0.97	0.99	0.99	0.87
	0	0.36	0.40	0.43	0.39	42	32	27	27	1.00	1.00	1.00	1.00	0.31	0.35	0.38	0.41	37	27	22	17	1.00	1.00	1.00	1.00	0.42	0.45	0.48	0.39	42	37	32	22	1.00	1.00	1.00	1.00
	15	0.36	0.37	0.37	0.28	37	32	32	32	1.00	0.98	0.96	0.93	0.32	0.32	0.32	0.27	37	37	32	32	1.02	0.99	0.97	0.94	0.41	0.43	0.42	0.29	37	42	32	22	0.98	0.97	0.96	0.92
	30	0.36	0.37	0.36	0.30	32	32	32	22	0.95	0.94	0.92	0.76	0.35	0.35	0.34	0.31	37	37	32	17	1.02	1.01	0.98	0.82	0.39	0.40	0.39	0.29	27	32	32	17	0.88	0.88	0.87	0.72
	45	0.41	0.42	0.42	0.40	27	27	27	17	0.90	0.89	0.86	0.56	0.42	0.42	0.42	0.42	32	32	27	12	1.04	1.04	0.99	0.66	0.43	0.43	0.42	0.38	22	22	22	12	0.78	0.79	0.77	0.49
	60	0.45	0.44	0.44	0.46	27	22	12	17	0.82	0.82	0.78	0.43	0.45	0.45	0.45	0.48	27	27	22	12	1.05	1.02	0.93	0.55	0.47	0.45	0.45	0.44	17	22	22	12	0.68	0.69	0.66	0.35
	75	0.43	0.42	0.41	0.42	27	27	17	17	0.75	0.75	0.69	0.32	0.42	0.41	0.41	0.43	32	27	22	12	1.04	0.97	0.85	0.43	0.48	0.46	0.44	0.43	22	27	27	27	0.61	0.61	0.57	0.26
	90	0.39	0.38	0.37	0.39	32	32	37	32	0.75	0.72	0.64	0.27	0.35	0.34	0.33	0.34	37	32	27	22	1.00	0.92	0.80	0.36	0.49	0.47	0.45	0.47	27	27	27	32	0.60	0.59	0.54	0.23
90°	-90	0.34	0.32	0.30	0.25	37	37	32	52	0.72	0.75	0.75	0.58	0.33	0.32	0.30	0.26	37	32	32	47	0.98	0.99	0.97	0.83	0.36	0.33	0.31	0.25	37	37	42	47	0.58	0.61	0.61	0.43
	-75	0.34	0.33	0.31	0.26	37	37	32	52	0.75	0.77	0.76	0.60	0.33	0.32	0.31	0.27	37	32	37	47	1.00	1.00	0.97	0.82	0.37	0.34	0.32	0.25	37	37	37	47	0.62	0.64	0.63	0.47
	-60	0.35	0.35	0.34	0.29	37	37	27	47	0.81	0.82	0.80	0.65	0.33	0.34	0.33	0.31	37	32	37	42	1.01	1.01	0.97	0.83	0.37	0.37	0.36	0.28	37	37	37	47	0.71	0.71	0.70	0.55
	-45	0.36	0.37	0.38	0.33	37	32	22	37	0.90	0.89	0.87	0.73	0.34	0.35	0.36	0.35	37	32	32	37	1.03	1.01	0.98	0.86	0.40	0.40	0.41	0.31	37	37	32	32	0.83	0.82	0.80	0.67
	-30	0.37	0.39	0.41	0.37	37	32	22	27	0.96	0.95	0.94	0.85	0.33	0.35	0.38	0.39	37	32	27	27	1.03	1.00	0.99	0.91	0.41	0.43	0.45	0.36	37	37	32	22	0.92	0.91	0.90	0.81
	-15	0.37	0.40	0.42	0.38	37	32	22	22	1.00	0.99	0.98	0.96	0.32	0.35	0.38	0.39	37	32	22	17	1.01	1.00	0.99	0.99	0.42	0.45	0.47	0.38	37	37	32	22	0.98	0.98	0.97	0.94
	0	0.36	0.40	0.43	0.39	42	32	27	27	1.00	1.00	1.00	1.00	0.31	0.35	0.38	0.41	37	27	22	17	1.00	1.00	1.00	1.00	0.42	0.45	0.48	0.39	42	37	32	22	1.00	1.00	1.00	1.00
	15	0.37	0.40	0.42	0.38	37	32	22	22	1.00	0.99	0.98	0.96	0.32	0.35	0.38	0.39	37	32	22	17	1.01	1.00	0.99	0.99	0.42	0.45	0.47	0.38	37	37	32	22	0.98	0.98	0.97	0.94
	30	0.37	0.39	0.41	0.37	37	32	22	27	0.96	0.95	0.94	0.85	0.33	0.35	0.38	0.39	37	32	27	27	1.03	1.00	0.99	0.91	0.41	0.43	0.45	0.36	37	37	32	22	0.92	0.91	0.90	0.81
	45	0.36	0.37	0.38	0.33	37	32	22	37	0.90	0.89	0.87	0.73	0.34	0.35	0.36	0.35	37	32	32	37	1.03	1.01	0.98	0.86	0.40	0.40	0.41	0.31	37	37	32	32	0.83	0.82	0.80	0.67
	60	0.35	0.35	0.34	0.29	37	37	27	47	0.81	0.82	0.80	0.65	0.33	0.34	0.33	0.31	37	32	37	42	1.01	1.01	0.97	0.83	0.37	0.37	0.36	0.28	37	37	37	47	0.71	0.71	0.70	0.55
	75	0.34	0.33	0.31	0.26	37	37	32	52	0.75	0.77	0.76	0.60	0.33	0.32	0.31	0.27	37	32	37	47	1.00	1.00	0.97	0.82	0.37	0.34	0.32	0.25	37	37	37	47	0.62	0.64	0.63	0.47
	90	0.34	0.32	0.30	0.25	37	37	32	52	0.72	0.75	0.75	0.58	0.33	0.32	0.30	0.26	37	32	32	47	0.98	0.99	0.97	0.83	0.36	0.33	0.31	0.25	37	37	42	47	0.58	0.61	0.61	0.43

complete calculatation performed with arc-length control unmarked

denotations:
G1 = isotropic G_2
G2 = 0.50 x isotropic G_2
G3 = 0.25 x isotropic G_2
G4 = G_2 = 5 MPa

	Q_1	x_f	|d|
HS	0.47	52	1.13
elastic	0.32	42	0.76

Table 6-1. Calculated values of Q_1, x_f and $|d|$ for different combinations of ratio $E_1:E_2$, shear moduli, dip and dip directions.

Preglednica 6-1. Izračunane vrednosti Q_1, x_f in $|d|$ za različne kombinacije razmerja $E_1:E_2$, stižnega modula, azimuta in vpada diskontinuitet.

Much larger scatter can be expected for dip directions 0° and 45° on the basis of the observed scatter of Q_1 and $|d|$, especially for dip angles in range [-45°,-90°] where Q_2* is in range [0.1,0.58] for dip direction 0° and [0.25,0.69] for dip direction 45°. The thickness of the highlighted zone for other dip angles is rather constant and has the maximum at 0.69 for both dip directions at dip angle of 15° for material set E_1:E_2 = *1:1* and isotropic value of G_2. The Hardening soil value of Q_2* represents the upper bound of possible values, except for higher stiffness parameters E_2 and G_2 at dip angles of 0° and 15° for dip direction 0°. For dip direction 45° the Hardening soil value of Q_2* presents mean value for dip angles in range [0°,30°] and the upper bound value for other dip angles except for higher stiffness parameters E_2 and G_2 at steeper dip angles.

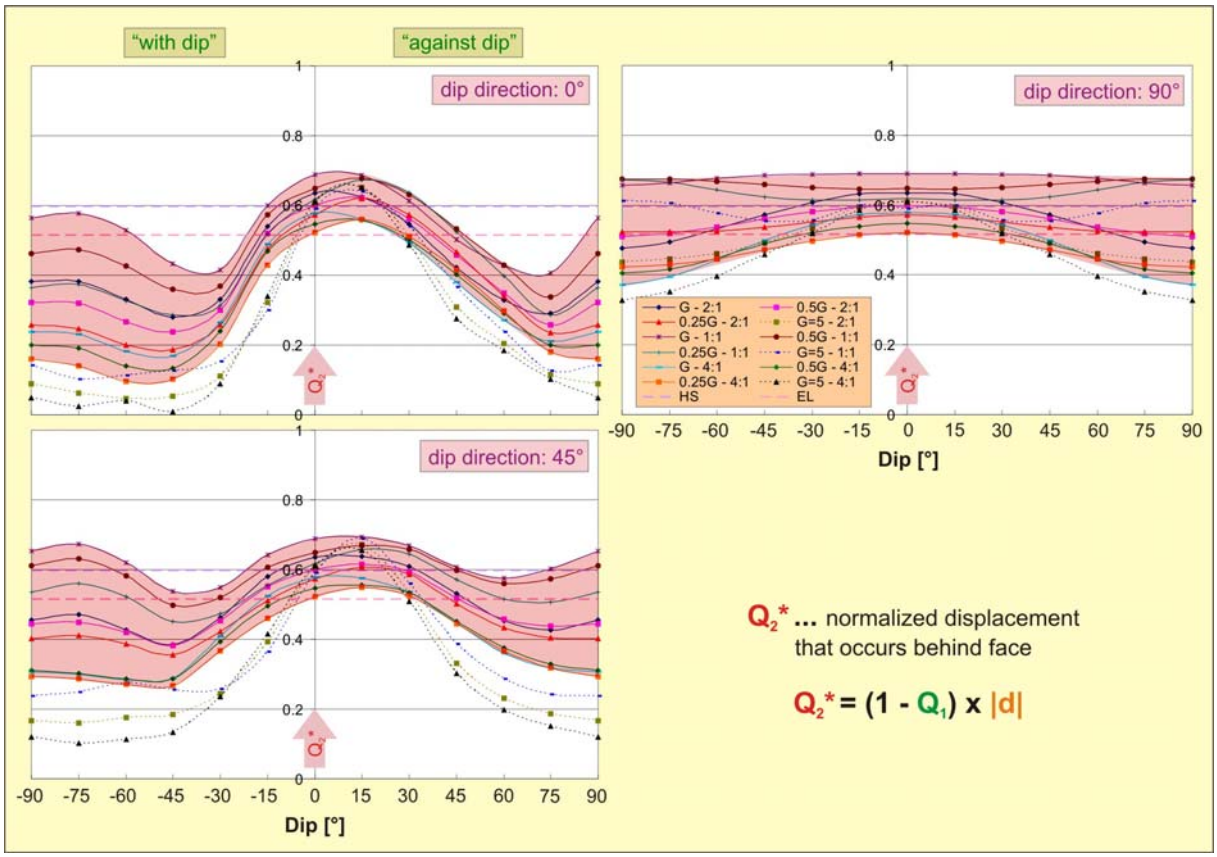

Figure 6-4. Normalized displacement (Q_2*) that occurs behind the tunnel face.

Slika 6-4. Normalizirane vrednosti pomika (Q_2*), ki se zgodi za čelom predora.

For more direct presentation of the influence of discontinuity orientation on the proportion of post-face displacements when tunnelling with and against dip, a ratio between Q_2*^{WD} (value of Q_2* when tunnelling with dip and Q_2*^{AD} (value of Q_2* when tunnelling with dip for the same dip angle as Q_2*^{WD}) was calculated using the lower equation in Fig. 6-5 and was named Q_2*(%). This parameter represents the magnitude of the tunnel crown point settlement for different material properties when

tunnelling against dip with regard to the settlement of the same point when tunnelling with dip in the same ground conditions.

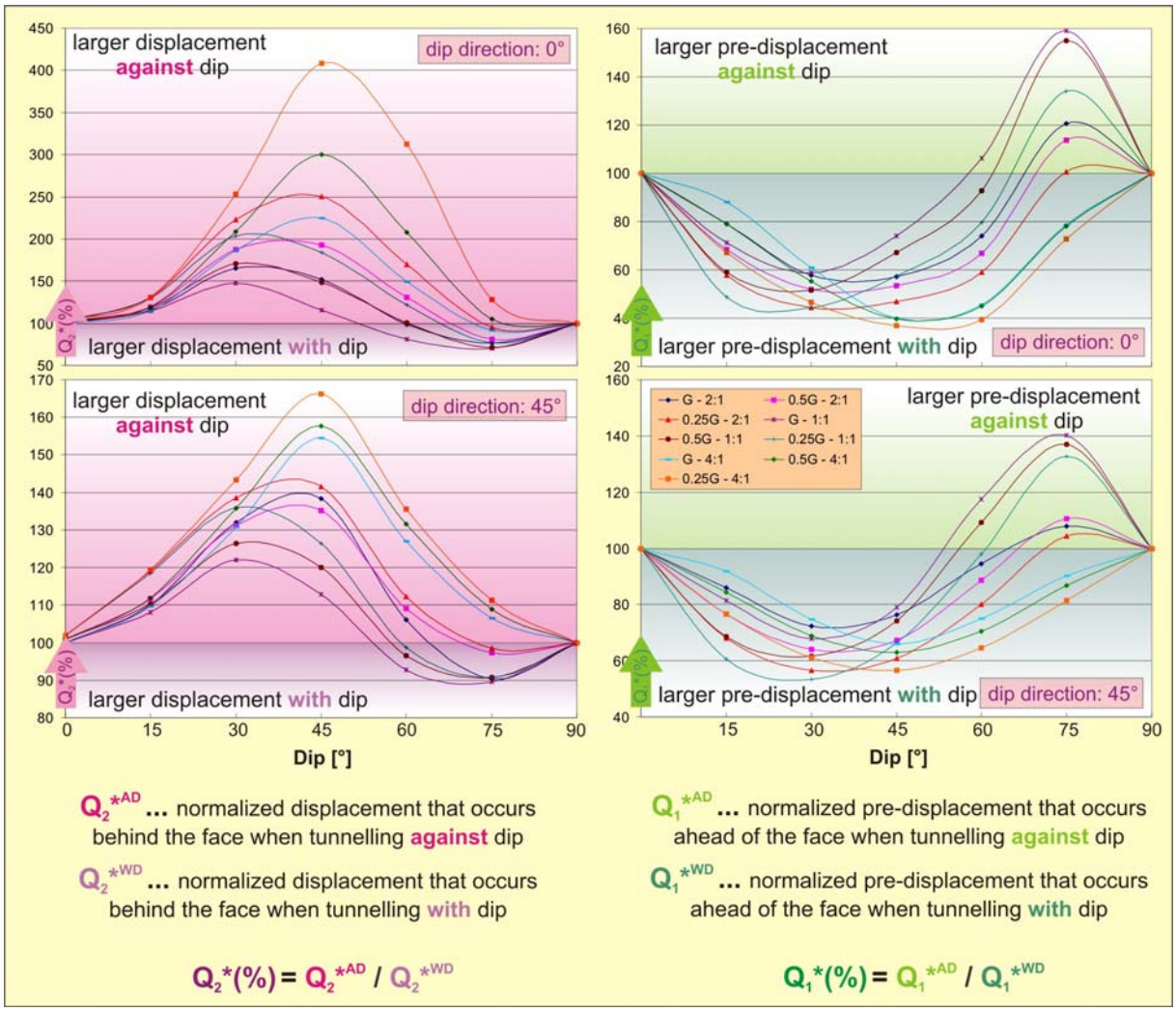

Figure 6-5. Proportion of the displacements when tunneling against/with dip occurring behind (Q_2*(%)) and ahead of the tunnel face (Q_1*(%)).

Slika 6-5. Delež pomikov pri izkopu predora proti/z vpadom plasti, ki se zgodi za čelom predora (Q_2*(%)) oz. pred čelom predora (Q_1*(%)).

For the dip direction 0° Q_2*(%) can reach more than 400% for the ratio of elastic moduli E_1:E_2 = *4:1*, shear modulus of 25% of the isotropic G_2 and dip angle of 45°, as seen in the upper plot at the left hand side of Fig. 6-5. In this case the measured displacement (i.e. the settlement that occurs behind the face) when tunnelling against dip would be more than 3 times larger than the settlement of the same point if the tunnel was excavated from the other direction. The lower bound is again a curve calculated with the ratio E_1:E_2 = *1:1* and isotropic shear modulus; the maximum amounts to 150% at the dip

angle of 30°. For better material parameters and steeper dip angles Q_2*(%) is slightly lower than 100%, which means that the settlement when tunnelling against dip would be somewhat smaller than when tunnelling with dip. The decreasing of the shear modulus causes proportional increase of Q_2*(%), while the decrease of the ratio E_1:E_2 results in the increase of Q_2*(%) and also in the shift of the curve maximum to the right, to steeper dip angles. The same observation stands also for the dip direction of 45°, only the magnitudes of Q_2*(%) are considerably smaller (upper bound of 165%, lower bound at 120% for gradual dip angles and 90% for steeper dip angles). The difference for G_2 = *5 MPa* is even more drastic and is not shown in Fig. 6-5.

Similarly to Q_2*(%) that was defined for post-face displacements, Q_1*(%) was further on defined for pre-displacements. Q_1*(%) presents the portion of the settlement of the future tunnel crown point when tunnelling against dip with regard to the settlement of the same point when tunnelling with dip in the same ground conditions.

The largest difference between pre-displacements when tunnelling against and with dip occurs at dip angle of 45° and 60°, where the Q_1*(%) amounts to as low as 35-40% for the dip direction of 0°, ratio of elastic moduli E_1:E_2 = *4:1* and shear modulus of 25% of the isotropic G_2. For the dip direction of 45° the minimum of Q_1*(%) = 55% is located at the dip angle of 30° for the ratio E_1:E_2 = *1:1* and shear modulus of 0.25G. Since Q_2 = 1 - Q_1, the highest values of Q_1*(%) coincide with the minimum of Q_2*(%). At the dip angle of 75° the maximum value of Q_1*(%)=160% is obtained for the dip direction of 0° and 140% for the dip direction of 45° when using the ratio E_1:E_2 = *1:1* and isotropic shear modulus.

6.3 Applications of calculated values Q_1 and x_f

On the basis of these numerical results it is now possible to explain some interesting displacement patterns from previously presented case histories (from Chapters 4 and 5).

6.3.1 Surface displacements above the Trojane tunnel

The comparison of surface settlements and settlements of the tunnel crown point in the Trojane tunnel was shown in Chapter 5.1. Although quite an effort was dedicated to reduce the large influence of the tunnelling process onto the surface (installing pipe roof umbrella and long rock bolts in the face; the distance between top heading and invert was kept at a minimum), the majority of the settlements occurred ahead of the face, as seen from Fig. 5-1. In some places only 1/3 of the surface displacements were monitored also in the tunnel, in general about 50-60% from chainage km 79+600 onwards. To chainage km 79+800 no general orientation of discontinuities could be observed; rock mass was

faulted and thus tectonically damaged to a high extent. Also the magnitudes of final tunnel displacements in this section are rather dispersed. From chainage km 79+800 to km 80+400 a general orientation of the discontinuities relative to the tunnel tube becomes more uniform. The tunnelling was performed with dip; strike was inclined about 45° to the tunnel tube, dip angles varied in the range from 15° to 45°. As seen from Fig. 5-1, the proportion between surface and tunnel crown settlements did not change significantly even in better ground conditions with GSI of up to 50.

If the ratio $E_1:E_2 = 2:1$ and isotropic value of shear modulus as back calculated in Chapter 4.1.2 is taken into account, the value of parameter Q_1 amounts to 0.42 for dip angle of 15° and 0.56 for dip angle of 45° (Table 6-1). The value obtained with isotropic Hardening soil model lies between these two values (0.48). In general the calculated values fit well the measured proportion. Nevertheless, it should be pointed out that some important aspects were not considered:

(1) the presented range of calculated pre-displacements does not comprise the displacement that occurs between the excavation of the round length and first measurement of the measuring section, which can not be reliably estimated (discussed in Chapter 5.5) and some more displacement is missed on the tunnel points; however, it could be monitored only above the tunnel;

(2) it is not likely that the whole deformation due to tunnelling is transferred to the surface as seen from the results of vertical extensometer in Fig. 5-3, and

(3) geology of the area can not be characterized as uniformly foliated rock mass. Therefore the calculated portions of pre-displacements can not be reliably proved, but can serve as possible explanation of the large influence of the tunnelling on the surface with only minor displacement measured inside the tunnel.

Preliminary analyses of the displacements of surface points in the performed numerical calculations revealed the same magnitude of surface settlement when tunnelling with and against dip with the same dip angle. The difference between the two cases was only in the “measured” portion of the tunnel displacement as displayed in Fig. 6-2.

6.3.2 Tunnel wall displacements at the breakthrough area of the Trojane tunnel northern tube

The obtained results were further on applied for the case history presented in Chapter 4.2.3 - area of breakthrough of the northern tube of the Trojane tunnel, where significantly different displacement

magnitudes were monitored when tunnelling with and against dip in rather uniformly foliated rock mass. In this area the prevailing dip direction was somewhere between 0° and 45° to the tunnel axis; dip angles were in the range from 30° to 60°. Normalized displacement (Q_2*) that occurs behind the tunnel face and Q_2*(%) curves for the mentioned discontinuity orientations are given in Fig. 6-6.

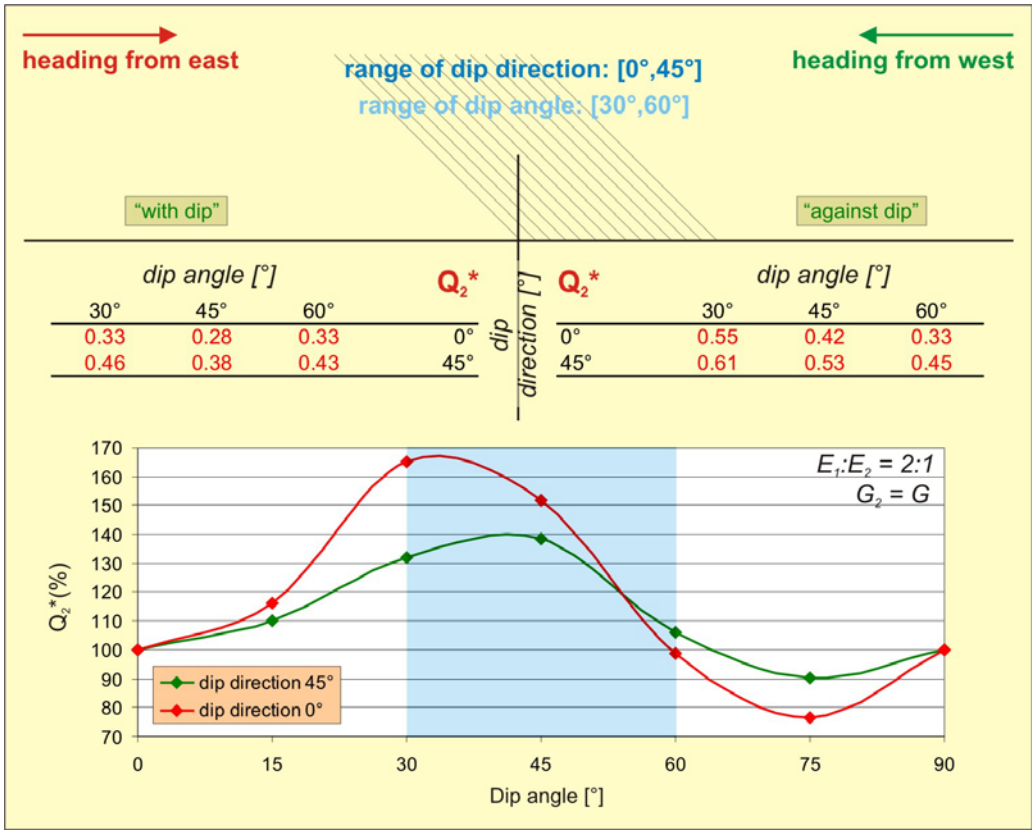

Figure 6-6. Normalized displacement (Q_2*(%)) that occurs behind the tunnel face in the breakthrough area of the Trojane tunnel northern tube.

Slika 6-6. Normalizirane vrednosti pomika (Q_2*(%)), ki se zgodi za čelom predora v območju preboja severne cevi predora Trojane.

If the dip angle of 45° is taken into account as an average dip, the displacement when tunnelling against dip is more than 150% (in case of dip direction of 0°) and almost 140% (for dip direction of 45°) of the displacement when tunnelling with dip for the ratio E_1:E_2 = *2:1* and isotropic value of shear modulus as back calculated in Chapter 4.1.2. For dip angle of 60° almost no difference can be noticed, while for dip angle of 30° and dip direction of 0° the calculated Q_2*(%) reaches 165%.

If the last 7 measuring cross sections (the closest measuring section to the breakthrough point in each of the lots is taken into account) the portion of average measured final displacement when tunnelling against dip compared to tunnelling with dip at the discussed section amounts to 197% for

the crown points and is thus slightly higher than calculated Q_2*(%). Nevertheless, the overburden above the western lot (tunnelling against dip) increases from around 70 m at the breakthrough area to more than 100 m at the end of the considered section. This fact also contributed to larger displacement magnitudes.

6.3.3 Displacement function when tunnelling with dip in the Trojane tunnel

The displacement function was fitted to the measured displacements in the breakthrough area attempting to verify the calculated Q_1 values. The output of the fitting procedure of one of the measuring sections when tunnelling with dip from eastern portal in the area close to breakthrough is shown in Fig. 6-7. The measured settlement of the crown point is plotted with blue crosses and the displacement function of the top heading with dashed line of black colour.

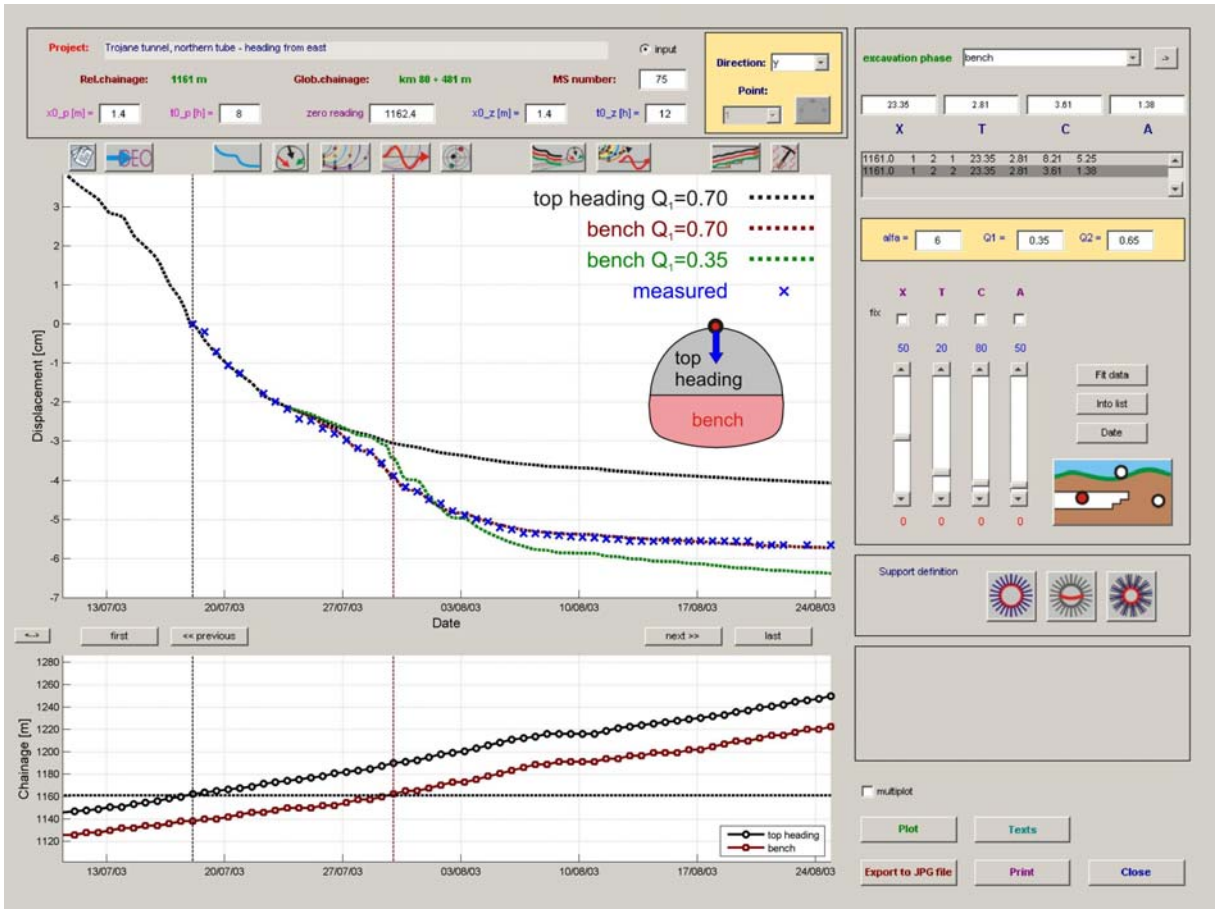

Figure 6-7. Fitted and monitored crown settlements of MS75 at chainage km 80+481 in the northern tube of the Trojane tunnel (heading from east).

Slika 6-7. Računsko prilagojeni in merjeni vertikalni pomiki stropne točke v merskem profilu MS75 na stacionaži km 80+481 v severni cevi predora Trojane (izkop iz vzhoda).

As the mapped relative dip direction in the vicinity of this measuring section is closer to 0° than 45° and the dip angle is around 45°, $Q_1 = 0.70$ (ratio of elastic moduli $E_1:E2 = 2:$1 and isotropic value of shear modulus) was adopted and applied for the displacement function of both excavation phases. The extent of pre-face domain ahead of the top heading face of 15 m was assessed on the basis of Table 6-1. The displacement function for bench using these two parameters (other parameters are displayed in Fig. 6-7) is plotted with dark red dashed line. If $Q_1 = 0.35$ (as generally used in the reviewed literature) is applied with the same parameters to the presented displacement curve for the bench excavation phase, the dashed line of green colour is obtained. It can not be satisfactorily fitted to the measured values with any combination of fitting parameters, especially without changing of the shape parameters X and T as suggested by Guenot et al (1985). With higher value of parameter Q_1 the values of fitting parameters X and T remain the same as obtained by fitting the function for top heading excavation only. The matching of calculated and measured values for bench and invert is then obtained only by adjusting parameters C and A. Values of fitting parameters for both excavation phases are listed in a list box in the upper right corner of Fig. 6-7 (the forth number in the row: 1 stands for the top heading and 2 for the bench excavation phase).

6.3.4 Displacement function when tunnelling against dip in the Trojane tunnel

Fitting procedure was performed also for a measuring section in the western lot of the breakthrough area as shown in Fig. 6-8 (tunnelling against dip). The discontinuity orientation is rather similar to the previously presented case (relative dip direction in the vicinity of this measuring section is closer to 0° than 45° and the dip angle is around 45°), so $Q_1 = 0.55$ (ratio of elastic moduli $E_1:E2 = 2:$1 and isotropic value of shear modulus) was selected and the pre-face domain extent was set at 20 m (see Table 6.1). Excellent match is obtained with same fitting parameters X and T as in previous case (tunnelling with dip) only by adjusting parameters C and A. For a comparison, displacement function of bench excavation phase is again plotted also for $Q_1 = 0.35$ with dashed green line.

Although both presented measuring sections were situated in similar ground conditions, the value of fitting parameter A needed to be altered to match the displacement function to the measured displacements, which does not comply completely with the suggestions by Guenot et al (1985) who claims (on the basis of observations from two tunnels) that function parameter A is like parameters X and T almost constant for the same tunnel. For the Trojane tunnel we can conclude that also parameter A needs to be adjusted to fit the displacement function satisfactorily to the measured displacements.

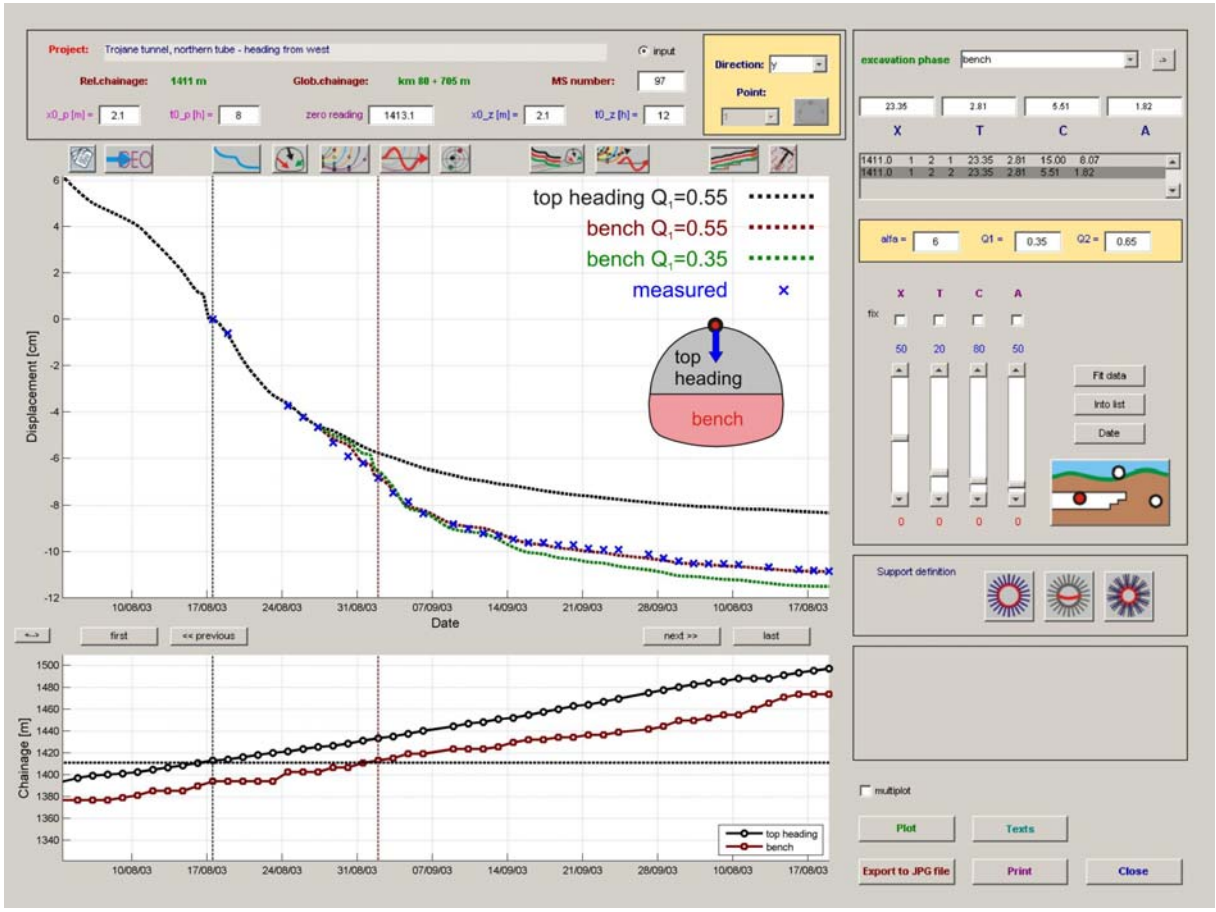

Figure 6-8. Fitted and monitored crown settlements of MS97 at chainage km 80+705 in the northern tube of the Trojane tunnel (heading from west).

Slika 6-8. Računsko prilagojeni in merjeni vertikalni pomiki stropne točke v merskem profilu MS97 na stacionaži km 80+705 v severni cevi predora Trojane (izkop iz zahoda).

7.0 Conclusion

The research work presented in the thesis consisted of several tasks:

- the development of Predor code that enables the collection, organization, graphical presentation and analysis of displacement monitoring data obtained from tunnelling projects,
- the collection of all displacement monitoring data from 13 tunnelling projects that were going on in Slovenia from 1998 onwards together with geological face logs,
- the execution of displacement measurements in the exploratory tunnel ahead of the main Šentvid motorway tunnel in the course of 7 months together with the analysis of results,
- the analysis of characteristic deformation patterns from extensive database related to: longitudinal displacements, portion of pre-displacements and geological structure (strike and dip of foliation with respect to direction of tunnel excavation).

The results of all these tasks brought us to some valuable conclusions.

7.1 Database

An extensive database with valuable monitoring data of the tunnels on Slovenian motorway network where 3D displacements of the primary lining were monitored was established in the framework of this thesis. For the time being it comprises displacement histories from 13 tunnel projects in different geological and geotechnical conditions. Displacements of the primary lining and surface displacements (where monitored) are included in the database. Additionally it comprises 3D displacement monitoring data ahead of the face of the Šentvid motorway tunnel and settlement disposition above the Trojane tunnel, measured with multi-point vertical extensometers. Such database can serve as an important source of documented experience that can be used in future projects, as long as the displacement histories are properly analyzed and interpreted. Comparison of the displacements in a wide range of geological and geotechnical conditions enabled identification of characteristic displacement patterns.

7.2 Predor code

In order to enable our own development and research in the field of analysis and interpretation of these monitoring data also with new graphical presentations, a task oriented computer code Predor was developed. Analyses of monitored displacements presented in this thesis were all performed and plotted with the Predor code. An automatic procedure was further on implemented for managing the monitoring data from construction sites and for the execution of comprehensive reports with graphical

presentation of the data in real time without intervention of an operator. To ensure full autonomy, the system needed to be accommodated to recognize the anomalies in the incoming data and to send a warning to data provider in case of gross errors or to recondition the displacement curves if the target position was mechanically shifted or the geodetic network in the tunnel was altered according to outer reference points. Automatic procedure was applied in three recent tunnel projects in Slovenia and can be evaluated as a reliable and autonomous system according to the number of recorded interventions of the operator and owing to no explicit complaints from clients regarding the overall performance.

7.3 Analysis of characteristic deformation patterns in foliated rock mass

Since the main subject of this thesis deals with tunnels in soft foliated rock mass of Permian and Carboniferous age, analyses were focused on the Trojane, Šentvid and Golovec tunnels. The encountered rock mass consists of foliated siltstone, claystone and sandstone. Rock mass is folded and intensely tectonically damaged; mapped fault zones are up to several meters thick and consist of low bearing and highly deformable gouge clay. Mechanical characteristics of the rock mass in case of the Trojane tunnel were worse compared to the Golovec and Šentvid tunnels. In the Trojane tunnel and especially in eastern part and close to the western portal the rock mass can be characterized as "BIMrock" (block-in-matrix rock). Better preserved geological structure was encountered only in the central part of the tunnel alignment under higher overburden. On the other hand, the geological structure in the Šentvid and Golovec tunnels was less tectonically damaged and thus the mapped foliation direction more uniform and well pronounced, which was reflected also on the monitored displacement patterns (different orientations of the displacement vector of a single target throughout the deformation process due to stress redistribution around an opening).

To identify appropriate material parameters in order to properly match calculated response and measured displacement pattern, 2D finite element numerical calculations with Plaxis software using anisotropic constitutive model (Jointed rock constitutive law) were performed. Sections of the Šentvid tunnel were selected, where strike of the foliation was parallel to the tunnel axis. Elastic modulus of the intact rock was obtained from presuremeter tests. Variation of strength parameters and elastic modulus normal to foliation down to the values that caused the instability of calculation could not reproduce the magnitude nor the shape of the measured displacement curves. Satisfactory match was obtained only when really low value of shear modulus along the foliation direction was applied. It should, however, be emphasized that no measurements of the shear modulus or strength parameters on the foliation planes were performed in the presented rock mass conditions, which is why one of the preferential tasks prior to any new projects in similar conditions would be to determine these

parameters. The same parameters were further on used also in the analysis of the Trojane tunnel displacements, but the best match of the measured and the calculated displacement pattern was obtained with isotropic value of the shear modulus, which again indicated less pronounced anisotropic behaviour of rock mass at the Trojane tunnel.

An interesting deviation from expected response was identified in the western part of the Trojane tunnel under the decreasing overburden towards the Učak valley. Measuring sections that were located under the increasing overburden displayed longitudinal displacements against the excavation direction (in the excavated area, which is according to reviewed literature "normal" behaviour), while the displacements of the measuring sections under decreasing overburden pointed in the excavation direction. The length of sections in both tubes amounted to about 320 m with a maximum longitudinal displacement in the excavation direction of 14.2 cm. Later on even more sections with longitudinal displacements in the excavation direction under decreasing overburden were recognized in the Trojane, Golovec, Jasovnik, Ločica and Podmilj tunnels (total length of these sections amounted to about 3.2 km; the longest unintermitting section of 500 m and maximum longitudinal displacement of 20.3 cm were recorded in the Jasovnik tunnel). Common to all these sections was dominating orientation of the discontinuities; foliation dip was oriented against the excavation direction into the excavated area (referred to as tunnelling against dip). Some authors reported longitudinal displacements in the excavation direction in soft ground due to sinking of the top heading section until the support ring was closed. If so, the longitudinal displacements of the crown points would be without exception larger than those of both sidewall points. No such pattern could be found in the entire 3.2 km of tunnels with recorded longitudinal displacements in the excavation direction. Due to the extreme lengths of these sections also the transitions from soft to stiff rock mass can be excluded as the general reason for such behaviour.

Deviations occuring repeatedly in similar conditions are no longer deviations but a phenomenon that needs to be thoroughly analysed. Therefore, 3D numerical calculations using Plaxis 3D Tunnel code were performed on a simplified model of a hill just before the Učak valley. Excellent match of calculated and measured response was obtained with isotropic Hardening soil model, except for the displacement magnitudes. Displacements would be more realistic if softening of the rock mass could be taken into account. Longitudinal displacements in the excavation direction in this case obviously occurred due to the morphology of the slope and belonging initial stress state. Initial assumption of deep sliding of potentially unstable slopes was not confirmed. The same model was further on used with anisotropic Jointed rock material parameters with low shear modulus to investigate the dependence of longitudinal displacements on anisotropy of the rock mass (synclinal geological

structure was modelled - tunnelling with dip under increasing overburden and against dip under decreasing overburden). As expected, the total displacements were rather similar on both sides of the "hill" and displacement vectors pointed in the same directions as monitored. Significant difference was, however, observed in the magnitude of the "measured" displacements, e.g. the displacements after the excavation of a section. These were significantly larger when tunnelling against dip and can be explained by more deformable rock mass in the direction normal to discontinuities. When approaching the observation point the deformation can hardly occur towards the rock mass ahead of the face and deformations start just after the section has been excavated.

The described deformation mechanism together with decreasing overburden obviously caused large longitudinal displacements in the excavation direction in the presented sections. The difference in magnitude of the measured displacements when tunnelling with and against dip was demonstrated on the case history from the breakthrough area of the northern tube of the Trojane tunnel, which was the only suitable section with regard to rather uniform orientation of the foliation found in the analyzed projects. There are some misleading factors, such as decreasing overburden towards east and some minor faults that were mapped in the area, but the monitored displacements were nevertheless significantly larger when tunnelling against dip in the western lot than when tunnelling with dip from eastern portal, despite higher GSI values at the western side of the breakthrough point. The monitored displacement vectors in longitudinal section pointed in the expected direction. The influence of the decreasing overburden and thus the stress state on the orientation of the displacement vectors was displayed in some measuring sections in the western lot.

7.4 Displacement measurements in the exploratory tunnel ahead of main motorway tunnel (Šentvid)

The exploratory tunnel that was constructed in the axis of the future Šentvid motorway tunnel has not only improved the knowledge on the geological structure of the Šentvid hill and thus allowed the determination of the micro location of the merging caverns, but also offered a unique opportunity to monitor 3D displacements ahead of the motorway tunnel excavation face and to observe the long-term impact of the surrounding rock mass on the primary lining.

Geodetic measurements were performed with the total station TCRP 1201R300 (Leica Geosystems Inc.) equipped with Automatic Target Recognition system that allowed to minimize the number of somewhat risky entries into the exploratory tunnel and still perform several, ideally 24 measurements per day. Despite extremely demanding working environment (dust, humidity) the system performed well during 7 months of operation and, in our opinion, presented an optimum choice for the task. The

accuracy of the determination of the control station position was about 1 mm, despite the fact that the total station had to be placed close to the monitored points, generally within the influence area of the tunnel excavation in order to get the highest number of executed measurements. The number of daily performed measurements ranged from 1 to 24, with the average value of 11.7, and it depended on dust, humidity, temperature, occasional accumulations of water on the floor of the gallery and on the distances from the total station to individual reflectors.

The weakest point of the system was in our case the Automatic Target Recognition system. It worked well if the reflectors were clean and dry and even if certain reflector (or a group of them) was not visible or removed. However, the system stopped and needed an operator intervention if the target was found but no accurate measurement could be obtained due to droplets of water, dust, and in some cases when the reflector was partially submerged.

This unique full scale experiment provided valuable data on rock mass behaviour ahead of the tunnel face in weak anisotropic rock mass conditions. A large amount of data was collected at about 250 m long section of the exploratory tunnel ahead of the face and in a cross-passage, perpendicular to the main tunnel axis (120 measuring cross sections, situated each 2 m along the tunnel axis in different geological and geotechnical conditions and ahead of the face of different sizes of the excavation cross sections).

The first documented observations of the sulphate attack to the shotcrete lining in Slovenia caused the modification of the support measures already at the present project (for the first time in Slovenian motorway tunnel the secondary lining was reinforced, bolts were grouted with sulphate resistant grout). For future projects in similar ground conditions (in rock mass that contains pyrite) proper support measures should be foreseen in the design stage to avoid the modification of the project during construction and consequently to avoid the increase of costs and time, needed for tunnel completion and especially to reduce operational costs and avoid needless closing of the tunnel during operation for the lining improvement.

Back analyses and interpretation of measured pre-face displacements allowed comprehensive interpretation of the rock mass – support response ahead of the face due to tunnel excavation, which is essential in case of tunnelling with shallow overburden under populated area. Since the performed measurements were of high precision, identification of some displacement patterns and other observations was possible, e.g.:

- the uplift of the points in stiff rock mass just after the transition from softer ground,

- distinctive bilinear deformation pattern was clearly observed in cross as well as longitudinal section, which enabled simple and reliable assessment of the turn point between the areas of large and small displacements,
- reliable determination of the beginning of the area of small displacements far ahead of the face, and
- observation of change in longitudinal displacement trend due to the installation of a large number of rock bolts ahead of the top heading face.

Extension of the area of small displacements or what is called pre-face domain and the magnitude of the displacements of the exploratory tunnel primary lining due to the main tunnel construction and its portion in all measured displacements are according to measurements strongly correlated to the stiffness of the rock mass. The comparison of the displacements ahead of the face with the those after the excavation of the main tunnel indicates that 15-45% of the measured displacements occur ahead of the face (less deformation in stiff and more in softer rock mass). Nevertheless, these observations could not be confirmed with numerical calculations. Normalized displacement curves calculated with higher and lower elastic parameters (the ratio $E_1:E_2$ was kept at *2:1* and the shear modulus at same ratio to E_1) compared to the back calculated values of the Šentvid tunnel were almost identical with the pre-face portion of total displacements of 45%. It was shown later on (when the numerical analyses of the influence of the anisotropy orientation on the portion of pre-displacements were performed) that the ratio $E_1:E_2$, and the magnitude of the shear modulus with regard to elastic modulus E_1 are the major influencing factors.

If the displacement curve of the unsupported region is anticipated on the basis of the displacement's tangent slope close to the excavation face and the time delay between the excavation and the first measurement of a certain cross section in range from 10- 25% of total displacements, the sum of these percentages gives the total percentage of the 'lost' displacements in range from 25-70%. The latter percentage stands for soft ground and is in fair agreement with pre-face portion of displacements measured with horizontal inclinometer and vertical extensometer at the Trojane tunnel. As observed, the extension of the pre-face domain depends mainly on alterations in stiffness of the rock mass and further more on extension of the poor ground ahead of the face. In general it reached 10-20 m ahead of the face for lining points and 20-25 m for bottom points with maximum of 42 m. Enlargement of the pre-face domain due to larger cross section could not be identified. We believe that the size of the excavation cross section, i.e. an equivalent tunnel diameter, certainly affects the extent of pre-face domain, but in the presented case the geological conditions had more significant influence

than the enlargement of the excavation cross section from 56 m^2 of the top heading face of the two-lane tunnel to 93 m^2 of the top heading face of cavern A.

During initial analysis the significant difference in the magnitudes of displacements of the point in the lining of the exploratory tunnel, measured during its construction and ahead of the main tunnel face, was ascribed partly to the distinction of the cross section area and partly to lost displacements during the construction of the exploratory tunnel. When the effect of the tunneling with and against dip on the displacement disposition ahead of and behind excavation face was identified, it was assumed that the majority of much larger displacements ahead of the face can be ascribed to this phenomenon.

In general no major influence of the number and length of face rock bolts on the longitudinal displacement trend line ahead of the face was observed. As partly confirmed by numerical studies, the exploratory tunnel acted like a reinforcement in longitudinal direction and like a stress absorber by allowing radial deformation of the rock mass ahead of the face due to stress redistribution. Therefore, only limited longitudinal displacements occurred just ahead of the top heading face where the lining was already cracked to a high extent and lost its bearing capacity. Numerical analysis displayed no difference in calculated displacement curves with or without rock bolts. This fact can be ascribed to the absence of plastic deformations in the model due to rather high strength parameters of the rock mass and extremely low value of shear modulus along the discontinuities.

Like in the excavated area, the displacement vector orientation L/S ahead of the face is also governed by the stiffness of the rock mass. The alterations of the displacement vector orientation trend line coincided with the transitions in the rock mass stiffness and not several meters before the transition as viewed in the literature. This phenomenon was also partly confirmed with numerical studies, which suggested the "normal" angle of around 60° in weaker material and around 30° in stiffer ground. Some alterations in the trend line of the measured displacement vector orientation really occurred at these values. Nevertheless, the "normal" angles could not be identified due to short sections of "homogeneous" rock mass.

7.5 The influence of discontinuity orientation on displacements during tunnelling

Since the dependence of the range of pre-displacements on the relative discontinuity orientation to the tunnel axis was observed: (1) in the breakthrough area of the northern tube of the Trojane tunnel when the excavation was performed with and against dip and (2) indirectly through the significant difference between measured displacements during the construction of the exploratory tunnel and

ahead of the face of the Šentvid motorway tunnel, a large number of 3D numerical analyses was performed to explore this dependence. Variations of dip direction, dip angle, shear modulus and elastic moduli ratio E_1:E_2 affect the portion of pre-displacements, the extent of the pre-face domain and also the final magnitudes of total displacements.

When tunnelling against dip, i.e. for dip direction 0° (strike perpendicular to the tunnel axis), the portion of pre-displacements mostly depends on the dip angle and only slightly on material properties. On the other hand, when tunnelling with dip the portion of pre-displacements depends on the dip angle as well as on the ground properties (the better the material properties, the lower the portion of pre-displacements and vice versa). The range of pre-displacement portion amounts from around 30% of total displacement of the observed point at dip angle of 15° (tunnelling against dip) to up to 90% for dip angle of 45° when tunnelling with dip. Rotation of dip direction from parallel to normal to the tunnel axis results in the decrease of the pre-face portion of displacements and also lower dependence on the material parameters. The decrease of the shear modulus and elastic moduli ratio causes the increase of the portion of pre-displacements. For the discontinuity strike parallel to the tunnel axis (dip direction 90°), the portion of pre-displacements varies in the range from 30-50% of total displacement, which is in the range of calculated values with the use of elastic parameters and the Hardening soil constitutive model.

The extent of pre-face domain reaches from 12 to 47 m for dip direction 0° (diameter of tunnel was 10 m) and depends on the dip angle and rock mass properties. The maxima of the pre-face domain extent coincide with the minima of the portion of pre-displacement. This means that where the large portion of total displacements occurs ahead of the face, it occurs in comparably shorter section ahead of the face. As opposed to that, at the dip angles where the portion of pre-displacements in total displacements is lower they start to develop at a larger distance ahead of the face. Rotation of dip direction from parallel to normal to the tunnel axis results in lower dependence of the pre-face domain extent on the dip angle and also limits the influence of the rock mass properties. For dip direction 90° the extent of the pre-face domain amounts to 22–42 m and is nearly independent of the dip angle. Magnitudes of the pre-face domain written above are somewhat larger than observed in the Trojane and Šentvid tunnels. We believe that the main reason is the small strain stiffness phenomenon which is not implemented in the Jointed rock constitutive model.

Further on it was noticed that the total displacement varies for different dip angles and directions, calculated with the same ground properties. The displacement curves were normalized to the curve at 0°/0° to compare all total displacements regardless their values and were calculated for different dip

directions, dip angles and $E_1:E_2$ ratios. The results were in the range from 50% to 120% of the total displacement at the discontinuity orientation 0°/0°. The displacement magnitudes for the same dip angle when tunnelling with and against dip are rather similar, except for dip direction 0° and dip angles from 15° to 65°.

To be able to more directly compare the effect of tunnelling with or against dip on the portion of post-face displacements, a parameter Q_2*(%) that presents the magnitude of the tunnel crown point settlement when tunnelling against dip with regard to the settlement of the same point when tunnelling with dip was calculated for dip directions 0° and 45°. It turned out that for dip direction 0° parameter Q_2*(%) is in the range from 70% at steeper dip angles to more than 400% at the dip angle of 45° and the poorest applied stiffness properties in the direction of discontinuities. For dip direction 45° Q_2*(%) is in the range from 90% to 165%. The maximum and minimum values of Q_2*(%) strongly depend on the rock mass properties. The decrease of shear modulus and elastic moduli ratio results in drastic increase of Q_2*(%). In the same way also parameter Q_1*(%) for the displacement was defined, occurring ahead of the face. The range of Q_1*(%) is from around 40 % to 160%, depending on the dip direction, dip angle and rock mass parameters.

The obtained results were then applied to previously mentioned breakthrough area of the northern tube of the Trojane tunnel. The calculated Q_2*(%) for the given discontinuity orientation and back calculated ground properties amount to 165%, while the portion of average measured final displacement when tunnelling against dip compared to tunnelling with dip was 197% for the crown points of the last 7 measuring cross sections on both sides of the breakthrough point. The difference between both values can be explained by higher overburden above the western lot and by inevitable differences in rock mass conditions.

The findings of the last chapter can be summarized with the following suggestion:

If the tunnel is to be excavated with shallow overburden under populated area in soft foliated rock mass with the discontinuity orientation that strikes perpendicular to the tunnel axis and for example with the dip angle of up to 45°, it would be more favourable to excavate it against dip, since the majority of the displacements would occur behind the face. These displacements could be partly controlled by stiff primary lining. In the opposite case the majority of the displacements would occur ahead of the face, where they can not be easily controlled and would unavoidably affect the infrastructure above.

If the tunnel is to be excavated in ground conditions as presented in previous passage under high overburden and/or no infrastructure located above, it would be more favourable to excavate the tunnel

with dip as the majority of the displacements would occur ahead of the face. The necessary amount of overexcavation would thus be considerably smaller as well as the loads transferred to the lining, which would result in more economic tunnelling.

8.0 Instructions for further work

A large database of monitoring data from Slovenian motorway tunnels in different geological conditions comprises at the time being more than 1800 tunnel measuring sections and only a small part of these sections was analyzed in the framework of this thesis. Thus, a major work will further on be to analyze the rest of the monitoring sections and compare the measured displacements to the geological model to identify more characteristic deformation patterns. The analytical displacement function will be fitted to measured displacements for all comprised tunnel projects to build a complete database of the function's parameters in very wide range of geological conditions. This database will serve for setting up an expert system which will enable reliable prediction of the magnitude of final displacements in advance for future tunnel constructions in similar ground conditions.

At the moment the presentation of the monitoring data is available to the clients only through delivered reports. Further development will allow the access to the database using the latest internet technologies according to the user proxy. Local installation of the Predor code at the client's computer to present monitoring data in the desired way will no longer be needed. A server system implemented in the code will provide the desired plot in real time. An automatic procedure will also be developed for fitting of the displacement function to the measured displacements for tunnels under construction, which will allow not only representation of the monitoring data but also automatic interpretation and analysis on the basis of extrapolation prediction method.

The analyses that were performed with the Jointed rock constitutive model and low value of shear modulus along the discontinuities for the phenomena observed ahead of the face in the Šentvid tunnel matched well some deformation patterns, while some could not be reproduced in details. Further analysis will hopefully provide more physically plausible material parameters of the soft foliated rock mass that will better fit the majority of the observed deformation patterns. It was also shown that the small strain stiffness problem affected the extent of the pre-face domain and that the differentiation of the stiffness moduli for loading and unloading conditions in the Jointed rock constitutive model could improve the calculated response. These two features should be implemented in the Jointed rock model for more realistic description of the soft foliated rock mass response. Alternatively, a new anisotropic material model should be developed for soft foliated rock masses.

We have shown that monitored behaviour in certain measuring sections can be reproduced by isotropic material models or with anisotropic model with isotropic G_2 value. Especially for measuring sections from the Šentvid tunnel the only way to reproduce numerically the observed behaviour was to use a very low shear modulus. The methodology is needed to predict the type of behaviour in advance.

The influence of the relative discontinuity orientation will be further investigated also for longitudinal displacements. One of important tasks will be to define the “normal” orientation of the displacement vector L/S for different dip directions and angles. Detailed analysis of the effect of discontinuity orientation on the displacements of surface points will also be performed.

9.0 Razširjen povzetek

9.1 Uvod

Zaradi dnevnih migracij in hitrega razvoja turizma postajajo prometnice v sodobnem svetu vse bolj obremenjene, gradnja novih ali razširitev obstoječih pa zahteva veliko razpoložljivega prostora. Tega primanjkuje predvsem v močno naseljenih urbanih središčih, na drugi strani pa je potrebno pri gradnji v občutljivih ekosistemih zadostiti vedno strožjim ekološkim kriterijem. Ena od možnih rešitev je kakovostna izraba podzemnega prostora. Nova znanja in tehnologije omogočajo varno in cenovno učinkovito izgradnjo predorov na prometnicah ter podzemnih objektov za potrebe elektrarn, skladišč za radioaktivne odpadke, parkirnih hiš, tovarn, ipd. Gradnja podzemnih objektov zato vedno pogosteje sega tudi v geološko-geotehnično zahtevna območja, v močno deformabilne in slabo nosilne hribine. Gradnja je v takšnih pogojih običajno povezana s precejšnjimi tveganji. Opazovalna metoda (Rabcewicz, 1965; Peck, 1969) se je izkazala kot najprimernejša za obvladovanje tveganj pri gradnji predorov in drugih podzemnih objektov s klasično metodo (metoda z brizganim betonom ali s pri nas bolj uveljavljenim imenom NATM). Analiza in ustrezna interpretacija izmerjenih in opaženih podatkov omogoča oceno ustreznosti vhodnih projektnih parametrov ter optimizacijo podporja in delovnih procesov glede na izmerjeni in pričakovani odziv podzemnega objekta (Schubert s sodelavci, 2003). V splošnem opazovalna metoda pri gradnji podzemnega objekta sestoji iz geotehničnega in geološkega opazovanja. Geološko opazovanje v slovenskih predorih temelji na izdelavi skic odkopnih čel in njihovo implementacijo v geološki model z interpolacijo in ekstrapolacijo opaženih struktur.

Geotehnično opazovanje se nadalje deli na geodetske in geotehnične meritve. Geotehnične metode običajno merijo vpliv gradnje predora zunaj vidnega polja (pomiki hribinske mase, sile v sidrih, napetosti v oblogi, ipd. (Kavvadas, 2003)), medtem ko geodetske metode služijo za določitev pomikov predorske obloge in ugrezkov površine v absolutnih koordinatah. Kljub hitremu razvoju terestričnih laserskih skenerjev, ki omogočajo določitev položaja ogromne množice točk, se predvsem zaradi premajhne natančnosti te metode za določanje prostorskih pomikov obloge v predorih še vedno uporabljajo izključno elektronski tahimetri. Z njimi se z nekaj milimetrsko natančnostjo določi prostorske položaje merskih prizem v primarni oblogi. Zaradi dobro raziskanega odnosa med pomiki in napredki izkopnega čela (Guenot et al, 1985) se pri interpretaciji meritev običajno uporabljajo radialni pomiki (vertikalna in horizontalna komponenta vektorja pomikov). S pomočjo analitičnih funkcij (Guenot et al, 1985; Barlow, 1986; modifikacija Sellner (2000)) lahko te pomike primerno modeliramo in z uporabo posebnih programov (Sellner, 2000) celo predvidimo končno velikost pomika in obliko krivulje za še ne izkopane prereze. Uporaba vzdolžnih pomikov je bila v geotehnični

praksi dolgo časa spregledana in šele s spoznanji Schuberta in sodelavcev so vzdolžni pomiki začeli pridobivati pravo veljavo, kajti prav ti omogočajo prepoznavanje sprememb v togosti hribinske mase precej pred čelom predora (Schubert s sodelavci, 2002; Schubert s sodelavci, 2005).

Intenzivna izraba podzemnega prostora se je po končani izgradnji železnic v začetku prejšnjega stoletja v našem prostoru začela pred približno dvemi desetletji. Večino gradenj predstavljajo predori na avtocestnem omrežju, poleg tega je bilo zgrajenih le še nekaj vodnih rovov in en železniški predor. V fazi načrtovanja je trajno podzemno skladišče radioaktivnih odpadkov, podzemno skladišče utekočinjenega plina in vrsta predorov na železnicah.

Sistematično merjenje 3D pomikov predorske obloge se je v Sloveniji pričelo s projektom predora Golovec leta 1997. V okviru naloge je bila izdelana obsežna baza 3D meritev pomikov primarne obloge iz predorov, kjer so se te meritve izvajale kontinuirano in sistematično. Za obdelavo in vstavljanje podatkov v bazo ter grafični prikaz in analizo je bil izdelan programski paket Predor, ki je bil nadalje nadgrajen z avtomatskim sistemom za obdelavo podatkov in pripravo grafičnih poročil. Avtomatski sistem je bil uspešno uporabljen na treh nedavno zgrajenih predorih (Barnica, Tabor, Leščevje). S pomočjo programskega paketa Predor smo sistematično primerjali izmerjeni odziv predorske obloge z geološko zgradbo prostora, da bi ugotovili morebitne karakteristične deformacijske vzorce pomikov v prečnem in vzdolžnem prerezu ter na površini. S povratnimi numeričnimi analizami smo poskušali določiti najbolj primerne materialne parametre za opis obnašanja mehke, skrilave hribinske mase.

Posebnost predora Šentvid je podzemno vozlišče avtocestnega predora in priključnega rova s Celovške ceste. Za določitev z vidika geoloških danosti najbolj primernega položaja priključnih kavern je bil izveden raziskovalni rov, ki je med gradnjo avtocestnega predora omogočil izvedbo 3D meritev pomikov ostenja raziskovalnega rova pred čelom glavnega predora. Po dostopnih podatkih je bil takšen eksperiment izveden prvič. Podan je celovit opis tega edinstvenega eksperimenta, rezultati so grafično prikazani in detajlno opisani ter na koncu nadgrajeni z numeričnimi analizami opaženih deformacijskih vzorcev.

Med analizo pomikov v vzdolžnem prerezu smo opazili vpliv orientacije diskontinuitet na velikost merjenih pomikov v izkopanem območju predora. Da bi ta fenomen bolje pojasnili in pokazali odvisnost deleža merjenih pomikov v celotnih pomikih glede na orientacijo diskontinuitet in različne materialne parametre, smo izvedli veliko število numeričnih analiz. Prikazani so rezultati in njihova uporaba s pomočjo prilagajanja analitične pomikovne funkcije merjenim pomikom v skrilavi, anizotropni hribinski masi.

9.2 Predori na slovenskem avtocestnem omrežju

S sprejetjem Nacionalnega programa izgradnje avtocest leta 1994 se je pričela intenzivna gradnja avtocestne infrastrukture, na kateri je bil zaradi razgibanega reliefa zgrajenih 15 dvo- ali tripasovnih predorov s skupno dolžino preko 30 km. V gradnji so še štirje predori s skupno dolžino 3,1 km, ki bodo predani prometu predvidoma v letu 2009 ali 2010. Od predora Golovec dalje se v vseh slovenskih predorih med gradnjo izvajajo meritve prostorskih pomikov predorske obloge. Podatki iz teh predorov so bili v okviru te disertacije zbrani v obsežno bazo, ki omogoča analize opaženega odziva in kot taka predstavlja na enem mestu zbrane dragocene izkušnje iz gradnje predorov v najrazličnejših geoloških pogojih. Baza trenutno obsega 13 projektov. Nekateri predori (Barnica in Tabor na hitri cesti Razdrto – meja Italija, Leščevje na AC A2 Ljubljana – Novo mesto pri Trebnjem, Dekani na AC A1 Ljubljana – Koper pri Kopru, Ljubno na AC A2 predor Karavanke – Ljubljana, Vodole na AC A1 Ljubljana – Šentilj pri Mariboru in Cenkova na AC A5 Maribor – Pince) so bili grajeni v relativno dobrih geoloških pogojih, kjer so bile izmerjene le manjše konvergence primarne obloge. Ker se ti predori ne nahajajo v skrilavih hribinah, analiza pomikov za te predore ni vključena v nalogo.

Podrobnejša analiza merjenih pomikov je bila izvedena za dvopasovne predore Trojane, Jasovnik, Ločica in Podmilj na avtocestnem odseku A1 Ljubljana – Šentilj preko Trojan, tripasovni predor Golovec na vzhodni ljubljanski obvoznici ter predorski sistem Šentvid, ki predstavlja navezavo AC A2 predor Karavanke – Ljubljana na ljubljansko obvoznico. Glede na makrotektonsko razdelitev Slovenije pripada območje teh šestih predorov Notranjim Dinaridom in Južnim Alpam (Placer, 1999a), iz strukturnega vidika pa Savskim gubam (Placer, 1999b). Starejša permo-karbonska osnova se običajno nahaja v antiklinalah, mlajše terciarne plasti pa v sinklinalah. Med njima se nahajajo kamnine različnih starosti, prevladujejo pa triasni skladi. Te mezozojske hribine so bile v geološki zgodovini narinjene na starejšo permokarbonsko osnovo. V kasnejših fazah so se zgodili tektonski premiki v smereh V-Z in SZ-JV (Dinarska smeri) (Premru, 1974).

Predor Trojane je s skoraj tremi kilometri dolžine najdaljši dvocevni predor na slovenskem avtocestnem omrežju. Trasa poteka pod zelo razgibanim terenom z nadkritjem od 2 do 140 m. Gradnja je potekala iz štirih napadnih mest hkrati med leti 2000 in 2004. Predor poteka pretežno v skladih mehkega skrilavega glinovca in meljevca, mestoma tudi peščenjaka. Hribina je tektonsko zelo poškodovana, pogosto se javljajo vertikalne do subvertikalne prelomne cone, večinoma zapolnjene s tektonsko glino. Pobočja nad predorom so potencialno plazovita in izkop predora je povzročil nekatera plazenja. Tekom gradnje se je sistematično beležilo geološki trdnostni indeks (GSI) hribinske mase (povprečna vrednost 20 do 25 (Štimulak s sodelavci, 2004)). Najbolj zahteven del projekta je bil izkop

z nizkim nadkritjem 10 – 25 m pod naseljem Trojane, kjer sta bili predorski cevi tudi razmaknjeni na 75 m medosne razdalje. Gradnja predora, predvsem južne predorske cevi, je povzročila velik vplive na površino in poškodovala bližnje zgradbe (Logar s sodelavci, 2004; Likar s sodelavci, 2004a). Izkop je bil začasno ustavljen, izvedene so bile dodatne preiskave. V izogib podobnim problemom pri nadaljnji gradnji pod naseljem Trojane je bil vzpostavljen kompleksen sistem opazovanja odziva hribinske mase (Likar s sodelavci, 2004b) (merjenje prostorskih pomikov površine v prečnih prerezih in vzdolž predorske osi, geodetsko opazovanje posedkov objektov v vplivnem območju predora, vertikalni in horizontalni ekstenzometri, inklinometri za merjenje horizontalnih premikov tal, horizontalni inklinometer za oceno vpliva gradnje pred čelo predora (Volkmann s sodelavci, 2005)). V predoru je bilo opazovanih skupno 389 merskih prerezov s petimi točkami.

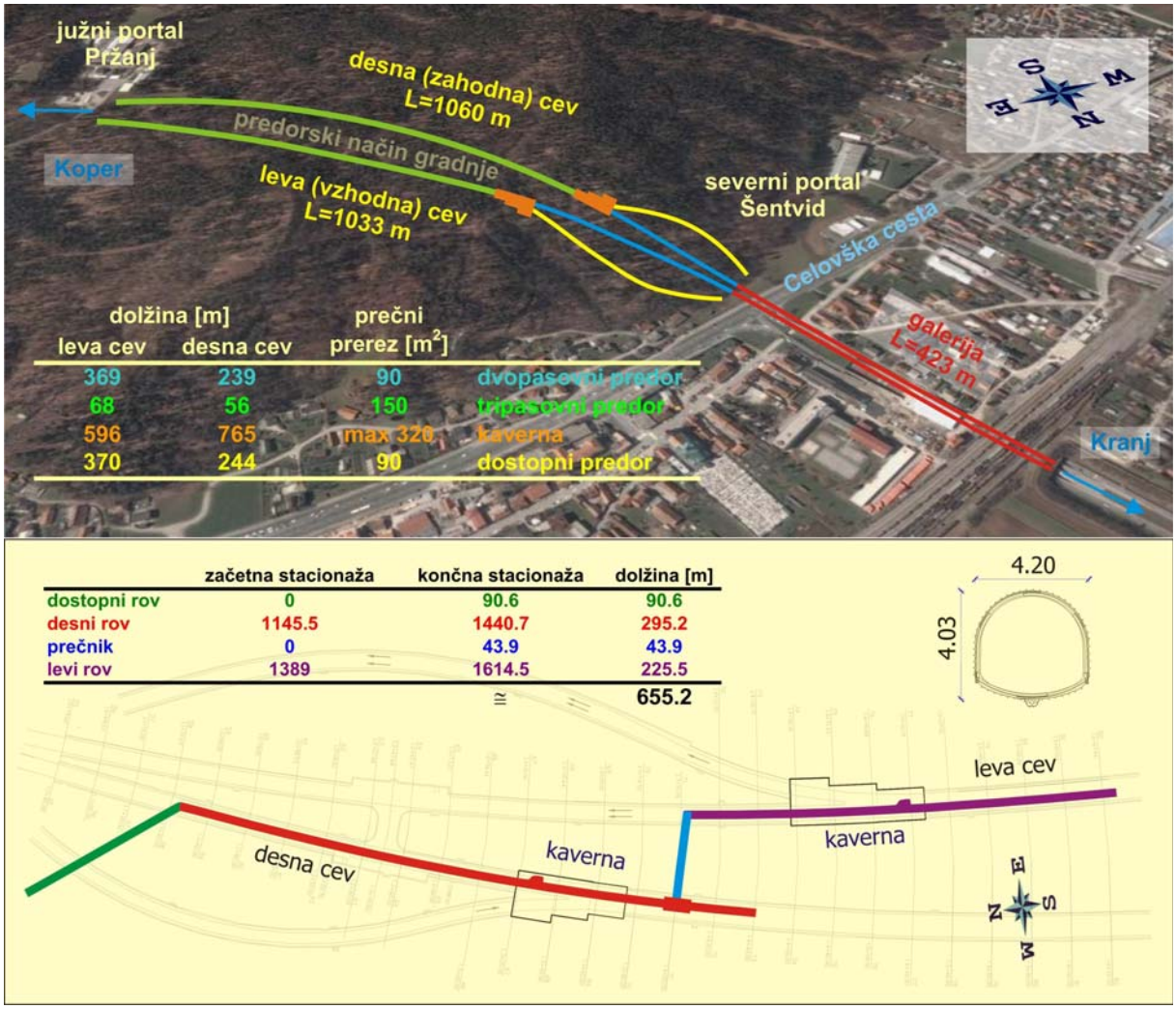

Slika 9-1. Izvedena situacija predora Šentvid (zgoraj), potek raziskovalnega rova in njegov prečni prerez (spodaj).

Predor Šentvid je generalno sestavljen iz dveh delov. Severni del predstavlja galerija dolžine 423 m in južni del dve predorski cevi dolžine približno 1050 m – slika 9-1. Prvotni načrti so predvidevali gradnjo dvopasovnega predora pod Šentviškim hribom in polovični priključek Celovške ceste na avtocesto preko obstoječe galerije. Zaradi močno povečanega prometa so bile opravljene številne študije izvedbe polnega priključka (Pulko, 2004) in glede na ekonomske dejavnike, prometno varnost in vidike gradnje je bila kot najugodnejša izbrana varianta z izvedbo podzemnih priključnih kavern (navezava Celovške ceste na avtocestni predor preko dostopnih predorov, dvopasovni predor od severnega portala do kavern, naprej proti južnemu portalu pa tripasovni predor). Izgradnja podzemnih prostorov izkopnega profila več kot 300 m^2 bi na podlagi tedanjega geološkega modela predstavljala preveliko finančno in tudi časovno tveganje, zato je skupina strokovnjakov priporočila predhodno gradnjo raziskovalnega rova (Žigon s sodelavci, 2004). Trasa predora namreč poteka v močno tektonsko poškodovanih skrilavih peščenjakih, meljevcih in skrilavcih permo-karbonske starosti ter tektonsko glino v več metrov debelih tektonskih conah. Gradnja raziskovalnega rova se je pričela v maju leta 2004 z 90 m dostopnim rovom do osi desne predorske cevi in nadaljnjim izkopom vzdolž te osi proti južnemu portalu. Ustrezni pogoji za gradnjo desne kaverne so bili najdeni 239 m od severnega portala. Raziskovalni rov je preko prečnika prešel v bodočo levo cev in se nadaljeval v dolžini približno 225 m. Na podlagi merjenih pomikov ter pridobljenih podatkov o zgradbi in tektonski poškodovanosti hribinske mase je bila kot najustreznejša za levo kaverno izbrana lokacija 369 m od severnega portala. Izvedena dolžina raziskovalnega rova je znašala 655 m (prečni prerez rova je znašal 13 m^2 (slika 9-1), zaradi pospešitve gradnje je bil večinoma grajen le z mikroarmiranim brizganim betonom in jeklenimi loki (Žigon s sodelavci, 2004).

Pomembnejši podatki za predore Golovec, Jasovnik, Ločica in Podmilj so podani v preglednici 9-1.

Preglednica 9-1. Osnovni podatki o predorih Golovec, Jasovnik, Ločica in Podmilj.

predor	opis	dolžina [m]	nadkritje [m]	hribina + geološka starost	število mer. profilov
Golovec	3 pasovi 2 cevi	578 + 545	do 80	permo-karbonski skrilavi peščenjaki in meljevci, močno tektonizirano, tektonska glina v prelomnih conah	97
Jasovnik	2 pasova 2 cevi	1612 + 1633	do 250	zgornjetriasne masivne karbonatne kamnine (1000 m), srednje triasni skrilavi (psevdoziljski) meljevci in glinovci, mestoma prehod v tuf (600 m)	65
Ločica	2 pasova 2 cevi	797 + 756	do 105	zgornjetriasni skrilavi meljevci v vmesnimi polami glinovca, lapornatega apnenca in peščenjaka	48
Podmilj	2 pasova 2 cevi	500 + 552	do 160	srednje triasni masivni dolomit (250 m), nato po stiku spodnjetriasnih skitskih plasti in grödenskih klastitov - hribina močno pregnetena	48

9.3 Programski paket Predor

Razvoj tehnologije za zajem in obdelavo podatkov omogoča, da pridobimo bolj podrobno informacijo o obnašanju predora med gradnjo s tem, da se razdalja med merskimi profili zmanjšuje, število točk v njih pa narašča. Z namenom čim bolj skrajšati čas gradnje se običajno izkopna dela izvaja iz obeh portalov hkrati, pri daljših predorih pa se celo uvedejo dodatna napadna mesta (Henke s sodelavci, 2004). V slabših pogojih se meritve obloge lahko izvajajo tudi večkrat dnevno. Tako se pridobi ogromna količina podatkov, ki jo je treba čim hitreje obdelati ter omogočiti analizo in interpretacijo izmerjenih pomikov. Na tržišču je za ta namen dostopnih nekaj komercialnih programskih paketov (*GeoFit*; *Tunnel:monitor*; Schmuck, 2009). Da bi si omogočili raziskovalno delo na področju interpretacije meritev pomikov iz predorov tudi z možnostmi novih grafičnih predstavitev rezultatov in razvojem dodatnih orodij, smo razvili interaktiven, uporabniku prijazen programski paket Predor. Omogoča obdelavo in grafično predstavitev merskih podatkov iz predora in površine nad predorom ter podatkov o napredkih gradnje. V okviru te naloge je bil program Predor zaradi prihranka časa pri obdelavi podatkov v realnem času med gradnjo predora nadgrajen z avtomatskim sistemom za pregledovanje in obdelavo podatkov iz predorov v gradnji ter njihovim shranjevanjem v bazo brez intervencije upravljalca sistema. Možna je tudi avtomatična izdelava strukturiranih grafičnih in tekstovnih poročil o obnašanju predora in napredkih gradnje za različne naročnike (nadzor, projektant, izvajalec).

Pred pričetkom avtomatskega spremljanja gradnje je za posamezno delovišče potrebno podati geometrijske podatke o osi predora, nadkritju in merskih prerezih ter mejne vrednosti pomikov za posamezno hribinsko kategorijo in njih razpored vzdolž osi. Nadalje je potrebno izdelati seznam pošiljateljev vhodnih podatkov ter prejemnikov poročil in opozoril v primeru grobih napak v vhodnih datotekah. Vhodni podatki sestojijo iz tekstovnih datotek z geodetskimi meritvami in napredki gradnje ter grafičnih datotek z geološkimi skicami izkopnih čel, ki jih izvajalci geološkega opazovanja oz. geodetskih meritev pošljejo z elektronsko pošto ali odložijo na dogovorjen FTP strežnik (slika 9-2). Ko jih avtomatski sistem zazna, najprej pregleda tekstovne datoteke glede grobih pogreškov. Če dobljeni podatki odstopajo od predhodno določenih mejnih vrednosti, sistem pošlje obvestilo o tem izvajalcem meritev, v nasprotnem primeru se podatki preračunajo v lokalni koordinatni sistem in zapišejo v bazo.

Veliko pozornosti je bilo med razvojem sistema posvečeno prepoznavanju odstopanj (napak) predvsem pri geodetskih meritvah. Na podlagi pridobljenih izkušenj z urejanjem podatkov iz že zgrajenih predorov so bili identificirani trije primeri odstopanj (prikaz na sliki 3-2): (1) odstopanje

zgolj ene meritve zaradi slabe natančnosti določitve položaja točke ali neustreznih pogojev merjenja, (2) odstopanje dela krivulje časovnega poteka pomikov zaradi mehansko poškodovane tarče in (3) odstopanje dela krivulje časovnega poteka pomikov zaradi spremenjenega položaja referenčnih merskih točk glede na zunanje točke kot posledica dolgotrajnih deformacij predorske obloge. Izdelan je bil algoritem, ki ustrezno prepoznava predstavljena odstopanja in jih sproti odpravlja, podatek o popravljeni krivulji se skupaj z originalno krivuljo shrani v bazo. Če so podane tudi geološke skice izkopnih čel, sistem za nov merski profil izreže skico iz po stacionaži najbližjega popisnega lista ter jo ustrezno obdela glede na kakovost skice in njen kontrast. Pri izdelavi poročil se jo lahko nato izriše pod izris vektorjev pomikov v prečnem prerezu in tako omogoči neposredno primerjavo pomikov z geološko strukturo.

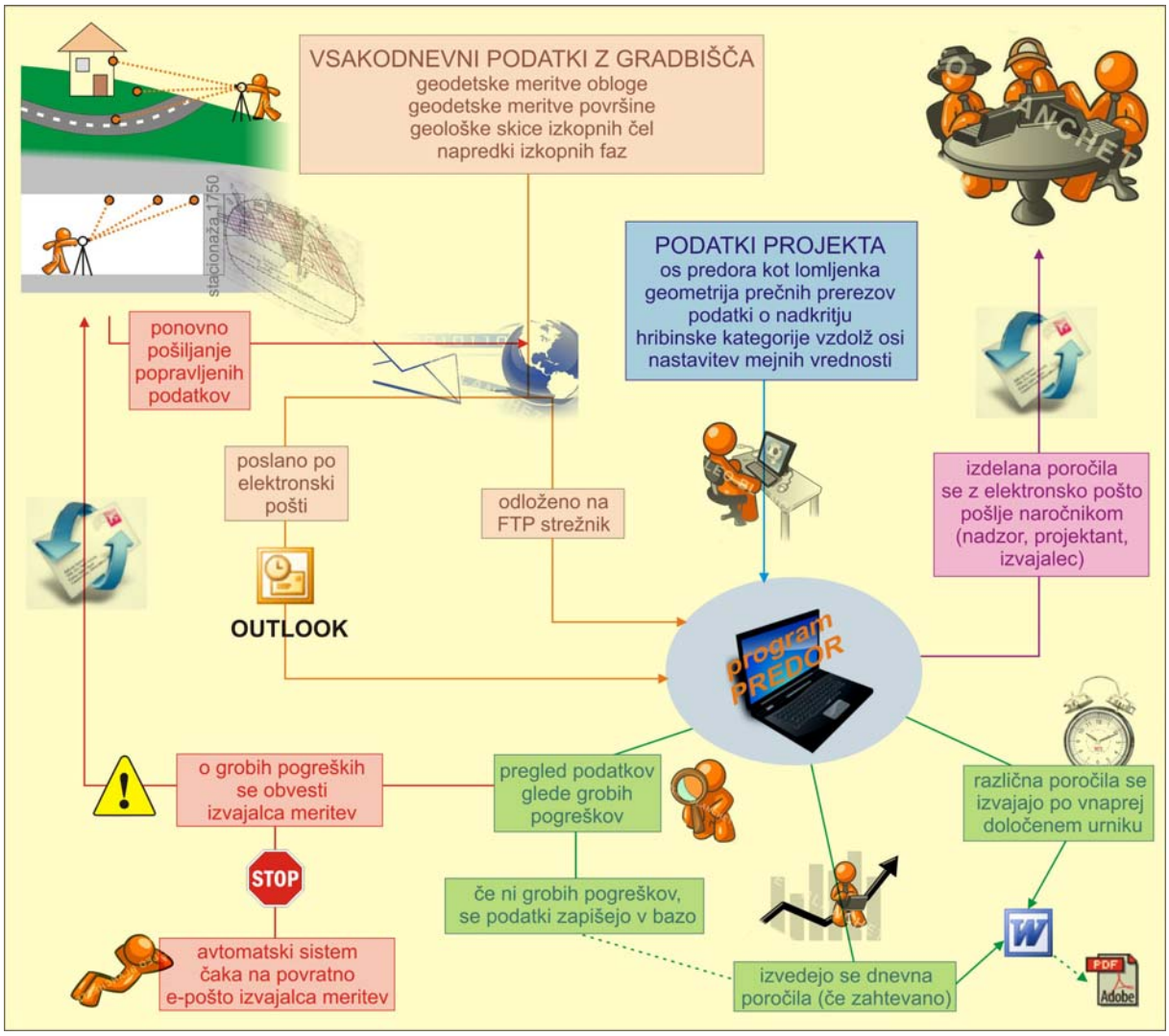

Slika 9-2. Shematski prikaz delovanja avtomatskega sistema za obdelavo podatkov geodetskega in geološkega opazovanja v predorogradnji.

Za avtomatizirano izdelavo poročil je potrebno podati ustrezno podlogo v programu Microsoft Word, kamor se nato vstavljajo teksti, tabele in grafični izrisi. Za kar najbolj koncentrirano obliko podajanja informacij v grafični obliki so bili razviti različni izrisi (izris relevantnih podatkov v merskem profilu v predoru ali na površini, izris različnih črt vzdolž predorske osi, situacija gradnje s položaji izkopnih čel ter situacija merskih profilov v predoru in na površini – prikazi so na slikah 3-4 do 3-9). Izdelana poročila se nato z elektronsko pošto pošlje vnaprej določenim prejemnikom.

Predstavljeni avtomatski sistem spremljanja gradnje predora je bil uspešno uporabljen pri gradnji predorov Barnica, Tabor in Leščevje.

9.4 Vpliv skrilavosti hribine na pomike predora

Izkop predora spremeni napetostno stanje v hribini in povzroči deformacije v izkopani prostor. Ti pomiki bi bili v primeru hidrostatskega napetostnega stanja radialni na konturo predora (Hoek, 2007). Vzorec deformacij se temeljito spremeni v heterogenih tleh, kjer je porazdelitev dodatnih napetosti in s tem pomikov odvisna od togosti zaledne hribinske mase. Vpliv bližnje tektonske cone na pomike je temeljito analiziralo že več avtorjev (Button, 2004b; Moritz s sodelavci, 2004; Schubert s sodelavci, 2002; Schubert s sodelavci, 2005). Še bolj kompleksen je deformacijski vzorec v anizotropnih pogojih (anizotropija pomeni različne lastnosti hribine v različnih smereh), ki izdatno vplivajo na njeno obnašanje (Leitner s sodelavci, 2006); običajno se nanaša na oslabljene ploskve v hribinski strukturi kot npr. skrilavost, plastovitost, prelomi, razpoke). Odziv izkopanega prostora torej močno zavisi od trdnostnih parametrov in relativne usmerjenosti diskontinuitet glede na izkopani prostor (Wittke, 1990; Solak, 2009). Za pridobitev ustreznih materialnih parametrov se izvede povratna numerična analiza opaženih vplivov, pri čemur je uporaba 2D izračunov opravičena le v primeru, ko je smer vpada diskontinuitet pravokotna na os predora. V vseh ostalih primerih so potrebni 3D numerični izračuni. Tonon (2003) je tako na podlagi 3D numeričnih analiz ugotovil, da vpliva relativna orientacija diskontinuitet tudi na velikost pomikov, ki se zgodijo pred čelom in za čelom predora. V primeru izkopa z vpadom diskontinuitet v čelo se večina celotnega pomika zgodi pred čelom, ker je hribina bolj deformabilna pravokotno na diskontinuitete kot vzdolž diskontinuitet in se torej deformacije lahko začnejo precej daleč od čela. Nasprotno pa se pri vpadu diskontinuitet v izkopani prostor večina pomikov zgodi šele za čelom v že izkopanem prostoru, kajti hribina se lahko le malo deformira v smer nadaljnjega izkopa.

Pregled literature s povratnimi analizami predorov Trojane, Golovec in Šentvid je pokazal, da so avtorji za povratne analize obnašanja uporabljali izotropne modele. Zato so bile za določitev izhodiščnih parametrov anizotropnega modela izvedene obsežne povratne 2D analize na odseku

kaverne v desni cevi predora Šentvid, kjer je bila skrilavost vzporedna z osjo predora. Uporabljen je bil program Plaxis, ki prostor opiše kot kontinuum. Uporaba takšnega modeliranja je opravičena, ker razmik med posameznimi diskontinuitetami ne vpliva na obnašanje izkopanega prostora (Leitner, 2006). Edina kombinacija parametrov, pri kateri je bil izračunani posedek točke v stropu kaverne enak izmerjenemu in elastični modul E_1 primerno velik glede na presiometrske preiskave, je bila z zelo nizkim strižnim modulom G_2=5 MPa. Izračunane parametre smo nadalje preizkusili še na dodatnem merskem profilu, kjer je iz slike 9-3 razvidno relativno dobro ujemanje merjenih in izračunanih velikosti pomikov, predvsem pa ujemanje poteka vektorjev pomikov. Ti parametri so bili nato uporabljeni v vseh nadaljnjih numeričnih analizah, razen pri predoru Trojane, ki je bil grajen v mehansko slabši različici kamnin kot predor Šentvid. Numerične analize so namreč pokazale, da ustrezen odziv dobimo, če je vrednost strižnega modula enaka izotropni vrednosti $G_2=0,5E_1(1+\upsilon_1)$.

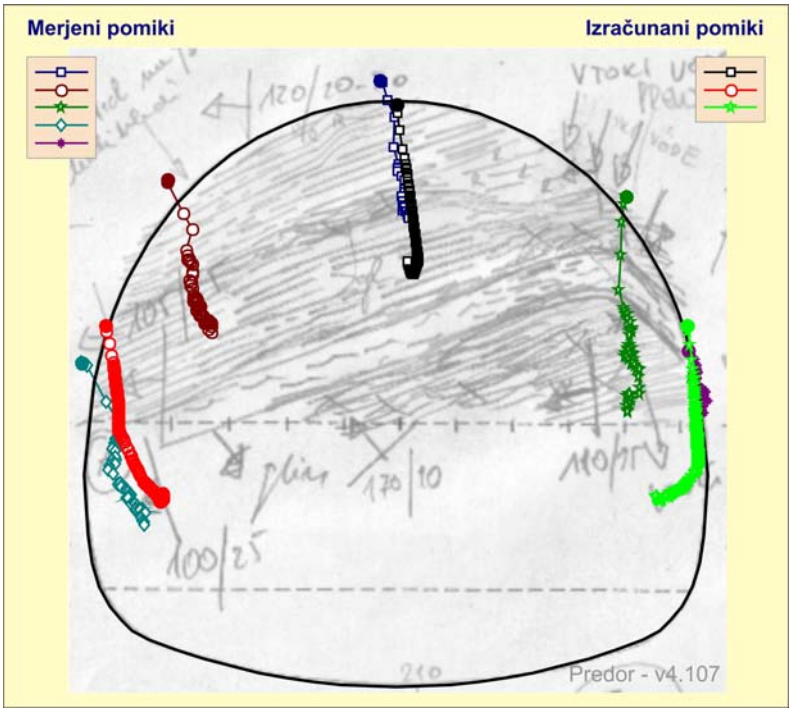

Slika 9-3. Primerjava merjenih in izračunanih pomikov v merskem prerezu MS6 na stacionaži km 1,1+23,2 v desni cevi predora Šentvid.

Med analizo merjenih pomikov v predoru Trojane smo naleteli na daljši odsek vektorjev pomikov z orientacijo v smer nadaljnjega izkopa. »Normalno« obnašanje je namreč glede na numerične izračune in izkušnje določeno kot odklon vektorja pomikov (razmerje med vzdolžnimi in vertikalnimi pomiki) z naklonom 8°-12° v izkopani prostor (Schubert s sodelavci, 2002). Pri približevanju območju mehkejše hribine se vektor odkloni še bolj v izkopani prostor (nazaj), v primeru približevanja boljši

hribini pa proti čelu (naprej). V literaturi kakšnih večjih pomikov v smeri izkopa na daljšem odseku nismo zasledili.

Ob izkopu predora Trojane iz zahodnega portala predor preči manjši hrib in se nato spušča proti dolini Učak (slika 9-4). Ko se je nadkritje nad predorom začelo zmanjševati, so bili izmerjeni vzdolžni pomiki v smeri napredovanja čela v obeh ceveh, pri čemer je presenetljiva predvsem velikost največjega izmerjenega pomika: 14,2 cm. Orientacija vektorja pomikov se je na tem odseku v severni cevi povečala celo do 70° naprej. »Normalna« orientacija vektorjev pomikov je bila znova izmerjena v dolini Učak. Glede na izkušnje (Schubert s sodelavci, 2005) bi pred čelom pričakovali območje res trdne hribine, a geološka interpretacija (Budkovič s sodelavci, 2005) kaže, da dolina Učak predstavlja večjo prelomno cono. V predoru Trojane je bilo prepoznano še eno območje s pomiki naprej (odsek T2 na sliki 9-4).

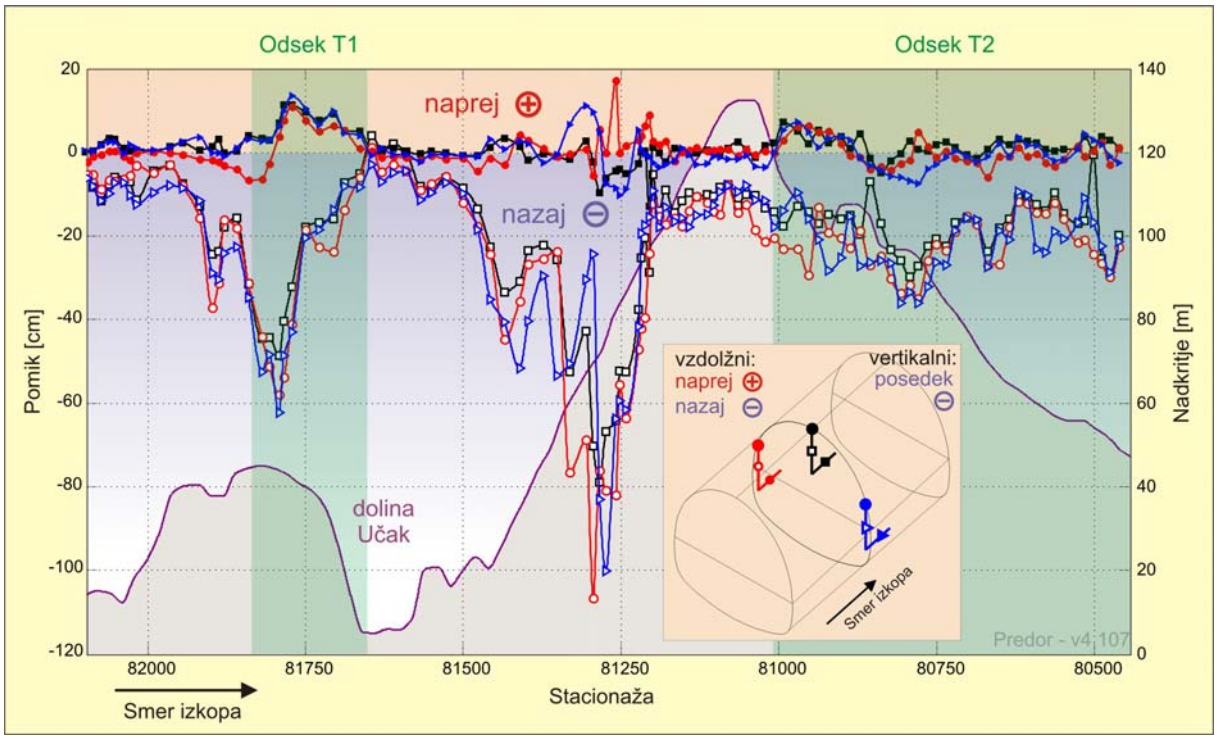

Slika 9-4. Kontura izmerjenih vertikalnih in vzdolžnih pomikov v južni cevi predora Trojane (izkop iz zahoda) z izrisanim nadkritjem; območja vzdolžnih pomikov v smeri napredujočega čela so obarvana zeleno.

Dolžina odseka T1 je okoli 180 m v južni in 145 m v severni cevi. Odsek T2 je precej daljši (približno 650 m v južni in 330 m v severni cevi; izkopa iz zahoda sta bila nato končana – mesto preboja), a zaradi lokalnih geoloških pogojev in višjega nadkritja pomiki niso na celotnem območju

usmerjeni vseskozi naprej. Sprememba orientacije vektorja pomikov se na odseku T1 zgodi pri nadkritju 45 m, na odseku T2 pa pri 135 m. Na obeh območjih prevladuje vpad skrilavosti s kotom približno 45° v izkopani prostor. Predvsem na območju T1 smo opazili zelo dolgotrajne deformacije, kjer je razdalja od merskega profila, ko se le-ta lahko smatra za umirjenega, do točke izgradnje celotnega podpornega obroča presegla 60 m. Običajno so se deformacije umirile približno na razdalji 15-25 m za dokončanim celotnim primarnim podporjem. Meritve površinskih točk v območju prebojev in doline Učak so pokazale, da je gradnja predora povzročila premikanje tal v smeri padnice pobočja. Možna razlaga pomikov predorske obloge v smer nadaljnjega izkopa ob padajočem nadkritju bi bila torej vsaj v primeru T1 vpliv morfologije terena in s tem povezano plazenje pobočja zaradi gradnje predora.

Območja spremembe orientacije vektorja pomikov v smer nadaljnjega izkopa ob enaki usmerjenosti skrilavosti in ob spremembi padnice terena nad predorom smo opazili še pri štirih predorih: Golovec, Jasovnik, Ločica in Podmilj. Podatki o dolžini teh območij, nadkritju, ko se zgodi sprememba orientacije in maksimalni pomik naprej so prikazani v preglednici 9-2.

Preglednica 9-2. Zbrani podatki o projektih predorov, kjer so bili izmerjeni vzdolžni pomiki v smeri napredovanja čela.

predor	cev	odsek	dolžina odseka [m]	nadkritje	maksimalni vzdolžni pomik [cm]	tarča
Trojane	severna	T1	145	35	14.2	strop
		T2	370*	130	6.1	leva
	južna	T1	180	45	13.7	desna
		T2	700*	135	7.3	strop
Golovec	vzhodna	G1	100**	75	9.7	desna
	zahodna	G1	130**	75	14.1	strop
Jasovnik	severna	J1	500	105+	12.8	desna
	južna	J1	500	110+	20.3	desna
Ločica	severna	L1	150	85	5.1	desna
	južna	L1	200	100	5.8	desna
Podmilj	severna	P1	150***	160	2.6	desna
	južna	P1	180***	145	2.2	desna

*preboj je bil izvršen ob koncu odseka T2; nadkritje se je še zmanjševalo v smeri izkopa
** preboj je bil izvršen ob koncu odseka G1; nadkritje se je še zmanjševalo v smeri izkopa (slika 4-16)
+nadkritje, ko so bili merjeni pomiki večji od merske natančnosti (slika 4-19)
*** preboj je bil izvršen ob koncu odseka P1; nadkritje se je še zmanjševalo v smeri izkopa (slika 4-25)

Zanimiv je predvsem predor Jasovnik. Kot je razvidno iz preglednice 9-2, se prvih 1000 m predora nahaja v dolomitu, kjer so bili izmerjeni pomiki zanemarljivi oz. v rangu merske natančnosti. Nato pa

se je izkop vršil v psevdoziljskih skrilavih meljevcih in glinavcih, kjer je bilo pod padajočim nadkritjem zabeleženo najdaljše območje neprekinjenih pomikov naprej (približno 500 m v vsaki cevi) in izmerjen tudi največji pomik: 20,3 cm ter hkrati edini predor, kjer ne moremo potrditi spremembe orientacije vektorja pomikov s spremembo padnice pobočja, kajti le-ta se zgodi še v dolomitu.

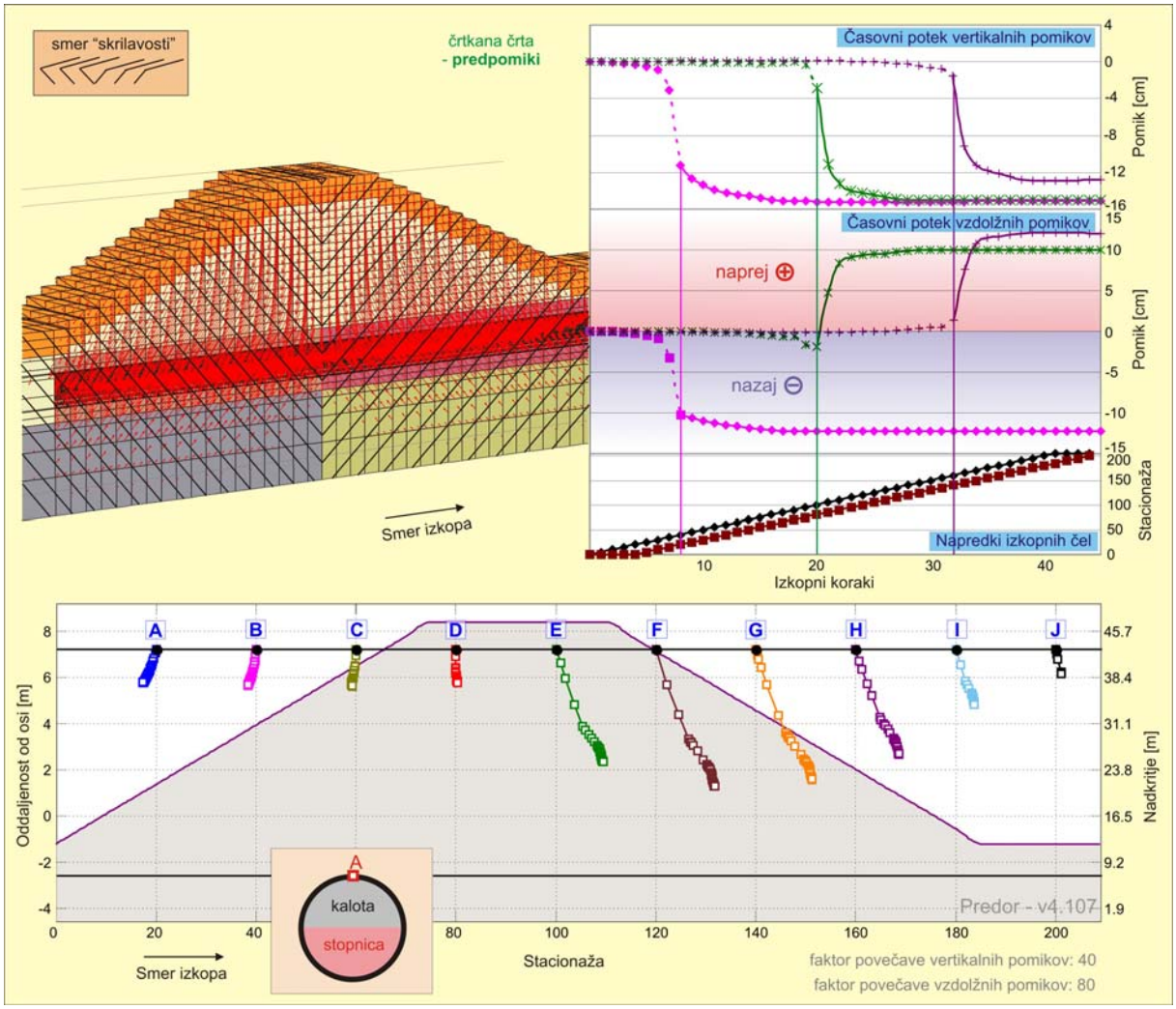

Slika 9-5. Izračunani vektorji pomikov po izkopu v vzdolžnem prerezu (spodnji izris), celoten potek vzdolžnih in vertikalnih pomikov za izbrane točke (zgornja desna izrisa) in prikaz pomikov s puščicami iz programa Plaxis ("Jointed rock" konstitutivni model).

Z željo pojasniti mehanizem, ki privede do znantnih pomikov naprej, smo izvedli 3D numerične analize. Geometrija modela je temeljila na poenostavljeni morfologiji hriba, kjer se nahaja odsek T1. V prvi fazi smo izračun opravili s »Hardening soil« konstitutivnim modelom v Plaxisu (iz zgoraj omenjene povratne analize in analiz drugih avtorjev lahko mehansko slabše različice skrilave hribine - kot to velja za predor Trojane - uspešno modeliramo tudi z izotropnimi modeli). Izračunani odziv je

bil zelo podoben dejanskemu na odseku T1 (pomiki izkopanega prostora v smeri padnice na obeh straneh hriba, celo dvižki v dolini Učak), le izračunani pomiki izkopanega prostora so bili precej manjši (do 2 cm), kar lahko pripišemo večjemu vplivnemu območju gradnje okoli predora z izrazito poslabšanimi lastnostmi hribine kot smo pa to upoštevali v modelu.

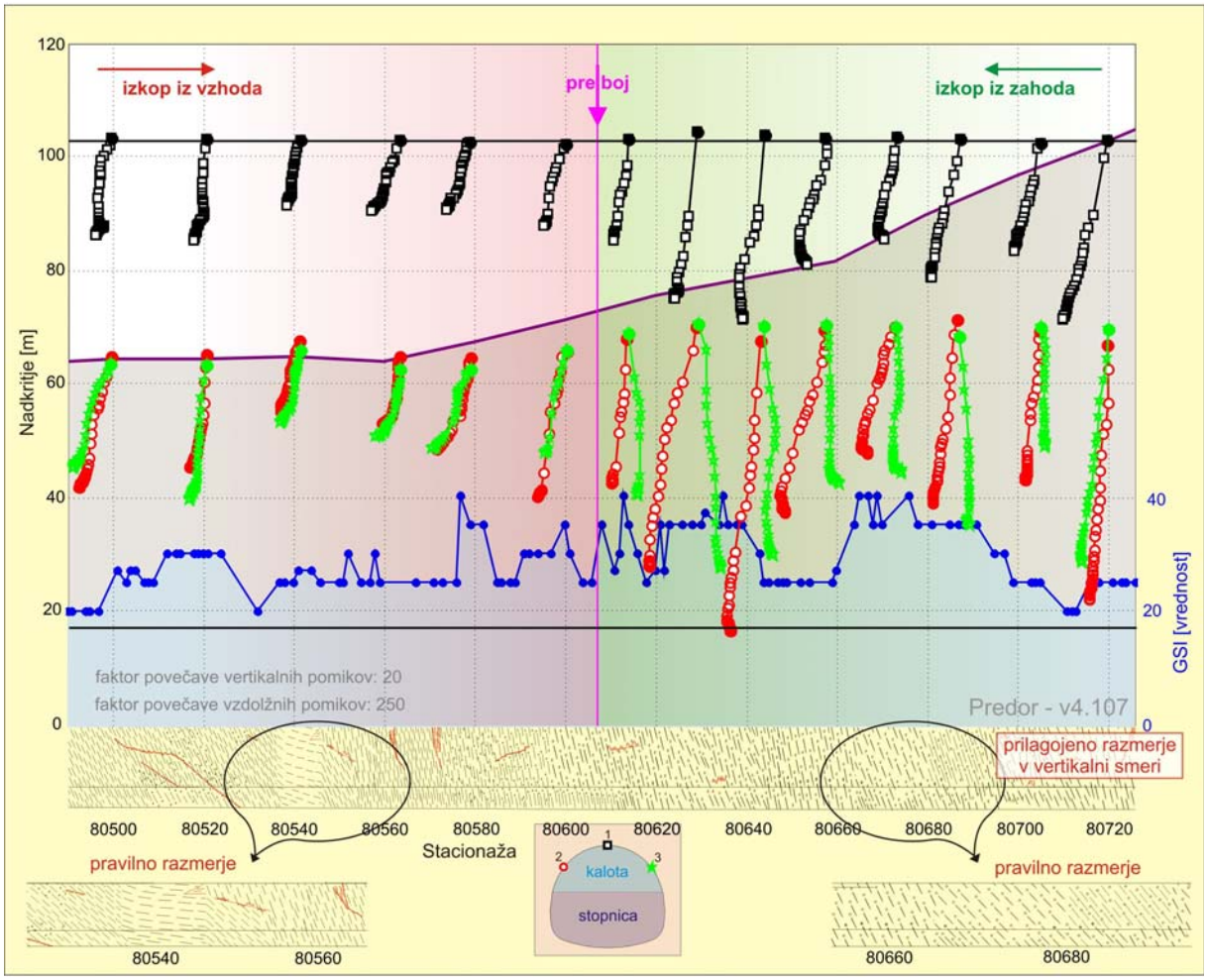

Slika 9-6. Vektorji pomikov v vzdolžnem prerezu na območju preboja v desni cevi predora Trojane z geološkim vzdolžnim prerezom (ni v merilu!) in pripadajočim GSI.

Da bi ugotovili morebiten vpliv anizotropije hribine na orientacijo vektorja pomikov in njihovo velikost, smo nato izvedli na enakem geometrijskem modelu še izračune z "Jointed rock" konstitutivnim zakonom s parametri iz predora Šentvid (nizek strižni modul G_2). Predpisana smer »skrilavosti« v numeričnem modelu je prikazana na sliki 9-5 in posnema poenostavljeno geološko zgradbo predora Ločica (sinklinalna guba, z vpadom plasti v izkopani prostor pod padajočim nadkritjem. Celotni izračunani pomiki so bili na obeh straneh »hriba« približno enake velikosti ter so bili usmerjeni v pričakovano smer (nazaj ob naraščajočem nadkritju in naprej ob padajočem – izris iz

programa Plaxis na sliki 9-5 zgoraj). Drugačno sliko pokaže primerjava pomikov v izkopanem prostoru (predpomiki niso zajeti) na sliki 9-5 spodaj, kjer je opaziti precej večje pomike izkopanega prostora v primeru vpada plasti v izkopani prostor (pod padajočim nadkritjem) kot pa v primeru vpada plasti v čelo. Izračunani odziv se sklada z ugotovitvami Tonona (2003).

Ker se je na predoru Ločica togost hribine vzdolž osi spreminjala, te ugotovitve nismo mogli podkrepiti z meritvami. Edina preostala možnost je bilo območje preboja v predorih Trojane in Golovec, kjer bi bil vpad plasti dokaj enoten in po možnosti ne preveč tektonsko premešan. Temu pogoju je zadostilo le območje preboja severne cevi predora Trojane. Hribina je na zahodnem delu sestavljena iz menjajočih se plasti meljevca in peščenjaka s povprečno vrednostjo GSI med 30 in 35 – slika 9-6. Na vzhodnem delu se plasti meljevca menjajo s plastmi glinovca in le podrejeno peščenjaka; povprečna vrednost GSI je zato tudi nižja kot na zahodni strani (približno 25). Globalno gledano so bili pogoji gradnje torej boljši na zahodnem delu. Generalno plasti v vzdolžnem prerezu padajo proti zahodu z naklonom 45° do 60° (slika 9-6) in jih kljub nekaj manjšim prelomom lahko smatramo za razmeroma enotne.

Izrisani vektorji pomikov v vzdolžnem prerezu so usmerjeni enakomerno na celotnem odseku (slika 9-6), na vzhodnem delu nazaj, na zahodnem naprej (konec odseka T2). Izmerjeni pomiki so na zahodu, kjer je izkop potekal z vpadom plasti v izkopani prostor precej večji kot pa na vzhodu, kjer je izkop potekal z vpadom plasti v čelo, čeprav je hribina na zahodu precej boljša. Del razloga za večje pomike na zahodu je tudi nekaj višje nadkritje. Na zahodnem delu je opaziti tudi razkorak med orientacijo vektorjev pomikov obeh bočnih točk, ki je posledica prostorskega vpada skrilavosti (po izkopu kalote se deformacije vršijo v smeri pravokotno na ravnino diskontinuitet, nato prevlada vpliv začetnega napetostnega stanja oz. nagnjenost terena z deformacijami v smeri padnice terena; po prehodu stopnice in talnega oboka so vektorji pomikov znova usmerjeni pravokotno na ravnine skrilavosti).

9.5 Meritve prostorskih pomikov pred čelom predora v raziskovalnem rovu predora Šentvid

Pomen geotehničnega opazovanja in interpretacije prostorskih pomikov predorske obloge je bil poudarjen v prejšnji poglavjih. Toda del deformacij hribine se zaradi prenosa napetosti v prostoru zgodi že pred čelom predora in med izkopom prereza ter prvo meritvijo položaja točke v tem prerezu (v nadaljevanju predpomiki). Za celovit odziv zaledne hribine na izkop predora moramo torej poznati tudi potek in velikost teh pomikov, ki jih z običajnimi geodetskimi metodami ne moremo izmeriti. Hoek (2007) trdi, da se deformacije hribine pričnejo približno pol premera predorske cevi pred čelom predora in dosežejo tretjino celotne radialne deformacije. Do podobnih zaključkov je na podlagi eksperimentov prišel

Lunardi (2008). Velikost predpomikov lahko ocenimo tudi iz primerjave posedkov površine in točk v predoru v primeru nizkega nadkritja. Takšna primerjava je bila narejena za vzhodni del predora Trojane v območju naselja Trojane, kjer so bili merjeni posedki merskih točk vzdolž osi. Ugotovili smo, da je na določenih predelih posedek stropa predora znašal le 35% izmerjenega posedka na površini (v povprečju okoli 50% - slika 5-1); dejanski delež je verjetno še nižji, če se celotna izguba volumna ni prenesla na površino). Še nekaj nižji delež izmerjenih pomikov obloge v celotnih pomikih je dala analiza rezultatov tritočkovnega vertikalnega ekstenzometra nad predorom Trojane (slika 5-3). Zadnja merska točka 4 m nad stropom predora je namreč izkazala trikratno vrednost posedka stropne točke v predoru. Ekstrapolacija vrednosti 4 m globlje izkaže le 27% delež merjenih pomikov stropa predora v celotnih pomikih. Vpliv gradnje je bil zaznan približno 20 m pred čelom predora. Podobne vrednosti so bile dobljene tudi ob analizi rezultatov horizontalnega inklinometra (slika 5-4). Slabost obeh merskih metod je merjenje le relativnih posedkov hribine in ne prostorskega odziva hribine zaradi bližajočega se izkopnega čela. Le-tega lahko merimo le, če se v območju izkopa bodočega predora nahaja rov z mnogo manjšim prečnim prerezom. Takšna priložnost se je ponudila v primeru raziskovalnega rova predora Šentvid in vzpostavljen je bil obsežen opazovalni sistem.

Zaradi zahteve po čim večji natančnosti meritev in varnostne omejitve vstopa v raziskovalni rov le na en dostop dnevno je bil za geodetske meritve položajev tarč izbran elektronski tahimeter Leica TCRP1201R300 z zmožnostjo avtomatskega prepoznavanja tarč. Standardne optične prizme so bile vgrajene v oblogi raziskovalnega rova na medsebojni razdalji približno 2 m v stropu ter 6 m na obeh bokih in tleh kot je razvidno iz slike 9-7. Opazovano območje pred čelom glavnega predora je bilo sprva določeno na podlagi literature in zgornjih opažanj na dva premera predorske cevi, a se je tekom opazovanja spreminjalo glede na opažene pomike prizem. Instrument je bil nameščen na jekleni konzoli na enem od obeh bokov (odvisno od (ne)ravnosti predora) in na dovolj veliki oddaljenosti od čela, da je bila nevarnost poškodbe z brizganim betonom, katerega bi izvajalec gradbenih del po nesreči brizgnil v raziskovalni rov, kar najmanjša (razdalja do čela ni bila manjša od 18 m). Zaradi možnosti poškodb predvsem talnih in bočnih točk z brizganim betonom ter padajočimi kosi brizganega betona iz poškodovane obloge so bile prizme blizu čela ter instrument zaščiteni z jeklenim ščitom. Referenčne točke so bile vgrajene na zadostni razdalji od napredujočega čela, da so se lahko smatrale kot stabilne. Prvi absolutni položaj teh točk je bil določen iz geodetske mreže v glavnem predoru. Razpored referenčnih točk je bil vedno enak: po ena točka na vsakem boku predora in na približno enaki oddaljenosti od instrumenta (čim večji horizontalni kot), medtem ko se je tretja točka nahajala na večji razdalji od instrumenta globlje v raziskovalnem rovu. Meritve merskih točk so se izvajale vsakih 60 minut v obeh krožnih legah. Ker se je instrument včasih že nahajal v vplivnem

območju gradnje (to smo opazili na precizni libeli in tudi iz analize položaja referenčnih točk), se je položaj instrumenta na novo določal ob vsakem izvajanju meritev.

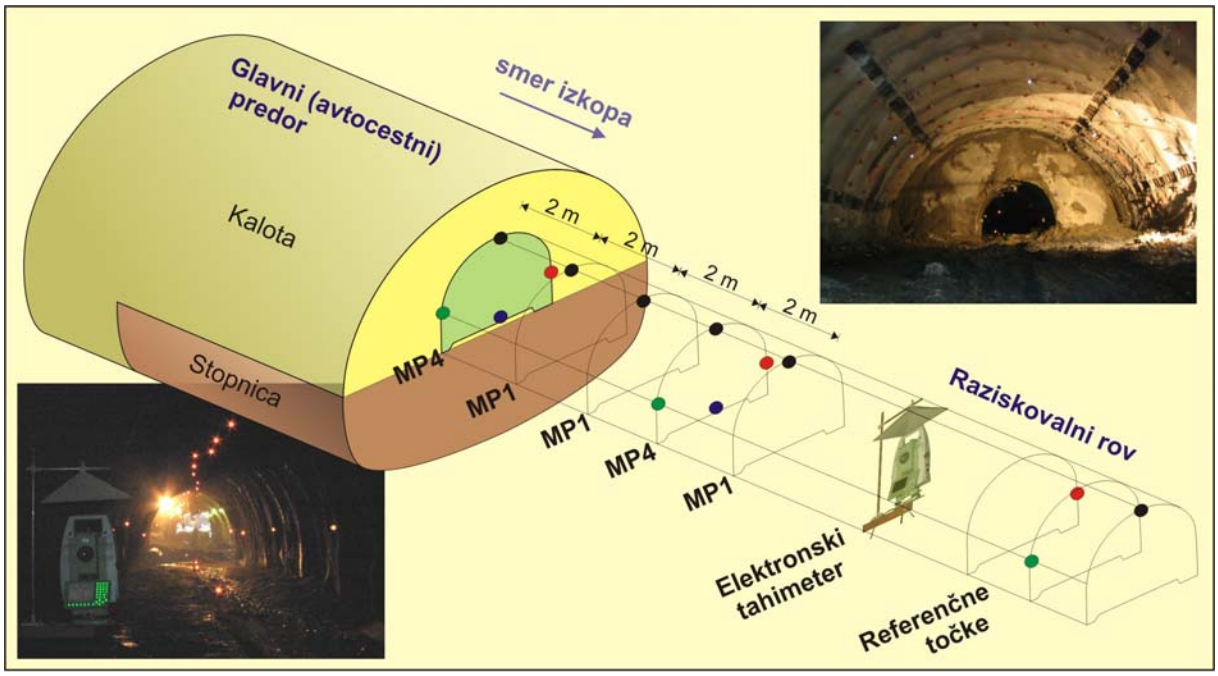

Slika 9-7. Shema eksperimenta v raziskovalnem rovu predora Šentvid.

Meritve prostorskih pomikov pred čelom predora so se pričele 22. septembra 2005 v desni cevi raziskovalnega rova (dva tedna prej so se izvajale posamezne meritve, da smo se spoznali z instrumentom in dokončno določili sistem opazovanja). V desnem rovu je bilo skupno opazovanih 37 merskih profilov na odseku dolžine 75 m (na 28 profilih je bila izmerjena celotna deformacijska krivulja od začetka vplivnega območja do izkopa prečnega prereza z merskim profilom). Glavni problem je elektronskemu tahimetru predstavljal prah, ki ga je povzročalo miniranje in pikiranje ob izkopnih delih in je povzročil zaustavitev instrumenta. Instrument smo vklopili ob ponovnem vstopu v rov naslednji dan. Izkušnje so pokazale, da je bilo izvedenih več meritev, če se je instrument nahajal bližje čelu in s tem merskim prizmam – slika 5-9. Ko se je izkop glavnega predora približal bodoči priključni kaverni, so se izmerjeni pomiki zmanjšali na nivo merske natančnosti in 27. oktobra so se stalne meritve v desnem rovu zaključile ter začele izvajati v levem rovu.

Že med izvajanjem meritev v desnem rovu smo izvedli posamezne meritve v prečniku med obema cevema, ko se je leva cev avtocestnega predora bližala stičišču prečnika in levega rova, kajti poleg vpliva pred čelom smo želeli zabeležiti tudi vpliv bližajočega se izkopnega čela pravokotno na os izkopa. Opazovanih je bilo 9 merskih profilov na odseku dolžine 20 m od desnega boka leve cevi glavnega predora.

Tako pričakovane kot dejanske geološke razmere v levem rovu so bile mnogo slabše kot v desnem in posledično so bile izmerjene deformacije mnogo večje. V levem rovu je bilo skupno opazovanih 72 merskih profilov na odseku dolžine 147 m, od tega je bilo 66 profilov merjenih od začetka vplivnega območja do izkopa prečnega prereza z merskim profilom. Zaradi drastičnega poslabšanja geoloških pogojev in s tem poslabšanja varnostne situacije je bilo merjenje prostorskih pomikov v predoru Šentvid po nekaj več kot sedmih mesecih zaključeno 24. aprila 2006. Za razliko od desnega rova je v levem rovu glavni problem predstavljala voda in z njo povezana večja zračna vlaga, ki se je kondenzirala na prizmah in povzročila zaustavitev instrumenta. Število opravljenih dnevnih meritev je bilo v neposredni povezavi s temperaturo zunanjega zraka (ventilacijski sistem je na čelo in v raziskovalni rov dovajal mrzli zunanji zrak) kot je razvidno iz slike 5-12. Nadalje je predstavljala problem voda, ki je pritekala iz raziskovalnih vrtin in zastajala pri vhodu v raziskovalni rov ter poplavila talne merske prizme (zaradi poslabšanih geoloških pogojev je bil izkop posameznega koraka razdeljen na več manjših korakov in je zato trajal mnogo dlje; voda je zastajala za izkopanim materialom in vstop v raziskovalni rov ni bil mogoč do konca izkopa). Instrument se je ustavil, če je bilo potopljene več kot pol in ne cela prizma.

Med vsakodnevnimi vhodi v raziskovalni rov smo predvsem v levem rovu opazili poškodovan, drobno razpokan brizgani beton rumene barve in rjavkasto oborino pod iztekajočo vodo iz raziskovalnih vrtin. Kemična analiza te oborine je pokazala vsebnost železovega hidroksida, pregled poškodovanega betona z elektronskim mikroskopom pa prisotnost nabrekljivih mineralov (sulfatna korozija betona – (Petkovšek, 2005)). Oboje je posledica razpada pirita, ki je bil v velikih količinah opažen v zaledni hribini. Ker so bili tudi v glavnem predoru identificirani vzorci sulfatne korozije, se je kot prvič v Sloveniji izvedlo armiranje notranje betonske obloge.

Izmerjeni pomiki so se dnevno obdelovali, analizirali in shranjevali v bazo podatkov. Na podlagi rezultatov se je po potrebi obveščalo projektante in nadzor o dogajanju pred čelom predora. Iz raziskovalnega vidika je leva cev mnogo bolj zanimiva kot desna, saj so bili v desni razen v začetnem delu (kjer pa se meritve niso izvajale nepretrgoma) pomiki majhni do zanemarljivi. Nasprotno pa so bili v levem rovu izmerjeni veliki pomiki (do 30 cm v vzdolžni in vertikalni smeri), menjavala so se območja boljše in slabše hribine, opažen je bil daleč segajoč vpliv gradnje.

Osnovni rezultat eksperimenta predstavlja časovni potek pomikov vsake opazovane točke. V vertikalni in vzdolžni smeri je krivulja parabolične oblike kot je predvidel že Barlow (1986), medtem ko je v prečni smeri viden izrazit vpliv anizotropije (slika 5-21). Na izrisu vektorjev pomikov v prečnem in vzdolžnem prerezu je tako viden izrazit bilinearni odziv (slika 9-8). Ko je merski prerez daleč od čela predora in je obtežba (sprememba napetostnega stanja zaradi razmeroma oddaljenega izkopa predora) majhna, prevladujejo deformacije vzdolž diskontinuitet, ko pa se čelo približa in so

spremembe napetosti večje, se hribina deformira pretežno pravokotno na smer skrilavosti. Prevoj med obema deformacijskima fazama se zgodi pri določeni oddaljenosti merskega profila od izkopnega čela predora (v povprečju 5 m pred čelom predora pri 35-50% končnega izmerjenega pomika kot je razvidno iz slike 5-24). Prevojna točka razdeli območje pred čelom na območje velikih deformacij (med čelom in prevojno točko) in malih deformacij (od prevojne točke naprej v smeri izkopa).

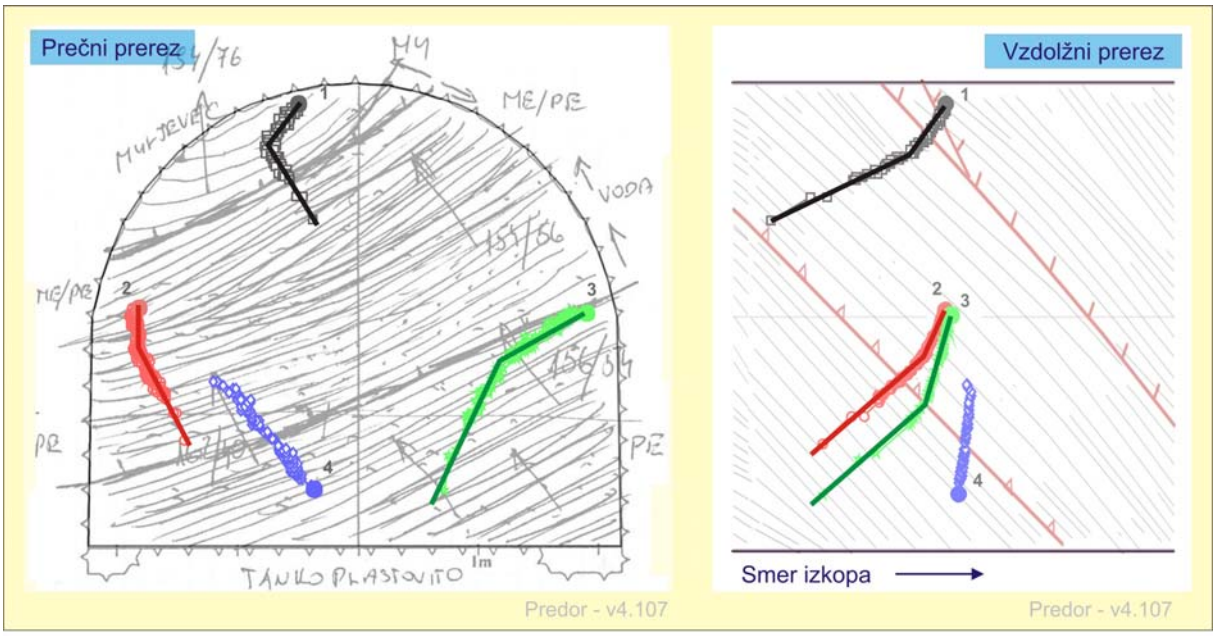

Slika 9-8. Bilinearni potek vektorjev pomikov v prečnem in vzdolžnem prerezu v merskem profilu na stacionaži km 1,4+55,8 v levi cevi raziskovalnega rova.

Odvisno od geološke zgradbe je bilo vplivno območje na talnih točkah zaznano v povprečju 18-25 m (maksimum 42 m), na stropnih točkah pa 10-20 m pred čelom predora (slika 5-26). Povečanje izkopnega profila v kaverni presenetljivo ni povzročilo povečanja vplivnega območja. Vplivno območje je glede na meritve odvisno le od geološke zgradbe tal oziroma togosti hribinske mase pred čelom predora – vpliv se izrazito poveča pred prehodom v slabšo oz. tektonizirano hribino in je odvisen od obsežnosti le-te. Nekoliko večje območje vpliva (25-30 m) smo zabeležili pravokotno na smer izkopa (v prečniku – slika 5-27). Vplivno območje gradnje pred čelom predora vsekakor je povezano z velikostjo prečnega prereza izkopa, a v prikazanem poskusu povečanje izkopnega profila iz 56 m^2 (kalota dvopasovnega predora) na 93 m^2 (kalota kaverne A) ni povzročila opaznega povečanja območja. To lahko pojasnimo z večjim vplivom geoloških struktur.

Primerjava pomikov, izmerjenih med gradnjo raziskovalnega rova, s pomiki, merjenimi pred čelom glavnega predora pokaže, da se hribina v obeh primerih odziva enako (bilinearni deformacijski

vzorec), le velikost pomikov je zelo različna. Vzrok je večplasten: (1) prerez raziskovalnega rova je precej manjši od glavnega predora, (2) pred čelom predora smo izmerili celotno krivuljo pomikov in (3) vpliv orientacije skrilavosti na velikost predpomikov in izmerjenih pomikov, ki je podrobneje opisan v poglavju 4. Primerjava merjenih pomikov pred čelom in v glavnem predoru omogoča oceno velikosti predpomika (oceno zato, ker točki nista bili vgrajeni na istem mestu in še vedno manjkajo pomiki med izkopom prereza in prvo meritvijo v merskem profilu in zato ker merjena velikost pomika v raziskovalnem rovu ni identična velikosti pomika, ki bi se v isti točki zgodil, če pred čelom ne bi bilo raziskovalnega rova). A na podlagi obeh krivulj merjenih pomikov, predvsem tangente med zadnjimi izmerjenimi vrednostmi in časa med zadnjo meritvijo pomikov pred čelom in prvo v glavnem predoru, lahko sklepamo o poteku manjkajočega dela celotne krivulje pomikov (na opazovanem odseku je bil ta delež pomikov ocenjen na 10%-25% celotnega pomika).

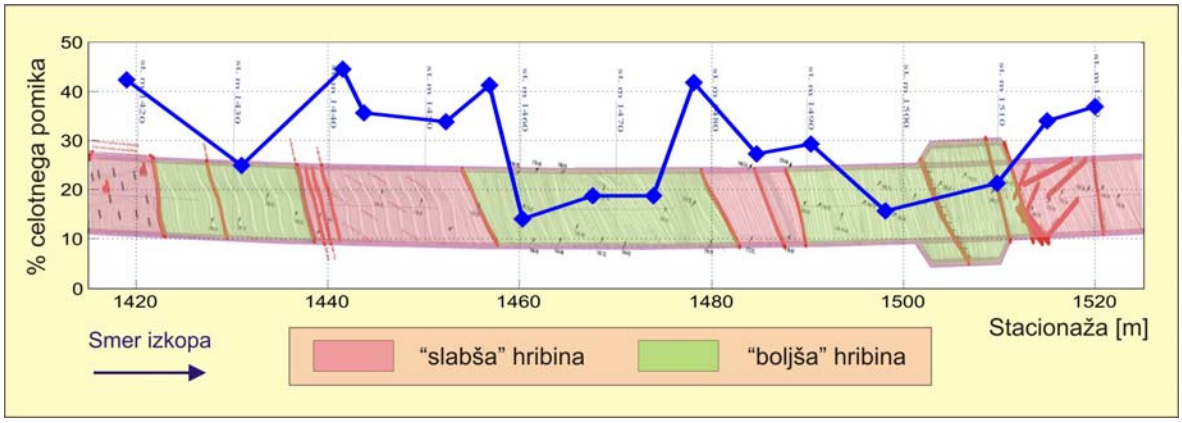

Slika 9-9. Delež posedkov stropne točke v raziskovalnem rovu, ki se zgodijo pred čelom avtocestnega predora glede na celoten izmerjen posedek te točke in točke v avtocestnem predoru, ki se nahaja nad raziskovalnim rovom.

Izmerjeni pomiki pred čelom predstavljajo 15%-45% celotnih izmerjenih pomikov odvisno od togosti hribine (več v slabših hribinah, manj v boljših – slika 9-9). Seštevek merjenih in ocenjenih deležev pomikov, ki se zgodijo pred prvo meritvijo merskega profila, tako znaša od 25%-70%. Numerične analize, ki so bile izvedene s programom Plaxis 3D Tunnel in anizotropnim "Jointed rock" konstitutivnim modelom, so pokazale, da samo spreminjanje elastičnega modula E_1 ob ohranjanju razmerja $E_1:E_2 = 2:1$ in vrednosti strižnega modula G_2 v odnosu na E_1 ne vpliva na povečevanje deleža pomikov pred čelom (slika 5-44). Normaliziran računski delež pomikov pred čelom predora v celotnih pomikih je bil tako v vseh računskih primerih skorajda identičen – 45%. Kasneje se izkazalo, da na delež predpomikov vpliva predvsem razmerje $E_1:E_2$ in velikost strižnega modula G_2 glede na vrednost E_1.

Nadalje smo podrobno analizirali obnašanje pred čelom predora pri približevanju in prečenju območij slabše hribine. Pri približevanju takšnemu območju se vertikalni in tudi vzdolžni pomiki povečajo zaradi koncentracije napetosti v boljši hribini (zaradi večje togosti lahko prevzame več napetosti kot mehkejša hribina). Edinole v tem primeru so bili v levem rovu izmerjeni večji vertikalni kot vzdolžni pomiki (slika 5-20). Vertikalni pomiki se vzdolž območja slabše hribine nato zmanjšujejo, medtem ko so vzdolžni največji tik pred koncem tega območja (slika 5-33), kar bi lahko vodilo do odvojitve bloka slabše hribine od boljše in posledično zruška, če čelo predora ne bi bilo ustrezno sidrano. Merski prerezi za območjem slabše hribine izkazujejo velike vzdolžne in relativno majhne vertikalne pomike, v nekaterih primerih celo dvižke v območju velikih deformacij (slika 5-34), ki so posledica razbremenitve boljše hribine ob koncu izkopa v slabši hribini.

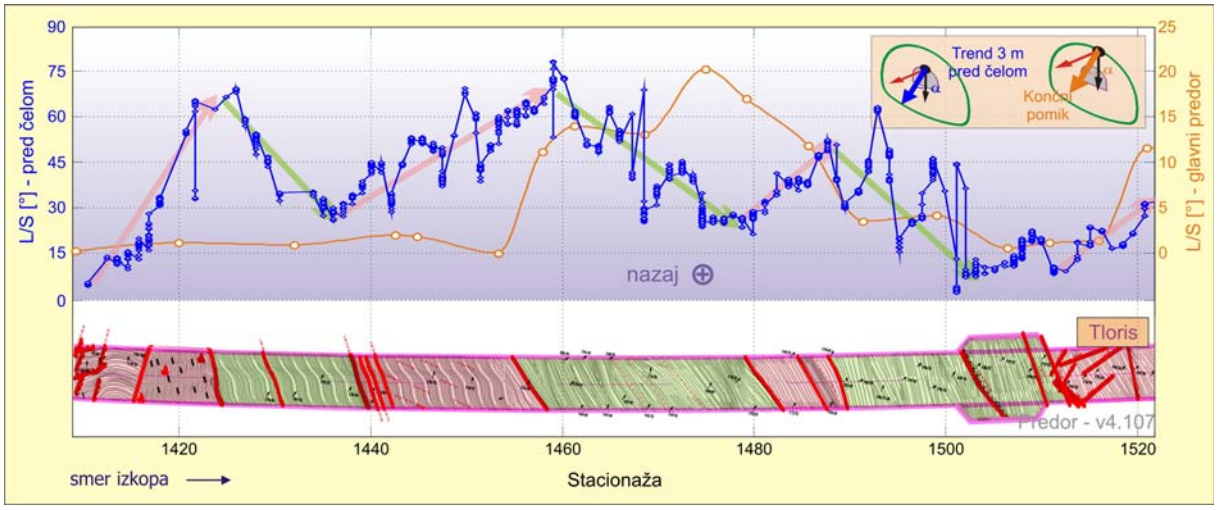

Slika 9-10. Orientacija vektorja pomikov L/S pred in za izkopnim čelom v levi cevi predora Šentvid.

Opazovali smo tudi spreminjanje orientacije vektorja pomikov pred čelom. Podobno kot za vektor pomikov v izkopanem prostoru tudi tu velja, da je orientacija odvisna od togosti hribinske mase. A za razliko od dognanj avtorjev (Steindorfer, 2000; Schubert s sodelavci, 2000), ki so opazovali spremembo orientacije vektorja pomikov predorskih točk precej pred spremembo togosti hribinske mase, sprememba trenda orientacije vektorja pomikov v primeru meritev pred čelom sovpada s spremembo v togosti hribinske mase kot je razvidno na sliki 9-10. Opažanja smo potrdili tudi z numeričnimi analizami, ki so kot »normalno« orientacijo v slabših pogojih izkazale velikost kota okoli 60°, v boljših pogojih pa okoli 30° v smeri proti napredujočemu čelu (slika 5-45). Zaradi pogostega menjavanja togosti hribinske mase »normalnega« kota orientacije vektorja iz merjenih podatkov ne moremo določiti. Se je pa večina opaženih sprememb v trendih zgodila pri zgornjih vrednostih kot je razvidno iz slike 5-45.

Primerjava vzdolžnih pomikov in števila sider v čelu na določenem odseku omogoča oceno učinkovitosti sistematičnega sidranja čela za zmanjšanje predpomikov. Na podlagi podatkov o razporedu osne sile v merskih sidrih, izmerjenem območju velikih deformacij in izkušenj predorskih delavcev smo določili krivuljo normalizirane nosilnosti sidra (3 m sidra naprej od čela ne prevzame nobene obremenitve, nato sila do 7 m pred čelom narašča do polne nosilnosti). Normalizirano nosilnost vseh sider (seštevek normaliziranih nosilnosti posameznih sider pred čelom predora za posamezen prerez) smo nato primerjali s trendnimi črtami pomikov 3 m pred čelom (slika 5-36) in ugotovili, da sistematično sidranje generalno ima določen vpliv na vzdolžne pomike pred čelom. Vendar zaradi relativno hitrega menjavanja odsekov slabše in boljše hribine zgolj vpliva sider ne moremo izolirati. Vpliv se opazi v manjšem merilu, kjer je vgradnja dodatnih sider botrovala precejšnji spremembi naklona krivulje časovnega poteka pomikov (slika 5-37).

Kot je bilo že omenjeno, se lahko 3D meritve pomikov pred čelom izvajajo le v primeru, ko je v osi bodočega predora zgrajen rov z zadosti majhnim prečnim prerezom. Gradnja takega rova spremeni napetostno stanje hribine pred čelom glavnega predora. Tako so tudi izmerjene deformacije drugačne kot če tega rova ne bi bilo. Da bi lahko glede na izmerjen odziv ocenili deformacije hribine pred čelom brez raziskovalnega rova, so bile izvedene obsežne numerične študije na modelu z enako mrežo končnih elementov (v enem primeru je bil rov izkopan, v drugem ne). Izračuni, izvedeni z izotropnima konstitutivnima modeloma »Hardening soil« in »Mohr-Coulomb«, zaradi izrazito anizotropnega odziva hribine pričakovano ne izkažejo odziva, ki bi bil primerljiv z opaženim (slika 5-39). Izračuni z "Jointed rock" materialnim modelom so bili izvedeni za obe prevladujoči orientaciji skrilavosti na opazovanih odsekih raziskovalnega rova. Vertikalni pomiki so v primeru raziskovalnega rova večji, ker se hribina lahko deformira v izkopani prostor. Tako se napetosti sproščajo v radialni smeri, medtem ko se v primeru brez raziskovalnega rova proces prerazporejanja napetosti pred čelom predora odraža v večjih vzdolžnih pomikih v smeri proti izkopnemu čelu. Analize so pokazale, da je bila izbrana lokacija (na platoju kalote) iz vidika vpliva raziskovalnega rova na pomike in notranje sile v primarni oblogi avtocestnega predora optimalna, saj večjih računskih vplivov nismo opazili. Iz raziskovalnega vidika bi bila bolj primerna lokacija, kjer bi temeni raziskovalnega rova in avtocestnega predora (teoretično) sovpadali, saj bi bili izmerjeni pomiki tako po velikosti kot časovnem poteku najbližje stanju brez rova pred čelom predora. A v tem primeru bi bili vplivi na pomike in notranje sile v predorski oblogi znatni.

9.6 Uporaba pomikovne funkcije v mehkih skrilavih hribinah

Kot je bilo že omenjeno v poglavju 9.4, izkop predora povzroči prerazporejanje napetosti okoli predorske cevi in posledično izzove deformacijo oz. konvergenco v notranjost izkopa, ki zelo zavisi od geoloških danosti prostora in tudi tehnologije gradnje. V heterogenih in anizotropnih tleh, kjer lastnosti

hribine zelo variirajo, je težko določiti primerne materialne parametre, zato je ocena velikosti potrebnega nadprofila ena zahtevnejših nalog inženirja pri gradnji predora. Nepravilna odločitev je v vsakem primeru povezana s stroški: če so dejanske deformacije večje od ocenjenih, je potrebno izvesti reprofiliranje, v nasprotnem primeru pa je treba višek zapolniti z betonom. Velikost nadprofila se v Sloveniji oceni na podlagi numeričnih analiz in izkušenj s podzemnimi gradnjami v primerljivih geološko-geotehničnih pogojih za vsako od predvidenih kategorij izkopa in podpiranja po ÖNORM B 2203. Bolj optimalna rešitev je analiza rezultatov opazovanja gradnje ter določitev velikosti nadprofila na podlagi pričakovanih pomikov in geoloških struktur. V ta namen je Guenot s sodelavci (1985) razvil enostavno, a učinkovito metodo, ki jo je nadgradil Barlow (1986) in nadalje prilagodil za uporabo v mehkih hribinah Sellner (2000). Pol-empirična analitična funkcija (v nadaljevanju pomikovna funkcija) hiperbolične oblike opisuje radialne pomike ostenja predora kot funkcijo napredovanja izkopnega čela in časovno odvisnega odziva hribine (Barlow, 1986). Pomikovno funkcijo prilagajamo merjenim pomikom s spreminjanjem prostih parametrov, ki opisujejo odziv sistema hribina – podporje ob upoštevanju faznosti gradnje. Glavna prednost pomikovne funkcije je enostavnost, saj omogoča hitro in zanesljivo oceno procesa stabilizacije prečnega prereza z upoštevanjem 3D vplivov gradnje in tudi časovne komponente gradnje (za razliko od analitičnih metod) ter je za razliko od numeričnih metod mnogo hitrejša kar se tiče porabe časa. Poleg tega za določitev »normalnega« obnašanja in končne velikosti pomika ne potrebuje materialnih parametrov, katere bi bilo potrebno določiti z dragimi in zamudnimi laboratorijskimi preiskavami. Zaradi teh prednosti je metoda primerna za vsakodnevno uporabo pri spremljanju gradnje predora (Sellner, 2000).

Pomikovna funkcija je sestavljena iz treh delov: 1. del predstavlja pomike, ki se zgodijo pred čelom; 2. del predstavlja pomike, ki se zgodijo med izkopom izkopnega koraka z merskim profilom in prvo meritvijo točk; 3. del predstavlja izmerjene pomike, ki se zgodijo za izkopnim čelom. Le zadnji del pomikovne funkcije lahko merimo in zanj je mogoče natančno določiti proste parametre s prilagajanjem funkcije merjenim pomikom, medtem ko sta prva dva dela določena na podlagi numeričnih simulacij in sta močno odvisna od dveh parametrov: Q_1, ki predstavlja delež celotne spremembe napetostnega stanja zaradi gradnje predora in se zgodi pred čelom predora in x_f, ki predstavlja velikost vplivnega območja pred čelom predora. Barlow trdi, da velikost predpomikov odraža velikost spremembe napetostnega stanja pred čelom predora. Analize rezultatov vertikalnega ekstenzometra in horizontalnega inklinometra v predoru Trojane in rezultati 3D meritev v raziskovalnem rovu pred čelom avtocestnega predora Šentvid izkazujejo do 75% delež predpomikov v celotnih pomikih.

Numerična analiza pomikov v izkopani prostor, različne velikosti merjenih pomikov v območju preboja desne cevi predora Trojane pri gradnji z vpadom plasti v izkopani prostor ali vpadom plasti v čelo in zelo

različne velikosti pomikov izmerjenih med gradnjo raziskovalnega rova in pred čelom predora so izkazale, da je velikost predpomikov razen od togosti hribine odvisna tudi od relativne usmerjenosti diskontinuitet glede na os predora. Izvedenih je bilo 350 3D numeričnih analiz s programom Plaxis 3D Tunnel, kjer smo variirali 3 različne azimute diskontinuitet (vzporedno z osjo – usmerjenost diskontinuitet 0°, 45° glede na os – usmerjenost diskontinuitet 45° in pravokotno na os – usmerjenost diskontinuitet 90°), vpade plasti smo variirali v območju [-90°,90°] s korakom 15°, spreminjali smo razmerje elastičnih modulov E_1:E_2 (1:1, 2:1, 4:1) in delež strižnega modula v odvisnosti od izotropne vrednosti G_2 (G, 0,5G, 0,25G in s povratnimi analizami v predoru Šentvid določenim G = 5 MPa). V nadaljevanju podani rezultati veljajo za vertikalne pomike stropne točke.

Numerični rezultati izkazujejo, da je pri gradnji predora z usmerjenostjo diskontinuitet vzporedno z osjo predora ter vpadom v izkopani prostor, velikost predpomika Q_1 odvisna predvsem od vpadnega kota in le malo od materialnih parametrov (slika 6-2). Pri gradnji predora z vpadom diskontinuitet v čelo je predpomik odvisen tako od vpadnega kota diskontinuitet in materialnih parametrov (boljša kot je hribina, manjši je delež predpomika v celotnih pomikih in obratno). Izračunane vrednosti parametra Q_1 so v razponu od 30% pri vpadu plasti 15° in izkopu predora proti vpadu diskontinuitet do 90% za vpad plasti 45° in izkopu predora z vpadom diskontinuitet v čelo predora. S spreminjanjem azimuta od smeri vzporedno z osjo predora proti pravokotno na os predora se velikost Q_1 zmanjšuje; zmanjšuje se tudi odvisnost od materialnih parametrov (zmanjšanje strižnega modula in razmerja elastičnih modulov E_1:E_2 še vedno povzroči večji delež predpomikov v celotnih pomikih). V primeru, ko je usmerjenost diskontinuitet pravokotna na os predora, delež predpomikov variira v razponu 30-50% celotnega pomika. Podobne vrednosti dobimo tudi v primeru izračuna z elastičnimi parametri in parametri »Hardening soil« konstitutivnega modela (slika 6-2).

Velikost vplivnega območja pred čelom za usmerjenost diskontinuitet vzporedno z osjo predora znaša 12 do 47 m (premer modeliranega predora je znašal 10 m) in zavisi od kota vpada in materialnih parametrov hribine (slika 6-3). Maksimalne vrednosti parametra Q_1 sovpadajo z minimalnimi vrednostmi parametra x_f in obratno. To pomeni, da se v primeru večjega deleža predpomikov le-ti razvijejo v primerjalno krajšem območju pred čelom oz. v primeru manjšega deleža predpomikov se le-ti pričnejo dogajati na večji oddaljenosti od čela predora. Spreminjanje usmerjenosti diskontinuitet proti pravokotni smeri povzroči manjšo variabilnost vrednosti parametra x_f za različne kote vpada; zmanjša se tudi odvisnost od materialnih parametrov. Pri usmerjenosti diskontinuitet pravokotno na os predora znaša velikost vplivnega območja med 22 in 42 m in je skorajda neodvisna od kota vpada plasti. Računske vrednosti x_f so nekoliko večje kot so bile opažene v predorih Trojane in Šentvid. Glavni razlog je fenomen velike togosti pri majhnih deformacijah, ki ni vgrajen v "Jointed rock" konstitutivni model.

Opazili smo tudi, da velikost celotnega izračunanega pomika variira za različne usmerjenosti in vpadne kote diskontinuitet pri enakih materialnih parametrih. Krivulje pomikov so bile tako normalizirane na krivuljo pri orientaciji diskontinuitet 0°/0°, da smo lahko primerjali krivulje za različne materialne parametre ne glede na njihovo velikost. Dobljene vrednosti (oznaka |d|) so bile v razponu od 50% do 120% celotnega pomika pri orientaciji diskontinuitet 0°/0° (slika 6-4). Velikosti pomikov so za enak vpadni kot pri izkopu predora z orientacijo diskontinuitet v izkopani prostor ali v čelo precej podobnega velikostnega reda, razen v primeru izkopa z usmerjenostjo diskontinuitet 0° in vpadne kote 15° do 60°.

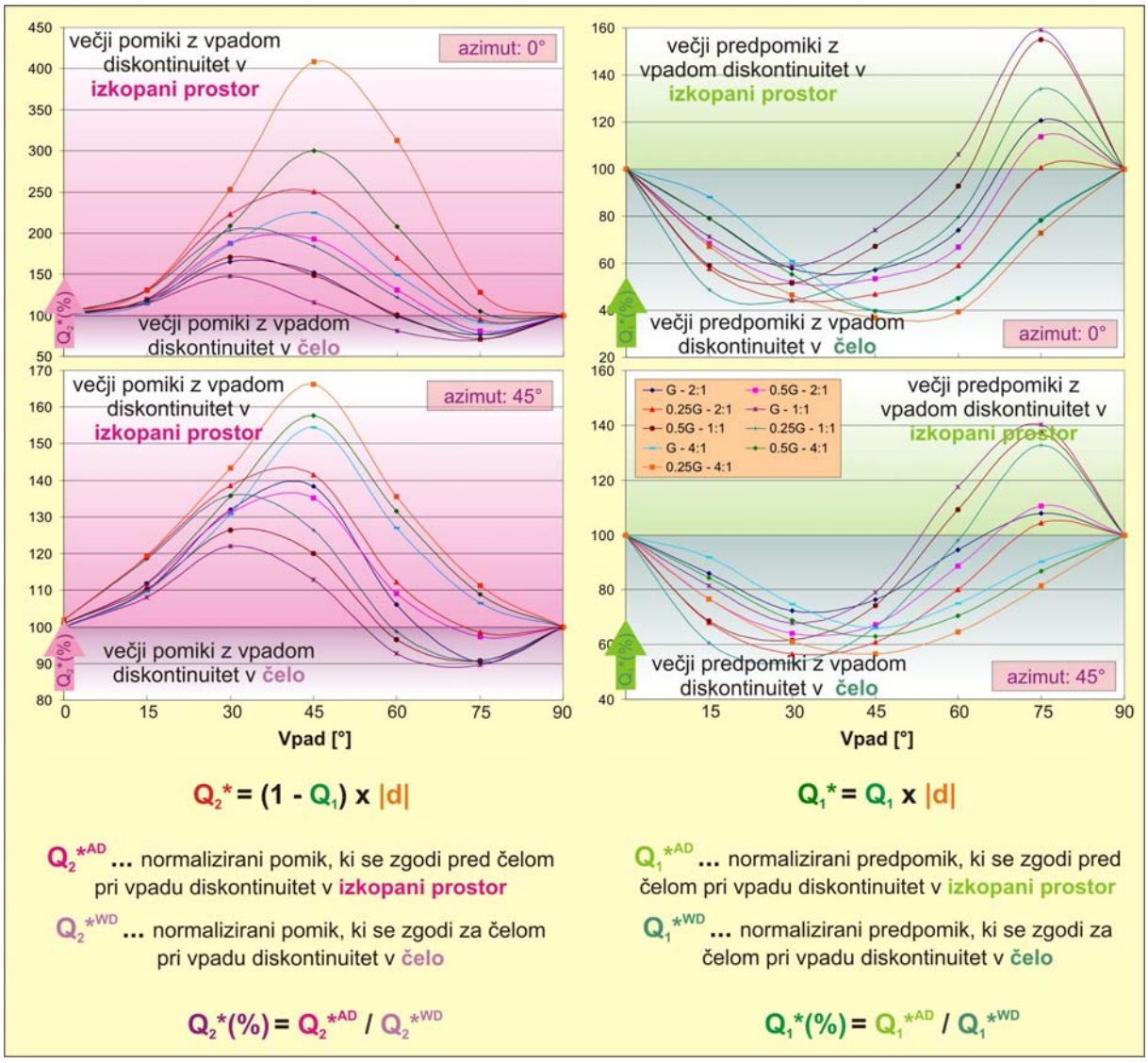

Slika 9-11. Delež pomikov pri izkopu predora proti/z vpadom diskontinuitet, ki se zgodi za čelom predora (Q_2*(%)) oz. pred čelom predora (Q_1*(%)).

Za lažjo primerjavo vpliva gradnje z različnimi vpadi diskontinuitet (v čelo ali v izkopani prostor) smo nadalje določili parameter Q_2*(%), ki predstavlja velikost posedka stropne točke v primeru gradnje z orientacijo diskontinuitet v izkopani prostor glede na posedek iste točke pri izkopu z orientacijo diskontinuitet v čelo (enačbe so zapisane na sliki 9-11). Za bolj strme vpadne kote in usmerjenost diskontinuitet 0° znaša Q_2*(%) od 70% do več kot 400% za vpadni kot 45° in najslabše uporabljene togostne materialne parametre v smeri diskontinuitet (levi zgornji graf na sliki 9-11). Za usmerjenost 45° so izračunane vrednosti Q_2*(%) v razponu od 90 do 165% (levi spodnji graf na sliki 9-11). Ekstremne vrednosti Q_2*(%) zavisijo od materialnih parametrov: znižanje togostnih parametrov vzdolž diskontinuitet (E_2 in G_2) povzroči drastično povišanje Q_2*(%). Na podoben način smo za predpomike definirali tudi parameter Q_1*(%). Razpon Q_1*(%) znaša med 40% in 160% in je odvisen od orientacije diskontinuitet in materialnih parametrov hribinske mase.

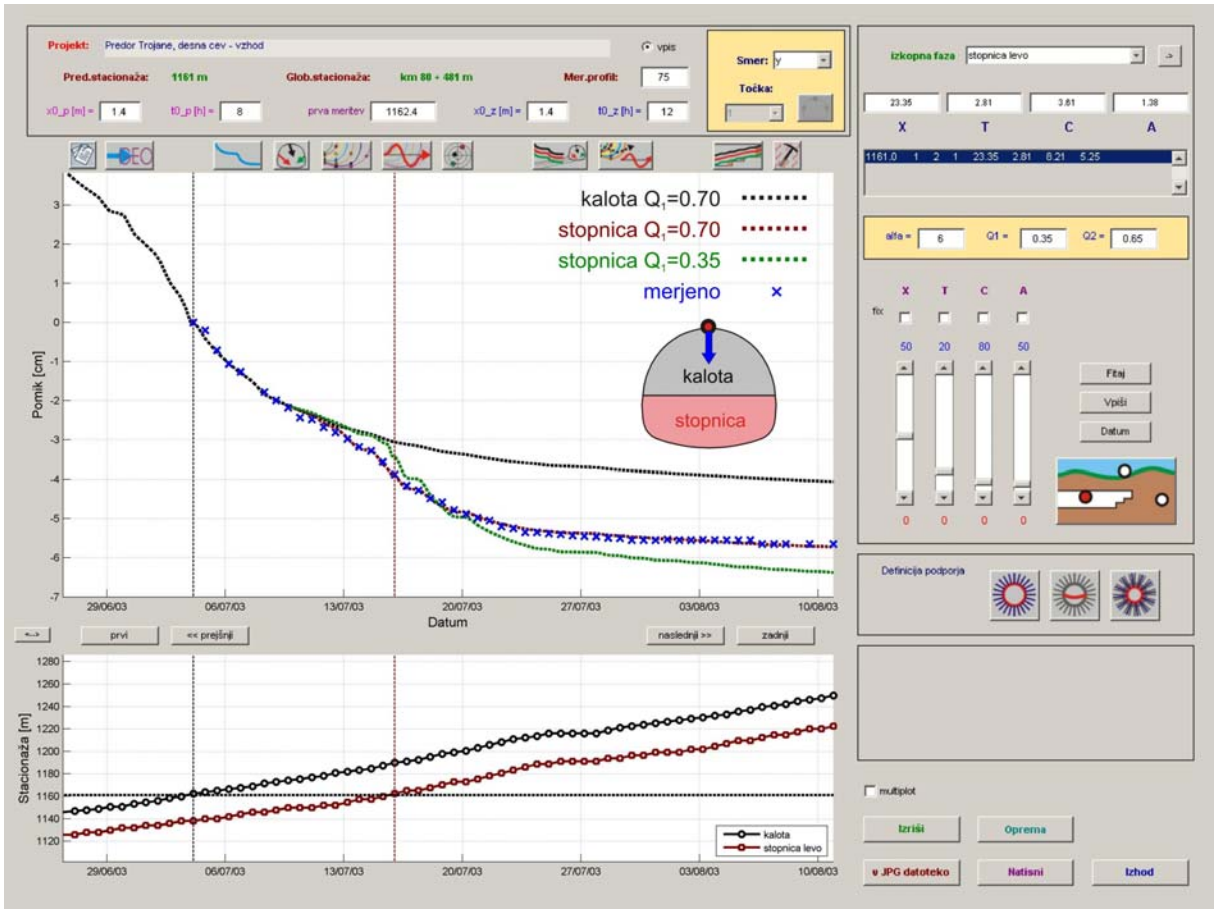

Slika 9-12. Računsko prilagojeni in merjeni vertikalni pomiki stropne točke v merskem profilu MS75 na stacionaži km 80+481 v severni cevi predora Trojane (izkop iz vzhoda).

Izračunani rezultati so bili nato med drugim uporabljeni na prej omenjenem območju preboja desne cevi predora Trojane. Izračunani Q_2*(%) za dano relativno orientacijo diskontinuitet glede na os predora

in s povratno analizo pridobljene materialne parametre znaša do 165%. Povprečni izmerjeni Q_2*(%) zadnjih 7 merskih profilov na vsaki strani mesta preboja (izkop iz vzhoda oz. zahoda) znaša 197%. Razliko med izračunanimi in izmerjenimi vrednostmi lahko pripišemo višjemu nadkritju nad izkopom iz zahoda (razvidno iz slike 9-6) ter razlikam v geološki strukturi na obeh straneh preboja.

Izračunane vrednosti Q_1 in x_f smo nato uporabili še pri prilagajanju analitične pomikovne funkcije krivuljam merjenih pomikov merskih točk v merskih profilih na območju preboja. Na sliki 9-12 je prikazano osnovno okno programa Predor z računsko prilagojenimi pomiki merjenim vrednostim za stropno točko merskega profila na vzhodni strani območja preboja. Merjene vrednosti so prikazane z modrimi križci, pomikovna funkcija kalote pa s črno črtkano črto (vrednost Q_1 za dano orientacijo diskontinuitet znaša 0,70). Z rdečo črtkano črto je prikazana pomikovna funkcija stopnice za isto vrednost Q_1, medtem ko je z zeleno prikazana pomikovn funkcija stopnice za $Q_1 = 0,35$, kakršno vrednost najdemo v literaturi. Slednje funkcije se ne da prilagoditi merjenim vrednostim, še posebej ne brez spreminjanja velikosti prostih parametrov X in T (Guenot s sodelavci (1985) je namreč ugotovil, da se vrednost parametrov X in T v podobnih pogojih vzdolž predora ne spreminja, bolj kot ne konstanten naj bi bil tudi parameter A). V obdelanih primerih smo morali spreminjati tudi velikost parametra A, da smo uspeli zadovoljivo prilagoditi računske vrednosti merjenim pomikom.

9.7 Zaključek

Obsežna baza podatkov o 3D meritvah pomikov predorske obloge in površinskih točk nad predorom, ki je bila izdelana v okviru naloge, je omogočila prepoznavanje zanimivih in do zdaj še ne dokumentiranih deformacijskih vzorcev, kamor sodijo veliki vzdolžni pomiki v smeri nadaljnjega izkopa. Baza podatkov trenutno vsebuje meritve iz 13 predorov; v analizi je bil uporabljen le manjši del podatkov izmed več kot 1800 merskih profilov.

Povratna 2D numerična analiza merjenih pomikov v kaverni predora Šentvid je pokazala, da je odziv skrilave hribinske mase z uporabo "Jointed rock" materialnega modela mogoče modelirati le z izredno nizkim strižnim modulom G_2 vzdolž diskontinuitet. Pri tem je treba poudariti, da v teh hribinah niso bile izvedene meritve strižnega modula ali trdnostnih parametrov vzdolž diskontinuitet, kar bi morala biti ena prednostnih nalog pred začetkom izkopa nadaljnjih predorov v podobnih geoloških razmerah. Vzdolžni pomiki v smeri nadaljnjega izkopa so bili v primeru padajočega nadkritja in orientaciji diskontinuitet v izkopani prostor opaženi na šestih daljših odsekih v skupni dolžini 3,2 km v petih predorih v različnih geoloških pogojih (Trojane, Golovec, Jasovnik, Ločica in Podmilj). Numerična analiza opaženega fenomena je pokazala, da je del velikih vzdolžnih pomikov v smeri nadaljnjega izkopa posledica morfologije terena in s tem povezanega začetnega napetostnega

stanja, drugi del pa zaradi nizkega strižnega modula večja deformabilnost hribine v smeri pravokotno na orientacijo diskontinuitet. Zadnji dejavnik vpliva tudi na velikost izmerjenih pomikov izkopanega prostora in je prikazan na območju preboja severne cevi predora Trojane, kjer so povprečni posedki stropnih točk zadnjih 7 merskih profilov pri izkopu iz zahoda kljub boljši hribini in deloma zaradi nekaj večjega nadkritja približno dvakrat večji kot pomiki zadnjih 7 merskih profilov pri izkopu iz vzhoda.

Raziskovalni rov predora Šentvid je poleg določitve najugodnejšega položaja priključnih kavern omogočil tudi izvedbo natančnih 3D meritev obloge raziskovalnega rova pred čelom glavnega predora. Meritve so se izvajale vsako uro z natančnim elektronskim tahimetrom in uporabo sistema za avtomatsko prepoznavanje tarč. Kljub izredno zahtevnim razmeram zaradi prahu in vlage je sistem deloval zanesljivo. V sedemmesečnem obdobju je bila pridobljena ogromna količina merskih podatkov, na podlagi katerih smo določili »normalno« obnašanje merskega profila pred čelom predora (izrazito bilinearni odziv z deformacijami vzdolž diskontinuitet, ko je obremenitev merskega profila majhna in pravokotno na smer diskontinuitet, ko je čelo predora bližje in se obremenitev poveča). Poleg tega so natančne in pogoste meritve omogočile določitev začetka območja majhnih deformacij oz. vplivnega območja pred čelom predora (bolj kot od velikosti predora je bil v našem primeru odvisen od geoloških pogojev) ter prevojne točke na krivulji pomikov, katera definira začetek območja velikih deformacij (večina deformacij se je zgodila v območju 4-6 m pred čelom predora). Natančne meritve so omogočile tudi opazovanje spremembe trenda vzdolžnih pomikov zaradi vgradnje velikega števila sider v čelo predora, medtem ko bolj izrazitega vpliva niso pokazale ne meritve ne numerični izračuni. Numerična analiza je tudi potrdila domnevo, da je raziskovalni rov deloval kot blažilec, ker je dovoljeval radialne deformacije v izkopani prostor zaradi prerazporejanja napetosti v zaledni hribini, katere bi se v nasprotnem primeru odrazile kot povečani vzdolžni pomiki proti izkopanemu prostoru. Zaradi raziskovalnega rova so bili izmerjeni trendi vzdolžnih pomikov z malo ali veliko sidri skorajda nespremenjeni.

Variacija materialnih parametrov hribinske mase in relativne orientacije diskontinuitet glede na os predora v numeričnih analizah je pokazala, da so delež predpomikov, velikost vplivnega območja pred čelom predora in tudi velikost pomika močno odvisni od orientacije diskontinuitet in togostnih parametrov hribine vzdolž diskontinuitet. S pomočjo opisanega deformacijskega mehanizma in izračunanih vrednosti lahko zadovoljivo razložimo predstavljene deformacijske vzorce.

Glavne ugotovitve teh numeričnih analiz lahko sklenemo z naslednjima odstavkoma:

Predpostavimo, da se predvideva gradnja predora z nizkim nadkritjem pod naseljenim območjem v mehki, skrilavi kamnini in z azimutom diskontinuitet, ki je vzporeden poteku osi predora, ter npr. vpadom diskontinuitet s kotom 45°. V takem primeru bi bilo z vidika čim manjšega vpliva gradnje na površino bolj ugodno izkop vršiti z vpadom plasti v izkopani prostor, saj se pri takšni smeri izkopa glede na diskontinuitete večina deformacij zgodi za čelom predora in jih lahko nadzorujemo s togim podporjem. Če bi potekal izkop iz druge smeri, bi se večina deformacij zgodila pred čelom predora, kjer jih ne moremo učinkovito nadzorovati, in bi gradnja predora tako neizogibno močno vplivala na objekte v vplivnem območju nad predorom.

Če bi gradnja predora v zgoraj opisanih hribinskih pogojih potekala pod visokim nadkritjem in/ali neposeljenim območjem, bi bilo iz vidika racionalnosti gradnje bolj ugodno graditi predor z vpadom plasti v čelo predora, saj se v tem primeru večina deformacij izvrši pred čelom predora. Potrebna velikost nadprofila bi bila tako precej manjša. Manjša bi bila tudi obremenitev primarnega podporja, kar bi se odrazilo v ekonomičnosti gradnje.

References

Ajdič, I., Štimulak, A. 2004. Geological Accompaniment to the Execution of the Trojane Tunnel and Rock Mass Classification, In: *Proceedings of the 4th Conference of the Slovenian Geotechnical Society*, Rogaška Slatina, Slovenia: Ljubljana, Slovenian Geotechnical Society; pp. 35-44 (in Slovene).

ALWAG, IBI self-drilling anchor. Producer homepage: http://www.alwag.com/products/anchors-and-rock-bolts/ibi-self-drilling-anchors.html (05.04.2009)

Barla, G.; Barla, M. 2000. Continuum and discontinuum modelling in tunnel engineering. *Gallerie e grandi opera sotterranee*, *61*: 15-35.

Barlow, J.P. 1986. *Interpretation of tunnel convergence measurements*. MSc thesis. The University of Alberta, Department of Civil Engineering, Edmonton, Alberta.

Barton, N. 1996. Investigation, Design and Support of Major Road Tunnels in Jointed Rock using NMT Principles. In: *Proceedings of IX. Australian Tunneling Conference*, Sydney, Australia; pp.145-160.

Beguš, T.; Sotlar, K. 2000. Engineering geological characteristics of the Golovec tunnel. In: *Proceedings of the 5th International symposium on tunnel construction and underground structures*, Ljubljana, Slovenia: University of Ljubljana, Faculty of natural sciences and engineering; pp. I-75 – I-84 (in Slovene).

Beguš, T.; Sotlar, K.; Jerše, Z.; Hoblaj, R. 2004. The Dekani motorway tunnel: Final report on geological and geotechnical accompaniment of the tunnel construction, Geoinženiring report 30-632/2002. Ljubljana, Slovenia: Ljubljana, Geoinženiring (in Slovene).

Beguš, T.; Kočevar, K.; Prestor, J.; Sotlar, K. 2003. Tunnels in karst and flysch in Slovenia, *RMZ – Materials and environment*, *50*: 17-20.

Beguš, T.; Sotlar, K.; Rupret, M.; Jakopin, D. 2005. Synthesis of the engineering geologic data of the Trojane tunnel. Geoinženiring report No. 30-2049/05, Ljubljana, Slovenia: Ljubljana, Geoinženiring (in Slovene).

Bensted, J. 1999. Thaumasite – background and nature in deterioration of cements, mortars and concretes. *Cement and concrete composites*, *21*: 117-121.

Beth, M.; Macklin, S.; Nichols, Z. 2003. King's Cross Station Redevelopment, London: Design of the Monitoring System. In *Proceedings of the FMGM 2003*, Oslo, Norway; pp. 731-738.

Brinkgreve, R.B.J; Vermeer, P.A. 2001. *Plaxis 3D Tunnel Material Models Manual, version 2*. A.A. Balkema.

Budkovič, T.; Čadež, F.; Petrica, R. 2005. Structural geological accompaniment to the execution of the Trojane tunnel for acquirement of an independent opinion about the tunnel condition, Geological Survey of Slovenia report No. J-II-30d/b4-7/41-9, Ljubljana, Slovenia: Ljubljana, Geological Survey of Slovenia (in Slovene).

Button, E.; Blümel, M. 2004a. Characterization of Phyllitic and Schistose Rock Masses: from System Behaviour to Key Parameters, In: *Proceedings of the ISRM regional symposium EUROCK 2004 & 53rd Geomechanics colloquy*, Salzburg, Austria: Essen, Verlag Glückauf GmbH; pp. 459-464.

Button, E. 2004b. Characterization of Phyllites for tunnelling. In: *Proceedings of International Symposium on Rock Mechanics SINOROCK 2004*, Three Gorges Dam Projects in Hubei province, China; pp. 215-220.

Button, E; Volkmann, G. 2004c. Inclinometer Measurements – Trojane Tunnel Left East Excavation: Report 107, *Unpublished report*, Technische Universität Graz: Graz, Austria, 5 p.

Cesar-LCPC CLEO3D. Software homepage: http://www.lcpc.fr/en/produits/cesar/presentation/index2.dml (03.05.2009)

Črepinšek, M. 2006. Evaluation of the Šentvid tunnel Construction (in Slovene). In: *Proceedings of the 8th international symposium on tunnel construction and underground structures*, Ljubljana, Slovenia: University of Ljubljana, Faculty of natural sciences and engineering; pp. 158-167.

Čadež, F.; Križnič, A.; Vukadin, V.; Trajanova, M. 2000. Engineering geological conditions of the Ločica tunnel construction. In: *Proceedings of the 5th International symposium on tunnel construction and underground structures*, Ljubljana, Slovenia: University of Ljubljana, Faculty of natural sciences and engineering; pp. I-85 – I-94 (in Slovene).

Čadež, F., Videnič, M., Merhar, B., Trajanova. 2001. Geological structure and rock classes in the Jasovnik tunnel. *RMZ – Materials and environment*, *48*: 433-446 (in Slovene).

Čadež, F.; Genser, W.; Kleberger, J.; Pöschl, I. 2004a. Šentvid motorway tunnel – Interim results from Slovenia's most recent exploration gallery. In: *Proceedings of the 7th international symposium on tunnel construction and underground structures*, Ljubljana, Slovenia: University of Ljubljana, Faculty of natural sciences and engineering, 2004; pp. 50-56.

Čadež, F.; Jelen, B.; Križnič, A.; Merhar, B.; Vukadin, V.; Trajanova, M. 2004b. Final report on geological and geotechnical accompaniment of the Podmilj tunnel construction, IRGO Consulting report 388/04, Ljubljana, Slovenia: Ljubljana, IRGO (in Slovene).

DARS, Built motorways and expressways. Motorway company of Republic of Slovenia homepage: http://www.dars.si/Dokumenti/About_motorways/National_motorway_construction_programme/Built_motorways_and_expressways_286.aspx (22.03.2009)

DARS, Predori. Motorway company of Republic of Slovenia homepage: http://www.dars.si/Dokumenti/O_avtocestah/Objekti_na_avtocestah/Predori_85.aspx (22.03.2009)

DGSI: Radial & Tangential Pressure Cells for Tunnels homepage (producer): http://www.slopeindicator.com/instruments/tpc-tunnels.html (15.05.2009)

Fifer Bizjak, K.; Petkovšek, B. 2004. Displacement analysis of tunnel support in soft rock around a shallow highway tunnel at Golovec. *Eng. geol. 75*: 89-106.

FLAC 3D. Software homepage: http://www.itascacg.com/flac3d/overview.php

Franc, D. 1999. Construction of the Golovec tunnel. In *Technical information book of SCT company 45*, Ljubljana, Slovenia: Ljubljana, SCT; pp. 20-28 (in Slovene).

Gaich, A.; Pötsch, M.; Schubert, W. 2006. Computer vision for rock mass characterization in underground excavations. Report of the *Workshop on Laser and Photogrammetric Methods for Rock Tunnel Characterization,* Golden, Colorado, 2006; pp. 33-48; published on web site: http://www.docstoc.com/docs/633930/Laser-and-Photogrammetric-Methods-for-Rock-Face-Characterization (13.06.2009)

GeoFit. Software homepage: http://www.geofit.3-g.at/ (21.04.2009)

Gogala, M. 2001. *Back analyses of presuremeter test results in Permian-Carboniferous rock mass*. Graduation thesis, University of Ljubljana, Faculty of Civil and Geodetic Engineering: Ljubljana, Slovenia; 69 p. (in Slovene)

Goricki, A.; Button, E.A.; Schubert, W.; Pötsch, M.; Leitner, R. 2005. The Influence of Discontinuity Orientation on the Behaviour of Tunnels. *Felsbau* 2005, *5*: 12-18.

Grossauer, K. 2009. *Expert System Development for the Evaluation and Interpretation of Displacement Monitoring Data in Tunnelling*. Doctoral dissertation, Technische Universität Graz: Graz, Austria.

Guenot, A.; Panet, M.; Sulem, J. 1985. A New Aspect in Tunnel Closure Interpretation. In: *Proc. 26th US Symposium on Rock Mechanics*, Rapid City, USA; pp. 445-460.

Henke, A.; Fabbri, D. 2004. The Gotthard Base Tunnel: Project Overview. In: *Proceedings of the 7th international symposium on tunnel construction and underground structures*, Ljubljana, Slovenia: University of Ljubljana, Faculty of natural sciences and engineering; pp. 107-116.

Hoek, E. 2007. *Practical rock engineering (2007 ed.)*, Chapter 12: Tunnels in weak rock, 204-221. Available at: http://www.rocscience.com/hoek/pdf/12_Tunnels_in_weak_rock.pdf (23.05.2009)

Huber, G.; Westermayr, H.; Alber, O. 2005. Einfluss der Gefügeorientierung am Strenger Tunnel. *Felsbau* 2005, *5*: 20-24.

ITA WG "Research". 2007. ITA/AITES Report 2006 on Settlements induced by tunneling in Soft Ground. *Tunn. undergr. space technol.*, *22*: 119-149.

Jemec, P. 2006. *Influence of the exploratory tunnel on the construction of the Šentvid motorway tunnel*. Graduation thesis, University of Ljubljana, Faculty of Civil and Geodetic Engineering: Ljubljana, Slovenia; 190 p. (in Slovene)

Jeon, J.S.; Martin, C.D., Chan, D.H., Kim, J.S. 2005. Predicting ground conditions ahead of the tunnel face by vector orientation analysis. *Tunn. undergr. space technol. [Print ed.]*, *20*: 344-355.

Kavvadas, M.J. 2003. Monitoring and modeling ground deformations during tunnelling. In: *Proceedings of the 11th FIG Symposium on Deformation Measurements*, Santorini, Greece; pp. 371-390.

Klopčič, J. 2004. V*isualization and analysis of the displacement monitoring data in tunneling.* Graduation thesis, University of Ljubljana, Faculty of Civil and Geodetic Engineering: Ljubljana, Slovenia (in Slovene)

Klopčič, J.; Logar, J.; Majes, B. 2005. Observations in the exploration gallery of the Šentvid tunnel: cracks in primary lining, inflow of water and sections with deteriorated shotcrete. Report KMTal 308-1-05, Ljubljana, Slovenia: University of Ljubljana, Faculty of civil and geodetic engineering (in Slovene).

Klopčič, J.; Logar, J.; Ambrožič, T.; Štimulak, A.; Marjetič, A.; Bogatin, S.; Majes, B. 2006. Displacements in the exploratory tunnel ahead of the excavation face of Šentvid tunnel. *Acta Geotech. Slov.* 2006, *2*: 16-33.

Klopčič, J.; Logar, J.; Ambrožič, T.; Bogatin, S.; Marjetič, A.; Majes, B. 2008. Numerical back analyses of measured displacements in the exploratory tunnel and executed part of the Šentvid tunnel. Report KMTal E-16-08, Ljubljana, Slovenia: University of Ljubljana, Faculty of civil and geodetic engineering (in Slovene).

Kontogianni, V.; Stiros, S. 2005. Induced deformation during tunnel excavation: evidence from geodetic monitoring. *Eng. Geol. 79:* 115-126.

Kontogianni, V.; Kornarou, S.; Stiros, S. 2007. Monitoring with electronic total stations: Performance and accuracy of prismatic and non-prismatic reflectors. *Geotech. News 25*: 30–37.

Leica Geosystems Inc. Instructions for use of TPS1200.

Leitner, R; Pötsch, M.; Schubert, W. 2006. Aspects on the Numerical Modelling of Rock Mass Anisotropy in Tunnelling. *Felsbau* 2006, *2*: 59-65.

Likar, J; Vukadin, 1997. V. Time-dependent Back Analysis of a Multianchored Pile Retaining Wall. *J. Geot. Env. Engng.*, 34: 117-125.

Likar, J. 1999. The analysis of predicted surface deformations above the Trojane tunnel. IRGO expertise, Ljubljana, Slovenia: Ljubljana, IRGO (in Slovene).

Likar, J.; Jovičić, V. 2004a. The causes of excessive settlement above Trojane Tunnel and remedial measures. *Tunn. undergr. space technol. [Print ed.]*, *19*: 386-387.

Likar, J. 2004b. Trojane Tunnel Construction in Time Dependent and Low Bearing Rocks. In: *Proceedings of the 7th international symposium on tunnel construction and underground structures*, Ljubljana, Slovenia: University of Ljubljana, Faculty of natural sciences and engineering; pp. 172-181 (in Slovene).

Likar, J.; Volkmann, G.; Button, E. 2004c. New Evaluation Methods in Pipe Roof Supported Tunnels and its Influence on Design During Construction, In: *Proceedings of the ISRM regional symposium EUROCK 2004 & 53rd Geomechanics colloquy*, Salzburg, Austria: Essen, Verlag Glückauf GmbH; pp. 277-282.

Logar, J.; Štimulak, A.; Ajdič, I. 2004. The influence of shallow tunnelling under Trojane village on surface movements and stability, In: *Proceedings of the ISRM regional symposium EUROCK 2004 & 53rd Geomechanics colloquy*, Salzburg, Austria; Essen, Verlag Glückauf GmbH; pp. 283-286.

Lunardi, P. 2008. The dynamics of tunnel advance. In *Design and construction of tunnels: Analysis of controlled deformations in rock and soils (ADECO-RS)*; Springer – Verlag: Berlin, Germany; pp. 3 – 13.

Mair, R.J.; Taylor, R.N.; Burland, J.B. 1996. Prediction of ground movements and assessment of risk of buiding damage duw to bored tunnelling. In *Geotechnical Aspects of Underground Construction in Soft Ground*, Balkema, Rotterdam; pp. 713-718.

Marinos, P.; Hoek, E. 2000. GSI: A geologically friendly tool for rock mass strength estimation. *Int. Conference on Geotechnical and Geological Engineering, Geoeng 2000, Melbourne*, Technomic Publishing Company, Inc. U.S.A.; pp. 1422–1440.

Marjetič, A.; Ambrožič, T.; Bogatin, S.; Klopčič, J.; Logar, J.; Štimulak, A.; Majes, B. 2006. Geodetic measurements in Šentvid tunnel. *Geodetski vestnik* 2006*, 1*: 11-24 (in Slovene)

Miklavžin, S. 2004. *Numerical model of the Trojane tunnel with shallow overburden below populated area*. Graduation thesis, University of Ljubljana, Faculty of Civil and Geodetic Engineering: Ljubljana, Slovenia; 125 p. (in Slovene)

Moritz, B.; Vergeiner, R.; Schubert, P. 2002. Experience Gained at Monitoring of a Shallow Tunnel Under a Main Railway Line. *Felsbau* 2002, *2*: 29-42.

Moritz, B.; Grossauer, K.; Schubert, W. 2004. Short Term Prediction of System Behaviour of Shallow Tunnels in Heterogeneous Ground. *Felsbau* 2004, *5*: 44-52.

Netzel, H.; Kaalberg, F.J. 2001. Monitoring of the North/South Metroline in Amsterdam. In: *Proceedings of the CIRIA Conference: The response of buildings to excavation induced ground movement*, London, UK.

O'Reilly, M.P.; New, B.M. 1982 Settlements above tunnels in the United Kingdom – their magnitude and prediction. In *Tunnelling'82*, London, UK; pp. 173–181.

Peck, R. B. State of the Art Volume: Deep Excavations and Tunneling in Soft Ground. *In Proc. 7th Int. Conf. on Soil Mechanics and Foundation Engineering,* Mexico City, Mexico, 1969; pp. 225-290.

Petkovšek, A.; Mladenovič, A.; Klopčič, J.; Logar, J.; Majes, B. 2005. Geological warning on recorded cases of large content of pyrite in the rock mass and consequently the sulphate corrosion of the shotcrete in the exploration gallery of the Šentvid tunnel. Report KMTal 278-1-05, Ljubljana, Slovenia: University of Ljubljana, Faculty of Civil and Geodetic Engineering (in Slovene).

Petkovšek, A. 2006. Importance of complementing routine geotechnical tests with performance related tests in geomaterials. *Panelist presentation of the Discussion session 6: Development of the modern transportation infrastructure - Role of geotechnical engineering at the XIII. Danube – European Conference on geotechnical engineering,* Ljubljana, Slovenia: Ljubljana, Slovenian Geotechnical Society.

Placer, L. 1999a. Structural meaning of the Sava Folds. *Geologija*, *41*: 191-221.

Placer, L. 1999b. Contribution to the macrotectonic subdivision of the border region between Southern Alps and External Dinarides. *Geologija*, *41*: 223-255.

Plaxis 3D Tunnel. Software homepage: http://www.plaxis.nl/?cat=features&mouse=3D%20Tunnel (03.05.2009)

Plaxis 2D. Software homepage: http://www.plaxis.nl/?cat=productinfo&mouse=Plaxis%202D (23.04.2009)

Popovič, Z.; Ločniškar, A.; Logar, J. 1998. Remediation of the landslide in the portal area of a tunnel in permo-carboniferous clastic rocks. *Engineering Geology and the Environment: Proceedings of the 8th International Congress of the IAEG*, Vancouver. Rotterdam; Brookfield: A.A. Balkema; pp. 3113-3120.

Popović, Z.; Beguš, T. 1999. Final report on geotechnical monitoring of the surface above the Golovec tunnel, Geoinženiring report 30-4344/99 ZP, Ljubljana, Slovenia: Ljubljana, Geoinženiring (in Slovene).

Popit, A.; Močilnikar, K.; Venta, M.; Kramberger, F.; Wilenpart, B.; Kuzman, R.; Rant, J. 2006. Excavation of the Šentvid tunnel. In *Proceedings of the 8th international symposium on tunnel construction and underground structures*, Ljubljana, Slovenia: University of Ljubljana, Faculty of natural sciences and engineering; pp. 173-185 (in Slovene).

Pottler, R. 1990. Time-dependent rock-shotcrete interaction. A numerical shortcut. *Comput. Geotech.*, *9*: 149–169.

Premru, U. 1983. General geological map of SFRJ 1:100000, paper Ljubljana. *Geologija*, *17*: 497-499.

Pulko, M. 2004. The Motorway Interchange in the Tunnel Šentvid on te Motorway Section Šentvid-Koseze. In *Proceedings of the 7th international symposium on tunnel construction and underground structures*, Ljubljana, Slovenia: University of Ljubljana, Faculty of natural sciences and engineering; pp. 273-281 (in Slovene).

Rabcewicz, L. 1964. *The New Austrian Tunnelling Method*. Water Power, part 1, 1964, pp. 511-515; Water Power, Part 2, 1965, pp. 19-24.

Rabensteiner, K. 1996. Advanced tunnel surveying and monitoring. *Felsbau* 1996, *2*: 98-102.

Sakurai, S. 1997. Lessons Learned from Field Measurements in Tunnelling. *Tunn. undergr. space technol.*, *12*: 453-460.

Schubert, P.; Klopčič, J.; Štimulak, A.; Ajdič, I.; Logar, J. 2005. Analysis of Characteristic Deformation Patterns at the Trojane Tunnel in Slovenia. *Felsbau* 2005, *5*: 25-30.

Schubert, W. 1993. Erfahrungen bei der Durchörterung einer Großstörung beim Inntaltunnel. *Felsbau*, 1993, *6*: 443-447.

Schubert, W.; Budil, A. 1995. The Importance of Longitudinal Deformation in Tunnel Excavation. In: Proceedings of 8th International Congress on Rock Mechanics, Fujii, T. (ed.), Tokyo, Japan, 1411-1414. Rotterdam: A.A. Balkema

Schubert, W. 1996. Dealing with squeezing conditions in Alpine tunnels. *Rock Mech. Rock Engng.* 1996, *3*: 145–153.

Schubert, W.; Moritz, B. 1998. Controllable Ductile Support System for Tunnels in Squeezing Rock. *Felsbau* 1998, *4*: 224-227.

Schubert, W.; Steindorfer, A.; Button, E.A. 2002. Displacement monitoring in tunnels – an overview. *Felsbau* 2002, *2*: 7-15.

Schubert, W.; Vavrovsky, G.M. 2003. Innovations in geotechnical on-site engineering for tunnels. In: *Proc.int.symp. on Geotecnical measurements and modelling*, Karlsruhe, Germany; pp. 35-44.

Schubert, W.; Riedmüller, G. 2005. Tunnelling in fault zones – State of the art in investigation and construction. *Felsbau,* 2005, *18*: 7-15.

Schmuck, C. 2009. Teil I: 2DOC als Basis zur strukturierten Erfassung und Analyse von Daten – eine Übersicht, *Felsbau magazin* 2009, 2: 74-83.

Sellner, P.J. 2000. *Prediction of displacements in tunneling*. Doctoral dissertation, Technische Universität Graz: Graz, Austria.

Sellner, P.J.; Grossauer, K.; Leitman, R. 2004. How to Predict Surface Movements & Prevent Damages of Surface Structures. In *Proceedings of the ISRM regional symposium EUROCK 2004 & 53rd Geomechanics colloquy*, Salzburg, Austria; Essen, Verlag Glückauf GmbH; pp. 245-250.

Shen, B; Barton, N. 1997. The Disturbed Zone Around Tunnels in Jointed Rock Masses. *Int. J. Rock Mech. Min. Sci.*, 34: 117-125.

Solak, T. 2009. Ground behaviour evaluation for tunnels in blocky rock masses. *Tunn. undergr. space technol., 24*: 323-330.

Steindorfer, A. 1998. Short Term Prediction of Rock Mass Behaviour in Tunneling by Advanced Analysis of Displacement Monitoring Data. Doctoral dissertation, Technische Universität Graz: Graz, Austria.

Suwansawat, S. 2006. Superposition Technique for Mapping Surface Settlement Troughs over Twin Tunnels. In: *Proceedings of the International Symposium on Underground Excavation and Tunnelling*, Bangkok, Thailand; pp. 353-362.

Šlibar, M. 2005. *Analysis of the monitored displacements in Golovec tunnel*. Graduation thesis, University of Ljubljana, Faculty of Civil and Geodetic Engineering: Ljubljana, Slovenia; 120 p. (in Slovene).

Štimulak, A.; Ajdič, I. 2002. Damage Risk Assessment and Geological-Geotechnical Monitoring of the MW Tunnel in the Area of Trojane Village, In *Proceedings of the 6th International Symposium on Tunnel Construction and Underground Structures*, Ljubljana, Slovenia: University of Ljubljana, Faculty of natural sciences and engineering; pp.81-94 (in Slovene).

Štimulak, A.; Ajdič, I. 2004. Influence of the Excavation of the Trojane Tunnel on Surface in the Area of Trojane Village, In *Proceedings of the 7th International Symposium on Tunnel Construction and Underground Structures*, Ljubljana, Slovenia: University of Ljubljana, Faculty of natural sciences and engineering; pp.17-24 (in Slovene).

Tonon, F.; Amadei, B. 2002. Effect of Elastic Anisotropy on Tunnel Wall Displacements Behind a Tunnel Face. *Rock Mech. Rock Engng.* 2002, *3*: 141–160.

Tonon, F.; Amadei, B. 2003. Stresses in anisotropic rock masses: an engineering perspective building on geological knowledge. *Int. J. Rock Mech. Min. Sci.,* 40: 1099-1120.

Tonon, F.; Kottenstette, J.T. 2006. Laser and Photogrammetric Methods for Rock Tunnel Characterization: A Workshop. Report of the *Workshop on Laser and Photogrammetric Methods for Rock Tunnel Characterization*, Golden, Colorado; pp. 5-10; published on web site: http://www.docstoc.com/docs/633930/Laser-and-Photogrammetric-Methods-for-Rock-Face-Characterization (13.06.2009)

Tunnel:Monitor. Software homepage: http://www.tunnelmonitor.com/home.7.0.html (21.04.2009)

Vavrovsky, G. M.; Ayaydin N. 1987. Die Bedeutung der vortriebsorientierten Auswertung von Messungen im oberflächennahen Tunnelbau. STUVA-Tagung, Essen, Germany.

Volkmann, G.; Schubert, W. 2005. The use of horizontal inclinometers for the optimization of the rock mass – support interaction. In *Underground space use: Analysis of the past and lessons for the future, World tunneling congress 2005*, Istanbul, Turkey; pp. 967-972.

Vukadin, V. 2001. *Suitability of different constitutive models of rock mass for analyses of supporting structures*. MsC thesis, University of Ljubljana, Faculty of Natural Sciences and Engineering: Ljubljana, Slovenia; 118 p. (in Slovene)

Wittke, W. 1990. *Rock mechanics*. Springer-Verlag, Berlin, Germany.

Žigon, A.; Žibert, M.; Jemec, P. 2004. The design of the Šentvid tunnel system. In *Proceedings of the 7th international symposium on tunnel construction and underground structures*, Ljubljana, Slovenia: University of Ljubljana, Faculty of natural sciences and engineering; pp. 125-147 (in Slovene).

Žigon, A.; Daller, J.; Proprenter, M.; Abazović, E.; Žibert, M.; Kleberger, J.; Pöschl, I; Genser, W. 2005. Tunnel Šentvid connecting cavern: feasibility report, Elea project 415484P, Ljubljana, Slovenia: Ljubljana, Elea iC.

Žigon, A.; Žibert, M. 2006a. Predor Šentvid – Complex or Simple Solution? In *Proceedings of the 8th international symposium on tunnel construction and underground structures*, Ljubljana, Slovenia: University of Ljubljana, Faculty of natural sciences and engineering; pp. 195-203 (in Slovene).

Žigon, A.; Proprentner M.; Žibert, M.; Jemec, P. 2006a. Šentvid tunnel. In *Proceedings of the XIII. Danube – European Conference on geotechnical engineering,* 2nd part, Ljubljana, Slovenia: Ljubljana, Slovenian Geotechnical Society; pp. 1025-1030.